The Interactions of *Toxoplasma gondii* with Epithelial Tight Junctions

Caroline Weight

Submitted for the degree of Doctor of Philosophy

Institute of Food Research
University of East Anglia

May 2011

(79,230 words)

Abstract

The integrity of the small intestinal epithelial barrier is essential for a healthy gut and preventing infection. Tight junction complexes maintain barrier function as they seal adjacent cells and regulate paracellular permeability. Their importance is exemplified by the many diseases and infections associated with dysregulated tight junction complexes, as observed in Inflammatory Bowel Disease. Tight junction complexes include proteins, such as occludin, claudins and Zonula-Occludens, that interact with each other and the cytoskeleton. The function of occludin is unclear, but studies show that it can contribute to the pathogenesis of various diseases and be affected by pathogens such as *Toxoplasma gondii* (*T. gondii*), during infection. A third of the world's population is thought to be infected with *T. gondii* and it can cause fatal Toxoplasmosis. *T. gondii* invades the host via the gastrointestinal tract, crossing the epithelial barrier to disseminate into the body and studies indicate that the paracellular pathway is important for this process.

The aim of this research was to ascertain whether or not *T. gondii* interacts with occludin during the invasion of and transmigration between epithelial cells. Epithelial cells derived from the small intestine were used to determine if *T. gondii* alters barrier integrity and tight junction physiology.

This thesis demonstrates that *T. gondii* can infect and disseminate between epithelial cells without affecting barrier integrity. In addition to altering cellular distribution, *T. gondii* co-localised with and bound to the extracellular loops of occludin, indicating that this protein could be a key component of the moving junction. In cells where the expression of occludin was reduced, transmigration was impaired, suggesting that interactions with occludin are a possible mechanism of transmigration between epithelial cells. Results identify possible regulators and binding partners of occludin, derived from both cells and *T. gondii*, which could represent targets for therapeutic intervention.

Contents

List of Figures

List of Tables

Acknowledgements

I would like to thank my supervisor, Simon Carding, for giving me the opportunity to undertake this project at the Institute of Food Research and allowing me to work in his laboratory.

I wish to thank past and present members of the Carding group. In particular, I would like to thank Isabelle Hautefort and Louise Wakenshaw for their advice, assistance and encouragement throughout my Ph.D. and also their help in proofing this thesis.

Thank you to Bruce Pearson and Duncan Gaskin for providing feedback and for keeping me entertained with their cheerful waves, coffee-time stories and amusing anecdotes.

I would like to acknowledge Roy Bongaerts, Fran Mulholland, Alex Jones, Kathryn Cross and Mary Parker for their collaborative work with Flow Cytometry, Mass Spectrometry and Electron Microscopy.

Finally, this thesis would not have been achievable without the loving support of my family and friends, especially my close friends Daniel Parnham and Gary Wortley.

Declaration

I hereby declare that this thesis and the work described herein are original, except where indicated by reference or otherwise, and has not previously been submitted for any degree at this or any other university.

Abbreviations

bp	base pairs
BSA	Bovine Serum Albumin
CAR	Coxsackie Adenovirus Receptor
CCL	Chemokine Ligand
CD	Crohns Disease
CD2	Cluster of Differentiation 2
DTT	DiThioThreitol
ECL	Extracellular loop
ERK	Extracellular signal-Related Kinase
FACS	Fluorescence-Activated Cell Sorting
FAE	Follicle Associated Epithelium
FBS	Foetal Bovine Serum
FITC	Fluorescein IsoThioCyanate
GEF	Guanine nucleotide Exchange Factor
GI	GastroIntestinal
GPI	GlycosylPhosphatidylInositol
GTP	Guanosine TrisPhosphate
HFF	Human Foreskin Fibroblasts
HSP	Heat Shock Proteins
IBD	Inflammatory Bowel Disease
ICAM	InterCellular Adhesion Molecule
IELs	IntraEpithelial Lymphocytes
Ig	Immunoglobulin
IFN	Interferon

IL	InterLeukin
IP	ImmunoPrecipitation
IPTG	IsoPropyl β-D-1-ThioGalactopyranoside
JAM	Junction Adhesion Molecule
KC	Keratinocyte Chemoattractant
LPL	Lamina Propria Lymphocyte
LPS	LipoPolySaccharide
LTR	Long Terminal Repeat
M cells	Microfold cells
MAGUK	Membrane Associated GUanylate Kinase homologue proteins family
MAPK	Mitogen Associated Protein Kinase
MARVEL	Myelin And lymphocyte and Related proteins for VEsicle trafficking and membrane Link
MCP	Monocyte Chemoattractant Protein
MIC	MICroneme
MICAL-L2	Molecule Interacting with CasL-like 2
MLCK	Myosin Light Chain Kinase
MHC	Major Histocompatibility Complex
Mo MuLV	Moloney Murine Leukemia Virus
MyD88	Myeloid Differentiation factor 88
NK	Natural Killer cell
NOD	Nucleotide Oligomerisation Domain
PBS	Phosphate Buffered Saline
PDZ	Post Synaptic Density Protein (PSD95), Drosophila disc large tumor suppressor (DlgA), Zonula Occludens-1 protein (ZO-1)
PET	PolyEthylene Terephthalate
PFA	ParaFormAldehyde
PI3K	PhosphoInositide 3-Kinase
PKC	Protein Kinase C

PPV	ParasitoPhorous Vacuole
RT	PCR Real-Time Polymerase Chain Reaction
ROCK	RhO associated Coiled-coil containing protein Kinase
RON	Rhoptry neck protein
ROP	Rhoptry bulb protein
SAG	Surface Antigen protein
SDS PAGE	Sodium Dodecyl Sulfate PolyAcrylamide Gel Electrophoresis
SEM	Scanning Electron Microscopy
scRNA	scramble RiboNucleic Acid
shRNA	short hairpin RiboNucleic Acid
siRNA	small interfering RiboNucleic Acid
SV40	Simian Virus 40
TCR	T Cell Receptor
TEER	TransEpithelial Electrical Resistance
TEM	Transmission Electron Microscopy
T. gondii	*Toxoplasma gondii*
TGF	Transforming Growth Factor
TLR	Toll Like Receptor
TNF	Tumour Necrosis Factor
UC	Ulcerative Colitis
VKER	Vitamin K Epoxide Reductase
YFP	Yellow Fluorescent Protein
ZO	Zonula Occludens

Chapter 1

Introduction

1.1 The Gastrointestinal Tract

1.1.1 Anatomy of the gastrointestinal tract

The human gastrointestinal tract (GI tract) is a $200m^2$ tubular organ the primary function of which is to absorb water and nutrients. The GI tract consists of the oesophagus, stomach, small intestine, large intestine, rectum and anus. The small intestine is the main site of digestion and absorption, and is divided into three sections called the duodenum, the jejunum and the ileum. In humans, the small intestine is 6m long and surface area is increased by longitudinal folds within the tube which are further folded into finger-like projections called villi, and tubular invaginations called crypts of Lieberkühn. Individual cells have microvilli on their surface to increase the absorptive area and limit adherence of microbes. Cells are covered in a mucus layer which acts as a primary defence against physical and chemical injury caused by food, the microbiota and pathogens in the lumen [Kim and Ho, 2010]. The microbiota, which consist of over 1000 species, comprise of microbes that reside in the GI tract that are important for extracting additional nutrients from the diet and producing vitamins, preventing harmful microbes (pathogens) from invading the epithelium, promoting peristalsis, regulating cell proliferation and differentiation, and stimulating the intestinal immune system [O'Hara and Shanahan, 2006; Hooper and Macpherson, 2010]. The intestinal immune system lies within and beneath the epithelium in a layer of connective tissue called the lamina propria, which resides on top of smooth muscle tissue called the muscularis mucosa. Collectively, the epithelium, lamina propria and muscularis mucosa make up the gut mucosa which rests on a network of blood vessels and lymphatic systems [Turner and Turner, 2010].

1.1.2 The intestinal immune system

The immune system consists of cells such as lamina propria lymphocytes (LPLs), intraepithelial lymphocytes (IELs), macrophages, dendritic cells, natural killer cells, neutrophils and secretory plasma cells.

IELs in the small intestine are predominantly $CD8^+$ T cells and express either the $\alpha\beta$ T-cell antigen receptor (TCR) or the $\gamma\delta$ TCR, the latter of which is present in the highest proportion [Guy-Grand et al., 1991]. IELs are situated at the basal domain of the mucosal epithelium and bind to cells via $\alpha_E\,\beta_7$ integrin [Taraszka et al., 2000]. IELs are thought to have a protective function and can respond to stress signals released from epithelial cells in conjunction with releasing their own. Stress signals include the secretion of small soluble signalling molecules called cytokines and chemokines (chemotactic cytokines) which can be anti-inflammatory and promote wound healing and cell proliferation [Chen et al., 2002b; Ismail et al., 2009]. In addition, they instigate the recruitment and activation of neutrophils, macrophages and antigen presenting cells such as dendritic cells to sites of infection, leading to inflammation [Shaw et al., 1998; Tramonti et al., 2006; Dalton et al., 2006; Komano et al., 1995]. Neutrophils and macrophages phagocytose bacteria while natural killer cells lyse bacteria, which leads to secretion of cytokines such as Tumour Necrosis Factor α (TNFα), Interferon γ (IFNγ) and hydrolytic enzymes like lysozyme [Colgan et al., 1993].

Epithelial cells, innate immune cells and subsets of T lymphocytes recognise microbes and microbial antigens by pattern recognition receptors on the cell surface known as Toll like receptors (TLRs), and in the cytoplasm, such as the nucleotide-binding oligomerisation domain (NOD) family of proteins, for example NOD2 [Hornef et al., 2003; Minns et al., 2006; Wesch et al., 2011]. Upon binding, signal transduction cascades are initiated through myeloid differentiation factor 88 (MyD88), resulting in activation of inflammatory pathways following NF$\varkappa$B (nuclear factor kappa light chain enhancer of activated B cells) translocation to the nucleus, that leads to the secretion of cytokines, chemokines and anti-microbial proteins.

Intertwined within the crypts and villi of the small intestine is the follicle-associated epithelium (FAE) containing specialised microfold cells (M cells), which lie in close proximity to Peyers Patches (PP, Figure 1.1). The antigens they absorb are detected by the underlying immune cells such as dendritic cells, macrophages and activating LPLs, which travel

through the lymphatic system to the lamina propria [Miller et al., 2007]. M cells are different to other enterocytes as they lack a defined brush border, have no glycocalyx mucus layer, and morphologically have an invaginated basal membrane in which lymphocytes can be found [Corr et al., 2008]. After microbial challenge the numbers of M cells increase which allows for higher antigen uptake and a rapid response from immune cells [Bahi et al., 2002; Kernéis et al., 1997].

Antigen uptake can also occur independently of M cells. Within the lamina propria, dendritic cells can migrate between cells and extend dendrites into the lumen and sample antigen from non-pathogenic bacteria [Rescigno et al., 2001; Rimoldi et al., 2004; Arques et al., 2009]. Having sampled antigen from the lumen, dendritic cells migrate to the Peyers Patches to induce B cell differentiation into plasma cells. Plasma cells migrate to the lamina propria where they secrete Immunoglobulin A (IgA) that is transcytosed across the epithelium via the polymeric Immunoglobulin receptor, to decrease microbial contact with the epithelium and regulate the composition of the microbiota [Macpherson et al., 2000].

Both enterocytes and dendritic cells express Major Histocompatibility Complexes (MHC) I and II, that process internal and external antigens respectively, and present the MHC-associated peptides to T cells. Dendritic cells have been shown to prime IELs via IFNγ production ([Moretto et al., 2007]) and are responsible for controlling tolerogenic or activating T cell effector responses following MHC presentation [Laffont and Powrie, 2009]. Tolerance describes the unresponsive nature of the immune system towards the microbiota and self antigens, and a breakdown in tolerance can lead to disorders of the GI tract such as Inflammatory Bowel Disease (IBD) [Weiner et al., 2011].

1.1.3 Structure and cells of the small intestine

Epithelial cells are derived from pluripotent stem cells in the base of the crypts that, by asymmetric division, produce one daughter cell and one stem cell [Marshman et al., 2002; Potten and Loeffler, 1990]. Most daughter cells migrate upwards along the crypt and becoming increasingly differentiated towards the villus. Differentiated cells have a specific function within the small intestine and these include Paneth cells, goblet cells and entero-endrocrine cells which are embedded within a single layer of enterocytes (Figure 1.1).

The 4 - 16 stem cells in each crypt divide every 12 - 32 hours, and with enterocytes surviving for 2 - 3 days in the small intestine in a process that

is responsive to the microbiota, they are constantly shed at the tip of the villi as they are forced upwards [Savage et al., 1981; Marshman et al., 2002; Potten and Loeffler, 1990]. The crypt contains approximately 250 - 350 cells of which approximately 150 proliferate twice a day [Potten and Loeffler, 1990; Watson et al., 2005]. Within each villus there are approximately 3500 cells that are derived from 2 or 3 individual crypts [Potten and Loeffler, 1990].

Entero-endocrine cells secrete peptide hormones such as gastric inhibitory polypeptide, substance P and glucagon like peptide 1, and contribute to the regulation of lipid absorption, gastric emptying, glycemia, cell proliferation and cell migration [Mellitzer et al., 2010]. Goblet cells are characterised by the presence of large vacuoles which contain mucin. Mucin along with other innate defence molecules are secreted from these cells to form the glycocalyx mucus layer that can be up to 150μm thick within the small intestine [Johansson et al., 2008]. Paneth cells are found at the base of the crypts and can live up to 70 days [Ouellette, 2010; Gordon and Hermiston, 1994]. They are characterised by large dense granules which contain anti-microbial proteins including defensins, angiogenin, cryptdins and lysozyme [Ouellette, 2010]. Anti-microbial proteins regulate microbial colonisation in the GI tract, alter the composition of microbiota present and, most importantly, kill pathogens [Vaishnava et al., 2008].

The single layer of enterocytes accounts for 95% of cells within the GI tract and express microvilli projections on their apical surface (brush border), which contributes to the high absorptive ability of the cells [Yu and Yang, 2009]. They are tall, columnar polarised cells approximately 20 - 30μm in height, with basally located nuclei [Massey-Harroche, 2000; MacDonald, 2003; Macpherson and Harris, 2004]. They produce various extracellular matrix proteins which may differ in composition along the crypt-villus axis according to the state of cell differentiation [Hahn et al., 1987b]. It is generally accepted that the expression of various microvilli hydrolases such as alkaline phosphatase, sucrase-isomaltase, lactase, dipeptidylpeptidase IV and aminopeptidase N serve as indicators of cellular differentiation for small intestinal cells grown in culture [Massey-Harroche, 2000; Beaulieu et al., 1989]. Enterocytes found within the lower villi and crypts are positive for the proliferation-associated antigen Ki67, whereas enterocytes found within the upper villi are positive for lactase-phlorizin hydrolase and maltase-glucoamylase [Pageot et al., 2000].

In culture, these molecules may not be expressed without extra sup-

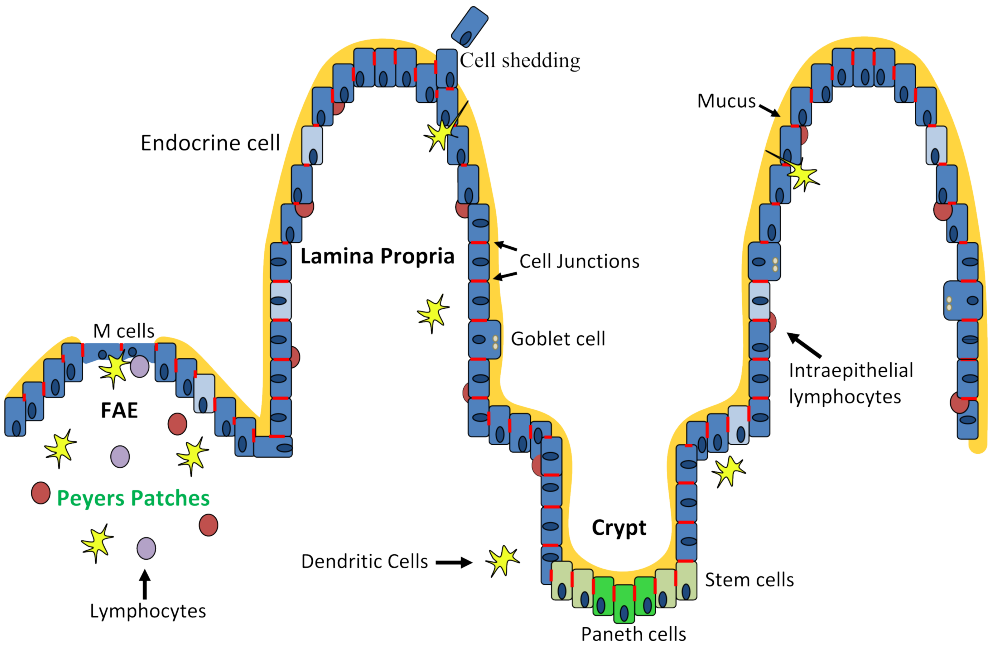

Figure 1.1: Anatomy of the small intestine. Cells are derived from stem cells in the base of the crypts. Paneth cells migrate downwards, while endocrine, goblet cells and enterocytes migrate upwards into the villi. All cells, except microfold cells (M cells, found in the follicle associated epithelium (FAE) within the Peyers Patches) are coated in a layer of mucus (yellow). Immune cells such as dendritic cells and lymphocytes are associated with and underneath the epithelium, in the lamina propria. Although cells are constantly being shed towards the tip of the villi, barrier integrity is maintained.

plementation of cofactors, matrices, non-essential amino acids and other stimulatory components [He et al., 1993]. Also, cells grown on different mediums such as collagen, laminin, and fibronectin extracellular matrix proteins [Rothen-Rutishauser et al., 2000; Sanders and Basson, 2000], Englebreth-Holm-Swarm sarcoma tumours extracellular matrix proteins (otherwise known as Matrigel, [Wood et al., 2003]), and a biomatrix [Hahn et al., 1987a], differ in degree of polarisation and differentiation [Simon-Assmann et al., 2007; Paul et al., 1993].

It should be noted that the structure and composition of the murine GI tract and the human GI tract are not identical, and recent publications have focussed on comparing these differences in order to address their significance [Haley, 2003; Mestas and Hughes, 2004]. For example, the numbers of M cells found in the human GI tract are lower than that of mice; human neutrophils are a source of defensins in humans but not mice, although murine Paneth cells secrete 20 types of defensins whereas human Paneth cells secrete only two types. Murine epithelial cells express the polymeric IgR receptor which can also bind IgM, whereas human cells express the IgA receptor. There are also differences within Immunoglobulin isotype production between species which may cause different signalling pathways to be transduced in response to microbial stimulation [Haley, 2003; Mestas and Hughes, 2004].

1.1.4 Cellular junctions

Epithelial cells are joined together by intercellular junctions (Figure 1.2). Tight junctions are found directly beneath the apical surface of the cells on the lateral domain, and are linked to the actin cytoskeleton. Tight junctions form the main barrier between adjacent cells and are discussed in detail in Section 1.2. Below the tight junctions are adherens junctions which link to cytoskeletal microfilaments and consist of calcium dependent proteins that contribute to cell - cell adhesion, through interactions with one another and with tight junction proteins [Knudsen and Wheelock, 1992; Hinck et al., 1994; Itoh et al., 1999]. They contain catenins (such as α, β, γ) and cadherins (such as E, N, P) which create a gap of 20nm between cells [Revel and Karnovsky, 1967; Knudsen and Wheelock, 1992]. Desmosomes, below adherens junctions, interlock adjacent cells and provide anchorage for intermediate cytoskeletal filaments which gives tensile strength to the cells [Green and Jones, 1996]. They include proteins such as desmogleins and desmocollins which produce gaps of 25nm [Farquhar and Palade, 1963; Green and Jones, 1996]. Hemidesmosomes

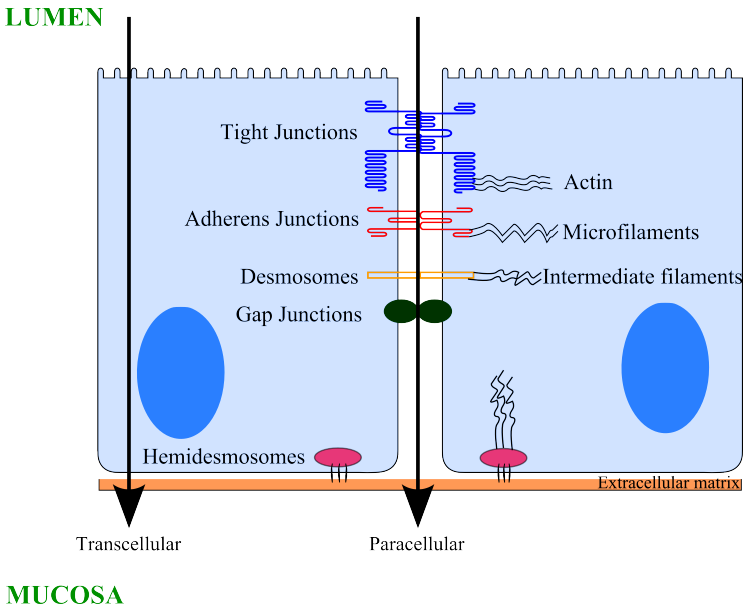

Figure 1.2: Cellular junctions. Cells are held together by tight junctions, adherens junctions, desmosomes and gap junctions, while hemidesomsomes adhere to the extracellular matrix. Water, ions and solutes from the lumen can pass through (transcellular pathway) or between cells (paracellular pathway).

include integrins and laminin-5 which adhere cells to the extracellular matrix (for example collagen, laminin, fibronectin and proteoglycans), and are connected to intermediate filaments of the cytoskeleton [Gagné et al., 2010; Teller and Beaulieu, 2001; Green and Jones, 1996]. Gap junctions act as communication channels and are permeable to molecules smaller than 1kDa which pass between cells via passive diffusion [Kumar and Gilula, 1996; Farquhar and Palade, 1963]. They maintain a distance between cells of 1.5 - 2nm, and are composed of connexins which form complexes with one another to generate a hexamer across the junction, binding through their extracellular loops that contain three conserved cysteine residues [Revel and Karnovsky, 1967; Kumar and Gilula, 1996].

1.2 Tight junction formation and regulation in the small intestine

The paracellular movement of molecules between cells accounts for 85% of all passive migration [Frizzell and Schultz, 1972], allowing molecules of 3.6 - 20Å (but up to 60Å in the crypts of Lieberkühn) to pass through the junctions, which are 10nm wide but spaced 18nm from centre-to-centre [Anderson, 2001; Furuse et al., 1996; Madara and Dharmsathaphorn, 1985; Fihn et al., 2000]. This allows molecules up to 20kDa to pass through the paracellular pathway at bicellular (joining of two

cells) junctions and 10kDa molecules at tricellular (joining of three cells) junctions [Krug et al., 2009]. The reason larger macromolecules cannot flow through the paracellular pathway is because of tight junction complexes found at the apical pole of epithelial cells [Farquhar and Palade, 1963]. Freeze fracture electron microscopy has been used to show that tight junctions appear as a network of anastomosing strands and grooves which form a continuous belt around each cell and restrict the diffusion of water, ions and solutes between cells [Staehelin, 1973]. This is defined as the gate function, with the belt consisting of transmembrane domain-containing proteins which are involved in the direct adhesion to adjacent cells. Cytoplasmic plaque proteins make up the remainder of the tight junction complex and are involved in scaffolding the transmembrane proteins to the actin cytoskeleton and initiating signal transduction pathways. There are over 50 proteins which make up the tight junction complex, of which five are the transmembrane domain proteins occludin, claudins, Junctional Adhesion Molecules (JAM), CoxsackieAdenovirus Receptor (CAR) and Crumbs3. The remaining proteins are referred to as cytoplasmic plaque proteins and include adaptors, regulatory proteins and transcriptional and post-transcriptional regulators.

Another function of tight junctions is to restrict the free flow of molecules within the apical domain (in contact with the gut lumen) from mixing with those from the basolateral domain (in contact with the gut mucosa and connective tissue), and this is defined as the fence function.

1.2.1 Generation of cell polarity

The fence function of tight junction complexes generates ionic and solute gradients across the cell surface which gives rise to cell polarity. Cell polarity is regulated in part by the conserved tight junction proteins Crumbs3 and PARtitioning defective 3 (Par) complexes [Roh et al., 2003]. Crumbs3 is a transmembrane domain protein with epidermal growth factor and laminin repeats which accumulate at the apical domain [Makarova et al., 2003]. Along with Protein Associated with Lin Seven 1 (PALS1), they stabilise the generation of the apical domain [Bachmann et al., 2001; Makarova et al., 2003]. Active Rho-GTPase cdc42 binds to Par6 which in turn increases the affinity of Par6 to bind to atypical protein kinase C (aPKC) [Garrard et al., 2003]. GTPases are enzymes that bind to guanosine triphosphate that have a range of functions including signalling transduction. Calcium is required to activate the adherens junction protein E-cadherin. E-cadherin and β catenin bind to α catenin which links

the adherens junctions to Zonula-Occludens 1 (ZO-1) and occludin complexes at the tight junctions [Müller et al., 2005; Drees et al., 2005]. Junctional adhesion molecule (JAM) and adherens junction protein E-cadherin, are thought to recruit Par3 to the tight junction complex so that it can bind to Par6-aPKC and cdc42 [Kim et al., 2000; Ebnet et al., 2001]. PALS1 recruits the Par6/Par3/aPKC complex to the apical domain [Straight et al., 2004] and interacts with PALS-Associated Tight Junction protein (PATJ) which binds to Zonula-Occludens 3 (ZO-3) [Roh et al., 2003; Lemmers et al., 2004; Roh et al., 2002]. Par3 suppresses the LIM kinase 2-induced phosphorylation of cofilin, an actin-sequestering protein which stabilises actin filaments to facilitate tight junction assembly [Chen and Macara, 2006].

The JAM family of proteins associate with cingulin, probably through the actin cytoskeleton, and binds to ZO-1 through PDZ domains (named after the three proteins originally identified; Post Synaptic Density Protein (PSD95), Drosophila disc large tumour suppressor (DlgA), and Zonula Occludens-1 protein (ZO-1)), and can form homodimers which are thought to play a role in cell-cell adhesion [Martìn-Padura et al., 1998; Ebnet et al., 2000; Bazzoni et al., 2000a,b; Blasig et al., 2006]. CAR also binds to ZO-1 and participates in cell adhesion and regulation of paracellular permeability (Figure 1.3) [Cohen et al., 2001].

Zonula occludens -1, -2 and -3 are central to the tight junction complex as they link the transmembrane proteins to the actin cytoskeleton [Itallie et al., 2009]. They have 3 PDZ domains, a src homology domain, and a guanylate kinase-like homologue domain and are therefore MAGUK proteins (Membrane Associated GUanylate Kinase homologue proteins family). MAGUK proteins have PDZ (PSD95/dIg/ZO-1), SH3 (src homology 3, consensus motive of SH3 domains), GuK (guanylate kinase homologue, sequence homology to the GuK domain in guanylate kinase) domains, acidic and proline rich regions [González-Mariscal et al., 2000]. ZO-1, -2, -3 bind to claudins 1 - 8 via the PDZ domains, which is considered one mechanism by which claudins cluster at the tight junction complex [Itoh et al., 1999]. ZO-1 dimerises through PDZ domains to form homodimers and heterodimers with ZO-2 and ZO-3 [Utepbergenov et al., 2006; Wittchen et al., 1999].

In a ZO-1 knock out epithelial cell line (murine Eph4 mammary cells), Umeda *et al.* 2004, showed that although cells appeared normal in terms of tight junction formation and cell morphology, observed subtle changes between parental cells and ZO-1 $^{-/-}$cells [Umeda et al., 2004]. This in-

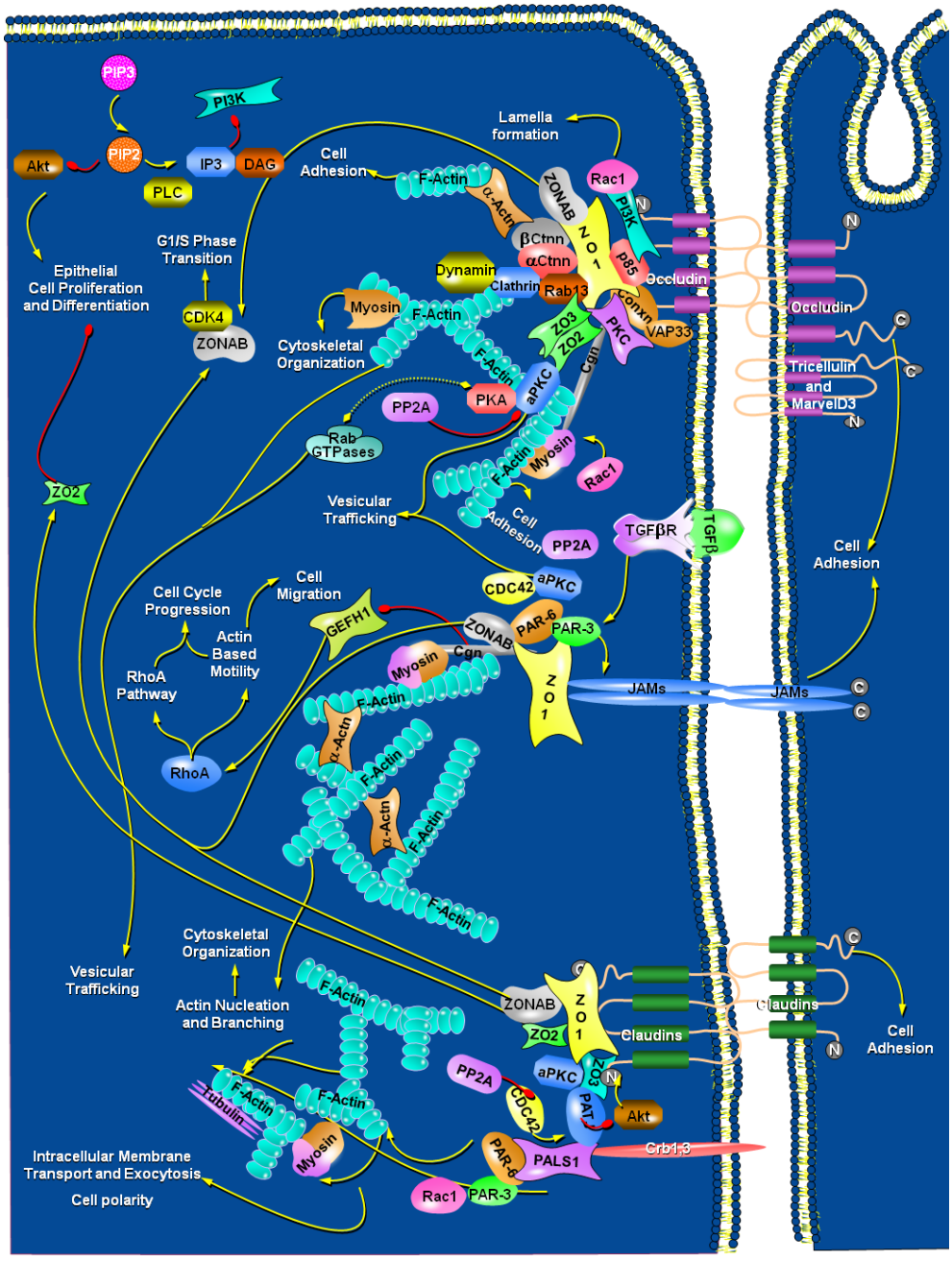

Figure 1.3: Tight junction associated proteins. Interactions between transmembrane and cytoplasmic plaque proteins of the tight junction complex are shown. Yellow lines indicate activation signalling whereas red lines indicate inhibitory signalling cascades. Actn - actinin, Cgn - cingulin, Conxn - connexins, Ctnn - catenin. Image adapted from Epithelial Tight Junctions, Pathway Central, SABiosciences, Qiagen.

cluded the redundant function of ZO-2 which was expressed at higher levels in the ZO-1$^{-/-}$cells, the lack of cingulin at the tight junctions, and the aberrant re-formation of tight junctions [Umeda et al., 2004]. The delayed formation was later identified to be caused by a lack of SH3 domain within ZO-1, showing the importance of MAGUK proteins in tight junction assembly [McNeil et al., 2006].

ZONAB (ZO-1 associated nuclear acid binding) protein is a Y-box transcription factor that normally binds to ZO-1. During cell cycle transitions when ZO-1 expression is low, ZONAB interacts with cell division kinase 4 which initiates S phase of the cell cycle [Balda et al., 2003].

1.2.2 Tight junction assembly and disassembly

Tight junction biogenesis commences in response to a number of intracellular triggers including calcium, kinases, protein phosphorylation, adenosine 3',5'-cyclic monophosphate (cAMP) and phospholipase C [Zhang et al., 2006; Staddon et al., 1995; Ward et al., 2002, 2003]. Tight junction disruption can be induced by calcium, cytokines, phosphatases and pathogens [Nunbhakdi-Craig et al., 2002; Jepson et al., 1995; Al-Sadi and Ma, 2007; Ma et al., 2004; Muza-Moons et al., 2004].

The initiation of tight junction biosynthesis following increases in calcium concentration using the calcium switch model has been widely employed to investigate tight junction assembly and disassembly. In the presence of 1.8mM calcium, tight junctions form and cells polarise and when extracellular calcium is reduced to levels of $\approx$ 5μM, cells become depolarised and loose cell-cell adhesion [Nigam et al., 1992]. This effect can be seen within 15 minutes of calcium withdrawal [Siliciano and Goodenough, 1988; Riesen et al., 2002]. The actin cytoskeleton is also important for generating tight junctions and a stable actin microfilament complex is important for the localisation of tight junction proteins such as occludin, phosphorylation of myosin and activation of PKC [Subramanian et al., 2007; Stuart and Nigam, 1995; Turner et al., 1997; Gonzalez-Mariscal et al., 1985].

Tight junction disassembly can be triggered by a number of events, both as a result of external and internal stimuli often resulting in protein endocytosis [Ivanov et al., 2004; Shen and Turner, 2005]. For example, upon calcium depletion, Rho guanine nucleotide exchange factor-H1 (GEF-H1), disassociates from microtubules and activates Rho associated kinase (ROCK) that leads to acto-myosin contraction via myosin light chain (MLC) phosphorylation and ultimately, a break down in the

tight junction complex [Samarin et al., 2007; Amano et al., 1996].

Tight junctions are dynamic in nature and using fluorescence recovery after photobleaching (FRAP) techniques, Shen *et al.* 2008, were able to show that 70% of occludin and ZO-1, but only 30% of claudin-1, was mobile within the complex [Shen et al., 2008]. This occurred through switching between membrane-associated and intracellular pools of ZO-1 and diffusion of occludin within the membrane [Shen et al., 2008]. This demonstrates that tight junctions are fluid and readily respond to changes in their environment as, for example, occludin proteins can rejoin within one hour [Wong and Gumbiner, 1997]. In the small intestine, the integrity of the barrier during antigen sampling by dendritic cells and lymphocyte migration (called extravasation) is maintained [Rescigno et al., 2001]. This is thought to occur because dendritic cells and intraepithelial lymphocytes express junctional molecules such as occludin, claudin-1, JAM, ZO-1, E-cadherin, β catenin, connexin 26 which may assist in forming new tight junction structures between the epithelial cells [Rescigno et al., 2001; Inagaki-Ohara et al., 2005; Alexander et al., 1998]. Occludin and E-cadherin are constitutively expressed in IELs, and at higher levels in γδ than αβ IELs, with only activated T lymphocytes expressing occludin [Alexander et al., 1998; Inagaki-Ohara et al., 2005]. Lymphocytes and dendritic cells are recruited to sites of infection by cytokines and chemokines secreted from epithelial cells, that can accelerate the rate of tight junction assembly through Adenosine Monophosphate-activated Protein (AMP) kinase activation and localisation of ZO-1 to the membrane complex [Tang et al., 2010a; Rimoldi et al., 2004]. AMP kinase is an ATP sensor molecule and can be triggered by cytokines such as TNFα [Tang et al., 2010a]. Modulation of other immune cells has also been demonstrated whereby JAM and occludin influence the migration of neutrophils between cells so that barrier function is not compromised [Martìn-Padura et al., 1998; Huber et al., 2000].

Cell turnover within the small intestine is of the order of one cell lost per minute [Potten and Loeffler, 1990]. Therefore the integrity of the barrier must remain intact in order to cope with such a fast renewal rate. Studies have shown that tight junction complexes relocate along the surface to maintain the functionality of the barrier by extruding adjacent cells and extending lamellipodia to form tight junctions with neighbouring cells [Madara, 1990; Watson et al., 2005; Matsuda et al., 2004]. Phosphorylated MLC Kinase (MLCK), which is associated with wound healing, was often found at areas of cell shedding [Bullen et al.,

2006]. However, only 9% of extensions have been shown to be positive for ZO-1 and claudins have been shown to internalise during cell movement, which suggests that other mechanisms are at play [Watson et al., 2005]. Watson *et al.* 2009, have identified gaps within the monolayer of the small and large intestines which is filled with an unknown substance that contributes to maintaining the barrier function [Watson et al., 2009].

1.2.3 Methods of determining barrier function

The majority of studies investigating tight junction biology have been performed with Madin-Darby Canine Kidney (MDCK) cells in which after 12 - 15 hours in culture, tight junctions are fully formed [Gonzalez-Mariscal et al., 1985]. There are two strains of MDCK cells which differ in their ionic conductivity, otherwise referred to as TransEpithelial Electrical Resistance (TEER). TEER is used as an indicator of ion selectivity and tight junction integrity and differs between cell types. Whereas the TEER of MDCK I cells can reach 3000 $\Omega.cm^2$, the TEER of MDCK II cells is only 100 $\Omega.cm^2$ [Stevenson et al., 1988]. TEER of T_{84} human colonic carcinoma epithelial cells can reach 1500 $\Omega.cm^2$ (tight monolayers), while murine small intestinal cells m-IC_{cl2} exert a TEER of 120 $\Omega.cm^2$ (leaky monolayers) [Madara and Dharmsathaphorn, 1985; Bens et al., 1996]. TEER within rat jejunum tissue is $\approx$97 $\Omega.cm^2$, and human ileum $\approx$186 $\Omega.cm^2$ [Banks et al., 2005]. TEER can be measured when cells are plated onto permeable supports (Figure 1.4), and when tissues are placed into an Ussing chamber. Both techniques provide a physiological method of introducing molecules, cells, microbes and drugs to the apical and/or basolateral compartments as permeable supports have holes within them to allow cells and other molecules to migrate into the different compartments [Chin et al., 2008; Sakaguchi et al., 2002; Ranaldi et al., 1992; Leonard et al., 2010].

This technique also allows the paracellular permeability of a monolayer to be analysed. Permeability through tight junctions is an indication of pore size and selectivity which is reflected by the degree of leakiness or tightness of a monolayer, with tight junctions being usually cation selective [Madara and Dharmsathaphorn, 1985; Claude and Goodenough, 1973]. Mannitol (182kDa, 3.6Å), inulin (5.2kDa, 11-15Å), and dextran (4 - 40kDa, 14-45Å), are often used to measure permeability. It is generally believed that the expression profiles of claudins control permeability, which is dependent on the type and number of claudins found [Morita et al., 1999].

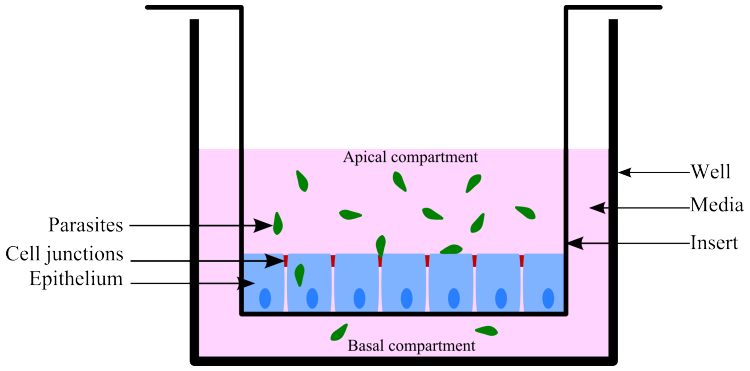

Figure 1.4: Cells grown on inserts can be used to measure TEER and permeability changes following experimental manipulation.

The claudin multigene family consists of over 20 members, which have molecular weights of 18 - 27kDa and span the membrane four times [Morita et al., 1999; Holmes et al., 2006]. They differ in tissue distribution with the number of strands seen by freeze fracture thought to represent the number of claudins present within cells [Sonoda et al., 1999]. Claudin 1 and claudin 2 were shown to induce strand formation in L-transfected cells (derived from stem cells) and claudin 1 can co-localise with occludin to strengthen the stability of the complex [Furuse et al., 1998]. Furuse *et al.* 1998 and 2001, showed that cells expressing claudin 1 exhibited tighter junctional complexes (that is, less leaky to dextran molecules), compared to cells expressing claudin 2, which provides evidence that claudins can dictate the permeability of the monolayer [Furuse et al., 1998, 2001]. Furthermore, the switch from claudin 1 to claudin 2 expression revealed that claudin 2 creates cation permeable channels [Amasheh et al., 2002].

Claudins have two extracellular loops that differ in their C-terminus but always end with a Y-V motif which interacts with PDZ domains of other proteins [Itoh et al., 1999; Morita et al., 1999] and can interact within and between isoforms [Furuse et al., 1999; Itallie et al., 2011]. The first extracellular loop, which contains signature residues W-GLW-C-C, is involved in selective permeability of the tight junctions whereas the second loop contributes to cell-cell adhesion [Anderson and Itallie, 2009; Chiba et al., 2008].

The distribution of claudins varies along the GI tract, along the villus-crypt gradient and within individual cells, which is unlike occludin and JAM proteins that are consistently expressed throughout the intestine [Holmes et al., 2006]. Claudins 2, 3, 7 and 12 are highly expressed in the ileum [Fujita et al., 2006]. Claudin 2 is expressed specifically in the apical domain of crypt and villi cells [Escaffit et al., 2005; Rahner et al.,

2001], claudin 3 and 7 expressed along the crypt-villus axis on all surface domains (especially the basolateral domain for claudin 7), claudin 8 at the basolateral domain, and claudin 12 and 15 on the apical domain of the villus [Fujita et al., 2006]. Claudin 4 is expressed in the dome region of the follicle associated epithelium, and at high levels on the basolateral domains of the villi [Tamagawa et al., 2003; Rahner et al., 2001]. The promoter for the claudin 4 gene is similar to the sucrose isomaltase promoter, (a marker of small intestinal epithelial cell differentiation) [Escaffit et al., 2005]. Claudin 8 expression increases along the intestinal tract, with claudin 15 showing the opposite profile [Holmes et al., 2006]. All these changes are thought to contribute to changes in permeability to different ions and solutes to maximise absorption along the GI tract. This is coupled with a change in pore size along the crypt-villi axis whereby small pores are present in the villus, and larger, but less accessible, ones present nearer the crypts [Fihn et al., 2000].

1.2.4 Diseases associated with tight junctions

Many diseases and disorders have been associated with losses in tight junction proteins and their protein signalling complexes [Furuse, 2009; Takehara et al., 2009]. Claudin 15 deficient mice have enlarged intestines associated with increased villi and decreased ionic conductance [Tamura et al., 2008], while mutations in claudin 16 causes hypomagnesemia hypercalciuria syndrome in humans [Simon et al., 1999]. Some claudins have been associated with carcinogenesis as reviewed by [Turksen and Troy, 2011]. For example, increased expression of claudin 3 and claudin 4 have been detected in human ovarian cancer cells, where they are present in a phosphorylated state [D'Souza et al., 2005, 2007], and claudin 7 mRNA is downregulated in human colorectal carcinogenesis [Bornholdt et al., 2011]. Increased occludin proteosome-mediated degradation has been demonstrated to occur in human irritable bowel syndrome [Coëffier et al., 2010].

Pathogens have been shown to affect epithelial barrier function. For example, reovirus infects the GI tract through M cells, which gives the virus access to the basolateral domain of enterocytes. Here, reovirus binds to JAM and causes signal transduction cascades to induce NFκB activation and apoptosis (as shown using human epithelial cells [Barton et al., 2001]). Another bacteria which infects via the basolateral domain is *Listeria monocytogenes* which infects at the top of intestinal villi, taking advantage of cell shedding events where E-cadherin may be temporarily

exposed to the lumen (as shown using MDCK cells [Pentecost et al., 2006]). Binding to E-cadherin activates tyrosine phosphorylation and ubiquitination of the adherens junction protein, which activates clathrin-mediated endocytosis (as shown using human epithelial cells [Bonazzi et al., 2008]).

IBD is a common disorder of the GI tract affecting 1 - 2 per 1,000 people across North America and Europe [Cosnes et al., 2011]. Two forms of IBD are Crohn's Disease (CD) and Ulcerative Colitis (UC) which affect the GI tract in different ways. CD affects across the entire length of the gut, but especially the terminal ileum, whereas UC affects the rectum and mucosal layers of the intestines resulting in mass inflammation and loss of water and solutes. There are many triggers that can lead to IBD onset which can be both environmental and genetic, with a dysregulation in the immune response to intestinal bacteria also thought to contribute to this phenomenon in humans [Ogura et al., 2001; Frank et al., 2007; Lam, 1993]. Loss of occludin, claudin 5, claudin 8, JAM-A and ZO-1, but enhancement of claudin 2, at the tight junctions has been implicated in barrier dysfunction associated with patients suffering from active IBD [Gassler et al., 2001; Kucharzik et al., 2001; Zeissig et al., 2007; Vetrano et al., 2008]. Claudin 2 upregulation has also been observed in apoptotic cells, indicating a dysregulation of tight junctions which is correlated with decreases in tight junction strands, TEER and increased permeability in active disease [Zeissig et al., 2007; Bojarski et al., 2004]. During inflammation, cytokines are secreted and polymorphonuclear leukocytes are recruited to sites of infection. This process disrupts barrier function resulting in decreased TEER and increased permeability in cultured epithelial cells [Nash et al., 1987]. Permeability increases are thought to be caused in part by the proinflammatory cytokine TNFα which signals through mitogen activated protein kinase (MAPK) to activate NF-$\varkappa$B, which increases the activity of the MLCK promoter that leads to microfilament contraction and inhibition or downregulation of tight junction associated proteins [Patrick et al., 2006; Ma et al., 2004; Boivin et al., 2009; Ye et al., 2006].

1.3 Occludin

1.3.1 Occludin family of proteins

The family of MARVEL (Myelin And lymphocyte and Related proteins for VEsicle trafficking and membrane Link [Sánchez-Pulido et al., 2002]) domain-containing proteins found within tight junctions are MarvelD3, tricellulin and occludin. They have four transmembrane domains with intracellular N- and C- termini and are concentrated in cholesterol-rich domains [Sánchez-Pulido et al., 2002]. The MARVEL domain within the C-terminus of occludin, MarvelD3 and tricellulin is conserved across vertebrate species and the occludin family of proteins are mainly found within epithelium especially the stomach, kidney, liver and lung [Raleigh et al., 2010]. In a comprehensive study, Raleigh *et al.* 2010, showed that MarvelD3, tricellulin and occludin possessed both unique and redundant functions within tight junctions [Raleigh et al., 2010]. Here, they demonstrated that while occludin specifically concentrates at bicellular junctions, tricellulin is normally specific to tricellular junctions and does not co-immunoprecipiate with occludin, whereas MarvelD3 is found at both bicellular and tricellular junctions, and co-immunoprecipitates with tricellulin [Raleigh et al., 2010; Ikenouchi et al., 2008, 2005; Steed et al., 2009]. In addition Raleigh *et al.* 2010 found that upon tight junction formation, occludin trafficked from the cytoplasm to the tight junction complex before MarvelD3 and tricellulin. They also showed that the binding site to cytosolic plaque protein ZO-1 differed between occludin and tricellulin, and that MarvelD3 and tricellulin responded differently to TNFα compared to occludin. This data support the notion of distinct functions of these proteins [Raleigh et al., 2010].

1.3.1.1 MarvelD3

MarvelD3 was identified by Steed *et al.* 2010, as being a 40kDa protein with a shorter C-terminus than tricellulin and occludin, and has two known splice variants which result from translation of either exon 3 or 4 [Steed et al., 2009]. MarvelD3 only appears to be expressed in vertebrates and the isoforms only expressed in mammalian species. The protein is approximately 40% conserved between mammalian species and the function of MarvelD3 is currently unknown.

1.3.1.2 Tricellulin

Tricellulin was originally identified by Ikenouchi *et al.* 2005, and migrates on Sodium Dodecyl Sulfate PolyAcrylamide Gel Electrophoresis (SDS-PAGE) gels as multiple protein bands between 66 - 72kDa suggesting that tricellulin is a phosphoprotein [Ikenouchi et al., 2005]. The protein sequence of tricellulin is relatively conserved between mammalian species (approximately 85% for mammals and 65% for birds and amphibians) and both tricellulin and occludin are found in tandem on murine chromosome 13 and have conserved C termini, suggesting they could have arisen as a result of gene duplication [Ikenouchi et al., 2005]. In contrast to Raleigh *et al.* 2010, Westphal *et al.* 2010, showed that tricellulin forms heteromers with occludin and dimerises with itself [Westphal et al., 2010; Raleigh et al., 2010]. Reasons for these apparent discrepancies could be related to different cell types or methods of immunoprecipitation. Ikenouchi *et al.* 2005, determined that tricellulin plays a role in TEER and permeability regulation and has functions within bicellular junctions as well [Ikenouchi et al., 2005; Krug et al., 2009]. It has been shown that the C-terminus targets tricellulin to bicellular junctions and the N-terminus targets to tricellular junctions during tight junction synthesis [Westphal et al., 2010]. Upon occludin recruitment to the tight junction, tricellulin relocates to tricellular junctions. Furthermore, when occludin expression was suppressed using RNA interference, tricellulin is expressed at bicellular junctions and this partially restores barrier function [Ikenouchi et al., 2008].

Tricellulin deficiency has been associated with loss of hearing in humans and four mutations within the C-terminus have been reported in humans [Riazuddin et al., 2006]. These mutations prevent ZO-1 from binding and are thought to represent crucial interactions to the cytoskeleton within the inner ear.

1.3.1.3 Occludin

Occludin was the first integral membrane protein of the tight junctions to be identified. Originally purified from chick liver by Furuse *et al.* in 1993, occludin is predicted to have four transmembrane domains with two extracellular loops, and an intracellular N- and C-terminus, with a molecular weight of ≈65kDa [Furuse et al., 1993]. The first extracellular loop contains many glycine and tyrosine resides (60%) with the second extracellular loop containing many tyrosine residues (18%) which are

thought to provide flexibility within the extracellular structure of the protein, to allow for dimerisation to occludin on adjacent cells [Itallie and Anderson, 1997; McCaffrey et al., 2008]. Occludin is found in a wide range of species and is highly conserved between canines, murines and humans (90%), but only 50% identical within the chicken and rat-kangeroo species [Ando-Akatsuka et al., 1996]. Occludin is expressed in a wide variety of epithelial tissue including the brain, heart, kidney, testes, stomach, kidney, jejunum, colon, lymph nodes and the lung [Kimura et al., 1997; Raleigh et al., 2010; Muresan et al., 2000].

1.3.2 Occludin variants

To date, three occludin variants have been described. Occludin 1B is found in different mammalian species and derives from the insertion of an exon resulting in translation of a longer protein sequence which migrates on SDS-PAGE gels as a 70kDa band [Muresan et al., 2000]. Differences arise within the N-terminus where the first 17 amino acids are replaced with a 56 amino acid sequence in the isoform. Occludin 1B is expressed alongside occludin and has the same cellular distribution [Muresan et al., 2000].

Occludin $TM4^{-}$ isoform lacks a 162bp sequence encoding the fourth transmembrane domain which causes the C-terminus to become extracellular [Ghassemifar et al., 2002]. This alternative splice variant is present in human and monkey cells but has not been detected in murine or canine cells. This 58kDa isoform is expressed at low levels alongside the 65kDa-occludin and may play a role in sub-confluent monolayers [Ghassemifar et al., 2002]. Confluency refers to the number of cells present, where a confluent monolayer represents 100% cell coverage over the substrate. A similar isoform has also been identified by Mankertz *et al.* 2002, who described both isoforms to be present in the cytoplasm of human cells [Mankertz et al., 2002].

A deletion in exon 9 (encoding a sequence within the C-terminus) represents another occludin splice variant detected in human cells [Gu et al., 2008]. Gu *et al.* 2008, provided evidence to suggest that the sequence within exon 9 is important for activating apoptotic pathways, as the variant isoform was not seen to affect levels of BAX and Bcl-2 genes [Gu et al., 2008]. This isoform prevented occludin from becoming associated with the membrane suggesting that the 44 amino acid sequence within exon 9 directs occludin to the membrane [Gu et al., 2008].

1.3.3 Occludin regulation

1.3.3.1 Promoter

The existence of multiple occludin isoforms led Mankertz *et al.* 2000, 2002, and Gu *et al.* 2008, to investigate the properties of the occludin promoter. They concluded that two promoters exist of which one is silenced by methylation within the CpG island region [Gu et al., 2008; Mankertz et al., 2000, 2002]. CpG islands are common within promoters and represent cytosine-guanine residues held together by phosphodiester bonds [Saxonov et al., 2006]. Epigenetic silencing of occludin was also demonstrated by Osanai *et al.* 2006, who provided evidence that occludin suppression by methylation prevented apoptosis and led to the development of carcinomas [Osanai et al., 2006]. The occludin promoters are also regulated by heat shock factor-1 (HSF-1), TNFα and IFNγ, showing that innate molecules and proinflammatory cytokines directly influence the expression of tight junction proteins and alter the integrity of the epithelial barrier [Mankertz et al., 2000; Dokladny et al., 2008].

1.3.3.2 Ubiquitination

E2 ubiquitin-protein ligase UBC4 and the E3 ubiquitin-protein ligase Itch target occludin for ubiquitination at the N-terminus in sertoli and kidney epithelial cells [Traweger et al., 2002; Lui and Lee, 2005]. Itch is a member of the HECT domain-containing subfamily of E3 ubiquitin-protein ligases that contains WW domains. WW domains represent two conserved tryptophan residues which are approximately 20 - 23 amino acids apart, and bind to proline rich domains [Sudol et al., 1995]. Traweger *et al.* 2002, demonstrated that two of the four WW domains within Itch interact with occludin and that Itch can target both cytoplasmic and membrane bound occludin for degradation [Traweger et al., 2002].

The addition of Vascular Endothelial Growth Factor (VEGF) to cells also induces endocytosis and subsequent ubiquitination of phosphorylated occludin by Itch [Murakami et al., 2009].

E3 ubiquitin-protein ligase Nedd4-2 targets occludin for ubiquitination at the C-terminus in kidney epithelial cells [Raikwar et al., 2010]. It was also found that overexpression of Nedd4-2 resulted in a decrease in TEER and increase in permeability which shows that occludin is involved in the development of tight junction barrier formation in the collecting duct. Similar findings were also described using proteosome inhibitors suggesting that occludin can be regulated by proteosome mediated de-

gradation, which has also been reported for other adhesion proteins such as connexin and β catenin [Raikwar et al., 2010; Traweger et al., 2002; Aberle et al., 1997; Musil et al., 2000]. Changes in phosphorylation status of a protein can change its conformation which induces signals to recruit degradation pathways [Fuchs et al., 1998]. As the function of occludin is heavily dependent on hyperphosphorylation, this may represent an important pathway in the regulation of occludin.

1.3.3.3 Turnover and Recycling

The turnover rate of occludin in gastrointestinal epithelial cells differs between reports, but most describe the half-life of occludin to be between 1.5 - 2 hours, although others estimate 6.5 hours [Traweger et al., 2002; Guo et al., 2005; Raikwar et al., 2010; Marchiando et al., 2010]. Discrepancies could be due to differences in experimental design, although this range is similar to that of connexin [Musil et al., 2000]. The half-life of occludin can be increased by inhibiting proteosome mediated degradation, or decreased by starving cells of polyamines [Guo et al., 2005]. Degradation of occludin has been shown to increase in polyamine deficient cells, where the half-life was reduced to 75 minutes [Guo et al., 2005]. Although the protein levels were altered there were no changes in mRNA levels, implying that regulation of occludin is predominantly at the post-transcriptional level. However, levels of occludin mRNA and other tight junction proteins can be suppressed by the transcriptional repressor Snail [Ohkubo and Ozawa, 2004]. Snail triggers the epithelial-mesenchymal (undifferentiated connective tissue) transition pathway whereby loss of E-cadherin and occludin result in disassembly of junctions to allow for cell movement [Ohkubo and Ozawa, 2004]. The transcription factor Hedgehog, activates Snail, and this pathway has also been implicated in brain tumorigenesis [Chou et al., 2010]. Transforming growth factor β (TGFβ) also induces epithelial-mesenchymal transition and it has been shown that occludin plays a role in recruiting TGFβ to the cell surface [Kojima et al., 2008; Barrios-Rodiles et al., 2005].

Occludin recycling is governed by endocytic pathways. Endocytosis is the process that involves invagination of the plasma membrane to engulf material from the plasma membrane. Tight junction proteins are then trafficked to late endosomes for degradation, or recycling endosomes to be returned to the plasma membrane [Utech et al., 2010]. Endocytosis of occludin can occur by clathrin mediated, caveolin mediated or micropinocytosis pathways.

The Rab family of proteins are small G proteins that are involved in vesicle transport pathways. They act as molecular switches which transition between GDP-GTP bound forms [Terai et al., 2006]. When MICAL-L2 (molecule interacting with CasL-like 2, also known as junctional Rab13-binding protein) binds to the GTP form of Rab13, it causes Rab13 to link to the actin cytoskeleton, becoming one of the cytosolic plaque proteins of the tight junction complex [Terai et al., 2006]. Here, it functions to continuously recycle occludin back to the membrane when occludin is endocytosed from the membrane in a clathrin dependent manner [Morimoto et al., 2005]. During cell polarisation, actinin 4 recruits the MICAL-L2/Rab13 complex to tight junctions and associates it with F-actin [Nakatsuji et al., 2008]. Actinin 4 complexes with clathrin heavy chain and dynamin, which are also part of endocytic pathways [Hara et al., 2007]. Actinin 4 may have protein transport functions both at the membrane and golgi complex, as molecules such as galectin can also be found within actinin 4 transfected cells [Hara et al., 2007]. Pathogens use endocytic pathways as a mechanism of infection and are therefore an important pathway to consider for therapeutic targets [Veiga et al., 2007].

Dynamin is also involved in caveolin-mediated endocytosis of occludin as shown in cells treated with latrunculin A, an inducer of actin depolymersiation [Shen and Turner, 2005]. Endocytosis was seen to occur in a caveolin I and dynamin II dependent mechanism and this was associated with a loss in TEER [Shen and Turner, 2005].

Caveolin mediated endocytosis of occludin can be initiated by myosin light chain kinase (MLCK) activation following TNFα stimulation [Marchiando et al., 2010]. This endocytosis was dependent on dynamin and cholesterol-rich domains. Occludin deficient cells may also have lower levels of caveolin associated with lipid rafts suggesting that occludin may play a role in tight junction remodelling in response to extracellular stimuli [Itallie et al., 2010]. The inhibition of TNFα-induced endocytosis of occludin prevented loss of water from the lumen, providing evidence that occludin has a functional role in maintaining barrier integrity within the GI tract [Marchiando et al., 2010]. NFκB has been shown to lead to TNFα-induced increases in permeability in epithelial cells and has been implicated as a causal factor towards the pathogenesis of IBD [Ma et al., 2004; Tang et al., 2010b]. TNFα leads to activation of PKCα, which in turn phosphorylates p115RhoGEF that activates RhoA-induced increases in occludin phosphorylation and F-actin rearrangements [Samarin et al.,

2007; Peng et al., 2011].

Micropinocytosis has been observed in cells exposed to IFNγ and results in occludin being targeted to recycling endosomes that also contain Rab4, Rab11 and actin coated vacuoles derived from apical plasma membrane [Bruewer et al., 2005; Utech et al., 2005]. This alteration in occludin may be triggered by IFNγ-activation of phosphoinositide 3-kinase (PI3K)/Akt pathways which activates NFκB signalling, and/or through Rho-induced ROCK activation which leads to endocytosis via myosin II-induced contraction [Boivin et al., 2009; Utech et al., 2005; Bruewer et al., 2005]. This, together with TNFα induced endocytosis of occludin, shows that proinflammatory cytokines can affect occludin signalling and molecules responsible for disrupting barrier integrity in the GI tract [Itallie et al., 2010].

1.3.4 Binding partners and functions of occludin

Unlike other tight junction proteins, the function of occludin has not been defined. Numerous studies have shown that occludin has a role in TEER and permeability, but this appears to be cell type and experimental design dependent.

1.3.4.1 Functions of occludin

The potential roles of occludin have been investigated at cellular, tissue, organ and whole organism levels.

Cellular level Occludin has been implicated to be important during the transition of cells as well as cell migration [Du et al., 2010; Ohkubo and Ozawa, 2004]. Occludin was found to be crucial for recruiting the aPKC-Par3/PATJ polarity complex towards the leading edge of migratory cells [Du et al., 2010]. Upon occludin tyrosine phosphorylation p85α, the regulatory subunit of PI3K, is recruited to the migratory cell edge which initiates PI3K and Rac1 activation, and the formation of lamellipodia [Du et al., 2010]. Polyamines are thought to be central for coordinating cell migratory signals and they also affect myosin II distribution [Rao et al., 1999]. Myosin II is located within actin arcs that form within the lamellipodia and may interact with occludin [Burnette et al., 2011]. Lamellipodia are present during the expulsion of cells from the villus tip where the tight junctional barrier must remain intact to prevent opportunistic infection, so proteins such as occludin that are found

at the leading edge are thought to play an important role in this process [Watson et al., 2005; Marchiando et al., 2011]. In a cancerous phenotype, the expression of occludin abolishes cell motility and appears to prevent tumour development and promote apoptosis [Osanai et al., 2006].

In concordance with this theory, cell extrusion following apoptosis can occur as a result of occludin signalling [Beeman et al., 2009; Yu et al., 2005; Osanai et al., 2006]. By overexpressing occludin in cancerous cell lines, Osanai *et al.* 2006, observed increases in apoptotic sensitivity, a process which was not seen when occludin was silenced [Osanai et al., 2006]. The authors demonstrated that a 44 amino acid sequence within the C-terminus of occludin was responsible for these signals. Furthermore, the transcriptional suppression of occludin by Slug has also been attributed to the progression of cancer invasiveness through lack of cell apoptosis [Kurrey et al., 2005]. Together, Slug and Snail induce epithelial-mesenchymal transitions, block the cell cycle and inhibit apoptosis [Vega et al., 2004]. Yu *et al.* 2005, showed that in occludin$^{-/-}$ monolayers, apoptotic cells could not be extruded [Yu et al., 2005]. These cells also failed to generate Rho-GTP. Rho-GTPases are members of the Ras family and are involved in many cell processes including organisation of the actin cytoskeleton and tight junctions [Gopalakrishnan et al., 1998; Samarin et al., 2007]. They switch between GTP-GDP forms via regulation by guanine nucleotide exchange factors and GTPase activating proteins [Benais-Pont et al., 2003]. RhoA signalling increases the levels of occludin phosphorylation and may trigger the assembly and disassembly of tight junctions [Gopalakrishnan et al., 1998; Yamamoto et al., 2008]. Recently, it has been shown that TNFα-induced activation of PKCα phosphorylates p115RhoGEF which activates RhoA [Peng et al., 2011]. This could represent a mechanism by which occludin is affected at the protein level by proinflammatory cytokines.

Tissue level: occludin overexpression Several groups have overexpressed chicken occludin in MDCK II cells and showed that an increase in the number of tight junction strands correlated with an increase of occludin at the surface, and an increased TEER and permeability [Itallie et al., 2010; Balda et al., 1996; McCarthy et al., 1996]. In addition, when chicken occludin was overexpressed in insect cells, multilamellar structures were seen in the cytoplasm [Furuse et al., 1996]. Therefore, occludin was considered to have a functional role in the tight junction complex.

Tissue level: occludin reduction When occludin alleles were made inoperative in murine embryonic stem cells, tight junctions still formed and an effective cell barrier was still evident. This suggests that tight junctions are able to function without occludin, which is probably due to redundant functions among other proteins for example, tricellulin and MarvelD3, that are also associated with the complex [Saitou et al., 1998].

Several groups have reduced occludin levels in MDCK II cells and show different results in terms of TEER and permeability. Reduction of occludin generally had little effect on TEER, but as each study was carried out using different cells, parameters and techniques, this is perhaps not surprising [Itallie et al., 2010; Yu et al., 2005; Balda et al., 2000; Al-Sadi et al., 2011; Huber et al., 2000]. However, changes in permeability were more varied. In the absence of occludin, permeability to non charged solutes or mannitol was not altered compared to parental cells [Itallie et al., 2010; Huber et al., 2000], but there was an increase in permeability toward monovalent organic cations and macromolecular molecules [Yu et al., 2005; Al-Sadi et al., 2011]. When deletions within the extracellular loops (ECLs) were made, occludin no longer associated with the membrane and caused a decrease in permeability to mannitol [Balda et al., 2000]. Although each study was not identical in design or procedure, the results suggest that occludin probably contributes indirectly to permeability and changes seen may be a result of decreased occludin within the tight junctions.

Organ level In occludin deficient mice, tight junction formation appeared normal and other associated proteins were still expressed at the membrane. Within the intestine, TEER was comparable to wild type mice and permeability was not affected [Saitou et al., 2000; Schulzke et al., 2005]. However, there was a lack of parietal cells and loss of acid secretion within the gastric corpus [Saitou et al., 2000; Schulzke et al., 2005]. This has a major impact on the acidity of the mucosa causing hypochlorhydria. Interestingly, Sonic Hedgehog is expressed in the gastric corpus and regulates the secretion of gastric acid in parietal cells [Waghray et al., 2010]. The proinflammatory cytokine IL-1β has been shown to suppress Sonic Hedgehog expression by preventing increases in intracellular calcium levels [Waghray et al., 2010]. IL-1β has also been shown to increase hyperphosphorylation of occludin which suggests that occludin could be upregulated at the tight junctional complex [Yamamoto et al., 2004]. The transcription factors Snail and Slug are induced as downstream targets

of Sonic Hedgehog and as described earlier, they act to repress occludin expression [Li et al., 2006; Fendrich et al., 2007]. This could provide a link between the lack of gastric acid secretion in occludin negative mice as in the presence of IL-1β, Sonic Hedgehog would be inhibited, which may suppress the functions of Snail and Slug to act towards occludin. The increase in hyperphosphorylation could therefore stimulate the release of acid secretion. However, in a different study, IL-1β was shown to decrease occludin expression both at the mRNA and protein level, after 48 hours of exposure [Al-Sadi and Ma, 2007]. Differences could be due to variations in cell type or exposure to IL-1β, but could also indicate activation of different downstream pathways. For example, increased levels of occludin phosphorylation were seen after activation of PI3K, whereas decreases in occludin expression occurred following MLCK-induced NKχB activation [Yamamoto et al., 2004; Al-Sadi et al., 2008].

Whole organism One of the most interesting studies on determining the functions of occludin was conducted by Saitou *et al.* 2000 [Saitou et al., 2000]. The generation of occludin deficient mice revealed a range of phenotypes affecting different organs. For example, calcification of the brain, thinner bones, abnormal striated ducts and testicular atrophy in older mice were observed, which affected overall growth of the mice [Saitou et al., 2000]. Furthermore, males were sterile and occludin deficient females failed to suckle their young [Saitou et al., 2000]. These results demonstrate a role of occludin in development at the whole organism level.

Therefore, occludin plays roles in the initiation of polarisation and differentiation of a monolayer; is a molecule that may be central to repairing damage to the epithelial barrier, initiates signalling cascades in response to internal (expulsion of cells from the villi) and external (pathogenic) stimuli and contributes towards the development and function of organs.

1.3.4.2 Roles and functions of occludin

Many studies have shown that different parts of the occludin protein have different and overlapping functions, and mediate interactions with other molecules (Figure 1.5).

N-terminus Huber *et al.* 2000, demonstrated multiple domains of occludin are necessary for controlling neutrophil transmigration (move-

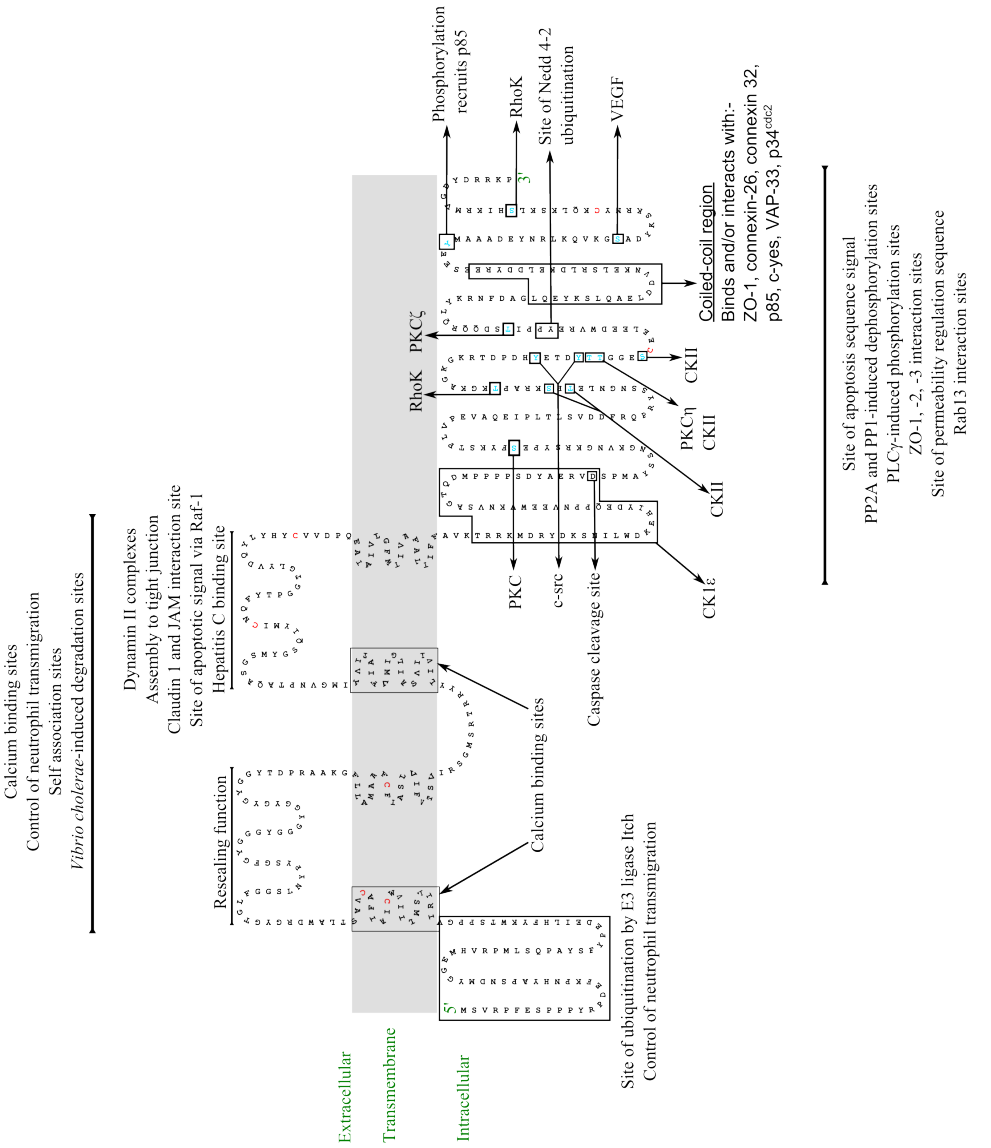

Figure 1.5: Functions, binding partners and kinases/phosphatases associated with occludin. Occludin has intracellular N- and C-termini and two extracellular loops. Cysteine (C) residues shown in red highlight areas where disulphide bonds may contribute to dimerisation and oligomerisation. Serine (S), threonine (T) and tyrosine (Y) residues that have been shown to be phosphorylated/dephosphorylated by kinases/phosphatases are shown in blue.

ment between epithelial cells) [Huber et al., 2000]. Modification within the N-terminus of occludin increases the rate of transmigration of neutrophils without affecting TEER or permeability, while mutations within the first extracellular loop of occludin result in decreased permeability and transmigration of neutrophils [Huber et al., 2000]. Mutations within the C-terminus did not affect neutrophil movement through the paracellular pathway, but did increase TEER and permeability. The authors also suggest that the N-terminus is functionally relevant in maintaining occludin at the tight junction complex.

The transmigration of neutrophils was shown to increase upon exposure to IFNγ [Colgan et al., 1993]. As IFNγ internalises occludin, this could imply that the N-terminus reacts to this proinflammatory cytokine. Consequently, the downregulation of occludin and increased neutrophil transmigration has been associated with the pathology of inflammatory bowel disease [Kucharzik et al., 2001].

Extracellular loops The extracellular loops of occludin are relatively uncharged and have a high tyrosine and glycine residue content that are thought to provide flexibility and an interlocking ability [Gorodeski, 2006; Senes et al., 2001; Aoki et al., 1997]. These loops consist of a helix motif, a calcium binding domain, and a residual loop segment which are hydrophilic in the absence of calcium, and hydrophobic in the presence of calcium [Gorodeski, 2006]. Gorodeski hypothesised that when calcium binds to the extracellular loops, a conformational change may occur which contributes to the sealing of the paracellular pathway [Gorodeski, 2006]. A cell adhesion recognition site has been identified within ECL2 which is considered to aid in cell-cell adhesion [Blaschuk et al., 2002]. Nusrat *et al.* 2005, demonstrated that an ECL2 peptide could form complexes with the surface of T_{84} cells and ECL1 can self-associate within the cell [Nusrat et al., 2005].

The initial observation that occludin could generate adhesive properties in cells that lacked tight junction complexes sparked off investigations into the functional roles of the extracellular loops [Itallie and Anderson, 1997]. The first study to investigate the effects on barrier function of the extracellular loops was carried out by Wong and Gumbiner, 1997 [Wong and Gumbiner, 1997]. They showed that a synthetic ECL2 peptide was responsible for decreasing TEER and increasing permeability of A6 Xenopus kidney cells, and provided evidence to suggest that ECL2 controls the resealing of tight junctions through regulating the turnover

of occludin [Wong and Gumbiner, 1997]. This was achieved without disruption to other tight junction proteins implicating an independent control mechanism of occludin [Wong and Gumbiner, 1997]. In Eph4 mammary epithelial cells, ECL2 peptides also affect cell morphology and β catenin localisation [Vietor et al., 2001]. This suggests that in different cell types, occludin may have different functions.

Other studies have also reported that ECL2 can regulate localisation to the tight junctions using MDCK cells, murine CSG epithelial cells, human T_{84} cells and occludin-null Rat-1 fibroblasts [Medina et al., 2000; Balda et al., 2000; Bamforth et al., 1999; Nusrat et al., 2005]. However, Balda *et al.* 2000, also found that ECL1 was important for occludin incorporation into the plasma membrane, and that both ECL1 and ECL2 mutants prevented interactions with ZO-1 [Balda et al., 2000]. It has been suggested that ECL1 may be more involved in recovery of occludin (recycling) to the tight junctions, following disruption [Lacaz-Vieira et al., 1999]. Discrepancies between studies could be due to the differences in residues that were deleted within the loops, cells used or the type of system employed to introduce the mutated occludin in the cells [Medina et al., 2000]. With a view to generating therapeutic modulation of tight junctions using synthetic peptides to the ECLs of human occludin, Tavelin *et al.* 2003, also found that the N-terminus of ECL1 was more important in controlling permeability [Tavelin et al., 2003].

Overall, these studies show that transmembrane domain proteins and extracellular loops are critical for stabilising occludin in the membrane and contributing to regulating permeability.

Oligomerisation Occludin forms homodimers and oligomers which can reach up to molecular weights of 300kDa [McCaffrey et al., 2007]. Within the transmembrane and extracellular domains, cysteine residues can be found which bind through disulphide links to create dimers and oligomers that function to seal the paracellular pathway [McCaffrey et al., 2008; Walter et al., 2009a]. Disruption of these bonds can cause conformational changes which increases the proportion of occludin associated within higher density membrane domains from lipid rafts [McCaffrey et al., 2008]. McCaffrey *et al.* 2008, 2009, propose that the cysteine residues within ECL2 covalently bind to ECL2 on adjacent cell occludin, the cysteine residues within the first and second transmembrane domains bind occludin within a cell and the two cysteines found in the C-terminus may also bind each other [McCaffrey et al., 2008, 2009;

Walter et al., 2009b]. Within the C-terminus, dimerisation is thought to occur in a coiled-coil domain [Nusrat et al., 2000; Blasig et al., 2006]. The observation that C-terminal-truncated occludin can still be found within the tight junction complex confirms that binding of occludin molecules may occur elsewhere [Matter and Balda, 1998; Chen et al., 1997]. Non-covalent bonds towards the edge of occludin dimers could be available to bind to proteins within the actin cytoskeleton and be subjected to conformational changes that may, for example, result from phosphorylation [McCaffrey et al., 2009]. This provides a mechanism by which occludin molecules can interlock with each other both within the cytoplasm and the external plasma membrane.

C-terminus Upon tight junction formation, occludin trafficks from the cytoplasm to the basolateral domain before complexing with the tight junctions, and this basolateral signal comes from within the C-terminus [Matter and Balda, 1998]. From the lateral membrane, occludin may become associated with cytosolic plaque proteins of the tight junctions such as ZO-1 [Furuse et al., 1994]. Phosphorylation of occludin could also contribute to relocation to the tight junction complex [Sheth et al., 2000].

The crystal structure of the highly conserved distal C-terminus (human residues 416-522) has been solved [Li et al., 2005]. The structure consists of three α-helices which form two anti-parallel coiled-coil loops with an N-terminal loop [Li et al., 2005]. Occludin binds from within the coiled-coil region (murine residues 455-473) of the C-terminus to the SH3-hinge-GuK region of ZO-1 (murine residues 606-618 and 759-766). The binding occurs through helical and ionic interactions and it is predicted that the positive lysine residues on the α-helices of occludin govern the binding to ZO-1 [Schmidt et al., 2004; Li et al., 2005]. It has since been found that α catenin and occludin bind to the same domain within ZO-1 and are predicted to form a four-helix bundle containing occludin or α catenin dimers, with ZO-1 dimers [Müller et al., 2005]. The dimerisation of these proteins was suggested to contribute to the stability of the tight junction complex [Müller et al., 2005]. The mutation of residue serine 490 prevented these interactions which were thought to be because of changes in charge distribution within the coiled-coil region [Sundstrom et al., 2009]. This mechanism could also explain how tight junctions become disrupted.

Li *et al.* 2005, stated that all known protein binding sites of occludin

are within the distal region of the C-terminus of occludin, with all known phosphorylation sites found in the proximal region [Li et al., 2005]. This led them to suggest that the proximal region regulates binding activities within the distal domain [Li et al., 2005].

A number of molecules have been shown to bind within the coiled-coil domain of occludin including cingulin, connexin 26, connexin 32, c-Yes, the regulatory subunit of PI 3-kinase (p85), PKC-ζ and ZO-3 [Nusrat et al., 2000; Kojima et al., 1999; Haskins et al., 1998; Cordenonsi et al., 1999; Sheth et al., 2003; Jain et al., 2011]. Other proteins have been shown to co-localise and bind with occludin via the C-terminus, such as JAM, cingulin, junction enriched associated protein and vesicle-associated protein 33 [Bazzoni et al., 2000b; Cordenonsi et al., 1999; Nishimura et al., 2002; Lapierre et al., 1999]. These co-localisations occur either directly, or indirectly via interactions with ZO-1 [Bazzoni et al., 2000b].

1.3.5 Occludin phosphorylation

Occludin has a lower molecular weight in cells that are non-polarised and non-differentiated (≈65 - 68kDa in MDCK cells), compared to those that are polarised and differentiated where tight junctions have formed (≈70 - 82kDa in MDCK cells) [Wong, 1997; Sakakibara et al., 1997]. This change in molecular weight appears to be due to phosphorylation, indicating that occludin location and functionality depends on its phosphorylation status [Wong, 1997]. Wong 1997, suggested that phosphorylation of occludin may act to stabilise the protein at the tight junctions and allow interactions within the C-terminus [Wong, 1997]. Occludin is phosphorylated on serine and threonine residues at lower molecular weights, but exclusively hyperphosphorylated on serine residues in higher molecular weights [Farshori and Kachar, 1999]. Sakakibara *et al.* 1997, found that these species corresponded to cytoplasmic or basolateral (detergent soluble) and tight junction associated (detergent insoluble) occludin, respectively [Sakakibara et al., 1997].

Murine occludin contains 34 serine/threonine and 17 tyrosine residues within the C-terminus, and to date a number of kinases have been identified which phosphorylate these residues (Figure 1.5).

Casein Kinase 1ε phosphorylates amino acids 265 - 318 of human occludin [McKenzie et al., 2006]. Phosphorylation increased when the last 48 amino acids of occludin were removed from the C-terminus which supports the observation that protein-protein interactions occur in the

distal region and phosphorylation in the proximal region [McKenzie et al., 2006; Li et al., 2005]. Casein Kinase 2 phosphorylates murine residues 328 - 439 with threonine 403 and serine 407 being likely candidates in brain cells [Smales et al., 2003]. In *Xenopus laevis* embryos, Casein Kinase 2 is predicted to phosphorylate threonine 375 and serine 379 [Cordenonsi et al., 1999].

$p34^{cdc2}$ and phospholipase Cγ have also been shown to phosphorylate occludin [Cordenonsi et al., 1999; Ward et al., 2002]. Phospholipase Cγ activates PKC by hydrolysing phosphatidylinositol 4,5-bisphosphate into inositol 1,4,5-triphosphate which increases calcium levels and diacylglycerol (DAG) [Ward et al., 2002]. Other activators of PKC have been shown to phosphorylate occludin such as phorbol 12-myristate 13-acetate and 1,2-dioctanoylglycerol, which phosphorylate occludin at murine residue serine 338 [Andreeva et al., 2001], and PKCη which phosphorylates human residues threonines 403 and 404 [Suzuki et al., 2009]. Here, phosphorylation resulted in localisation at the tight junction complex and increased barrier integrity, but for Phospholipase Cγ hyperphosphorylation was associated with impaired barrier function [Ward et al., 2002]. This suggests that PKC may exert multiple effects on occludin that regulate the protein following different stimuli. Furthermore, the phorbol ester, 12-0-tetraecanoylphorbol-13-acetate, activates PKCα to translocate from the cytoplasm to the tight junction complex, which is associated with a decrease in threonine phosphorylation of occludin [Clarke et al., 2000]. PKCα could inhibit the activity of PKCη, as decreased threonine phosphorylation of occludin was observed following knockdown of PKCη [Suzuki et al., 2009]. Recently, PKCζ has been shown to phosphorylate occludin on threonine residues 424 and 438 which contributes to tight junction assembly in epithelial cells [Jain et al., 2011].

In endothelial cells, VEGF phosphorylates serine residue 490 (human occludin) and causes an increase in permeability within 10 minutes [Sundstrom et al., 2009; Antonetti et al., 1999]. Tyrosine phosphorylation of ZO-1 was also seen when cells were treated with VEGF and lead to the dissociation from occludin. Occludin is trafficked into early and late endosomes and subsequently ubiquitinated by Itch [Murakami et al., 2009].

Tyrosine phosphorylation of occludin has also been studied. For example, it was shown that oxidative stress marker c-src binds to and phosphorylates occludin on human tyrosine residues 398 and 402, preventing occludin from binding to ZO-1, ZO-2 and ZO-3 [Kale et al., 2003; Elias et

al., 2009]. Additionally, p85 interaction with occludin increases following oxidative stress, resulting in increased permeability [Sheth et al., 2003]. Epidermal growth factor prevents the disruption of occludin following oxidative stress induced by hydrogen peroxide, via activation of extracellular signal related kinase which binds to the C-terminus of occludin [Basuroy et al., 2006]. However, tyrosine phosphorylation of occludin has also been implicated in tight junction assembly and barrier function [Chen et al., 2000, 2002a]. This could suggest that tyrosine phosphorylation of occludin has varying functions within different cell types following different stimuli.

Protein phosphatases PP2A and PP1 have been shown to interact directly with the C-terminus of occludin where PP2A dephosphorylates occludin at threonine residues and PP1 at serine residues [Seth et al., 2007]. Na-K-ATPase inhibits the activity of PP2A and prevents dephosphorylation of occludin [Rajasekaran et al., 2007]. Na-K-ATPase also binds to PLCγ1 suggesting that it contributes to occludin regulation. [Rajasekaran et al., 2007]. These findings indicate that threonine and tyrosine phosphorylation are important for occludin assembly at the tight junction complex, and serine phosphorylation is important for the stability and interactions with other proteins at the tight junction complex. Deficiencies in occludin phosphorylation and oligomeric assembly in the blood brain barrier have been suggested to lead to the onset of hypoxia, hyperalgesia and multiple sclerosis as a result of increased barrier permeability [Morgan et al., 2007; McCaffrey et al., 2009, 2008].

1.4 *Toxoplasma gondii*

Toxoplasma gondii (*T. gondii*) was first identified in 1908 in the African rodent *Ctenodoactylus gundi* and has since been found to infect virtually all animals [Sukthana, 2006; Weiss and Dubey, 2009]. It is estimated that over one third of the human population is infected, although prevalence varies between countries [Sukthana, 2006; Weiss and Dubey, 2009]. *T. gondii* is an obligate intracellular parasite of the phylum Apicomplexa which includes *Plasmodium*, *Cryptosporidium*, *Neospora* and *Eimeria*. *T. gondii* has a complex life cycle in which only members of the felidae family can host the sexual phase and release oocysts containing sporozoites into the environment [Hill and Dubey, 2002; Elmore et al., 2010]. There are three dominant clonal lineages of *T. gondii* present in Europe, North America and Africa and are 98 - 99% identical in terms of nucleotide

sequence. These are called Type I (for example RH and GT1), which are highly virulent and migratory in terms of tissue dissemination; Type II (for example ME49) which are less virulent and migratory, but more likely to activate a robust immune response and convert to bradyzoites, and is the most common lineage found in nature; and Type III (for example VEG) which are less virulent than I and II and less migratory [Howe et al., 1997; Velmurugan et al., 2008]. Expansion of the common three dominant lineages coincides with the domestication of the cat and changes in human agricultural practices 10,000 years ago [Su et al., 2003]. Multiple infections of different strains can result in the production of a large number of recombinant and atypical forms, which are highly prevalent in South America where ancient/exotic strains such as COUG, MAS and CAST are also found [Lindström et al., 2008; Dubey et al., 2011; Sibley et al., 2009].

1.4.1 Life cycle

Humans and other animals become infected through congenital transmission, transfusion and transplantation of infected blood and organs, ingestion of contaminated water and undercooked meat containing bradyzoite cysts, the slow replicating form, and ingestion of contaminated soil containing sporozoites (Figure 1.6) [Kijlstra and Jongert, 2008; Derouin et al., 2008].

When individuals of the feline family become infected with *T. gondii,* the bradyzoites or sporozoites are released into the small intestine and multiply by schizogony (multiple nuclei and cytoplasm divisions) to produce merozoites [Dubey et al., 1998]. This is thought to initiate the sexual phase of the life cycle whereby gametogenesis leads to the rupture of infected epithelial cells. The oocysts are shed in the feline faeces and sporulation occurs in the environment within five days [Dubey et al., 1998]. The oocysts can survive and remain highly infectious in the environment for many years [Black and Boothroyd, 2000].

Bradyzoites and sporozoites released from oocysts infect cells in the small intestine where they convert to the fast replicating and highly invasive tachyzoite. Asexual replication takes place by endodyogeny whereby two daughter cells form within one parasite [Sheffield and Melton, 1968]. Tachyzoites disseminate throughout the body and reside in long lasting tissues and organs such as the muscle and brain. Here, due to pressure from the immune system, parasites convert back into the bradyzoite form and remain dormant in cysts which are invisible to immune attack, un-

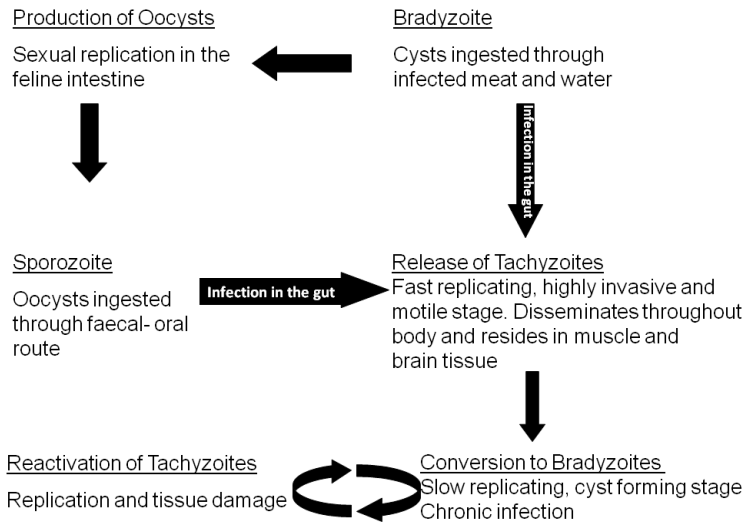

Figure 1.6: The life cycle of *T. gondii*. Sporozoites (generated in the felidae gut) and bradyzoites are ingested by animals. Conversion to tachyzoites leads to activation of the immune system and dissemination throughout the body. Once tachyzoites reach long lasting tissues they convert back to bradyzoites to establish a chronic infection. Reactivation occurs following immune suppression and results in inflammation.

til reactivation [Scharton-Kersten et al., 1996]. Reactivation can occur following host stresses such as illness and causes clinical symptoms such as encephalitis and chorioretinitis. The infection of *T. gondii* occurs at an impressive speed, taking less than 40 seconds to infect a cell in the small intestine, to being present in the lamina propria after one hour, transported to lymph nodes after two hours, conversion to tachyzoites after 18 hours, and reaching the brain within six days of initial contact with the host [Buzoni-Gatel et al., 1999; Courret et al., 2006; Morisaki et al., 1995; Dubey, 1997; Hirai et al., 1966]. Parasites infect towards the distal half of the intestine and only tachyzoites are thought to migrate through the body and infect the brain and muscles, where they convert to bradyzoites and form a non-immunogenic cyst [Dubey, 1998a, 1997].

With the exception of the immunocompromised and pregnant women, *Toxoplasma gondii* causes a relatively asymptomatic infection in humans and animals of typical fever-like symptoms. During pregnancy in mice, T cell responses and levels of IFNγ are suppressed allowing *T. gondii* to take advantage which can result in death of the host following a primary infection [Shirahata et al., 1992]. The parasite can cross the murine placenta and as a result, infect and replicate inside the unborn foetus as the immune system is too immature to respond, causing fatality if a new infection occurs within the first trimester of pregnancy [Roberts and Alexander, 1992]. This congenital transmission is thought to cause the

same pathology in humans as it does in sheep, the latter of which is a large scale problem for farmers in economic terms, as reviewed by Dubey, 2009 [Dubey, 2009].

T. gondii is one of the most common secondary opportunistic infections to occur in immunocompromised people where reduced numbers of T cells results in mass systemic inflammation and pathology [Nissapatorn, 2009]. Reactivation of *T. gondii* from cysts to tachyzoites can also cause loss of vision and fatal encephalitis [Weiss and Dubey, 2009].

In addition, the effects of a chronic infection have been shown to influence behaviour in immunocompetent hosts as infected rats are attracted towards cat odours, and show decreased learning potential and increased levels of dopamine [Stibbs, 1985; Berdoy et al., 2000; Webster, 2001]. Dopamine is an important neurotransmitter for controlling movement, mood, memory and thought, which may explain the changes in conscientiousness, sensitivity and sociability observed in infected individuals [Flegr, 2007]. Studies have shown that infection with *T. gondii* makes humans more susceptible to car accidents probably because of delayed reaction times caused by the altered dopamine levels [Flegr et al., 2002], and might possibly be a causal factor in the onset of Schizophrenia [Yolken et al., 2009].

Interconversion between stages results from changes in temperature, pH, chemical stress and stress from the immune system, and can occur spontaneously [Soête et al., 1994; Jerome et al., 1998]. The surface of *T. gondii* is covered in glycosylphosphatidylinositol (GPI)-anchored proteins which include surface antigen (SAG) 1, and SAG1-related sequences [Manger et al., 1998]. SAG1 is the most abundant protein in tachyzoites and contains 12 conserved cysteine residues that are thought to maintain secondary structure [Burg et al., 1988; Manger et al., 1998]. SAG1 is thought to contribute to virulence as the virulent RH strain expresses fours times the mRNA levels compared to the avirulent NTE strain [Windeck and Gross, 1996]. Furthermore, SAG1 antibodies prevent invasion in different cell types indicating its importance in adherence to the cell surface [Mineo et al., 1993]. Tachyzoites and bradyzoites both express SAG3 and dense granule proteins 1 - 7 whereas bradyzoites exclusively express the SAG1-related sequence bradyzoite specific recombinant 4, and bradyzoite antigen 1 (BAG1), which has homology to small heat shock proteins (HSP) [Manger et al., 1998].

Morphologically, tachyzoites and bradyzoites look similar although tachyzoites have a central nuclei, few microneme proteins and rhoptry

proteins, but numerous dense granules (secreted from specialised organelles from the apical cytoplasmic complex), whereas bradyzoites have a basally located nucleus, many microneme and rhoptry proteins, but few dense granules [Dubey et al., 1998].

1.4.2 Invasion strategies of *T. gondii*

Individual *T. gondii* parasites either infect enterocytes of the small intestine, or migrate between them. To date, it is not known whether parasites that infect enterocytes can exit through the basal domain before replication occurs although invasion of cells decreases once they become polarised, suggesting that receptors for invasion are located on the lateral or basal domains [Velge-Roussel et al., 2001]. Parasites that move between cells have been shown to do so without affecting the integrity of the monolayer, but upregulate adhesion proteins such as intercellular adhesion molecule-1 (ICAM-1) [Barragan et al., 2005]. Additionally, migration occurs more in Type I strains than Type II and III, which is one factor used to define virulence [Barragan and Sibley, 2002]. It is probable that given Type I can survive outside cells longer than Type II or III, these parasites are capable of migrating between cells independently, as well as in immune cells [Saeij et al., 2005; Aliberti et al., 2003].

T. gondii preferentially attaches and invades enterocytes within the villi of the small intestine that are in mid-S phase of the cell cycle, during the upregulation of surface receptors [Dubey et al., 1998; Grimwood et al., 1996]. It has also been shown that *T. gondii* influences the cell cycle to remain in S phase by deregulating molecules such as cyclin E1, cyclin dependent kinase 4 (CDK4) and CDK6 [Molestina et al., 2008]. Once inside the cells, parasites remain below the cell surface above the nucleus within a parasitophorous vacuole, and may replicate six hours after infection [Woodmansee, 2003; Jerome et al., 1998; Sasono and Smith, 1998].

1.4.2.1 Attachment and parasite movement

To date, only a few cell surface receptors involved in *T. gondii* invasion have been identified. For example, it has been shown that *T. gondii* can attach via GPI-anchored proteins such as SAG1, to host glucosamine receptors [Mineo et al., 1993], and via laminin binding to β1 integrin receptor α6β1 on host macrophage, fibroblasts and ovarian cells [Furtado et al., 1992b,a]. GPIs from *T. gondii* can also bind to galectin-like mo-

lecules on the cells surface [Debierre-Grockiego et al., 2010]. Galectins are involved in the formation of the microneme MIC1-MIC6 protein complex which is secreted during infection [Saouros et al., 2005]. Sulfated glycosaminoglycans (GAGs) also mediate binding to host cells as demonstrated by the addition of soluble GAGs (heparin, heparin sulfate and chondroitin sulfate A), GAG deficient cells and enzymatic treatment of GAGs [Carruthers et al., 2000]. These treatments resulted in decreased binding, attachment and parasite motility and showed that GAGs (in particular O-sulfated GAGs), which are expressed on many cells, represent one class of receptors that *T. gondii* targets for invasion [Carruthers et al., 2000]. SAG3 mediates binding to heparin sulfated proteoglycans [Jacquet et al., 2001], and sialic acid residues on host cells may also be important for parasite binding and invasion [Monteiro et al., 1998].

Following attachment, the parasite reorientates itself so that the apical cytoskeletal complex (which is made of a tubulin polymer and called a conoid) is in contact with the host membrane (Figure 1.7) [Carruthers and Boothroyd, 2007; Hu et al., 2002]. The parasite moves into the cell by conoid extension in an anterior to posterior fashion using an actin-myosin motor (gliding motility) [Håkansson et al., 1999; Pezzella-D'Alessandro et al., 2001; Dobrowolski and Sibley, 1996; Dobrowolski et al., 1997; Hirai et al., 1966]. Gliding motility includes three forms of movement; circular gliding, describing an anti-clockwise movement of the parasite from a fixed point; helical gliding, describing rotation along a longitudinal axis when the parasite is horizontal which results in a flipping movement; and twirling, where the parasite is vertical and rotates around a fixed point at one end [Hirai et al., 1966; Håkansson et al., 1999].

Actin polymerisation is essential for parasite motility to occur and actin filaments must be expressed in a polarised manner to initiate directed gliding motility into cells [Wetzel et al., 2003]. Actin polymerisation within the host may also assist in internalisation and establishment of the moving junction during invasion [Gonzalez et al., 2009]. Myosin light chain kinase induces the contraction of myosin through calmodulin-dependent increases in calcium levels within the parasite, and to initiate microneme binding [Pezzella-D'Alessandro et al., 2001]. This process shows that active penetration of the parasite is required for invasion to occur and is different to phagocytosis as no membrane ruffling occurs. In addition, microfilaments are not reorganised during active penetration, the opposite of which is true during phagocytosis [Hirai et al., 1966; Morisaki et al., 1995]. Butcher and Denkers, 2002, also demonstrated

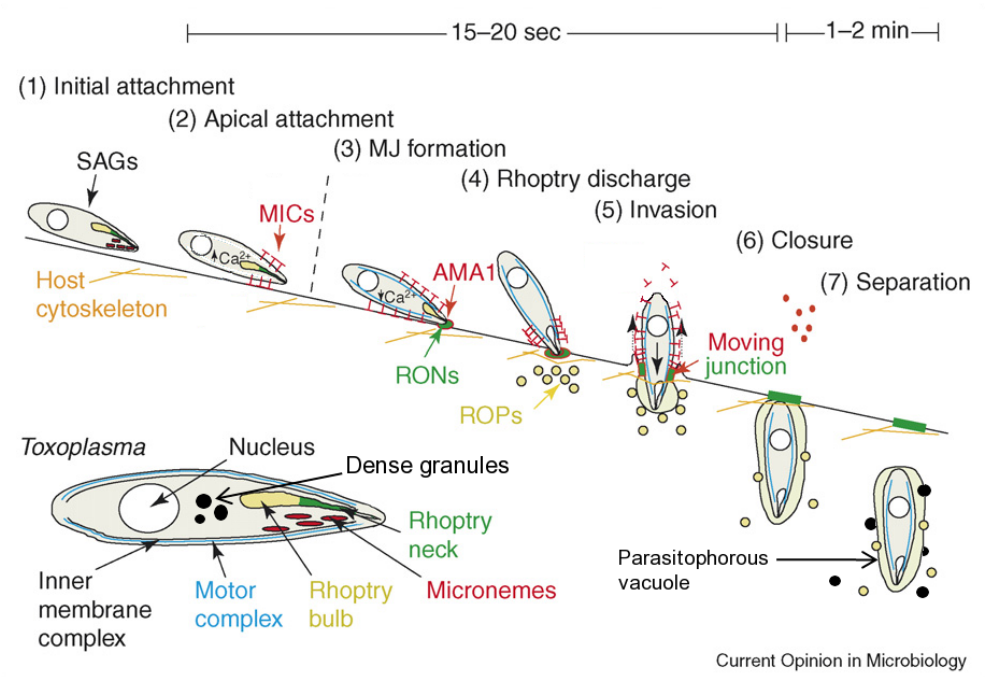

Figure 1.7: Invasion process of *T. gondii*. (1) Following initial engagement with the cell surface through molecules such as SAG1, parasites reorientate and attach (2). As invasion commences, microneme proteins are secreted and a moving junction forms to stabilise interactions between the parasite and cell (3). Rhoptries (green) are secreted from the parasite during penetration which locate on the parasitophorous vacuole, or are secreted into the host cytoplasm (4, 5). Internalisation of the parasite (6) leads to completion of the parasitophorous vacuole and dense granule proteins are secreted that maintain parasite growth and replication within the cell (7). The apical complex containing micronemes, rhoptries, dense granules and the motor complex is depicted in the bottom left corner. Figure taken from Carruthers and Boothroyd, 2007 [Carruthers and Boothroyd, 2007].

that active penetration is necessary to induce an immune response by macrophages, providing further evidence that invasion is an active process instigated by live parasites [Butcher and Denkers, 2002]. Although *T. gondii* actively invades cells, host dynamin (a GTPase involved in vesicle transport), endocytosis pathways and membrane tubule formation are also necessary for the parasite to internalise, as inhibition of Dynasore-treated cells prevents invasion by 80% [Caldas et al., 2009].

1.4.2.2 Invasion

Micronemes Following increases in parasite intracellular calcium, microneme proteins such as apical membrane antigen 1 (AMA1) are secreted from the apical complex which aid in attachment to the host membrane [Alexander et al., 2005; Lovett and Sibley, 2003; Carruthers and Sibley, 1999]. Impairment of AMA1 signalling causes decreased invasion, providing evidence that these molecules are important for host-parasite cell surface interactions [Alexander et al., 2005]. Microneme proteins are homologues of vertebrate adhesive proteins and contain thrombospondin type I repeats, integrin-like domains, epidermal growth factor-like domains and lectin-like domains suggesting they bind to cell surface receptors [Meissner et al., 2002; Saouros et al., 2005; Fourmaux et al., 1996; Wan et al., 1997]. Microneme proteins such as the MIC2-M2AP complex, are involved in invasion and motility and directly participate in host cell binding. MIC2 has been shown to immunoprecipitate with ICAM-1, possibly indicating transmigration could occur following this interaction [Barragan et al., 2005; Huynh et al., 2003]. MIC6 and MIC8 act as escorts for other MIC protein complexes [Meissner et al., 2002] through binding to cytoskeletal molecules such as adolase, to provide a gateway between the actin-mysoin motor and the cell surface [Zheng et al., 2009]. MIC4 is complexed with MIC1 and MIC6, and contains cysteine residues that form disulphide bonds within six conserved apple domains [Brecht et al., 2001]. Binding to cells indicates that MIC1 and MIC4 proteins act as a bridge between the parasite and host cells [Brecht et al., 2001; Fourmaux et al., 1996].

Rhoptries Rhoptry proteins derive either from the neck (RON) or the bulbous (ROP) part of the rhoptries, and are another type of specialised organelle containing approximately 40 proteins [Bradley et al., 2005]. AMA1 complexes with rhoptry neck proteins RON2, RON4 and Ts4705, and RON2 attaches to the moving junction via AMA1 [Lamarque et al.,

2011]. This complex binds and integrates with the host membrane and thereby providing a gateway for secreted RON4, RON5 and RON8 to commence formation of the parasitophorous vacuole, progressively eliminating host proteins from the invaginated surface [Alexander et al., 2005; Straub et al., 2009; Lamarque et al., 2011]. RON8 also adheres to an as yet unidentified cell cytoskeletal molecule [Straub et al., 2009]. Straub *et al*, 2011 recently demonstrated that RON8 contributes to virulence and is required for attachment and invasion as deficient parasites were less able to do so, in addition to not binding the cell cytoskeletal molecules [Straub et al., 2011].

ROP18 is associated with the PPV, has active serine/threonine kinase activity and is involved in controlling parasite replication [Hajj et al., 2007]. ROP18 shows high sequence divergence between strains which correlates to high Type I virulence [Taylor et al., 2006]. RON16 is also a serine/threonine kinase that enters the cell nucleus where it induces variable levels of IL-12 secretion from macrophages, depending on the strain of *T. gondii* [Saeij et al., 2007]. Rab11 and Toxophilin have also been identified to be rhoptry proteins [Bradley et al., 2005]. Rab11 controls cholesterol recycling while Toxophilin binds to parasite G-actin and may play a role in assisting the actin-myosin motor during invasion [Hölttä-Vuori et al., 2002; Poupel et al., 2000]. Parasite protein phosphatases have been identified that translocate to the cell nucleus upon infection to act on rhoptry proteins or host proteins [Gilbert et al., 2007; Jan et al., 2009; Delorme et al., 2002]. This suggests that phosphorylation and dephosphorylation events are important during invasion and growth of *T. gondii* inside cells [Jan et al., 2009].

Dense Granules Rhoptry proteins associate with dense granule proteins which play a role in maintaining the parasitophorous vacuole for intracellular parasite replication [Nam, 2009]. For example, RON2 and RON4 are present with dense granule protein GRA 7, which is involved in parasite nutrient acquisition, and is essential for lipid-microtubule formation around the PPV [Coppens et al., 2006; Dunn et al., 2008].

Moving junction and formation of the Parasitophorous Vacuole The enclosure of the moving junction correlates with a change in conductance within the host cell but without altering the integrity of the membrane [Suss-Toby et al., 1996]. The parasitophorous vacuole (PPV) derives initially from host cell membrane invagination as part of

the moving junction that forms during invasion, and remains connected to the host via fibrous and tubular material which is used as a gateway for accessing host cell nutrients [Schatten and Ris, 2004]. The vacuole membrane contains parasite derived molecules such as dense granule proteins, rhoptries, ubiquitin ligases, kinases and superoxide dismutases, and is permeable to molecules up to ≈1.9kDa [Martin et al., 2007; Schwab et al., 1994; Pacheco-Soares and Souza, 1998]. Host GPI-anchored proteins and cholesterol are present but host transmembrane proteins and protein complexes are thought to be excluded over time so that the vacuole remains undetected by phagosomes, lysosomes and the immune system [Mordue et al., 1999; Straub et al., 2009]. The PPV induces alterations in the host cytoskeleton through microtubule rearrangements, which are involved in intracellular vesicle trafficking, and associates with γ-tubulin and intermediate filaments such as vimentin [Walker et al., 2008; Halonen and Weidner, 1994].

Egression Following invasion, *T. gondii* prevents cells from undergoing apoptosis by inhibiting the production of reactive oxygen species and pro-apoptotic molecules such as Bas and caspases, by blocking p38 MAPK pathways and enhancing anti-apoptotic molecules such as Bcl2 [Choi et al., 2011]. However, decreases in host cell potassium levels, or increased death receptor ligation due to cell stresses such as nutrient depletion or irreversible cell expansion, can cause *T. gondii* to increase calcium levels via activation of Phospholipase C [Moudy et al., 2001]. Parasites then secrete perforin-like proteins in a calcium dependent manner, which creates pores in the membrane and releases them from the PPV and the cell [Kafsack et al., 2009; Persson et al., 2007].

1.4.3 Immune responses to *T. gondii*

Upon exposure to *T. gondii*, intestinal epithelial cells, intraepithelial lymphocytes, natural killer cells, macrophages and dendritic cells all respond to and activate immune responses towards the parasite, which is crucial in controlling the outcome of infection [Ronet et al., 2005; Buzoni-Gatel et al., 2001, 1999; Ju et al., 2009; Hou et al., 2011; Lepage et al., 1998]. The SAG1 protein on tachyzoites has been shown to be largely responsible for generating a robust immune response, although dense granule protein GRA15 can also activate the immune system via NFκB in Type II parasites, illustrating that multiple molecules are probably involved in the immune response to *T. gondii* infection [Rachinel et al.,

2004; Rosowski et al., 2011].

T. gondii is recognised by TLR2 and TLR9 expressed on epithelial and immune cells, and the TLR11-UNC93B1 protein complex expressed by dendritic cells (not present in humans), which binds to parasite actin-binding protein profilin (Figure 1.8) [Yarovinsky et al., 2005; Pifer et al., 2011; Minns et al., 2006; Ju et al., 2009; Mun et al., 2003]. These TLRs activate myeloid differentiation factor 88-induced secretion of T_H1 proinflammatory cytokines such as IL-1, IL-8, IL-12, IL-18 and IFNγ, of which the early secretion of IL-12 from dendritic cells plays a critical role in controlling gastrointestinal pathology caused by *T. gondii* [Hou et al., 2011; Ju et al., 2009]. Within 30 minutes of infection, IFN-inducible GTPases (also termed immunity-related GTPases or IRGs) act upon the PPV to create pores within the membrane, resulting in both parasite death and cell necrosis [Zhao et al., 2009]. However, as IRGs are not present in humans, other mechanisms to kill intracellular parasites are employed which include IFNγ-induced production of nitric oxide, reactive oxygen species and tryptophan degradation, that inhibits parasite growth within macrophages and activates stage conversion [Pfefferkorn, 1984; Bohne et al., 1994]. However, ROP18 can bind to IRGs to prevent destruction and promote survival within macrophages [Fentress et al., 2010]. In addition, *T. gondii* has been shown to inhibit the production of proinflammatory cytokines and nitric oxide in macrophages by preventing translocation of NF-$\varkappa$B to the nucleus [Butcher et al., 2001; Guillermo and DaMatta, 2004]. Nod2 signalling is also required to prompt an efficient T cell response against *T. gondii,* as deficient mice are unable to produce sufficient levels of IL-2 that drives T cell expansion [Shaw et al., 2009].

Infected epithelial cells activate MAPK and NF$\varkappa$B signalling pathways and secrete cytokines and chemokines such as Macrophage Inhibitory Protein (MIP) -1α and MIP-1β, IL-8, and monocyte chemoattractant protein-1 (MCP-1) which recruit IELs, neutrophils and macrophages, respectively [Denney et al., 1999; Ju et al., 2009; Luangsay et al., 2003; Mennechet et al., 2002]. This recruitment is essential in preventing a high parasite burden, as for example, mice that are deficient in IL-17 are more susceptible to infection than wild type mice due to a lack of neutrophil activation from natural killer cells [Passos et al., 2010; Kelly et al., 2005].

Neutrophils secrete soluble factors such as chemokine ligand 5 (CCL5), IL-12 and TNFα which attract natural killer cells and activate dendritic cells and IELs [Bennouna et al., 2003; Khan et al., 2006; Luangsay et

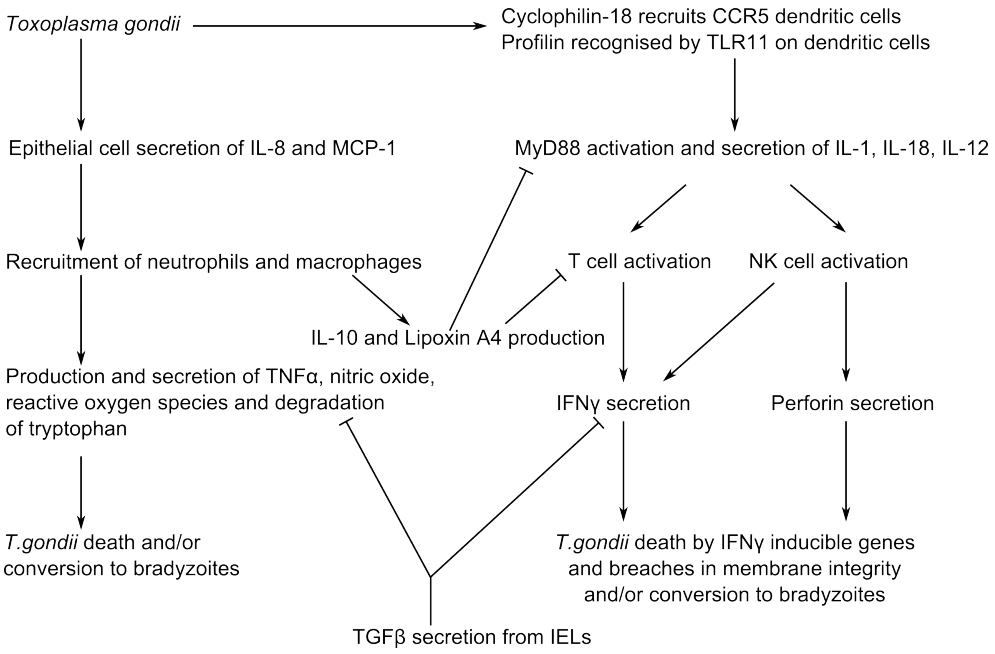

Figure 1.8: Immune response initiated by infection with *T. gondii*. *T. gondii* stimulates the recruitment of dendritic cells by the expression of cyclophilin-18 and activates cells through TLR11. This drives the production of proinflammatory cytokines such as IL-12 which recruit T cells and activate them to produce IFNγ. IFNγ leads to parasite death or stage conversion. Epithelial cells also respond to the parasites by secretion of chemoattractants which recruit neutrophils, natural killer (NK) cells and macrophages to sites of infection. Production of cytotoxic products drives the clearance of parasites and infected cells, but increases the probability of stage conversion. IELs, macrophages and dendritic cells also suppress the immune response to decrease pathology within the host, by secreting anti-inflammatory molecules such as IL-10, TGFβ and Lipoxin A4.

al., 2003]. Binding of CCL5 to its receptor on dendritic cells and natural killer cells triggers the production of perforin which kills parasites, but also IL-12 which regulates the secretion of IFNγ that is necessary for the activation of antigen-specific and cytotoxic T cells [Yarovinsky et al., 2008; Guan et al., 2007; Parker et al., 1991]. Infected dendritic cells can also present *T. gondii* antigen through MHC class I to recruit cytotoxic T cells [Gubbels et al., 2005]. The production of IL-7 and IL-15 from T cells and epithelial cells drives the expansion and survival of $CD8^{+}$and γδ T cells, that also results in increased IFNγ levels [Lee et al., 1999; Bhadra et al., 2010]. Additionally, IL-7 and IL-15 have been shown to upregulate anti-apoptotic protein Bcl2 [Bhadra et al., 2010]. Translocation of NFκB to the nucleus enhances anti-apoptotic molecules and is a mechanism that *T. gondii* employs to promote survival within the cell, as IκB, the inhibitory subunit of NFκB, becomes associated with the PPV following infection [Molestina et al., 2003].

The production of IFNγ is critical in controlling parasite burden as studies have shown that without IFNγ, the host is unable to survive an acute infection [Scharton-Kersten et al., 1996]. IFNγ induces the conversion of tachyzoites into bradyzoites, preventing the parasite being targeted by the immune system and thereby establishing the chronic phase of infection [Scharton-Kersten et al., 1996; Bohne et al., 1993].

Parasitic cyclophilin-18 is a mimetic of CCL5 and also binds to its receptor on dendritic cells, recruiting them to sites of infection, and then using them in a trojan horse mechanism to disseminate out of the gut into lymph nodes [Aliberti et al., 2003]. Furthermore, it has been shown that *T. gondii* preferentially invades immature dendritic cells and that infected dendritic cells migrate into lymph nodes at a faster rate than non-infected cells [Lambert et al., 2006; McKee et al., 2004]. This increased migratory capacity is strain dependent, favouring type II and type III lineages over type I which migrate in an extracellular manner via virulence factors [Lambert et al., 2009]. In a similar trojan horse mechanism, NK cells kill infected dendritic cells by releasing substances such as perforin, but *T. gondii* can use this process to then infect NK cells and evade the immune system [Persson et al., 2009].

IELs also play an important role during *T. gondii* infection as they have been shown to be both destructive (cells positive for MCP-1 receptor) and protective (TGFβ secreting cells) depending on whether parasitic load is high or low, respectively [Egan et al., 2009, 2005; Buzoni-Gatel et al., 2001, 1997]. Up-regulation of the anti-inflammatory molecule

lipoxin A_4 by *T. gondii* also suppresses the production of dendritic cell-induced IL-12 and slows down the immune response [Aliberti et al., 2002]. Dendritic cells from mesenteric lymph nodes, primed with *T. gondii* antigens, also suppress the immune response by the production of TGFβ, IL-10 and IgA [Dimier-Poisson et al., 2003]. γδ IELs protect the epithelium barrier by preventing the redistribution of tight junction proteins and changes in occludin phosphorylation, decreasing parasite transmigration and are involved in establishing long term immunity to *T. gondii* infection [Buzoni-Gatel et al., 1997; Lepage et al., 1998; Dalton et al., 2006]. IELs expressing TCR-Vγ7$^+$appear to be responsible for controlling infection within the small intestine and TCR-Vγ1$^+$IELs for controlling systemic infection to eliminate infected immune cells that have disseminated out of the GI tract [Egan et al., 2005; Dalton et al., 2006].

1.4.4 Therapies for treatment and prevention of Toxoplasmosis

Drugs used for the treatment of Toxoplasmosis include Spiramycin which is used during pregnancy for the reduction of congenital transmission, and Pyrimethamine and Sulfadiazine (with Folinic acid) to prevent nucleic acid synthesis, but are often associated with adverse side effects and are therefore not a long term solution for the control, or indeed prevention, of *T. gondii* infection. Molecules up-regulated upon bradyzoite conversion, such as heat shock proteins have also been targeted for drug development, and the antibiotic geldanamycin has been shown to prevent stage conversion via inhibition of ATP binding to HSP90 [Bedin et al., 2004]. HSP90 is a heat shock protein and chaperone implicated in assisting protein folding and assembly of other molecules important for invasion [Ahn et al., 2003; Echeverria et al., 2005].

The most efficient method to prevent Toxoplasmosis is to vaccinate against it and stimulate cell-mediated immune responses. However, to date there are no human vaccines for *T. gondii*, although there is one commercially available live vaccine, Toxovax, for administration in sheep to prevent congenital toxoplasmosis [Buxton and Innes, 1995], and one experimental live vaccine aimed at reducing oocyst shedding in cats as the T-263 strain used is unable to produce oocysts [Frenkel et al., 1991]. Toxovax uses the S48 strain which has naturally lost its ability to convert into bradyzoites and undergo the sexual stage of the life cycle in feline species [Buxton and Innes, 1995]. If these options were to be practiced on a large scale across countries, this would undoubtedly reduce the prevalence of Toxoplasmosis in all humans and animals.

However, live vaccines carry the risk of reverting into a virulent form and so the production of dead or knock out strains such as the type II KU80 strain with a knock out of the gene encoding de novo pyrimidine synthesis pathway, created by Fox and Bzik, are also being investigated for their efficiency as vaccines [Fox et al., 2011; Mévélec et al., 2010].

Research into DNA vaccines can also provide a high level of stimulation for cell-mediated immune responses and efforts have focused on using surface antigens, microneme, rhoptry, and dense granule proteins as targets in the presence of adjuvants [Martin et al., 2004; Petersen et al., 1998; Ismael et al., 2003; Huynh and Carruthers, 2006; Bhopale, 2003]. For example, combinations of microneme proteins MIC1 and MIC4, or MIC3 used to immunize mice were found to generate high levels of IgG specific antibodies, increase IFNγ and IL-10 production, prolong host survival and decrease parasite burden in the brain [Lourenço et al., 2006; Ismael et al., 2003]. The virulence factor ROP16, was shown to trigger a strong immune response in mice following intramuscular injection and improved the life expectancy of infected individuals [Yuan et al., 2011] and a cocktail of GRA1 - GRA7 generated proliferation of lymphocytes and IFNγ production in pigs that were intradermally immunised [Jongert et al., 2008].

Non-therapeutic solutions to decreasing the prevalence of *T. gondii* within the human population include simple awareness of transmission routes and hygiene techniques which will prevent individuals becoming infected. Such examples include thorough cooking of meats, washing raw vegetables before eating, washing hands after the preparation of food and after gardening.

1.5 Rationale

T. gondii is a parasite found within all mammals and birds worldwide that can result in the fatality of immunocompromised people and unborn foetuses. The parasite causes chronic infections by residing in long lived tissues such as muscle and the brain where it can alter the behaviour and perception levels of infected individuals, and be a causal factor for the onset of psychological disorders such as Schizophrenia [Lafferty, 2006; Yolken et al., 2009]. Furthermore, the financial burden that *T. gondii* infection exerts within the farming industry due to the death of lambs caused by congenital toxoplasmosis, means that research into prevention is necessary.

This requires detailed understanding of mechanisms and pathways of host invasion by *T. gondii* to prevent chronic infection. *T. gondii* normally enters the host through contaminated meat and water consumption. Consequently, the gastrointestinal tract is the point of initial contact between the host and parasite. Mechanisms of invasion through the GI tract are currently unknown, although studies suggest that the paracellular pathway is important for parasite dissemination [Barragan et al., 2005]. Therefore, investigations into the effects on tight junctions following exposure to *T. gondii* in small intestinal epithelial cells is examined in this thesis. Findings may contribute to a further understanding of tight junction regulation and identify novel molecules involved in maintaining the integrity of gastrointestinal epithelial cell barriers, as well as identify parasite-derived molecules important during *T. gondii* infection in the small intestine.

1.6 Hypothesis

In small intestinal epithelial cells, occludin plays an important role in the invasion and transmigration of *T. gondii.*

1.7 Aims

1. To establish an *in vitro* system to investigate changes within barrier function and tight junction complexes.

2. To define *T. gondii* infection in small intestinal epithelial cells in terms of barrier function and tight junction complexes, and further investigate the effects on occludin [Dalton et al., 2006].

3. To determine if *T. gondii* can directly interact with occludin and suggest candidate pathogen-associated molecules.

4. To identify regulators of occludin following *T. gondii* infection.

All experiments (with the exception of one) were performed using tachyzoites. This life stage was used as it is the invasive form of the parasite which disseminates throughout the body to infect multiple tissues. In this thesis the findings could be transferable to more relevant cell types such as infection of the brain. However, it must be noted that the bradyzoites and sporozoites are the infective forms of the parasite which invade the GI tract. Therefore, caution should be taken in the interpretation of these results although an individual experiment was carried out using bradyzoites which resulted in similar, but not identical, findings.

Chapter 2

Materials and Methods

2.1 Commercial Suppliers

A full list of names and addresses of suppliers used can be found in Appendix A. Unless stated otherwise, reagents were obtained from Sigma-Aldrich (Dorset, UK).

2.2 Secondary Cell lines

All cells and parasites were cultured in 25cm^2 flasks (Starstedt, Leicester, UK).

Hs27 Human Foetal Foreskin Fibroblasts (HFF) were obtained from the European Collection of Cell Cultures (ECACC, no. 94041901) and maintained by serial passage in Dulbecco's Modified Eagle's Medium (DMEM, Lonza, Basel, Switzerland), supplemented with 2mmol/L L-Glutamine and 10% Foetal Bovine Serum (FBS, Biosera, East Sussex, UK) at 37°C in 5% CO_2/ 95% air atmosphere.

Murine small intestinal epithelial cells (m-IC$_{cl2}$ cells) were kindly provided by Alain Vandewalle (Inserm U246, Paris, France, [Bens et al., 1996]) and cultured in 1:1 volume of DMEM:HAM's F-12 (BioWhittikar/Lonza, Basel, Switzerland), 60nmol/L selenium, 50mmol/L dexamethasone, 5µg/ml apo-transferrin, 2mmol/L L-Glutamine, 20mmol/L N-2-hydroxyethylpiperazine-N'-2-ethanesulfonic acid (HEPES), 5µg/ml insulin, 1nmol/L tri-iodothyronine, 2% FBS, 3.6g/L D-glucose, 10ng/ml epithelial growth factor (EGF), at 37°C in 5% CO_2/ 95% air atmosphere. After 10 passages had been reached, cells were discarded and cultures restarted to prevent changes in cell behaviour, growth and morphology that are typical with cells maintained in culture. For experimental use, centrifugation of m-IC$_{cl2}$ cells was always 260g for 5 minutes.

Human adenocarcinoma colonic epithelial $CaCo_2$ cells, and the derivative clonal cell line, C2BBe1, were obtained from the ECACC (86010202) and American Type Culture Collection (CRL-2102), respectively. Both cell lines were grown in 10% FBS in DMEM supplemented with 2mmol/L L-Glutamine (and also 0.01mg/ml apo-transferrin for C2BBe1 cells). Cells were maintained at 37°C in 10% CO_2/ 90% air atmosphere.

Murine fibroblast Ψ CRE cells were obtained from the ECACC (no. 94090902) and cultured in DMEM supplemented with 10% FBS and 2mmol/L L-glutamine at 37°C in 5% CO_2/ 95% air atmosphere.

2.3 Parasite culture

Virulent type 1 strain RH, *Toxoplasma gondii* tachyzoites that stably express the tandem yellow fluorescent protein (YFP) were maintained by continuous passage in confluent monolayers of HFF cells at 37°C in 5% CO_2/ 95% air atmosphere [Gubbels et al., 2003]. Bradyzoite production was induced in culture by the high pH shock method as described by Soete *et al.* 1996 [Soête and Dubremetz, 1996]. Supernatent from an infected monolayer of HFF cells (naturally lysed to approximately 70 - 90%) was collected and centrifuged at 1000g for 15 minutes. The pellet was resuspended in 5 - 10mls of bradyzoite induction medium (2% FBS, 50mM HEPES and 2g/L sodium hydrogen carbonate (pH 8.2) in Roswell Park Memorial Institute media (RPMI, Lonza)) and added back onto the remaining HFF monolayer for 48 hours. Bradyzoites were collected from the supernatent by centrifugation at 1000g for 15 minutes. The conversion from tachyzoites to bradyzoites was checked by means of fluorescence (bradyzoites were YFP negative [Egan et al., 2005], nor expressed the tachyzoite specific surface antigen 1 protein (anti-SAG1 antibody from Abcam, Cambridge, UK)).

2.4 Parasite treatments

Parasites were killed by either the freeze-thaw method or the heat shock method [Koshy et al., 2010]. Briefly, parasites were centrifuged at 1000g for 15 minutes, supernatent discarded and replaced with 1× phosphate buffered saline (PBS, Oxoid, Basingstoke, UK). Parasites were either frozen in 1:1 volume of 100% ethanol and dry ice for 5 minutes, before thawing in a 37°C water bath. This process was repeated three times. Alternatively, parasites were heated at 65°C for 20 minutes.

2.5 Parasite Viability

Having been resuspended in PBS, parasites (live or dead) were incubated with LIVE/DEAD® Fixable Green (488nm excitation) or LIVE/DEAD® Far Red (633 or 635nm excitation) Dead Cell Stain Kit (Invitrogen) for 10 minutes before centrifuging in 1% Bovine Serum Albumin (BSA) in PBS. Parasites were then fixed in 2% PFA for 20 minutes, centrifuged and resuspended in PBS. Samples were run through the FACS Calibur by Roy Bongaerts (Institute of Food Research, Norwich, UK).

2.6 Invasion and Transmigration Assay

m-IC_{cl2} cells were plated in a volume of 100µl onto the apical (top) compartment of polyethylene terephthalate (PET) cell culture transwell inserts (6.5mm diameter, 8µm pore size, BD Biosciences, Oxford, UK), within a 24 well plate (Starstedt), and soaked in 1ml of cell media in the basal (bottom) compartment. An insert containing just cell media was used as a blank. Cells were grown at 37°C in 5% CO_2/ 95% air atmosphere. After 24 hours, the volume of media in the apical compartment was adjusted to 500µl. Apical media was replaced every 24 hours and transepithelial electrical resistance (TEER) was measured every 24 - 48 hours using an Epithelial Tissue Volt Ohmmeter 2 (EVOM2, World Precision Instruments, (WPI), Stevenage, UK). Basal media was replaced every 48 hours after a TEER reading was taken. TEER was calculated using the following equation:

$$Resistance = (R_C - R_i)\pi r^2$$

where R_c is the resistance of cells on the insert, R_i is the resistance of the insert and r is the radius of the insert.

On day 12, TEER was recorded and inserts with confluent, polarised monolayers of cells (indicated by a consistent TEER over time) were transferred to new 24 well plates with 700µl pre-warmed (at 37^0C) cell media per well (basal compartment). Apical media was replaced with 200µl fresh pre-warmed media. On day 13 TEER was recorded using an ENDOHM (WPI) that contained 700µl pre-warmed cell media, in which each insert was placed and allowed to calibrate for 2 minutes before measuring. These volumes of liquid created equal levels in the apical and basal compartments to ensure the readings were as accurate as possible. The insert was then placed back into the 24 well plate. Media

was removed from the apical compartment and was used to resuspend pelleted RH-YFP *T. gondii* tachyzoites or bradyzoites in a volume of 200µl. In some cases, 1000µg/ml 3 - 5kDa FITC-conjugated Dextran was also added to the apical media, in order to assess changes in permeability during infection. Inserts were returned to 37°C in 5% CO_2/ 95% air atmosphere during infection. TEER was then recorded using the ENDOHM as before. Apical and basal media were removed and kept for later analysis of FITC-dextran permeability (Section 2.9) and numbers of parasite transmigration (Section 2.10). Cells were transferred to new plates and prepared for confocal microscopy following the immunocytochemistry protocol outlined below.

2.7 Immunocytochemistry

Live cells were washed in 1× PBS and fixed at 25°C in either 2% paraformaldehyde for 20 minutes, or acetone for 5 minutes followed by 5 minutes in rehydration buffer (1% BSA in PBS). Cells were then permeabilised in 0.2% Triton X-100 for 10 minutes and blocked in blocking buffer (0.2% Triton X-100, 3% BSA, 3% goat serum, 3% fish skin gelatin in PBS) for 1 hour. All incubations were applied to both the apical and basal compartments of transwell inserts. Primary antibodies diluted in blocking buffer were added to the apical compartment, with blocking buffer maintained on the underside of each insert for 20 hours at 4°C (Appendix B). Controls consisted of either no primary antibody or relevant IgG in place of the primary antibody. Solutions were removed and cells washed in PBS three times. Secondary and tertiary antibodies were then added to cells and incubated on a shaker in the dark at 25°C for 1-2 hours, washing in between incubations with 1× PBS. Where different antibodies were raised in the same species, secondary and tertiary antibodies were applied to one protein before continuing with the other, in order to avoid non-specific binding. Finally, the PET membrane was extracted from the insert using a scalpel and placed cell side up onto a glass microscope slide. A drop of DePeX (BDH, Dorset, UK) or Vectashield Hard-Set Mounting medium with DAPI (4',6-diamidino-2-phenylindole, Vector Labs, Peterborough, UK) was applied to the sample. It was then covered with a glass coverslip and stored in the dark at 4°C.

To visualise intracellular parasites, cells were grown to confluency on 13mm diameter glass coverslips (BDH). RH-YFP tachyzoites were added to cells for 2 hours before removing and discarding unattached parasites.

Cells were briefly washed with PBS and fixed in 2% paraformaldehyde for 20 minutes. The samples were permeabilised in 0.2% Triton-X 100 for 10 minutes, soaked in Haematoxylin for 1 minute, washed 3 times in PBS, soaked in Eosin for 1 minute, before rinsing and mounting onto a microscope slide with DePeX or DAPI mountant.

2.8 Confocal and Fluorescent Microscopy

Cells were viewed using an upright or inverted Zeiss AxioVert 200M microscope with LSM510 META image analysis software and AxioVision image viewer. Z stacks were composed of 1μm interval sections with the 40× oil objective unless stated otherwise. Rhodamine and Texas Red fluorochromes were excited by the 543-nm helium neon 1 laser. YFP-RH *T. gondii* was captured using the argon 488-nm laser, DAPI and Pacific Blue by the 405-nm diode laser and Cy5 by the 633-nm helium neon 2 laser. All laser intensities for the same protein-antibody complex were consistent throughout the duration of sample collection both within and between experiments.

2.9 Paracellular Permeability

Samples were collected in 1ml eppendorfs and centrifuged at 1000g for 10 minutes using a bench top centrifuge (Eppendorf, Cambridge, UK). The supernatent was transferred to a new eppendorf and 100μl was used for fluorescent analysis in black 96 well plates (Matrix Technology Corporation, Wilmslow, UK). The concentration of FITC-dextran was determined from a standard curve. Samples were read using the FLUOstar OPTIMA microplate reader (excitation 490nm, emission 520nm, BMG Labtech, Aylesbury, UK).

2.10 Parasite Transmigration

The pellet containing parasites, collected from Section 2.9, was resuspended in 2% paraformaldehyde for 20 minutes and transferred to 5ml round bottom FACS falcon tubes (BD Biosciences). Data was acquired with side scatter trigger for 2 minutes on a low flow speed using a Cytomics FC500 MPL (Beckman Coulter, High Wycombe, UK) or a FACS Calibur (BD Biosciences). Detector voltages and threshold settings were adjusted based upon sample blanks and negative controls. For the FC500MP,

green fluorescence was collected in the FL-1 channel (515nm - 535nm), yellow fluorescence in the FL-2 channel (568nm - 583nm), orange fluorescence collected in the FL-3 channel (615nm - 620nm), red fluorescence in the FL-4 channel (660nm - 690nm) and far red fluorescence in the FL-5 channel (725nm - 785nm). For the Calibur:- green fluorescence was collected in the FL-1 channel (515nm - 545nm), yellow fluorescence collected in the FL-2 channel (564nm - 606nm), far red fluorescence in the FL-3 channel (>670nm), and red fluorescence in the FL-4 channel (653nm - 669nm). Quantum dots conjugated to Alexa Fluor 655nm were collected in the FL-4 channel (653nm - 669nm) at a high flow rate. All parameters were collected as logarithmic signals. Data was analysed post-collection using FlowJo version 7.6 (TreeStar).

2.11 Cytokine Bead Array

Cells were grown to confluency on 6 well plates and infected with *T. gondii* tachyzoites for 24 hours. Supernatent was collected and centrifuged at 1000g for 15 minutes to remove parasites. The supernatent was snap frozen in liquid nitrogen and stored at -80°C. Beads from the Cytometric Bead Array kit (BD Biosciences, 30 Plex Bead Mixture) were vortexed for 15 seconds and 0.5µl of each capture bead in 24.5µl of assay diluent was used per reaction. 200µl of thawed supernatent was added to the bead solution in FACS tubes for 1 hour in the dark at 25°C. After vortexing for 15 seconds, 0.5µl of Phycoerythrin detection reagent was resuspended in 24.5µl assay diluent and this was incubated with the sample, shaking for 1 hour at 25°C in the dark. 1ml of wash buffer (1% BSA in PBS) was added to each tube and centrifuged at 200g for 5 minutes. The supernatent was carefully removed and replaced with 600µl wash buffer. Samples were read using the FC500 Flow Cytometer.

2.12 Electron Microscopy

A collagen gel solution (1:1 mixture of bovine derived collagen I gel:cell media, set for 2 hours at 37°C) was set onto thermanox coverslips. These coverslips are designed specifically for electron microscopy sample preparation and were placed within a 35mm µ-dish (Ibidi, Martinsried, Germany). m-IC_{cl2} cells were plated onto the gel and cultured for 8 days before infecting with RH-YFP *T. gondii* tachyzoites for 2 hours. Media was removed and cells were rinsed in PBS before fixing with 3% glut-

araldehyde (Agar Scientific, Stansted, UK) in 0.1M cacodylate buffer (pH 7.2) for 2 hours. The fixative was removed and then replaced with three washes of 0.1M cacodylate buffer. Kathryn Cross and Mary Parker (Institute of Food Research, Norwich, UK) kindly further prepared the samples for scanning electron microscopy (SEM) and transmission electron microscopy (TEM) from this point onwards. The experiments were carried out once with biological replicates for SEM and TEM.

For TEM, an additional fixing step was applied to the samples using a 2% aqueous osmium tetroxide solution for 1 hour, before dehydrating the samples through a series of ethanol solutions (from 10% to 20% to 30%). A $1cm^2$ portion of the cell layer was cut and removed from the coverslip using a razor blade. This portion was then processed through an additional ethanol dehydration series (40, 50, 60, 70, 80, 90, 3 $\times$ 100%). The ethanol was replaced with a 1:2 mix of LR White medium grade resin (London Resin Company Ltd, London, UK) to 100% ethanol and incubated on a rotator for 17 hours at 25°C.

This resin was removed and replaced with solutions containing first a 1:1 and then a 2:1 mix of LR White resin: 100% ethanol and finally a 100% resin was applied to the sample with 4 hours between each change. The resin solutions were changed twice more with a 100% resin and incubated for another 4 hours each time. The cell layers were laid flat in embedding capsules with fresh resin and polymerised for 17 hours at 60°C.

Sections approximately 90nm thick were cut using an ultramicrotome (Ultracut E, Reichert-Jung, Labquip, Ontario, Canada) with a glass knife, collected on film/carbon coated copper grids, and stained sequentially with uranyl acetate (saturated in 50% ethanol) and Reynold's lead citrate.

For SEM, sections of the supporting dishes were carefully cut away ensuring that the cell layers remained immersed in buffer. Sections were dehydrated through a series of ethanol solutions (10, 20, 30, 40, 50, 60, 70, 80, 90, 3x 100%) and critical point dried in a Polaron E3000 critical point drier using liquid carbon dioxide as the transition fluid. The sections were mounted such that the cell layers were face up on aluminium SEM stubs using quick drying condicutive silver paint (Agar Scientific). The samples were coated with gold in Agar high resolution sputter-coater apparatus.

Samples were visualised using a Zeiss Supra 55 VP FEG SEM, operating at 3kV (Zeiss).

2.13 Protein analysis

2.13.1 Protein sample collection

Cell lysates were prepared as follows. Approximately 2 - 3 x 10^6 m-IC_{cl2} cells can be collected from a confluent monolayer growing on a $25cm^2$ flask for 8 days. To prepare cell lysates for protein analysis, media was removed and replaced with 1ml of ice-cold PBS. PBS was removed and replaced with 400µl of ice-cold soluble lysis buffer: 1% Triton X-100, 100mmol/L NaCl (Fisher Scientific, Loughborough, UK), 25mmol/L Tris-HCl, pH 7.4, 1mmol/L sodium orthovanadate, 5mmol/L ethylenediaminetetraacetic acid (EDTA), 2mmol/L ethyleneglycoltetraacetic acid (EGTA), 50mmol/L phenylmethysulfonyl fluoride (PMSF), 25mM sodium fluoride, 10× protease inhibitor cocktail and a 15-fold dilution of phosphatase inhibitor cocktail. Cells were removed from the flask using a cell scraper (BD Biosciences) and transferred to a pre-chilled eppendorf tube. Cells were lysed 10 times using a 19 gauge needle before being centrifuged at 16,100g for 10 minutes at 4°C. The supernatent (soluble, cytoplasmic fraction) was kept on ice while the pellet (insoluble, membrane-associated fraction) was prepared. The pellet was resuspended vigorously in 300µl of insoluble lysis buffer (soluble lysis buffer supplemented with 6M urea and 0.5% sodium lauryl sulfate (SDS), with additional protease and phosphatase inhibitor cocktails), vortexed, sonicated three times for 30 seconds at 4°C before centrifuging for 5 minutes at 16,100g. The supernatent (insoluble, membrane associated fraction) was transferred to a new eppendorf tube and the pellet (mainly containing DNA) was discarded. An aliquot of fractions were taken for protein quantification and the remainder was snap frozen in liquid nitrogen.

Protein content was determined using a Bio-Rad DC Protein Assay Kit according to manufacturers instructions (BioRad Labs, Hemel Hempstead, UK). Protein standards were established using various concentrations of BSA from 0.0825mg/ml to 1.48mg/ml, including a blank (soluble and insoluble lysis buffer only). Colorimetric measurement was performed using a microtitre plate reader (SpectraMax $Plus^{384}$).

2.13.2 Immunoprecipitation and gel electrophoresis

The immunoprecipitation (IP) was carried out according to manufacturers instructions. Briefly, Dynabeads Protein G (Invitrogen) were resuspended and for each IP, 50µl (1.5mg) were transferred into an eppendorf

tube. The tube was placed on a magnet (Invitrogen) to separate the beads from the solution. Having removed the solution and tube from the magnet, 4μg of anti-occludin antibody (Invitrogen) in 200μl of PBS containing 0.02% Tween 20 was added to the beads and rotated at 25°C for 90 minutes. The tube was then placed back onto the magnet and supernatent removed. The antibody-bead complex was gently washed with 200μl of PBS containing 0.02% Tween 20. The beads were resuspended with cell lysates in a volume of no less than 200μl and rotated at 25°C for 90 minutes. The tubes were then placed back on the magnet and supernatent removed. The bead-antibody-protein complex was gently washed twice with 200μl of PBS, separating the solution from the beads using the magnet. In order to discard proteins that had bound to the tube wall, the complex was resuspended in 100μl of PBS and transferred to a new tube. The beads were separated from the supernatent again, before eluting the protein in 20μl of 1× RunBlue Lithium Dodecyl Sulfate sample buffer (LDS, Expedeon, Harston, UK) and 1× dithiothreitol reducer (DTT, 100μg/ml, Expedeon) in double distilled water (ddH_2O).

For denaturing gels, samples were added to a mixture of 1× RunBlue LDS Sample Buffer and 100μg/ml DTT reducer. A constant volume of sample was prepared in ddH_2O. These samples were then heated to 70°C for 10 minutes before loading onto a precast Sodium Dodecyl Sulfate PolyAcrylamide GEls (SDS-PAGE, 8%, 10% or 12%, RunBlue, Expedeon). Equal amounts of protein were used to load in each lane and samples were run alongside a pre-stained protein molecular marker (10 - 170kDa, Fermentas, St. Leon Rot, Germany), at 150V for 1 - 2 hours in running buffer according to manufacturers instructions.

2.13.3 Densitometry

Gels were incubated in Coomassie Brilliant Blue stain for 1 hour and washed in water. Proteins were visualised under white light and photographed. For purposes of ensuring equal loading across samples, densitometry analysis was performed by Francis Mulholland (Institute of Food Research). Gels were scanned using a GS-800 scanner and imaged using Quantity One software (version 4.6.1). Protein bands were aligned across lanes according to molecular weight, as shown in Appendix C, and relative quantities were estimated using the intensity (measured from the optical density) of each protein band and subtracted from the background signal from the gel.

2.13.4 Mass Spectrometry

For mass spectrometry analysis all sample preparation was performed by Francis Mulholland. Gels were stained with SYPRO Ruby and protein bands were extracted from the gel as follows. Samples were washed twice for 15 minutes in 400mM ABC in Acetronitrile (Fisher Scientific) and rinsed in acetronitrile for 10 minutes. Samples were air dried before adding 10mM DTT in 50mM Ammonium Bicarbonate and incubated for 30 minutes at 60° C using a PCR machine. Liquid was removed and replaced with 100mM Iodoacetamide in 50mM Ammonium bicarbonate Iodoacetamide solution for 30 minutes at 25° C, in the dark. This step was repeated three times before washing in acetonitrile for 10 minutes. After air drying, 25µg Chymotrypsin in enzyme buffer (20mM Ammonium Bicarbonate in 1M Calcium Chloride Dihydrate) and 5µg Trypsin Gold (Promega) in 50mM Acetic Acid in enzyme buffer were added together at kept at 4° C. Samples were incubated at 37° C for over three hours in the presence of protease solution and enzyme mixture. Finally, 1% Formic Acid was added to samples and incubated for 10 minutes before freezing.

Samples were acquired through an LTQ OrbiTrap (Thermo Fisher Scientific), database searches were performed by Alex Jones (Sainsbury Lab, Norwich, UK), and results were analysed using MASCOT (Matrix Science) software.

2.13.5 Immunoblotting

For the detection and visualisation of specific proteins, samples were transferred onto Hybond C+ nitrocellulose membranes (Amersham Biosciences, Little Chalfont, UK) at 100V for 1 hour at 4°C in transfer buffer (3g ultrapure Tris Base, 14.4g glycine (Fisher Scientific), 200mls methanol (Fisher Scientific), 0.05% SDS and 800mls ddH_2O). Membranes were blocked in 5% BSA in Natt buffer (150mM NaCl, 20mM Tris Base, 0.1% Tween-20, pH 7.4), shaking for 1 hour at 25°C. Primary antibodies diluted in 1% BSA in Natt buffer were applied to a sealed bag with the membranes inside, to incubate for 24 hours 4°C. Membranes were washed 5 - 6 times for 1 hour in Natt buffer, before incubation with secondary horseradish peroxidase (HRP) conjugates (Santa Cruz, California, USA) in 1% BSA in Natt buffer, for 1 hour at 25°C. Membranes were washed again for 1 hour 5 - 6 times with Natt buffer, before the addition of 1:1 volume of enhanced chemiluminescence substrate (SuperSignal West

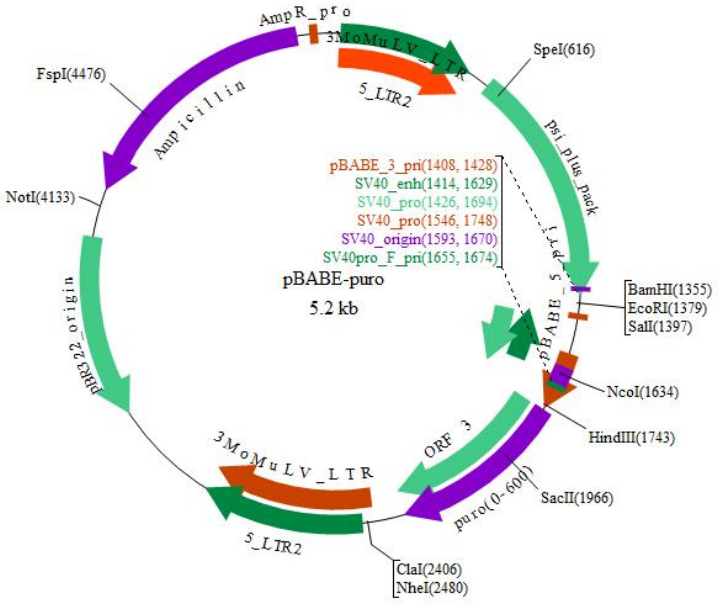

Figure 2.1: pBABEpuro plasmid vector. Map extracted from `http://www.biovisualtech.com/bvplasmid/pBABE-puro.htm`

Pico Chemiluminescent substrate (Pierce Chemical Company, Cramlington, UK)) for 5 minutes and developed using a Fluor-S-Multi Imager (Bio-Rad) and Quantity One software (version 4.5.2).

In order to probe for another protein, membranes were stripped by incubating in a 1:20 dilution of acetic acid in 1× PBS for 1 hour, pH 2.59. Before and after stripping, the membrane was washed for 30 minutes in Natt buffer.

2.14 FLAG-tagged occludin in the pBABEpuro vector

The retroviral pBABEpuro vector with FLAG-tagged full length murine occludin was kindly provided by Britta Engelhardt (Theodor Kocher Institute, University of Bern, Switzerland) [Bamforth et al., 1999]. The pBABEpuro plasmid is a high copy plasmid and contains genes that confer resistance to ampicillin and puromycin (Figure 2.1).

To amplify the pBABEpuro plasmid vector, it was transformed into competent DH5α *Escherichia coli* (*E. coli*) cells (Invitrogen) by incubating on ice for 30 minutes. Bacteria were heat shocked at 42°C for 2 minutes and returned to ice for 5 minutes. Super Optimal broth with catabolite repression (SOC) media was added for 1 hour and incubated in an orbital shaker set at 37°C, 225rpm (revolutions per minute). Bacteria was grown for 20 hours at 37°C on ampicillin-containing lysogeny

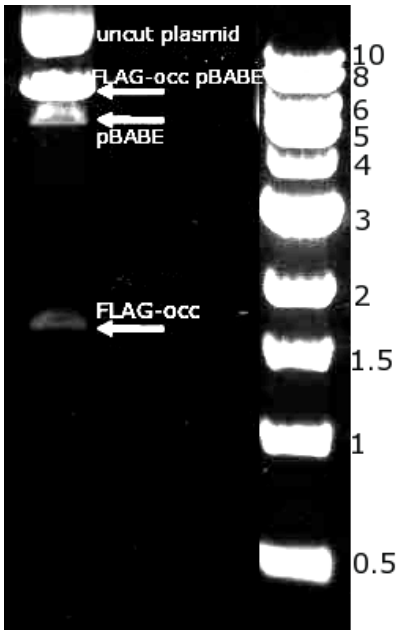

Figure 2.2: Digestion of FLAG-tagged occludin pBABEpuro plasmid vector. Following digestion using *Ngo*MIV and *Sal*1 restriction enzymes. FLAG-tagged occludin migrates on a 0.8% agarose gel as a 1.6kbp band. Supercoiled, uncut plasmid is also present on the gel after staining with ethidium bromide. Image produced by Mohamed Bencharab (visiting worker in the Institute of Food Research).

broth (LB) agar plates (100µg/ml), and colonies selected and grown in 3 - 5mls of LB media with ampicillin. Using a miniprep kit (Qiagen, Crawley, UK), DNA was purified according to manufacturers instructions. The insert size was checked and confirmed by digesting the plasmid with *Ngo*MIV and *Sal*1 enzymes in Buffer 3 (New England Biolabs, (NEB) Hitchin, UK) for 1 hour at 37°C (Figure 2.2). The plasmid vector is 6774 base pairs (bp) long, and following digestion, releases full length occludin with the FLAG tag, resulting in a DNA band of 1601bp, leaving the plasmid vector at 5173bp.

The plasmid sequence was checked and confirmed by The Genome Analysis Centre (TGAC, Norwich, UK) using Set1F, Set1R, Set2F, Set2R, Set3F and Set3R primers (Appendix D and Appendix E).

2.15 Production of recombinant occludin protein fragments

High quality DNA from a large scale preparation kit (Qiagen) of the FLAG-tagged occludin-pBABEpuro plasmid vector was used as a template to amplify different portions of the occludin sequence to create recombinant protein fragments as described below. These portions were then ligated into the pET3a vector (a kind gift from Lora Hooper (Wash-

ington University School of Medicine, Missouri, USA)), which carries an N-terminal T7•Tag® sequence.

2.15.1 Production of recombinant proteins in *E. coli*

To generate a fragment containing the extracellular loops 1 and 2 (ECL1 and ECL2) of occludin, (Appendix F), the pBABEpuro vector containing FLAG-tagged occludin was amplified by Polymerase Chain Reaction (PCR) with 5 units of Phusion high fidelity polymerase (New England Biolabs), 10mM dNTPs, and 10μM each of the pECL1 forward and pECL2 reverse primers (Appendix D) using the following protocol: initial denaturation at 98°C for 30 seconds, 35 cycles each of ten seconds, denaturation at 98°C for 30 seconds, annealing at 50°C for 30 seconds and 1 minute extension at 72°C. A final extension step was performed at 72°C for 10 minutes. PCR products were checked on a 2% agarose gel, before ligating into the pET3a vector using a 1:1 ratio of insert:vector and the protocol described in Section 2.14. The pET3a vector was digested with *Bam*H1 and *Nde*1 restriction enzymes. DH5α *E. coli* was transformed and 10 - 20 colonies were screened for the presence of the inserted occludin fragment within the plasmid.

Having established this, the bacteria were grown in 15mls of LB media containing ampicillin and large scale DNA purification was performed using the miniprep kit previously mentioned. Approximately 200ng of plasmid DNA was transformed into the competent BL21 Codon Plus (DE3) RIL strain of *E. coli,* chosen for expressing the protein and recombinant fragments due to the presence of a large number of rare tRNAs. Colonies were picked and plasmids were checked by restriction digest to determine whether the insert was still the correct size and when confirmed (Figure 2.3), DNA was sent for sequencing using the T7 primers to TGAC (Appendix D).

BL21 cells containing the correct recombinant plasmids were grown in 5mls of LB media supplemented with ampicillin for 20 hours at 37°C shaking at 225rpm. A 1:100 dilution of culture was sub-cultured in 25mls of pre-warmed LB media supplemented with 1% glucose in a 250ml conical flask at 37°C and allowed to grow whilst shaking at 250rpm (Scientific Innova 44, New Brunsuick), until the optical density reached 0.35. Expression of the heterologous protein fragments was induced by adding either 4mM of isopropyl-beta-D-thiogalactopyranoside (IPTG), and incubated for a further five hours. IPTG is an activator of the *lac* operon and causes an increased rate of the T7 polymerase transcription to oc-

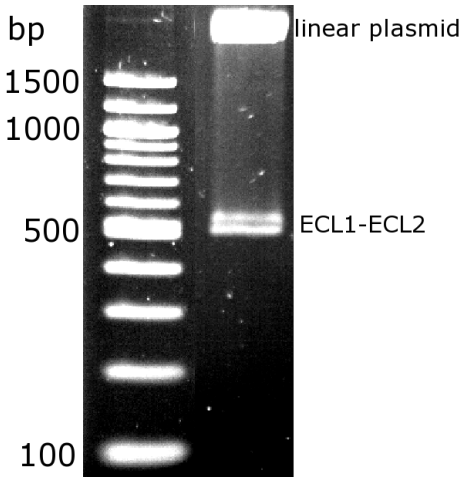

Figure 2.3: Insertion of ECL1-ECL2 into pET3a plasmid vector. The insert was ligated into the pET3a vector using a 1:1 ratio of insert:vector. The pET3a vector was then digested with *Bam*H1 and *Nde*1 restriction enzymes. ECL1-ECL2 was present at 500bp on a 2% agarose gel after staining with ethidium bromide.

cur. The cultures were transferred to ice-cold 50ml falcon tubes and centrifuged at 8228g for 10 minutes at 4°C (Eppendorf 5810R centrifuge). Supernatent was removed and the pellet was frozen and stored at -20°C.

2.15.2 Expression of recombinant proteins in *E. coli*

In view of the subsequent protein purification, the solubility of the heterologous protein and protein fragments were checked. A fraction of the bacterial pellets were resuspended in wash buffer (20mM TrisHCl, pH7.5, 10mM EDTA, pH8, 1% Triton X-100 in MilliQ water) and lysed on ice by serial sonication impulses at 10 seconds (using a 10 - 11 intensity setting) each for nine or ten times until the suspension turned clear. The lysed bacteria were then centrifuged at 10,000g for 10 minutes at 4°C in order to separate inclusion bodies from membrane-associated and soluble cytoplasmic proteins. Supernatents were transferred to a clean eppendorf and centrifuged at 16,100g for 10 minutes. The second supernatents contained the soluble cell protein fraction, and the pellets contained the membrane-associated fraction. Samples from each fraction were run on a 4 - 12% SDS-PAGE gel (Invitrogen) using 2-(N-morpholino)ethanesulfonic acid (MES) buffer according to manufacturers instructions, and then stained with Coomassie Brilliant Blue to detect the location of the recombinant protein.

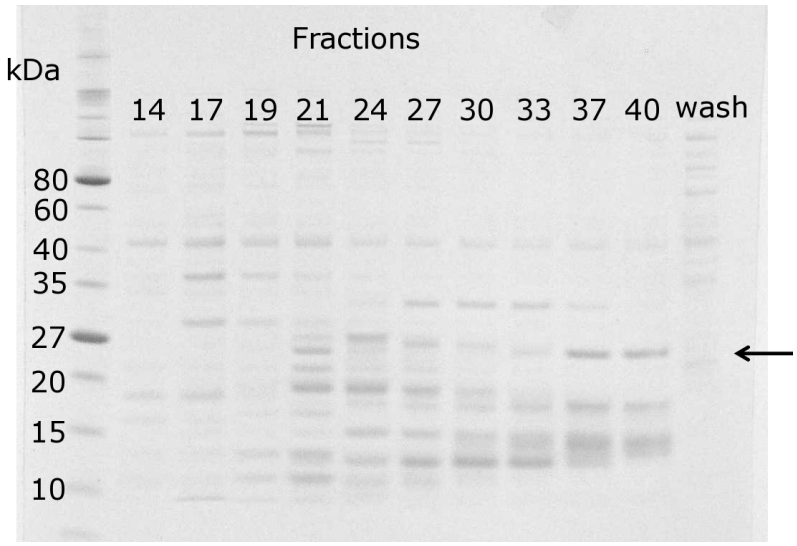

Figure 2.4: Eluted fractions for ECL1-ECL2. A selection of fractions were electrophoresced on a 4 - 12% gradient SDS-PAGE gel which was stained with Coomassie Brilliant Blue. The size of ECL1-ECL2 was approximately 27kDa, as indicated by the arrow.

2.15.3 Recombinant protein purification

Recombinant ECL1-ECL2 protein bacterial pellets were resuspended and pooled together in 25mM TrisHCl, pH7, and sonicated until the solution became transparent. Using a cationic exchange chromatography SP Sepharose column, the protein was run through the system following a wash with 25mM TrisHCl, pH7, and 0.2M NaCl. Forty protein fractions were eluted in 500µl aliquots with 25mM TrisHCl, pH7, and 0.6M NaCl. A selection of collected fractions were subjected to gel electrophoresis on 4 - 12% gradient SDS-PAGE gels and subsequently Coomassie Brilliant Blue-stained for the detection of recombinant protein. Elution of the heterologous protein or protein fragments was observed after fraction 17, peaked at fractions 22 and 23 and tailed off by fraction 40 (data not shown). To check that all the protein had been eluted within the 40 fractions, a final fraction (called wash) was included on the gel. It was seen that the majority of recombinant protein (≈27kDa) was found in fractions 33 - 40 (Figure 2.4). Fractions 37 - 40 were pooled together and desalted on a PD-10 column (Amersham Biosciences, Buckinghamshire, UK). Following protein quantification using a Bradford assay, recombinant fragments were concentrated using a 3000MWCO PES Viva column (Sartorius, Goettingen, Germany). This column separated the proteins based on size, excluding any above 30kDa. Proteins were centrifuged at 12,000g at 25°C for 2 x 15 minutes. Approximately 150µl of purified protein at a concentration of 780µg/ml was collected and stored at -80°C.

2.16 Generation of cells with reduced occludin

2.16.1 shRNA treated cells

2.16.1.1 Construction of shRNA plasmid vector

The pBABEpuro vector backbone was used to express a short hairpin siRNA (shRNA). The sequence of the shRNA was described by Yu *et al.* 2005, (Figure 2.5) [Yu et al., 2005]. Restriction enzyme sites for *Ngo*MIV and *Bam*H1 were added onto the ends of the shRNA sequence.

The pBABEpuro occludin plasmid was reduced in size by removing occludin with *BamH1* and re-ligated using T4 ligase. The shRNA was then ligated into this intermediate plasmid at a ratio of 1:1000 with T4 ligase for 20 hours at 4°C using restriction enzymes *Ngo*MIV and *Bam*H1 (NEB). In order to compute the ligation reaction, the following equation was followed:-

$$q_i = \frac{vs_i}{s_v}$$

where q = quantity of insert (i) in ng, v = vector, s = size in base pairs. The quantity of insert required was relative to 50ng of vector.

The shRNA was pre-prepared by adding 1µl of each oligonucleotide to 48µl of annealing buffer (100mM potassium acetate, 30mM HEPES pH 7.4, 2mM magnesium acetate) and amplified by PCR (95°C for 4 minutes, 70°C for 10 minutes and finally 4°C for 10 minutes). The plasmid was transformed into competent DH5α *E. coli.* Colonies were picked and bacteria grown in LB media containing ampicillin and purified using a miniprep kit (Qiagen). Plasmid DNA containing the shRNA sequence were verified by digesting with *Bam*H1 and *Ngo*MIV restrictions enzymes and the sequence was analysed using Set1F and Set3b primers (Appendix D). All DNA was amplified by large scale plasmid DNA preparation once correct sequences had been confirmed (Qiagen, Appendix G).

2.16.1.2 Production of retrovirus

In order to transfect m-IC_{cl2} cells with the cloning products described in Section 2.14 and Section 2.16.1.1, it was necessary to incorporate the products into a Ψ-CRE cell line. These cells are derived from the murine NIH 3T3 cell line and have been transformed with the Moloney murine leukaemia virus [Danos and Mulligan, 1988]. In the presence of pBABEpuro vector, they generate helper free recombinant retroviruses

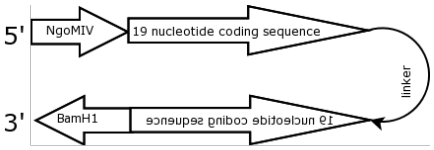

(a) Example of an shRNA molecule

CCGGCGTGAAGAGTACATGGCTGCTTCAAGAGAGCAGCCATGTACTCTTCAC-TTTTTG
GCACTTCTCATGTACCGACGAAGTTCTCTCGTCGGTACATGAGAAGTG-AAAAACCTAG

(b) The sequence of shRNA for occludin

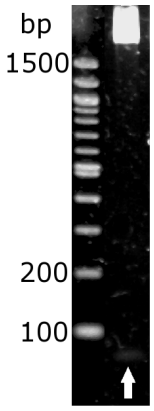

(c) shRNA

Figure 2.5: shRNA molecule for reducing occludin expression. The structure of an shRNA is shown in Figure 2.5a. At both ends are sequences for restriction enzymes *Bam*H1 and *Ngo*MIV, followed by the sense and antisense strands and joined by the hairpin loop. A short termination sequence is also included. The sequence of shRNA for reduction of occludin that was incorporated into the pBABE vector was adapted from Yu *et al.* 2005, [Yu et al., 2005] (Figure 2.5b). Underlined letters illustrate the restriction enzymes while the black letters represent the sense and antisense strands. Red lettering indicates the hairpin loop. The annealed shRNA oligonucleotide was ligated at a ratio of 1 : 1000 (vector : insert) using *Bam*H1 and *Ngo*MIV. After staining the 2% agarose gel with ethidium bromide, shRNA was present at ≈50bp (Figure 2.5c).

without the production of helper virus or transferring the packaging function to the virus (Health Protection Agency, London, UK). Cells were washed and trypsinised for 5 minutes before centrifuging at 150g for 5 minutes. Supernatent was discarded and the cells were resuspended in 10mls of Ψ-CRE cell media and plated into a 10cm dish (Greiner Bio-One, Stonehouse,UK) at a density of 3.2 x 10^6 cells. Cells were incubated for 20 hours at 37°C, 5% CO_2 and grown until 70 - 90% confluent. Up to 10μg of DNA was added to 1.5mls of OptiMEM without serum in a sterile bijou and mixed gently for 5 minutes. In a separate bijou, 36μl of Lipofectamine™ 2000 (Invitrogen) was added to 1.5mls of OptiMEM without serum and mixed gently for 5 minutes. The two solutions were mixed together and allowed to incubate gently shaking at 25°C for 20 minutes, before adding to the Ψ-CRE cells, in a drop-wise fashion. Cells were incubated at 37°C, 5% CO_2 for 20 hours before discarding the media and replacing with an additional supplementation of 1mM of sodium pyruvate, 1 x non essential amino acids, 1% L-Glutamine, 1% Penicillin and Streptomycin (Invitrogen), and 1% FBS in Ψ-CRE cell media, for up to 48 hours at 37°C, 5% CO_2. Supernatent containing viral particles was collected and centrifuged at 1600g for 15 minutes at 4°C, to remove cell debris. The remaining solution was then filtered using a 0.45μm filter. Virus was either stored in aliquots at -80°C or added directly onto m-IC_{cl2} cells.

2.16.1.3 Stable Cell Line Production

Preparations of virus (up to 2mls of viral prep per well) were added to m-IC_{cl2} cells on 6 well plates in the presence of 0.1μg/ml polybrene (Hexadimethrine Bromide) for 24 hours at 37°C, 5% CO_2. Polybrene was removed and replaced with normal m-IC_{cl2} cell media for 24 hours. Transduced cells were selected for by the addition of 1.5μg/ml of puromycin into the media because at this concentration, puromycin will kill non-transduced cells within 2 - 6 days of addition. This was confirmed both by visualisation of cell detachment and TEER, which plummeted after day 6 (data not shown). Therefore, any transduced cells grown in the presence of puromycin that were alive 14 days post transfection were considered to be carrying the virus.

Puromycin was added every other time the media was changed (therefore once every 4 days) and after 10 days the concentration of puromycin was increased to 3μg/ml and added every time the media was changed thereafter. This gave the cells a chance to survive following transduction,

and although this may have allowed a small fraction of non-transduced cells to survive, it was clear the cells would not replicate in the presence of puromycin. After six weeks of culture, the cells started to reach confluency and were transferred from a 6 well plate into a 25cm^2 flask. Media was changed every 3 - 4 days and replaced with 3μg/ml puromycin in normal m-IC$_{cl2}$ cell media. Cells were tested for the presence of the FLAG tag or shRNA by western blot analysis and immunofluorescence.

2.16.2 siRNA treated cells

m-IC$_{cl2}$ cells were cultured in 6 well plates and 13mm coverslips for 24 hours, or on inserts for 11 days. For each transfection, 3μl of siRNA to murine occludin (0.375μg, containing a mixture of three short target specific nucleotides (nt), 19 - 25nt in length, Santa Cruz) was added in 100μl transfection medium (OptiMEM, Invitrogen). 6μl of transfection reagent (Santa Cruz) was added in 100μl transfection medium and both solutions incubated for 5 minutes at 25°C. The solution containing the siRNA was then transferred into the solution containing the transfection reagent and incubated for a further 20 minutes at 25°C. The cells were rinsed with 1 ml of transfection medium before adding the siRNA-transfection reagent complex to them, in an additional 800μl transfection medium. The cells were incubated at 37°C, 5% CO_2 for 6 hours before adding either 1ml (for 6 well plates) or 0.5ml (for inserts) of normal growth medium containing 2× FBS for a further 24 hours. The media was then replaced with normal growth media for a further 24 hours before the cells were used on day 13. As a control, cells were transfected with a control scramble siRNA (Santa Cruz). Cells were tested for reduction of occludin by immunoblotting and immunofluorescence.

2.17 Bioinformatics

The murine protein sequence of occludin was used to search for potential binding proteins within the *T. gondii* database [1] using the default settings for parameter limitations (Expectation value 10, Maximum descriptions 50, Maximum alignments 50, low complexity filter). Proteins were BLASTed against the VT1, ME49 and VEG genomes. Proteins identified were aligned with occludin using the EMBOSS Pairwise Alignment Algorithms[2].

[1] http://www.toxodb.org

[2] `http://www.ebi.ac.uk/Tools/emboss/align/index.html`

2.18 Statistical Analysis

Error bars on all graphs presented in this thesis represent the standard error of the mean. All data was assessed for normal distribution using the Kolmogarov-Smirnoff test and for homogeneity of variance by the Levene test. For parametric data, either an independent t test, a paired t test, or a one way ANOVA was carried out. For non-parametric data the Mann-Whitney U test, the Kruskal-Wallis test, or the Wilcoxon Signed Rank test was used. Post-hoc analyses were carried out using the LSD test. Data was analysed using the Student Package for the Social Sciences Software (SPSS, version 19). P values of less than 0.05 were considered significant. Any data points that were more than two or more standard deviations away from the mean were considered outliers and disregarded from the analyses.

Chapter 3

Optimisation of a cell culture model for investigating interactions between epithelial cell tight junctions and *Toxoplasma gondii*

3.1 Introduction

Dalton *et al.* 2006, reported that infection by *T. gondii* caused a redistribution of claudin 3, occludin and ZO-1 in mice that were deficient in the T-cell receptor V$\gamma 7^+$ subset of intraepithelial lymphocytes [Dalton et al., 2006]. This thesis extends current knowledge on the effects of occludin following *T. gondii* infection, using an *in vitro* epithelial cell model.

There are three main ways to culture epithelial cells *in vitro*. These are by using primary cells, secondary cells or immortalised cells. Primary cells are derived directly from an organism and retain most, if not all, the functions of the original cell type, but are generally not sustainable in culture as the cells eventually die. Secondary cells are derived from explants of an organism and given the right culture conditions can survive for a prolonged period of time. However, they too may lose some of their functions and will eventually die. Immortalised cells can be derived from either primary or secondary cells that have been transformed usually by a viral oncogene such as the human papillomovirus (for example [Ryan et al., 1994]), the epstein-barr virus (for example [Amoli et al., 2008]), and the large T-antigen of simian virus 40 (SV40, for example [Gluzman, 1981; Whitehead et al., 1993]). Cell lines derived from cancer patients will have been transformed by unknown aetiologies.

SV40 works by inactivating Senescence-6 (SEN-6), p53 and Retinoblastoma genes, which regulate senescence [Resnick-Silverman et al., 1991;

Banga et al., 1997]. These cells continue to grow *in vitro* under the right culture conditions but due to their very nature, tend to loose characteristics of their normal cellular counterparts. However, to study epithelial cell biology, stable cell lines are always preferred and although will be somewhat different to *in vivo* cells, immortalised cell lines currently provide the best model.

Small intestinal cell lines Two rodent immortalised cell lines derived from the small intestine that are currently used and reported in the literature are the IEC-6 rat cell line and the m-IC_{cl2} murine cell line [Quaroni et al., 1979; Bens et al., 1996].

Intestinal epithelial cells -6 (IEC-6) cells were extracted from different areas of the intestine by scraping the intestinal mucosa and collecting crypt and villus cells [Quaroni et al., 1979]. All four epithelial cell types of the small intestine could be identified from cells that had grown in contact with mesenchymal factors [Quaroni et al., 1979; Kedinger et al., 1998]. Being non-transformed cells, they offer advantages over immortalised cell lines such as $CaCo_2$ in studying early cellular differentiation events and remain non-differentiated when cultured in the absence of mesenchymal factors [Wood et al., 2003]. They have been used to investigate changes in the replication of *T. gondii* in the presence of IFN γ [Dimier and Bout, 1993].

Murine intestinal cells, clone 12 (m-IC_{cl2}) cells were created by Bens *et al.* 1996, who used the SV40 T-antigen for generation of this trans-immortalised cell line [Bens et al., 1996]. Cells were derived from the lower part of the intestinal villus within the duodenum and jejunum, from 20 day old foetuses of L-type pyruvate kinase (L-PK)/TAg1 transgenic mice. The SV40 T-antigen is under the regulatory control of the 5' L-type pyruvate kinase gene, the expression of which is activated by D-glucose [Lefrançois-Martinez et al., 1994], and provides the cells an opportunity to become partially differentiated in culture under the right conditions [Bens et al., 1996]. This partial polarisation and differentiation state is representative of the cells found along the lower crypt-villus axis showing that in culture, the cells remain similar to when they were first extracted from the mice. However, they do express a defined apical membrane with short microvilli and villin, as well as ZO-1 and desmosomes. They are reported to accumulate sucrase isomaltase in their cytoplasm, express the polymeric Immunoglobulin receptor and Cystic Fibrosis Transmembrane conductance Regulator (CFTR) Cl^- channel, which confirms their

crypt like phenotype [Bens et al., 1996]. Furthermore, m-IC$_{cl2}$ cells may retain the ability to produce Paneth cells, staining positive for α-L-fucose glycoconjugates. In culture, the cells are reported to grow rapidly with a doubling time of 30 hours, and are fairly homogeneous in shape. They form a confluent monolayer, which is not flat but contains domes where the cells grow on top of each other. Bens *et al.* 1996, report that when the cells were grown on cell culture inserts they reach a transepithelial electrical resistance (TEER) of approximately 120Ω.cm^2 and are impermeable to ^{3}H inulin after 6 hours of addition [Bens et al., 1996]. The cell culture media is supplemented with various hormones, cofactors and growth factors to achieve the characteristics described. These include D-glucose for the activation of the L-PK gene; insulin to absorb glucose; tri-iodothreonine to increase metabolic rate stimulate protein synthesis and glycogen breakdown; transferrin for iron binding via plasma glycoproteins; selenium which acts as a cofactor for reducing anti-oxidant enxymes; and dexamethasone which acts as an anti-inflammatory to stress responses.

To date only a few reports have been published that use the m-IC$_{cl2}$ cell line. Of these, their response to LPS and infection of *Helicobacter hepaticus* and *T. gondii* have been investigated [Sterzenbach et al., 2007; Mennechet et al., 2002; Hornef et al., 2003]. These pathogen studies focussed on cellular responses via toll like receptors (TLRs) and interactions with lamina propria CD4$^+$T lymphocytes in m-IC$_{cl2}$ cells, respectively [Sterzenbach et al., 2007; Mennechet et al., 2002]. Both reports indicate that the cells are capable of producing and responding to various cytokines and other immune stimuli. Furthermore, they have been used to compare the rate of passage of botulinum toxin through small intestinal epithelial cells against that of the colonic epithelium [Couesnon et al., 2008]. m-IC$_{cl2}$ cells have been studied to determine the degree of virulence between different strains of *Salmonella enterica* subspecies; as a model for infection of *Salmonella* and rotavirus infection in the GI tract [Macartney et al., 2000; Suar et al., 2006]. These studies were all carried out using different substrates as the cells were cultured on inserts, 24 well plates or collagen I-coated plates, demonstrating that they can be used in a range of different applications. m-IC$_{cl2}$ cells have also been used in co-culture systems with lymphocytes derived from Peyers Patches to induce M cell development during a temperature shift; and bone marrow derived dendritic cells to investigate signalling pathways in the presence of enteric bacteria [Bahi et al., 2002; Zoumpopoulou et al., 2009]. This

provides additional evidence that these enterocytes are functional in an *in vitro* system.

The m-IC_{cl2} cells were chosen as a model of small intestinal epithelial cells in this thesis. This is because although the IEC-6 cell line is the most popular choice of small intestinal models, the cells are unresponsive to certain stimuli and differentiation of the cells seems difficult to achieve in normal cell culture systems [Quaroni et al., 1999]. They are also derived from the rat, making the cell line not compatible with original findings that this thesis is based upon [Dalton et al., 2006]. The m-IC_{cl2} cells, being trans-immortalised in the way they are, means that the cells maintain a differentiated state even when proliferating, providing a more physiological *in vitro* model for studying cells found along the crypt-villus axis [Bens et al., 1996].

To our knowledge, no study has yet reported any further information on the distribution of tight junction proteins (other than ZO-1), or adherens junction proteins within the m-IC_{cl2} cell line and, with the exception of the original paper, there is little information regarding cellular polarisation and differentiation when they are cultured on different substrates. However, the reports listed above clearly show the cells are responsive to infection, and that they are capable of being infected by *T. gondii*.

The first point of contact *T. gondii* has with its host is the small intestine although it is also capable of infecting the colon [Kowalik et al., 2004]. Murine colonic cell lines tend to be very specific to their required purpose and were therefore not a viable option for this study [Brattain et al., 1980; Kanaya et al., 2008]. Use of the human $CaCo_2$ cell line is well established within the field of cell culture, especially with ion transport studies [Ning et al., 2010; Roberts et al., 2010; Lau et al., 2011]. The cells derive from a colonic adenocarcinoma and are widely used for investigating intestinal cell biology. They exhibit a highly heterogenous phenotype displaying mixed characteristics of colonic and small intestinal enterocytes. The C2BBe1 cell line is a derivative of the $CaCo_2$ line that was selected for exclusive expression of villin on the apical membrane, and are considered to be more similar to the cells found in the small intestine than the colon [Peterson and Mooseker, 1992]. For the purpose of this thesis, these cell lines were used to determine the reproducibility of results obtained from the m-IC_{cl2} cells that have not been as extensively used as colonic epithelial cells.

3.2 Results

Initial characterisation was performed in order to develop the optimal conditions for investigating tight junction dynamics during infection by *T. gondii*, by testing a variety of growth substrates for developing a polarised and differentiated m-IC_{cl2} cell monolayer.

3.2.1 Characterisation of tight junction expression in m-IC_{cl2} cells grown on different substrates

The cells were grown on a number of substrates including glass, plastic, matrices and PET membranes, and tested for their ability to express tight junction and adherens junction proteins.

3.2.1.1 m-IC_{cl2} cells express adherens junction and tight junction proteins when grown on glass coverslips

Plating cells onto glass coverslips is a simple and efficient way of obtaining a confluent monolayer in a short space of time. When cells were plated at a density of more than 1 x 10^5 per ml onto 13mm circular glass coverslips, they reached confluency (100% cell coverage over the coverslip) after 24 hours. Figure 3.1 shows that cells were partially polarised, expressed the adherens junction protein β catenin at the lateral junctions, occludin at the membrane and in the cytoplasm, and carbohydrates N-acetylglucosamine and galactosyl (β-1,3) N-acetylgalactosamine (referred to as surface carbohydrates from this point onwards) on the lateral and apical surfaces. However, the cells did not survive for more than four days, and were only 10µm in depth, whereas small intestinal epithelial cells *in vivo* are approximately 20 - 30µm in depth [Massey-Harroche, 2000].

3.2.1.2 Cells are cuboid and polarised when cultured with an extracellular matrix complex

m-IC_{cl2} cells were plated onto either a collagen I and fibronectin matrix (1:1 ratio) or a collagen I gel, within a 6 well dish. After eight days, morphology and tight junction protein expression was assessed. Rationale for choice of extracellular matrix is based on the fact that these proteins are naturally found in cells of the small intestine [Rothen-Rutishauser et al., 2000]. This enabled a increased rate of adherence to the substrate and decreased the time required to reach a differentiated state (Figure 3.2).

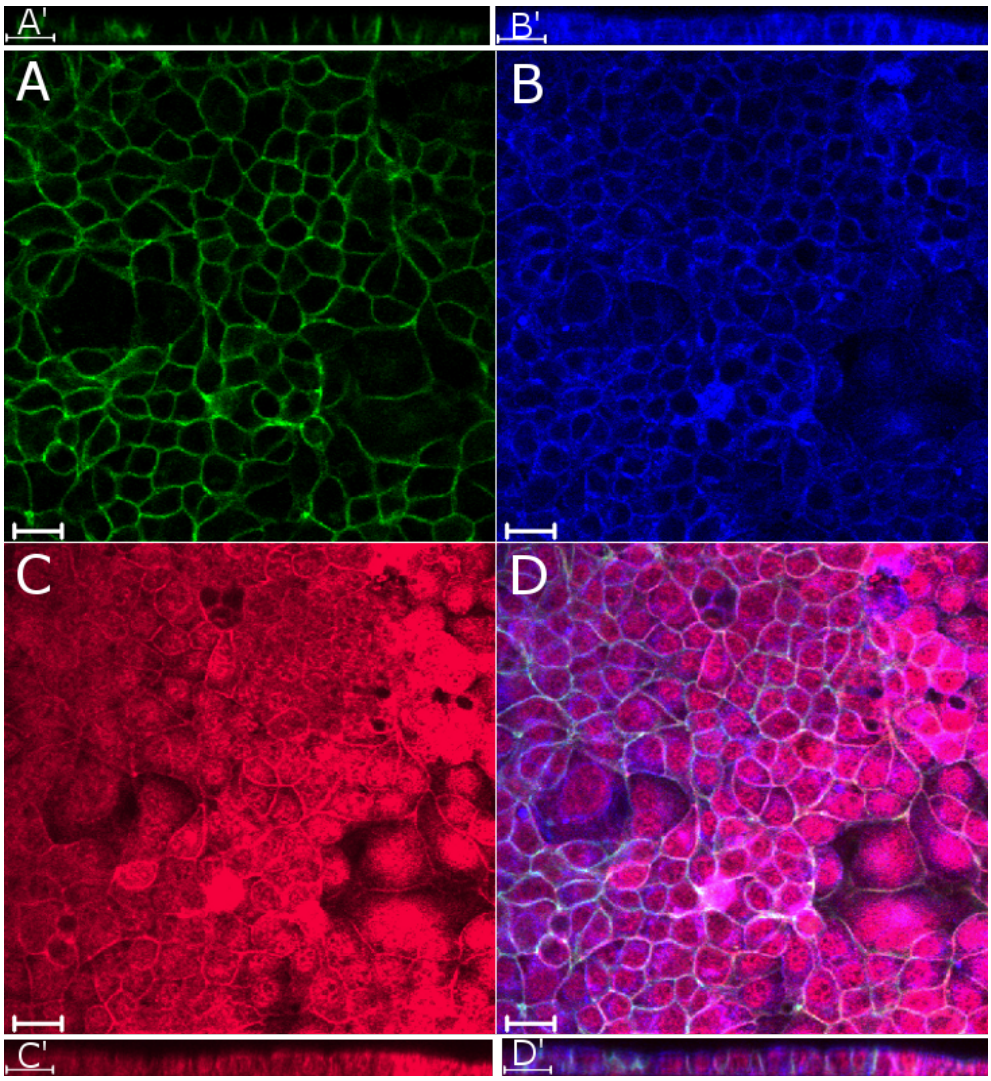

Figure 3.1: Morphology of m-IC$_{cl2}$ cells grown on glass coverslips. Cells were plated onto coverslips, fixed with 2% paraformaldehyde (PFA), and stained for cellular proteins. β catenin is shown in green (A), occludin in red (C), and surface carbohydrates labelled in blue (B). Merged images are shown in D. (A-D) represent XY plane images (where the Z-axis is perpendicular to the substrate) and (A'-D') represents XZ plane images. Scale bar = 20µm.

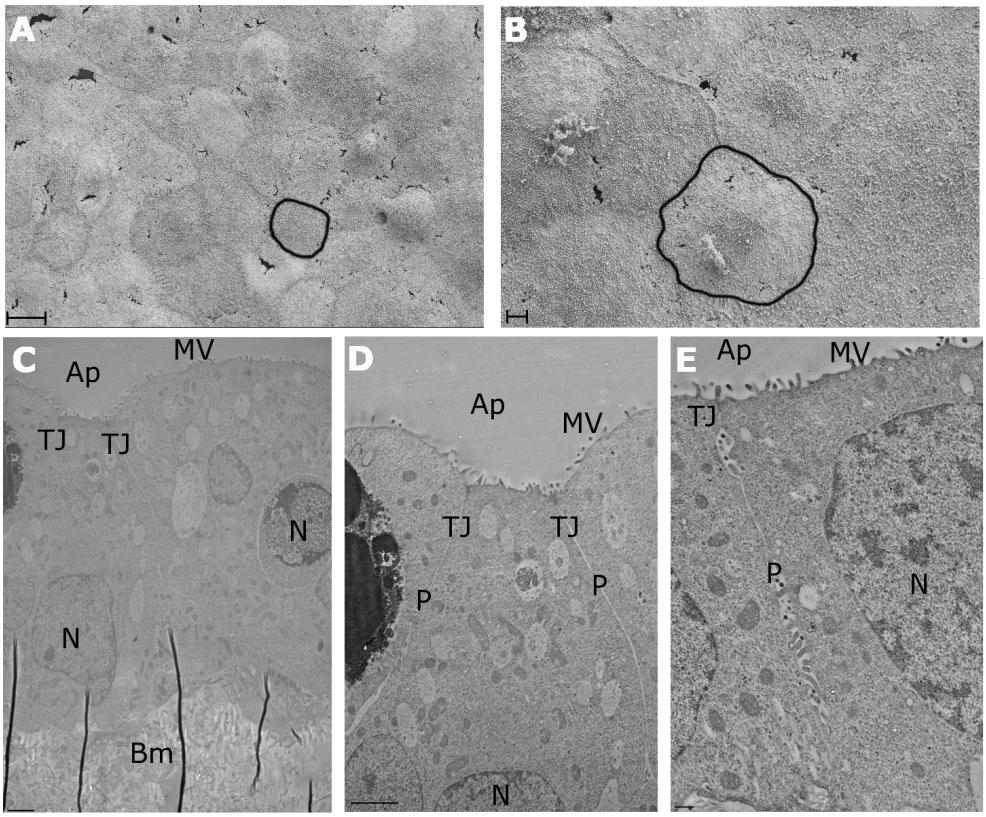

Figure 3.2: Cell morphology of m-IC$_{cl2}$ cells grown with extracellular matrix molecules. Cells were cultured for 8 days on either a collagen I and fibronectin matrix, or a collagen I gel and analysed by SEM (A and B) and TEM (C-E). (A) Magnification 3000×, scale bar 10µm; (B) magnification 8000×, scale bar 2µm. The black solid line represents an example of a cell outline. Using TEM, tight junctions (TJ) and the paracellular pathway (P) are visible, as are microvilli (MV) on the apical (Ap) surface, and basally located nuclei (N). The extracellular matrix can also be seen (Bm). (C) Magnification 1100×, scale bar 2µm; (D) magnification 2100×, scale bar 2µm; (E) magnification 3500×, scale bar 500nm.

These substrates also allow there to be a substance between the basal membrane of the cells and the plastic dish, creating a more physiological system.

After eight days of culture, cells were confluent and a tight monolayer had formed with visible cell junctions (Figure 3.2). Microvilli were seen on the apical surface of the cells, and the nuclei basally located, which are all indicators the cells have become polarised [Wakabayashi et al., 2007]. Cells survived for up to 10 days on these extracellular matrices before they begin to detach and die.

Cells cultured in the presence of extracellular matrices expressed defined β catenin staining at the lateral membrane, clear apically located carbohydrates and apically located occludin (Figure 3.3). Cells were approximately 15µm in depth. This substrate increased the potential for the m-IC$_{cl2}$ cells to form a polarised and differentiated monolayer

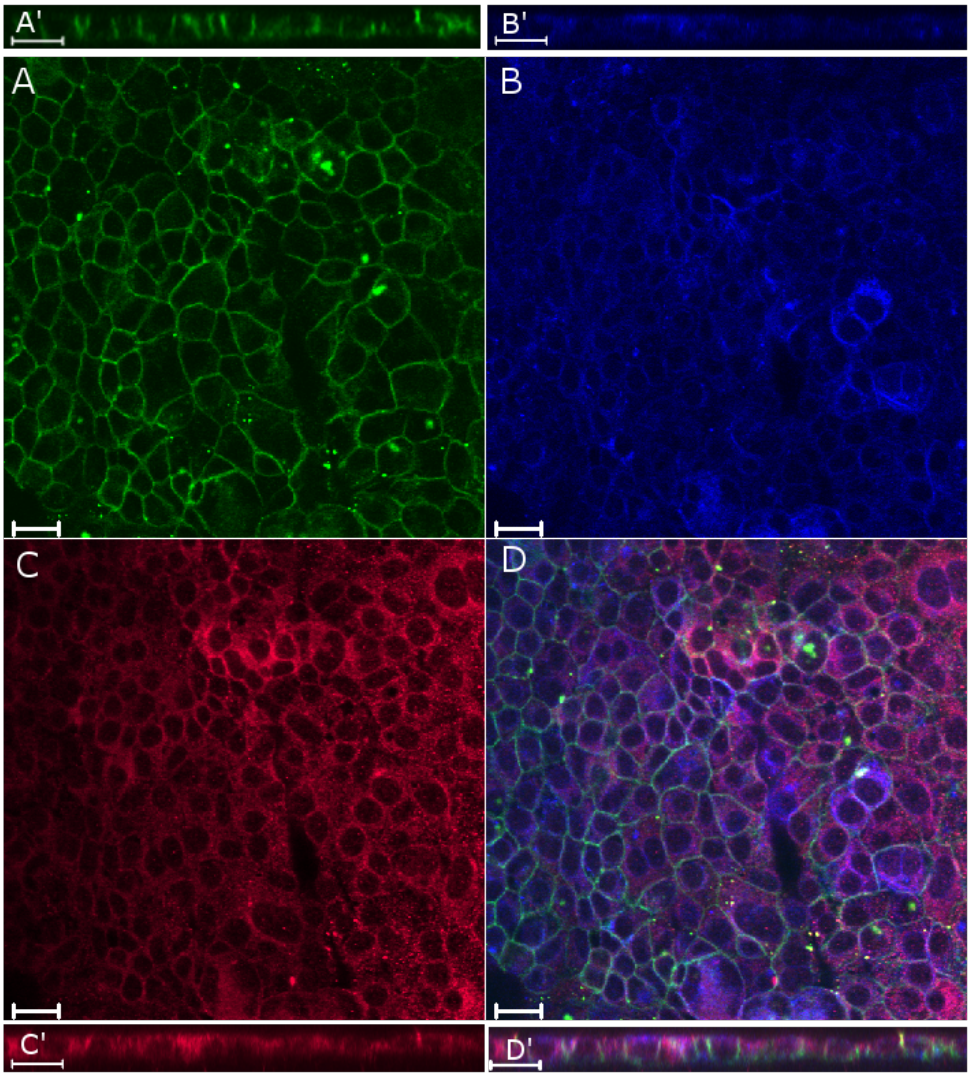

Figure 3.3: Protein expression of m-IC$_{cl2}$ cells grown with extracellular matrix molecules. Cells were grown on a collagen and fibronectin matrix or a collagen gel for 8 days. Cells were fixed with acetone and stained for β catenin (green, A), surface carbohydrates (blue, B) and occludin (red, C). Z stack images are shown in A'-D'. Scale bar 20µm.

that was embedded within an extracellular matrix. As occludin appeared to be only expressed on the apical domain and not concentrated at the tight junctions, the cell conditions were still not optimal for evaluating occludin regulation.

3.2.1.3 Cells cultured on plastic form dome-like structures

m-IC$_{cl2}$ cells plated at a density of 2 x 10^5 cells reached confluency on a plastic substrate, within 48 hours (Figure 3.4a). This is indicative of a high numbers of cells adhering to the substrate, and/or rapid replication. They also possessed the capacity to form dome like structures within the monolayer (light areas), which represent the apparent crypt-like pheno-

type as described by Bens *et al.* 1996, and observed by Paul *et al.* 1993, when using a rat small intestinal cell line (Figure 3.4a) [Bens et al., 1996; Paul et al., 1993]. Cell recovery was typically 2 - 2.5 x 10^6 cells, from a 25cm^2 flask eight days after plating. The amount of occludin increased in both the soluble (cytoplasmic) and insoluble (membrane-associated) fractions over time and was most prominent around day 9 - 21 (Figure 3.4b).

When other tight junction proteins were analysed, claudin 2 was found to be associated with the membrane fraction, claudin 4 was expressed in both the cytoplasm and the membrane, but claudin 7 was only detected at low levels in both fractions (Figure 3.4c). ZO-1 was mainly found within the cytoplasm, but was also associated with the membrane fraction. Occludin was present in both the cytoplasmic and membrane-associated fractions. The shift in molecular weight in the membrane-associated fraction of occludin was predicted due to the increased phosphorylation status when present at the tight junctions [Wong, 1997]. β catenin was also present in both the cytoplasm and membrane-associated fractions.

3.2.1.4 Cells cultured on transparent polyethylene terephthalate (PET) tissue culture inserts are optimal for studying barrier function and tight junction proteins.

Culturing cells on a collagen base provided some depth underneath the monolayer. However, as the occludin distribution was not optimal at the tight junctions, and barrier function would be difficult to quantify, a different approach was investigated. Bens *et al.* 1996, grew cells on a collagen-coated semi-permeable transparent filter with a pore size of 0.4µm [Bens et al., 1996]. However, as these cells will be used in this thesis for infection with *T. gondii,* which is approximately 2µm by 7µm, a pore size large enough to accommodate transmigration of parasites was required [Swedlow et al., 2002]. Therefore, cells were grown on PET inserts with a pore size of 8µm. In this thesis, coating the insert membrane with collagen was not seen to improve cell monolayer integrity or levels of polarisation and differentiation (data not shown), and was not included in subsequent experiments.

After six days, plating at a density of 5.5 ± 3.5 x 10^5 cells, a confluent monolayer had formed, and after 14 days, domes had also formed, indicated by the darker patches of cells seen in Figure 3.5.

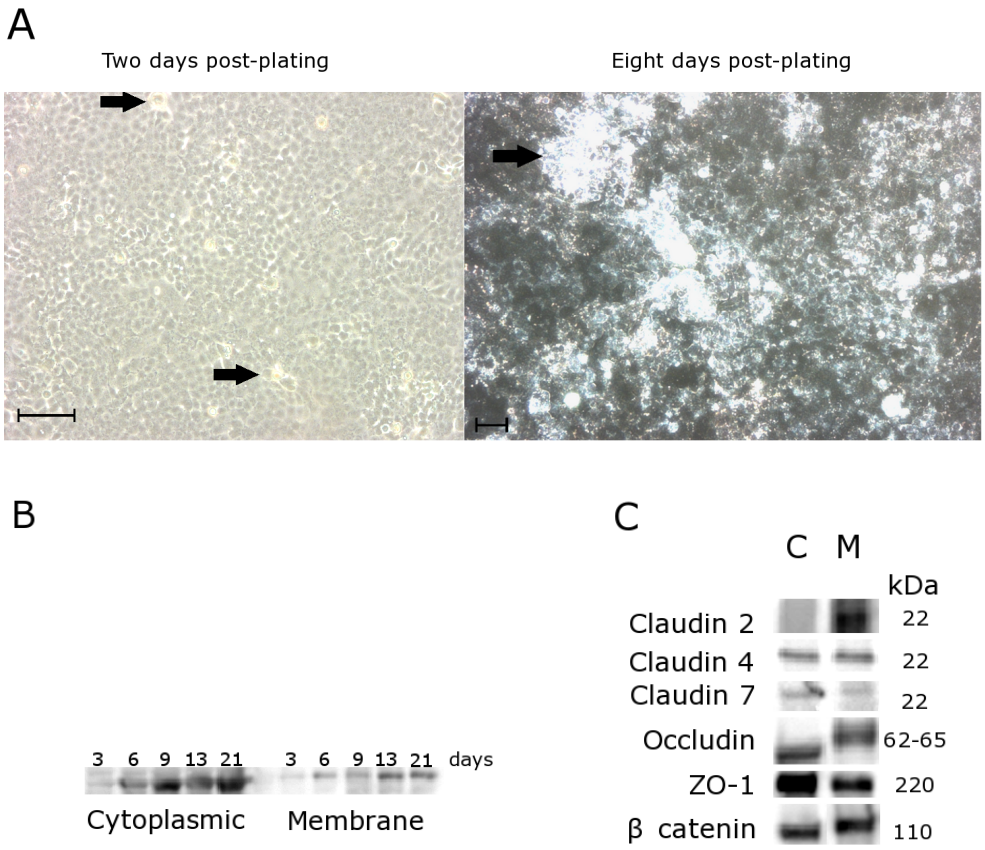

Figure 3.4: Characterisation of m-IC$_{cl2}$ cells cultured on plastic surfaces. Cells were plated on 6 well dishes or 25cm^2 cell culture flasks. Figure 3.4a shows cells after two (left) and eight (right) days of culture on 6 well dishes. Arrows indicate examples of cell doming. Magnification 10×, scale bar 50µm. Cells cultured on 25cm^2 flasks for 3 - 21 days were analysed by immunoblotting for the presence of occludin (Figure 3.4b). The expression of claudin -2, -4, -7, ZO-1, occludin and β catenin in the cytoplasmic (C) and membrane associated (M) fractions were also tested (Figure 3.4c).

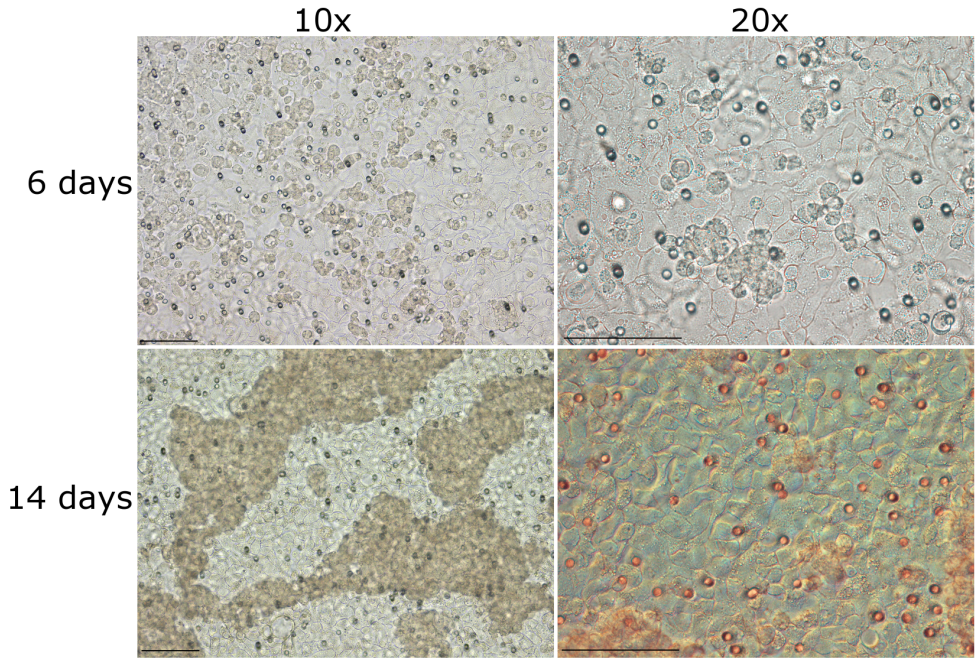

Figure 3.5: m-IC$_{cl2}$ cells cultured on PET inserts. Cells were grown for 14 days and analysed by light microscopy. Insert pores were visible as distinct circles (white arrows). Black arrows represent dome formation. Magnification on left 10×, on right 20×. Scale bar = 100μm. Images taken by Mary Parker (Institute of Food Research, Norwich, UK).

3.2.2 Characterisation of cells on PET inserts

Having established the ability of m-IC$_{cl2}$ cells to grow on PET inserts, it was important to determine the optimal time post-seeding to use the cells. Barrier function was determined by measuring transepithelial electrical resistance (TEER), permeability and the expression of tight junction proteins [Anderson and Itallie, 2009; Al-Sadi and Ma, 2007]. The expression of occludin at the tight junctional complex was imperative for the purposes of this study.

3.2.2.1 The expression of tight junction and adherens junction proteins in cells cultured on PET inserts

Approximately 9 x 10^5 cells were cultured on inserts for either 4, 8 or 13 days. An established homogeneous monolayer was observed after 13 days of plating, coinciding with localisation of occludin to tight junctions and lateral localisation of β catenin (Figure 3.6).

Confirmation of specific immunofluorescent staining was performed using negative isotype controls in place of the primary antibody (Figure 3.7).

By day 13 the cells were approximately 14μm in depth and were

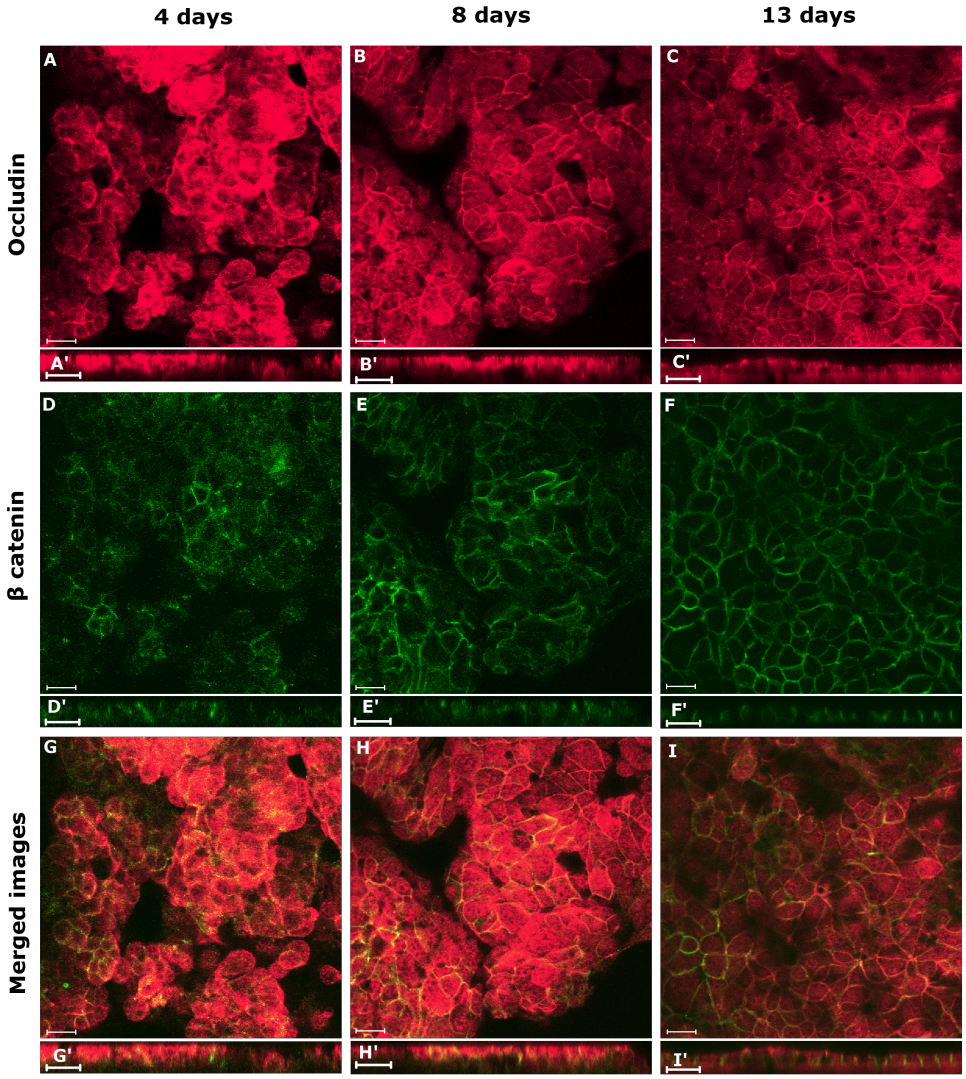

Figure 3.6: Expression of occludin and β catenin in cells cultured on inserts for 4 - 13 days. Cells were cultured on inserts for either 4 days (A,D,G), 8 days (B,E,H) or 13 days (C,F,I). Cells were fixed with 2% PFA and stained with antibodies specific for occludin (red, A,B,C) and β catenin (green, D,E,F), and analysed by confocal microscopy. Merged images are shown in G,H, and I. A - I represents images in XY planes, and A' - I' represents images from XZ planes. Scale bar = 20μm.

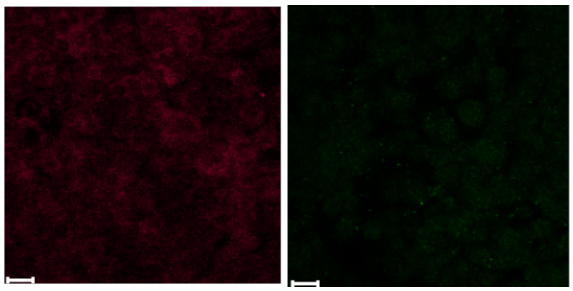

Figure 3.7: Negative controls for occludin and β catenin. Negative controls for occludin (red, rabbit IgG) and β catenin (green, mouse IgG). Controls for other tight junction proteins also revealed minimal background staining (data not shown). Scale bar = 20μm.

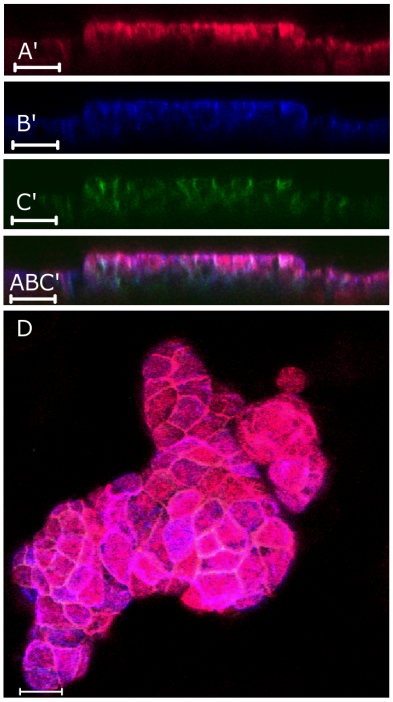

Figure 3.8: Doming of m-IC$_{cl2}$ cells cultured on PET inserts. Cells were cultured for 13 day, fixed with 2% PFA and stained for occludin (red, A'), surface carbohydrates (blue, B') and β catenin (green, C'). Individual XZ planes are shown and the merged image is shown in ABC'. A merged XY image illustrating a dome like structure is depicted in (D). Scale bar 20μm.

cuboid in shape. Cell depth increased to approximately 20μm where dome-like structures were evident (Figure 3.8). A confluent monolayer was still present within these structures.

Other tight junctional proteins (claudin 2, claudin 4, ZO-1) were analysed to determine their expression profile on the PET substrate. Claudin 2 and ZO-1 were present in both the cytoplasm and the membrane, whereas claudin 4 was concentrated at the membrane (Figure 3.9).

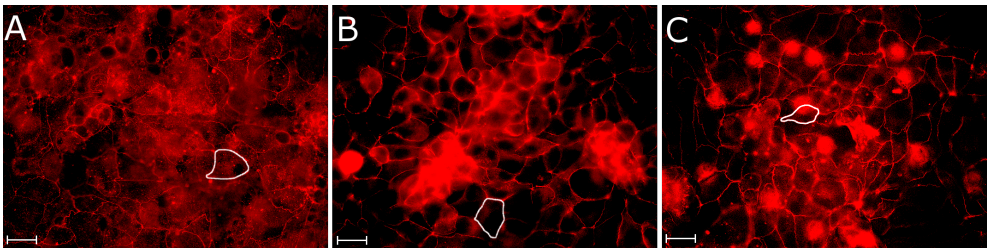

Figure 3.9: Expression of tight junction proteins in cells cultured on PET inserts. Claudin 2 (A), claudin 4 (B) and ZO-1 (C) were visualised by confocal microscopy. White lines highlight a cell outline. Circular-like objects where staining is intensive, is non-specific and highlights the positions of the pores (Appendix I). Scale bar = 20μm.

3.2.2.2 Tight junctions and adherens junctions in human colonic epithelial cells

As a comparison, immortalised colonic epithelial cell lines $CaCo_2$ and C2BBe1 were plated onto 8µm PET inserts and cultured for 16 days. These additional cell lines were used to test that any effects seen from m-IC_{cl2} cells were similar to colonic derived cell lines. Both colonic cell lines show occludin localisation at the tight junctions and β catenin at the lateral membrane, using surface carbohydrate markers as an indicator of the apical membrane (Figure 3.10).

3.2.2.3 Membrane integrity of small intestinal and colonic cell lines on PET inserts

Tight junctions form an efficient barrier between the apical and basolateral domains. TEER and permeability (using a 3kDa FITC-dextran molecule) were assessed as measures of barrier function.

Approximately 7 x 10^5 cells were plated onto 8µm PET inserts and cultured for up to 17 days. TEER was recorded every 24 - 48 hours. Intra- and inter-experimental variation was low (Figure 3.11a). TEER gradually increased from 20Ω.cm^2 to 120Ω.cm^2 before declining after day 16 as the cells detached from the insert membrane and died. This matches values obtained in other studies [Bens et al., 1996]. TEER was highest between day 10 and 14. Each time point represented data from 20 - 245 inserts over 3 - 14 experiments, with the exception of day 14 onwards. These data represent only one insert, as following on from results seen in Figure 3.4b and Figure 3.6, occludin was expressed at higher levels after 9 days at the tight junction complex and therefore it was not considered necessary to extend cell culture on inserts for more than 13 days.

On day 13, cells were counted using a haemocytometer (2.3 x 10^5, n = 4) or from an estimate of cells per field of view by confocal microscopy (1.2 x 10^5). Numbers equated to approximately 30% of the original cell number plated. As a comparison, 2.65 x 10^5 C2BBe1 cells were counted after 13 days of culture (55.8% of original number added).

The permeability of the monolayer was measured by the amount of FITC-dextran present in the basal compartment after two hours of addition to the apical compartment. A blank insert was used as a control to determine the maximum amount of dextran that could leak through the insert membrane, which was approximately 4.6%. In the presence of cells this was reduced to 0.3%. Approximately 15.5% of FITC-dextran

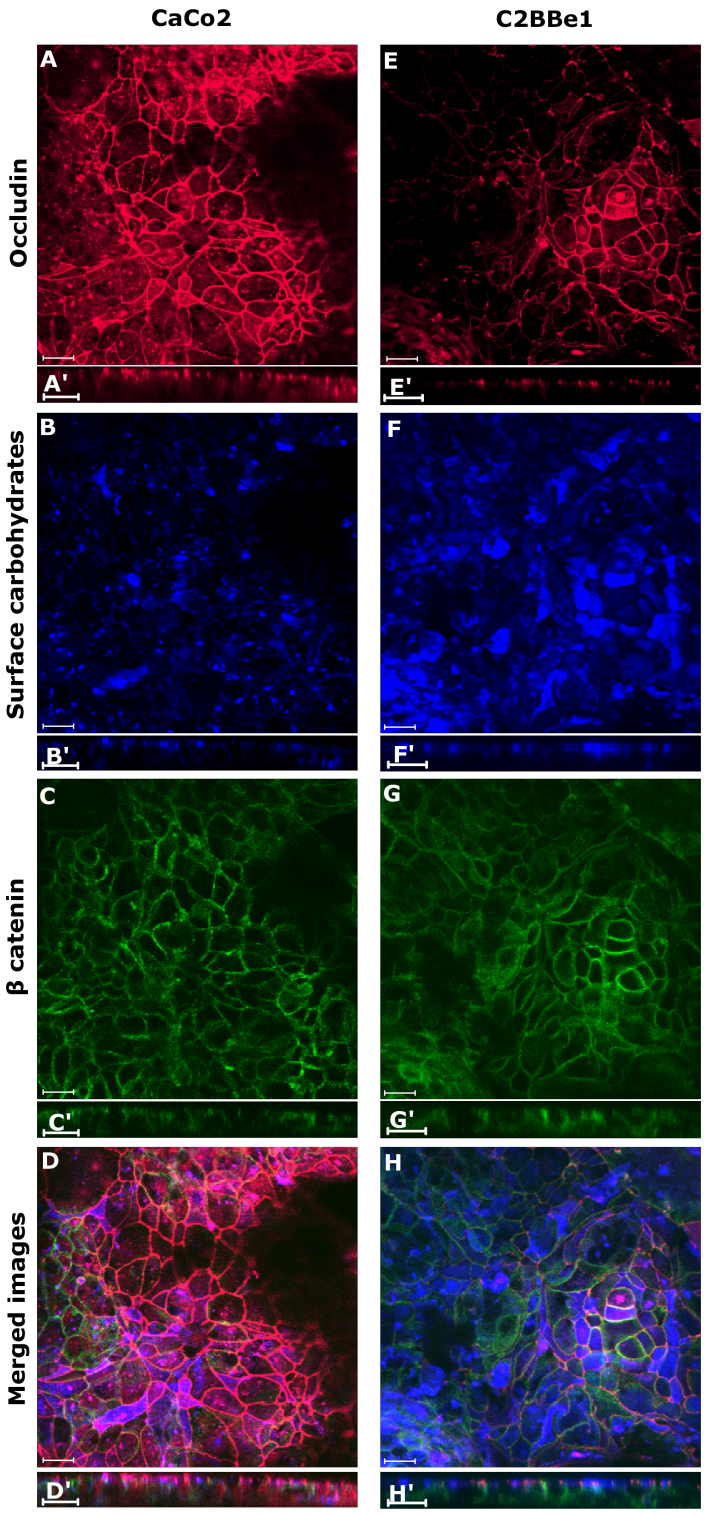

Figure 3.10: Junctional protein staining in $CaCo_2$ cells and C2BBe1 cells. $CaCo_2$ cells (left hand panel) and C2BBe1 cells (right hand panel) were cultured on inserts and fixed with acetone. Cells were stained for occludin (red, A, E), β catenin (green, C, G), and surface carbohydrates (blue, B, F). Merged images shown in D and H. A - H shows cells in the XY plane, A' - H' shows cells in the XZ plane. Scale bar = 20μm.

was associated with or absorbed by the cells, or within the membrane itself (Figure 3.11b).

TEER was also measured every 48 hours in CaCo2 and C2BBe1 human colonic epithelial cells (Figure 3.12). TEER increased more rapidly in $CaCo_2$ cells and C2BBe1 cells compared to m-IC_{cl2} cells. After 16 days both colonic cell lines reached a TEER of 450 $\Omega.cm^2$, nearly 4 times higher than m-IC_{cl2} cells. These figures match the numbers expected from the supplier.

C2BBe1 cells were permeable to 0.2% of total FITC-dextran following 2 hours of addition (data not shown).

All three cell lines produce a resistant, selectively impermeable monolayer after 13 days of culture on PET inserts, with colonic cells generating a tighter barrier compared to m-IC_{cl2} cells.

3.2.3 Calcium withdrawal decreases TEER and disrupts the m-IC_{cl2} cell monolayer

Calcium is required for the formation and development of tight junctions [Nigam et al., 1992]. Calcium withdrawal and subsequent addition (known as the calcium switch method) is a widely used technique to disrupt tight junctions and was used in this study as an indicator of the responsiveness of cells to stimuli [Nigam et al., 1992]. In order to determine whether changes in TEER and permeability could be detected, cells were cultured on PET inserts for 12 days before replacing normal m-IC_{cl2} cell media with calcium-free DMEM (Invitrogen) supplemented with 2% FBS, L-glutamine and HEPES, for 24 hours.

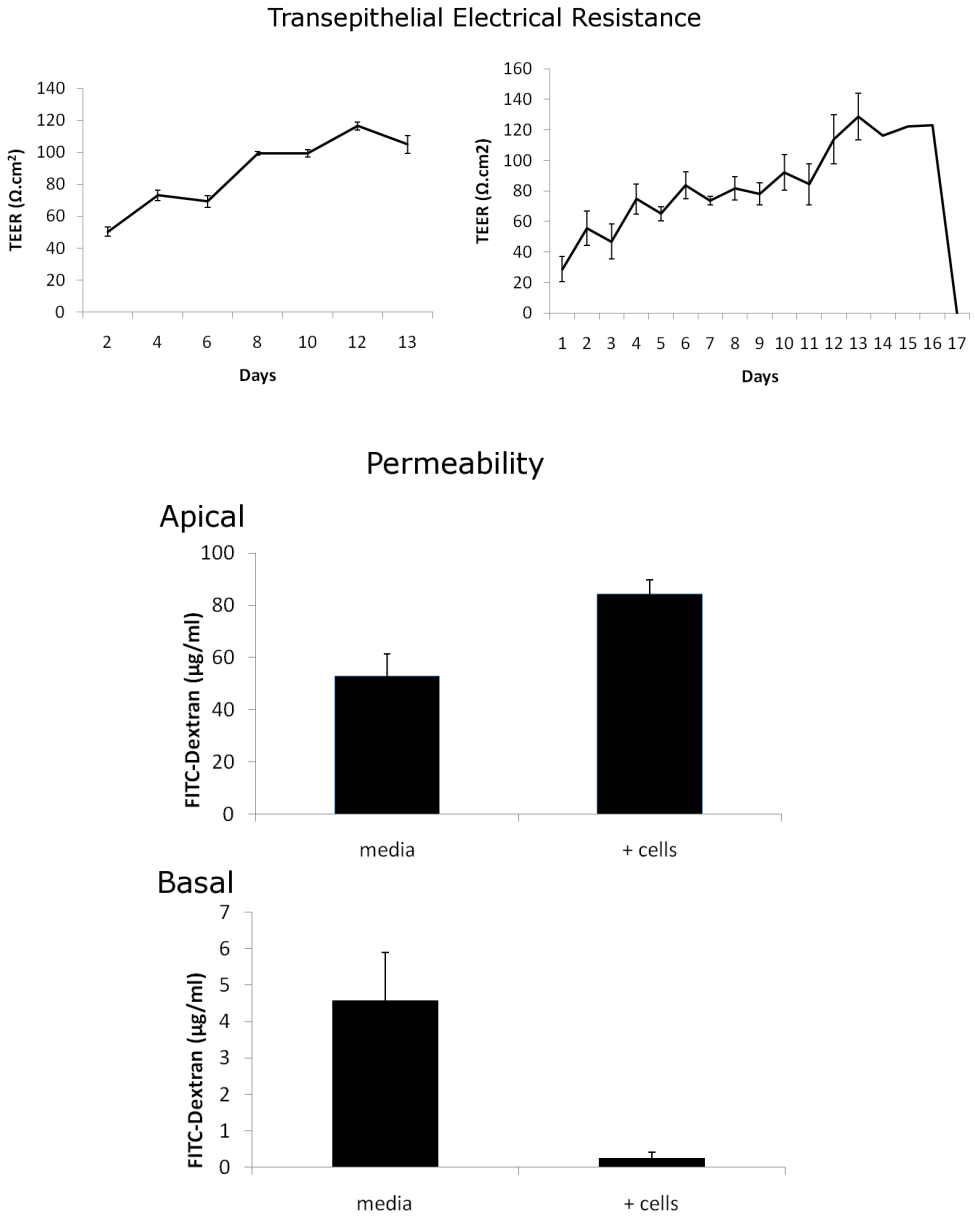

Figure 3.11: Assessment of barrier function in m-IC$_{cl2}$ cells cultured on PET inserts. TEER was recorded every day for 17 days. Within an experiment (left), and between experiments, TEER is similar between inserts. Data represents an experiment with biological replicates (left) and 15 independent experiments each with biological replicates (with the exception of day 14 onwards, right).
Permeability was measured by the amount of 3kDa FITC-dextran that could be found in the basal compartment after 2 hours of addition to the apical compartment. Results represent data from 7 independent experiments.

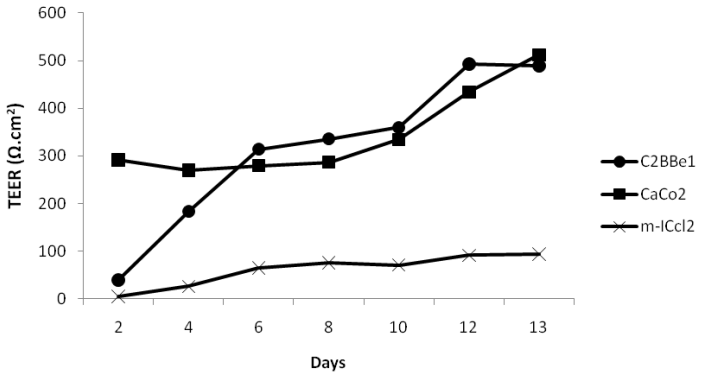

Figure 3.12: Comparative analysis of TEER in m-IC_{cl2} cells, $CaCo_2$ cells and C2BBe1 cells. TEER was recorded every 48 hours after plating the cells. Data represents one experiment with biological replicates.

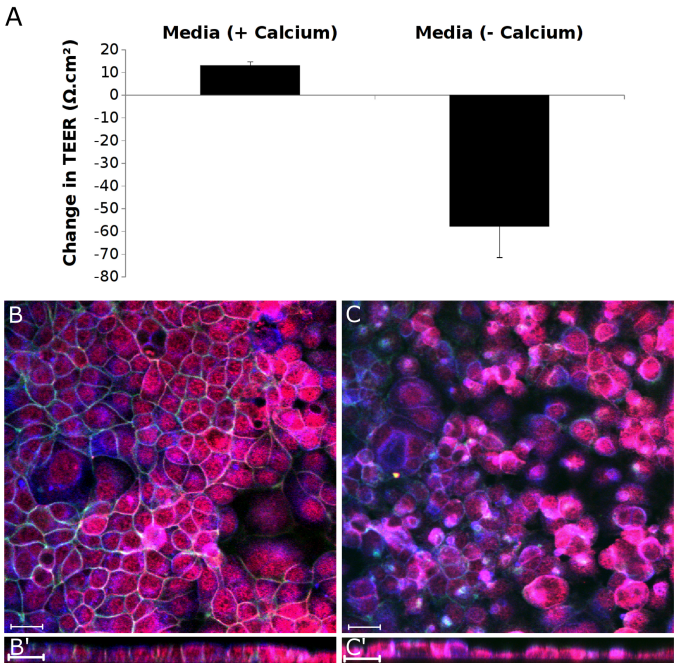

Figure 3.13: Calcium withdrawal negatively affects barrier function in m-IC_{cl2} cells. Cells were cultured on inserts (A) or coverslips (B-C). Calcium was removed from the media and effects on TEER, occludin (red) β catenin (green) and surface carbohydrates (blue) were assessed. Change in TEER is shown as the difference before and after treatments. Data represents an experiment for (A) and 4 independent experiments for (B-C). Scale bar 20µm.

As expected, TEER significantly decreased after calcium withdrawal, by 48.5% over 24 hours, in contrast to cells in media containing calcium, whose TEER increased by 10% ($P<0.001$, Figure 3.13). Cells cultured on PET inserts for 24 hours in calcium-free media did not survive the immunofluorescent staining protocol. However, an example of how cells on coverslips were affected by removing calcium from the media is illustrated in Figure 3.13.

These results show that the cell culture insert system is capable of

detecting changes in TEER and permeability following treatment.

3.3 Discussion

An *in vitro* assay was developed to use in this thesis for the infection of epithelial cells by *T. gondii.* Barrier integrity was measured by TEER and permeability, and polarisation and differentiation of cells measured by the expression of junctional proteins.

To date, the use of m-IC_{cl2} cells has been mainly limited to investigations in the response to pathogenic stimuli, with a focus on cellular immune responses. Since the tight junctions have not yet been characterised in this cell line, it was necessary to do so whilst determining the optimal growth conditions for promoting polarisation and differentiation of the cells. Results presented here show that the cells are capable of growing on glass coverslips, collagen I and fibronectin matrix or gel, plastic and PET substrates, with an increasing degree of polarisation and differentiation respectively. Optimal growth occurred on plastic and PET membranes, where the cells survived for up to 21 and 16 days, respectively.

On glass coverslips the cells expressed lateral β catenin and apical surface carbohydrates (N-acetylglucosamine and galactosyl (β-1,3) N-acetylgalactosamine), indicating that initial stages of polarisation had occurred. The staining of occludin was not concentrated to the tight junctions and the cells were vertically thin. However, this substrate was used for measuring changes in invasion rates by *T. gondii*, as it provided the most feasible method of calculating infection of m-IC_{cl2} cells (Table 3.1).

Substrate	Experiment	Method	Chapter
Glass coverslips	Proportion of infected cells	H&E	4, 5
Collagen/ fibronectin gel/ matrix	Location of parasites within and between cells	Electron and confocal microscopy	4, 5
Plastic	Quantification of changes in occludin distribution following infection, occludin-binding partners	Immunoblotting, immunoprecipitation and mass spectrometry	4, 5, 6
PET	Location of parasites, visualisation of tight junction proteins, measurements of barrier function	Confocal and fluorescent microscopy, TEER and FACS	4, 5, 6

Table 3.1: Summary of different substrates used for experiments throughout this thesis.

A more defined monolayer was achieved by culturing the cells on either a collagen I and fibronectin matrix, or a collagen I gel. This provided a basement membrane for the cells to adhere to and for the purposes of this study, would provide a medium for transmigrating parasites to enter. This monolayer produced polarised cells, as indicated by the lateral staining of β catenin and the apical staining of surface carbohydrates, tight junction formation, a basal nucleus and microvilli on the apical surface. Occludin was apically located although not concentrated at the tight junctional complex, suggesting that the cells were not fully differentiated. This substrate was chosen for electron microscopy analysis because it provided the most efficient method to prepare the cells for visualisation (Table 3.1).

Cells cultured on plastic often formed dome-like structures, possibly mimicking crypt-like formations. The cells expressed a variety of selected tight junction proteins and their location in the membrane-associated fraction provides evidence of cellular polarisation and differentiation. This substrate was used for investigating quantitative changes to junctional protein location in cytoplasmic and membrane-associated regions, upon *T. gondii* infection (Table 3.1).

PET cell culture inserts offered the most accessible method for providing a luminal domain, where substances can be added to the apical side of a monolayer, and a mucosal domain, where substances can be detected from the basal side of a monolayer (and vice versa) [Wakabayashi et al., 2007]. To determine when the cells were polarised, differentiated, and expressing tight junctional proteins, TEER and permeability were measured as indicators of ionic conductivity and molecular flux through the paracellular pathway, in combination with immunofluorescence. By day 13, cells were homogeneous in morphology, cuboid in shape and approximately 14μm in depth. Permeability to 3kDa sugar was low and the cells exerted a stable TEER across the PET membrane indicating that the epithelial barrier was functional and intact.

Polarisation was progressive, whereby the expression of β catenin at the lateral junctions increased from day 4 to 13. By day 13, the expression of occludin was found at both the tight junction complex and in the cytoplasm. To visualise junctional proteins, cells were fixed with either acetone or 2% PFA, each of which resulted in different staining patterns (Appendix H). Fixation with acetone enhances the visual degree of membrane-associated occludin and fixing with PFA shows a higher degree of nuclear and cytoplasmic occludin in addition, which could be

non-specific staining. PFA cross-links proteins during fixation and preserves structure, but decreases antigenicity which could account for the increased cytoplasmic staining. Differences in immunofluorescent staining according to fixative have been observed and discussed by Matter and Balda, 2003 [Matter and Balda, 2003]. The reason that both methods were employed in this thesis was because YFP-fluorescent signals associated with the *T. gondii* strain used in this study, were lost with acetone but retained with PFA fixation (Appendix H).

The cell number after 13 days of culture was surprisingly low compared to the original number of cells added. This may be due to several reasons, one of which is that although every care was taken to add the cells directly onto the membrane, light microscopy images revealed that cells could grow up the sides of the insert, probably in preference to the plastic over the PET. Additionally, cells were able to grow on the underside of membranes after migration through the insert pores, although these cells never became confluent or polarised (data not shown). The low number could also suggest that cells did not replicate to a high extent and a large number of cells may not have initially adhered to the membrane. After 48 hours of plating, the media was changed, with non-adherent cells being discarded at this point.

Expression of claudin 2, claudin 4 and ZO-1 showed that the tight junction complex is fully developed on inserts by day 13. Claudin 2 is involved in the formation of cation-selective channels, whereas claudin 4 decreases cation selectivity, being a channel to chloride ions and a barrier to sodium ions [Amasheh et al., 2002; Chiba et al., 2008]. These proteins are expressed along the crypt-villus axis in a gradient like fashion [Chiba et al., 2008]. Claudin 7 has similar functions to claudin 2 and although it is expressed along the crypt - villus axis, its involvement in colorectal tumour genesis suggests a more important role in the colon than the small intestine, which may explain the low levels in m-IC_{cl2} cells [Darido et al., 2008; Bornholdt et al., 2011; Fujita et al., 2006]. ZO-1 is a cytoplasmic plaque protein and links occludin to the tight junctional complex [McNeil et al., 2006]. Claudin 2, claudin 4 and ZO-1 are all located at the tight junctional complex in m-IC_{cl2} cells.

Having determined the parameters of cell culture on inserts, a calcium switch method was used to check the responsivity of the cells. The lack of calcium in the media destroyed tight junctions, depolarised cells and resulted in detachment from the insert membrane. The extent of calcium withdrawal was visualised by confocal microscopy, showing complete in-

ternalisation of occludin and β catenin. Therefore, the insert culture system was deemed functional and suitable for use in subsequent studies to evaluate the effects of *T. gondii* on tight junction barrier function (Table 3.1).

This chapter represents a first attempt to characterise different tight junction proteins in the m-IC_{cl2} cell line.

Chapter 4

Infection of small intestinal epithelial cells with *Toxoplasma gondii*

4.1 Introduction

Toxoplasma gondii is an obligate intracellular parasite that has the ability to infect all cell types [Carruthers and Boothroyd, 2007; Lei et al., 2005]. Most natural infections occur following consumption of contaminated food or water. Thus the first point of contact between the parasite and the host is the gastrointestinal tract. Previous evidence has shown that the parasite can pass through the cells of the small intestine using a range of different mechanisms. The first is via active penetration of a host cell [Morisaki et al., 1995], the second via the paracellular pathway [Barragan et al., 2005] and the third by using localised mucosal immune cells such as dendritic cells, in a trojan horse-like mechanism [Lambert et al., 2006].

Although the process of invasion that *T. gondii* employs to infect a cell has been previously documented [Morisaki et al., 1995], it is not clear from the literature whether or not tachyzoites are capable of exiting intestinal epithelial cells from the basolateral membrane following short term infection (that is, before parasite replication). Sporozoites and bradyzoites have been shown to leave host cells without lysing them, and infect neighbouring cells, suggesting that invasion via the lateral membrane is possible [Speer et al., 1997; Dzierszinski et al., 2004].

Of all the proteins involved in the junctions of the paracellular pathway, only claudin 3, ZO-1, ICAM-1 and occludin have been studied in regards to *T. gondii* infection. ZO-1 remained unchanged but an upregulation of ICAM-1 was observed in MDCK II cells following infection [Barragan et al., 2005]. In mice that lacked the TCR-V$\gamma 7^{+}$ subset of intraepithelial lymphocytes (IELs), a redistribution of claudin 3, occludin and ZO-1 occurred following infection by *T. gondii* [Dalton et al., 2006].

The trojan horse mechanism suggests that as immune cells, such as dendritic cells, sample the environment for foreign antigen, they become more susceptible to *T. gondii* infection. Furthermore, the parasites may increase the migration of these cells into the proximity of the lumen, in order for this opportunistic infection to occur [Bierly et al., 2008; Lambert et al., 2006]. The parasites would then be trafficked to the lymph nodes and hence succeed in quick dissemination from the small intestine.

The ability of *T. gondii* to infect any nucleated mammalian cell is a property that makes the parasite an attractive model for investigating how cells respond to pathogens. Previous work by Dalton *et al.* 2006, suggested a protective role for localised γδ iIELs in the small intestine as in their absence, the small intestinal epithelial barrier was compromised when exposed to *T. gondii* [Dalton et al., 2006]. Furthermore, occludin location and phosphorylation was altered. Following on from this work in the murine model, this thesis set out to enhance knowledge and understanding of these observations *in vitro,* in order to identify the nature of occludin disruption in small intestinal epithelial cells.

4.2 Results

The infection mechanisms of *T. gondii* in epithelial cells derived from the small intestine were investigated with a specific view to identifying effects on tight junction physiology using m-IC_{cl2} cells as a model of small intestinal epithelial cells.

4.2.1 Determination of infection kinetics in m-IC_{cl2} cells

Parasites are present in the lamina propria after one hour of infection by oral gavage *in vivo*, indicating dissemination out of the GI tract occurs quickly [Dalton et al., 2006]. To determine the optimum length of infection to use for further studies *in vitro*, parasites were added for various time periods to cells cultured on inserts. The number of parasites that were associated with the cells increased over time although after six hours, no differences in the proportion of infected cells were observed (data not shown). Additionally, cells could be infected by more than one parasite, as illustrated in Figure 4.1, and cell monolayers remained alive after 24 hours exposure to the parasites. However, for the *in vitro* studies, an infection time of 2 hours was chosen to detect changes in tight junction physiology as disturbances within the epithelial barrier can occur rapidly following stimulation [Siliciano and Goodenough, 1988; Dalton

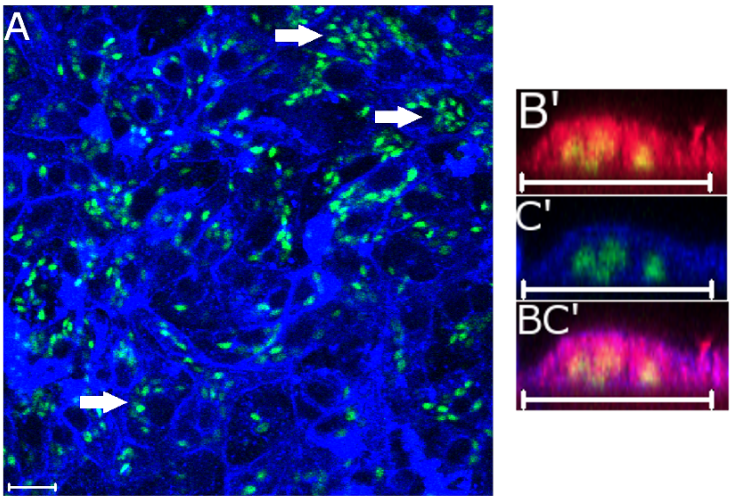

Figure 4.1: Parasite infection of epithelial cells after six hours. Cells were analysed for the expression of surface carbohydrates (blue) and occludin (red). Arrows indicate examples of cells with more than one intracellular parasite, as viewed from an XY plane. Scale bar 20μm. B', C', and BC' represent a cell infected with four parasites, as viewed from an XZ plane. Co-localisation of parasites and occludin appear yellow. Scale bar 10μm.

et al., 2006; Antonetti et al., 1999], and was also when many parasites were associated with the cells, as visualised by confocal microscopy.

In order to determine the proportion of infected cells, cells were grown on glass coverslips, as it proved difficult to calculate the numbers of infected cells grown on inserts. Media was temporarily removed from the cells to resuspend the parasites, before replacing and allowing infection to occur for two hours. Cells were counter-stained with Haemotoxylin and Eosin and the presence of a parasitophorous vacuole, indicated by a white halo around a parasite, was used as a marker for infection (highlighted by the arrows in Figure 5.10). Infection rates were calculated to be between 8.5% and 21.6%, which is comparable to figures reported in the literature [Dimier and Bout, 1993; Kowalik et al., 2004]. The ratio of cells to parasites made no difference to the proportion of cells infected and overall, the number of infecting parasites with regards to the original number added, was in the order of 0.1%. This value is likely to be an underestimate, due to the difficulties encountered in obtaining the data.

4.2.2 Cells secrete chemokines following *T. gondii* infection

The production of cytokines and chemokines from epithelial cells is recognised as an important factor in controlling *T. gondii* infection [Miller et al., 2009]. Therefore, to check that the cells were responding in the presence of parasites, a cytokine and chemokine analysis was carried out.

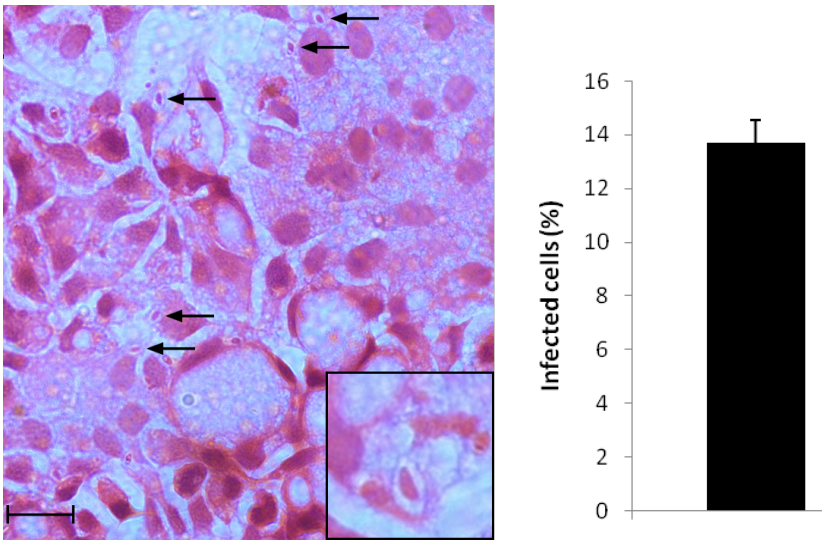

Figure 4.2: *T. gondii* infected 13% of cells following two hours exposure. Cells were cultured on glass coverslips for 48 hours and infected with *T. gondii* for two hours. Intracellular parasites were identified by the presence of a parasitophorous vacuole, as indicated by black arrows, and illustrated in the magnified image (bottom right hand corner). Scale bar = 20μm. The percentage of infection was calculated to be 15.05 ± 6.55. Data represents six independent experiments.

Previous studies have shown that the m-IC_{cl2} cells are capable of secreting a wide range of cytokines and chemokines [Zoumpopoulou et al., 2009]. IFNγ, IL-6, IL-10, IL-12, TNFα, KC (Keratinocyte Chemoattractant, the murine homologue of IL-8), MCP-1 (Monocyte Chemoattractant Protein-1), MIP-1α and MIP-1β were tested following infection for 24 hours, although only IL-10, KC and MCP-1 were detected.

A slight increase in IL-10 was observed, but KC and MCP-1 were significantly increased following exposure to both live and dead parasites ($P<0.001$, Figure 4.3). The concentration of KC produced by cells exposed to live parasites was 13 times higher compared to the control (no parasites), and 5 times higher for dead parasites. The concentration of MCP-1 production was 2.7 times higher compared to the control for live parasites and 2 times for dead parasites. These results were comparable to those previously reported in the literature, although only for the presence of live parasites [Ju et al., 2009; Mennechet et al., 2002; Denney et al., 1999].

4.2.3 Parasites cluster around cellular junctions

Parasites have been detected in the lamina propria of mice within one hour of infection [Dalton et al., 2006]. This rapid dissemination suggests that *T. gondii* exploits the paracellular pathway to enter the mucosa. The ability of parasites to transmigrate through the paracellular pathway *in*

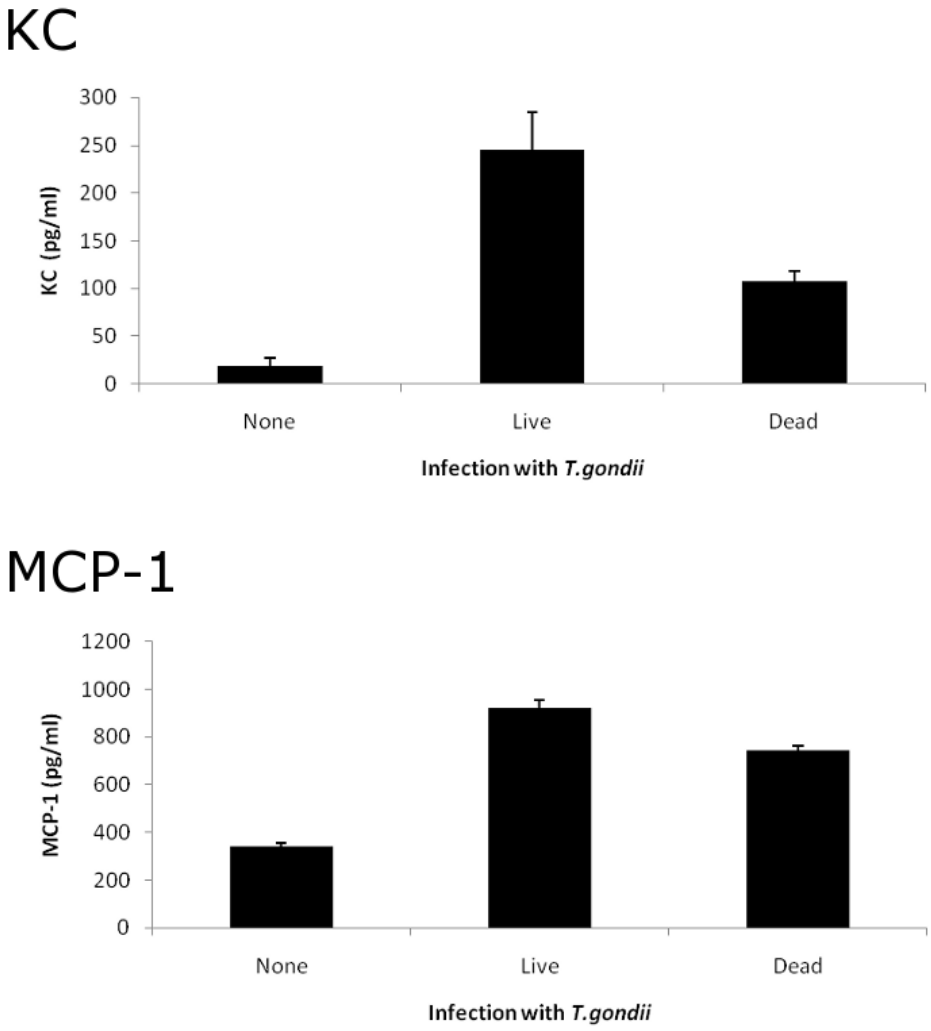

Figure 4.3: Cells respond to *T. gondii* by secretion of KC and MCP-1. Cells were cultured in 6 well dishes for three to five days. Approximately 1.5×10^6 live or dead (killed by freeze thawing or heat shock) parasites, were added to the cells for 24 hours. Media was collected and analysed for the secretion of cytokines and chemokines using a cytokine bead array kit (BD Biosciences). Data represents 3 independent experiments with biological replicates.

vitro was therefore tested.

Cells cultured on inserts were infected with ≈1.5 x 10^6 parasites and following two hours of infection, parasites were often found to be in close proximity to the lateral junctions of cells (Figure 4.4).

Having established that the parasites localised to junctions, it was necessary to assess their ability to transmigrate through the cells, via the paracellular pathway. Evidence collected using both immunofluorescence and electron microscopy techniques showed that parasites could be found between cell boundaries and underneath an intact cell monolayer (Figure 4.5). With cell culture inserts, it was possible to count the number of parasites that transmigrate through the monolayer, using their YFP-fluorescent signal as a means of distinguishing them by flow cytometry. The numbers of transmigrating parasites increased up to two hours of addition to the cells, but did not increase thereafter (Figure 4.6).

Overall, approximately 0.3% of parasite inoculum transmigrated into the basal compartment, with a range of 0.04 - 1.4% over 16 independent experiments. This equated to approximately 1,700 parasites. As a measure of maximum parasite numbers that could migrate through the pores, a blank insert was used and showed that this was on average 7.7%, with a range from 1 - 20%.

4.2.4 Epithelial barrier function was not affected by *T. gondii*

The ability of the parasites to transmigrate through the paracellular pathway suggests they may affect the integrity of the epithelial cell barrier. Therefore, the transepithelial electrical resistance (TEER) and permeability were measured following 2 hours exposure to parasites. As a control, cells received just media. After 2 hours, a slight but significant decrease in TEER was always observed in the controls ($P = 0.008$), whereas for infected samples, three experiments showed an increase in TEER, three showed a decrease, and for one experiment TEER was not altered (Figure 4.7). Therefore, when comparing the average change in TEER across all experiments, there was no significant difference between control and infected samples ($P = 0.279$).

To detect changes in paracellular permeability following exposure to *T. gondii*, FITC-dextran (molecular weight 3 - 5kDa) was added to the apical compartment along with the parasites. Apical and basal media were measured and quantified by fluorescence. The permeability of the cell monolayer was not affected by the presence of *T. gondii* ($P = 0.391$).

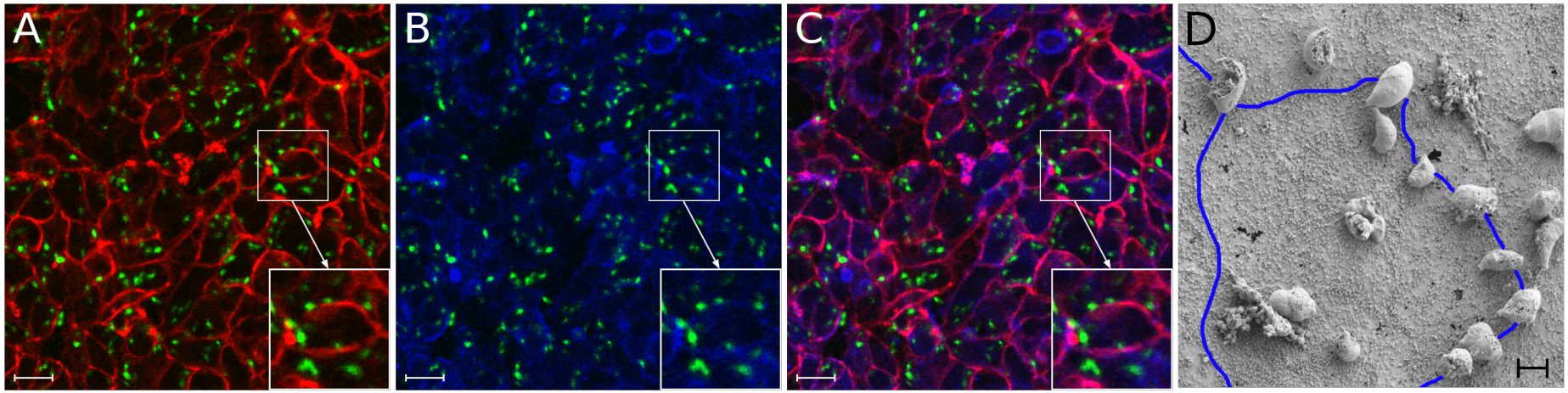

Figure 4.4: Parasites cluster around cellular junctions. Cells cultured on inserts were grown for 13 days before exposing to *T. gondii* for 2 hours. Parasites (green) were seen to be near the perimeter of epithelial cells, the lateral membrane being represented by the adherens junction protein, β catenin (red, A), and apical surface carbohydrates (blue, B). The merged image is shown in C. The enlarged images show six parasites surrounding the edge of one cell. Scale bar = 20 µm. Further evidence of lateral localisation of parasites was provided by scanning electron microscopy, where the cells were cultured on a collagen gel (D). The cell edge is outlined in blue, with the parasites clustered around it. Image (D) was captured by Kathryn Cross (Institute of Food Research, UK). Scale bar = 2 µm, magnification 8000×.

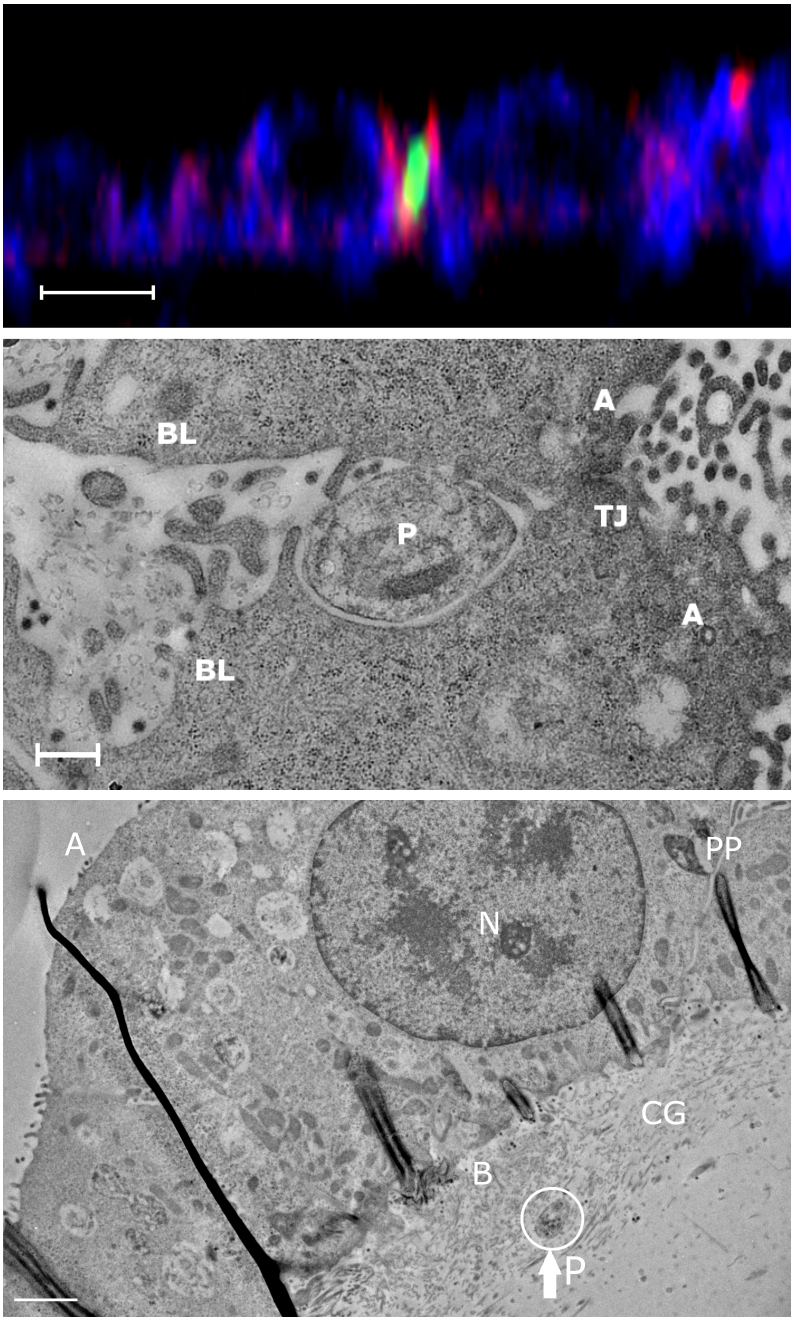

Figure 4.5: Parasites can penetrate the paracellular pathway. Cells were cultured on a collagen I gel for eight days before infecting with *T. gondii*. A YFP-fluorescent parasite (green) between two cells is shown by β catenin (red) highlighting the lateral membrane of cells and surface carbohydrates (blue) outlining the membrane (top image). Scale bar = 20 µm. Further evidence for use of a paracellular route by parasites (P) can also be seen by transmission electron microscopy where A is the apical domain of cells, TJ is the tight junction complex and BL marks the basolateral domain (middle panel). Scale bar = 500 nm, magnification 6500×. Parasites were found underneath the cell monolayer (B, basal domain) embedded within the collagen gel (CG) (bottom image, highlighted by the arrow). Also marked are a nucleus (N) and the paracellular pathway (PP). Electron microscopy images were taken by Kathryn Cross. Scale bar = 2µm, magnification 1700×.

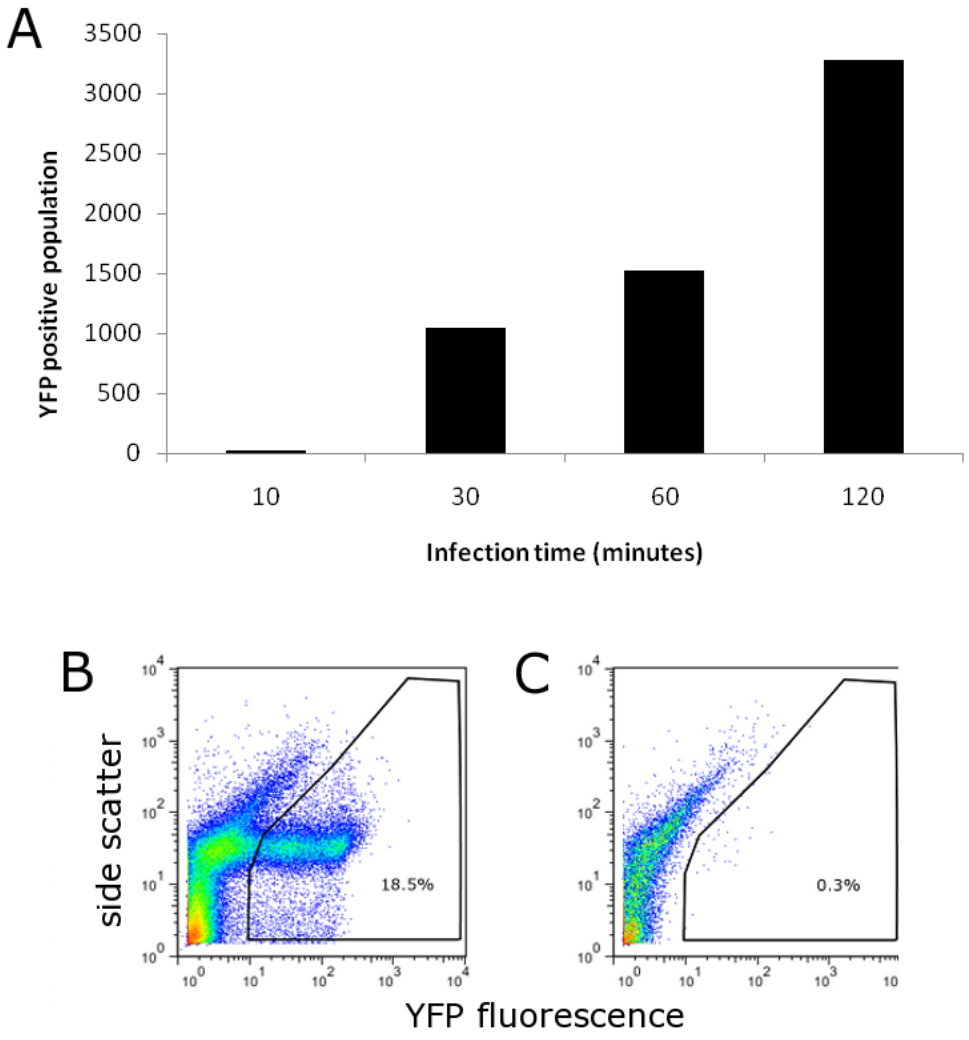

Figure 4.6: Parasites transmigration increases with time. Parasites that had transmigrated through the cells into the basal compartment were counted by flow cytometry. Numbers of parasites detected increased with time (A). Parasites were counted in the basal compartment by collecting samples positive for YFP-fluorescence within the FL-1 channel (B). Background autofluorescence of cells and/or media is represented in (C). Data represents one of two independent experiments.

These findings agree with data presented in the literature [Barragan et al., 2005].

A time-course of infection was also performed for which there were no detectable changes in either resistance or permeability between non-infected and infected cells at 30 minutes, 6 hours or 24 hours (data not shown). Additionally, the number of parasites added to the apical compartment did not make a difference to TEER or permeability (data not shown).

4.2.5 *T. gondii* affects the cellular distribution of occludin

Following infection, the effects on individual tight junction proteins were assessed by immunofluorescence. It was found that the distribution of occludin was dramatically altered in the presence of *T. gondii* with a decrease of occludin from the tight junction complex to a more intracellular-apical location (Figure 4.8).

To examine the kinetics of occludin redistribution, a time-course of infection was performed (Figure 4.9). After 30 minutes, subtle changes were seen in expression whereby occludin appeared more concentrated at tricellular junctions compared with the control. Additionally, slight aggregation of the protein was also observed. After 2 hours the changes in occludin redistribution were more apparent, becoming more apically distributed within the cytoplasm. Following 6 hours of infection, the presence of occludin at the tight junction complex was fractured compared to the control, and was found increasingly in the cytoplasm. After 24 hours this phenomena was even more profound. To rule out the possibility that antibody complexes were binding to the parasites, immunocytochemistry was performed on the parasites alone. There was no evidence of non-specific occludin staining with the parasites for the primary, secondary or tertiary antibodies (data not shown, anti-occludin antibodies are shown in Appendix B).

As it was not easy to quantify changes in occludin distribution by microscopy, cell lysates were analysed for the presence of occludin in the cytoplasmic fraction (soluble) and the membrane-associated fraction (insoluble) by immunoblotting. After 30 minutes of infection, both the cytoplasmic and membrane-associated fractions of occludin decreased in concentration, compared to non-infected samples. However after 6 hours, there was an increase in cytoplasmic occludin, but a further decrease in membrane-associated occludin (Figure 4.10). After 24 hours, an elevated level of cytoplasmic occludin and a depressed level of membrane-

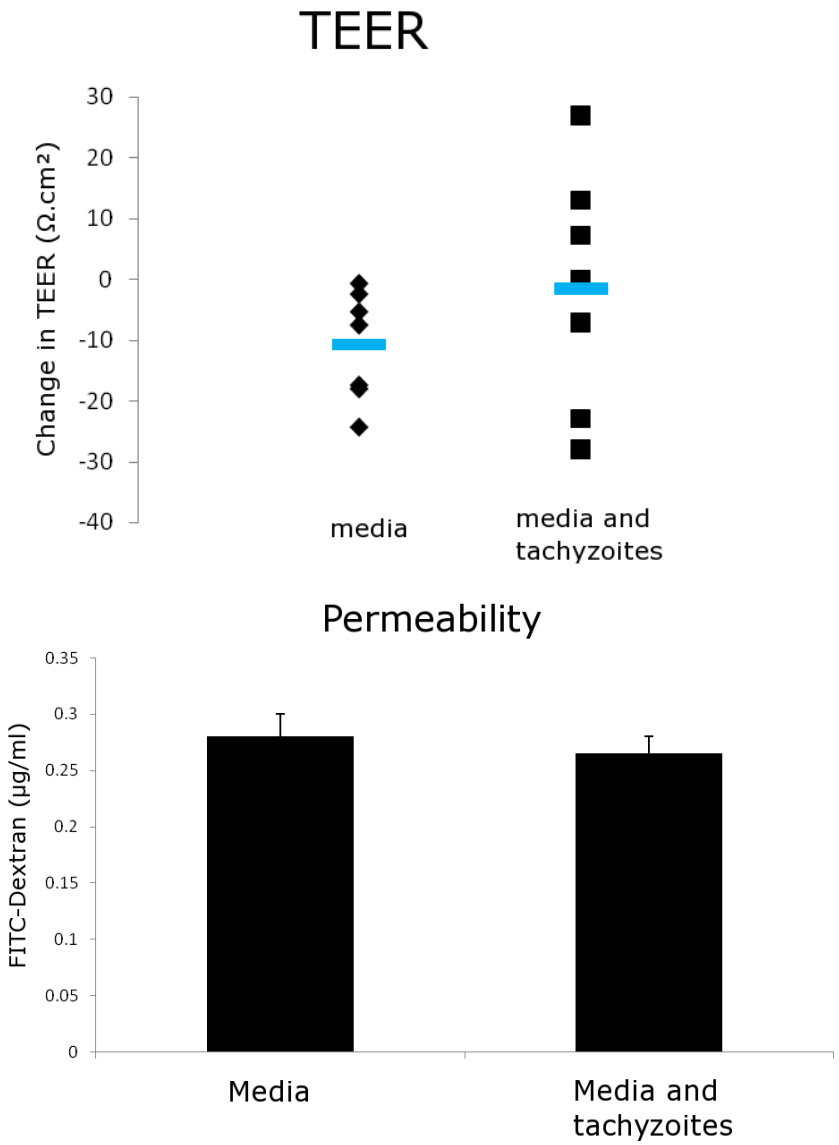

Figure 4.7: The integrity of the epithelial barrier was not affected by *T. gondii*. Approximately 6.5 x 10^5 cells were plated on 8µm PET inserts and cultured for 13 days. Approximately 2.3 x 10^6 parasites were added with dextran to the cells and TEER was measured before and after the addition of parasites. TEER (top) and permeability (bottom) were not altered in cells following 2 hours exposure to *T. gondii*. Data represents results from 7 independent experiments with biological replicates. Permeability was measured by the amount of FITC-dextran that was present in the basal compartment following addition to the apical compartment. Data represents 3 independent experiments with biological replicates.

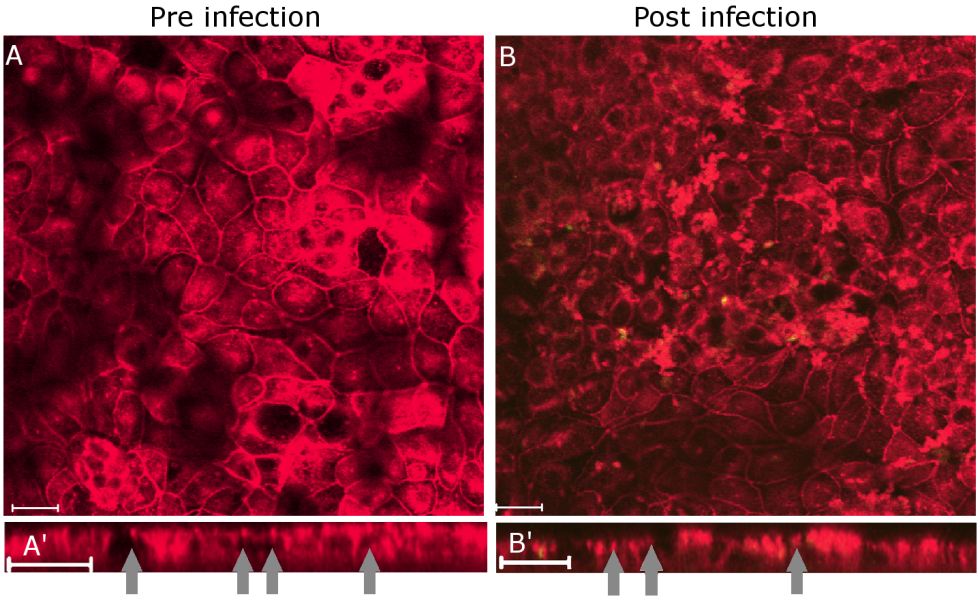

Figure 4.8: Occludin was affected by *T. gondii*. Cells were cultured on PET inserts and infected with parasites for 2 hours, fixed with 2% PFA and stained with anti-occludin antibodies (red). (A) Cells without parasites and cells with parasites (B, green). Co-localisation results in yellow staining. Z stacks are illustrated in (A', B'). Arrows represent occludin expression at the tight junctions. Scale bar = 20µm. Images are typical of those collected over 16 independent experiments.

associated occludin was observed.

These data provide evidence that occludin distribution and levels of protein expression are affected by *T. gondii,* even though the patterns are not identical to the immunofluorescent results. Overall, cytoplasmic occludin increases 6 hours post infection, while membrane-associated occludin decreases.

A further occludin species of approximately 45kDa was visible in the cytoplasmic fraction after 6 hours of infection, which may correspond to a degradation product, or cleavage of occludin, and similar results have been observed following infection with other pathogens [Lytton et al., 2005; Wu et al., 2000].

Occludin is a phospho-protein whose function is governed by levels of phosphorylation [Sakakibara et al., 1997; Farshori and Kachar, 1999]. The phosphorylation status of occludin in m-IC_{cl2} cells proved extremely difficult to quantify by immunoblotting. Preliminary data suggested that there was a decrease in phosphorylated serine residues after 6 hours of infection in the membrane-associated fraction and an increase in the cytoplasmic fraction, compared to the control (data not shown). These results match the expression profile of occludin seen in Figure 4.10. In order to amplify the levels of phosphorylated occludin detectable by immunoblot-

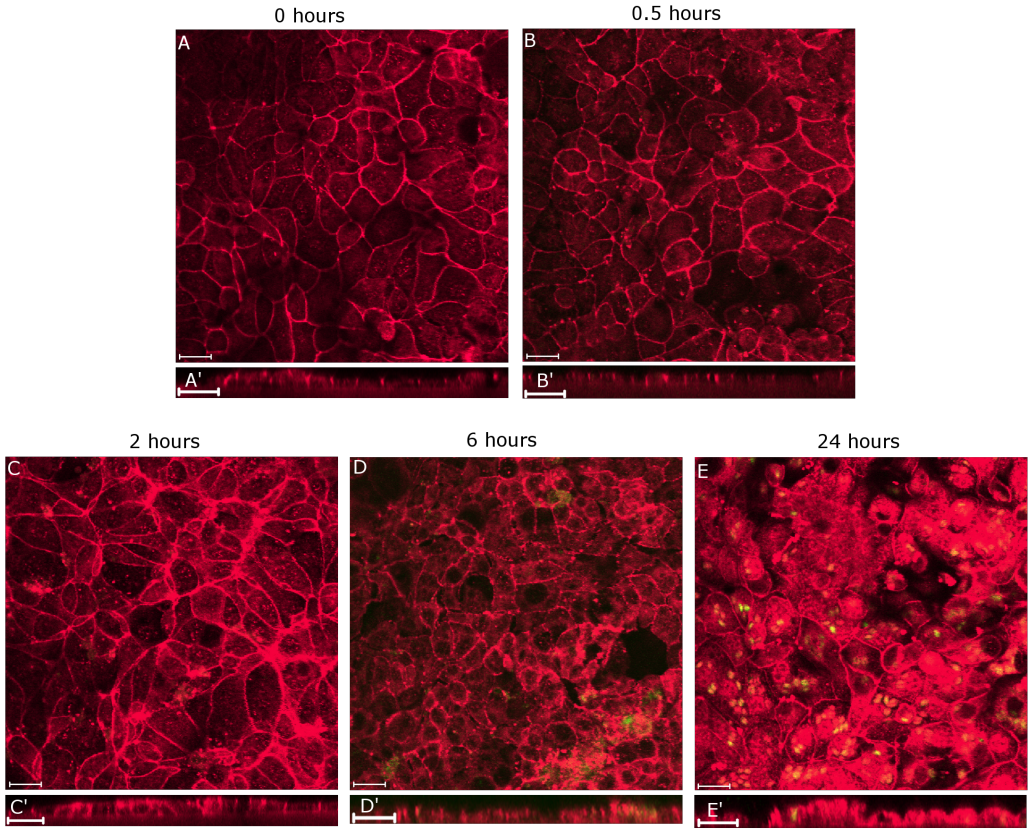

Figure 4.9: Length of infection increases the effects on occludin redistribution. Cells cultured on inserts were fixed with acetone and the expression of occludin (red) after infection from *T. gondii* (green) was visualised. (A) shows a representative image of cells that were not exposed to parasites and (B - E) shows representative images of cells exposed to parasites for different amounts of time. A' - E' are corresponding XZ images. The experiment was repeated on 3 separate occasions. Scale bar = 20μm.

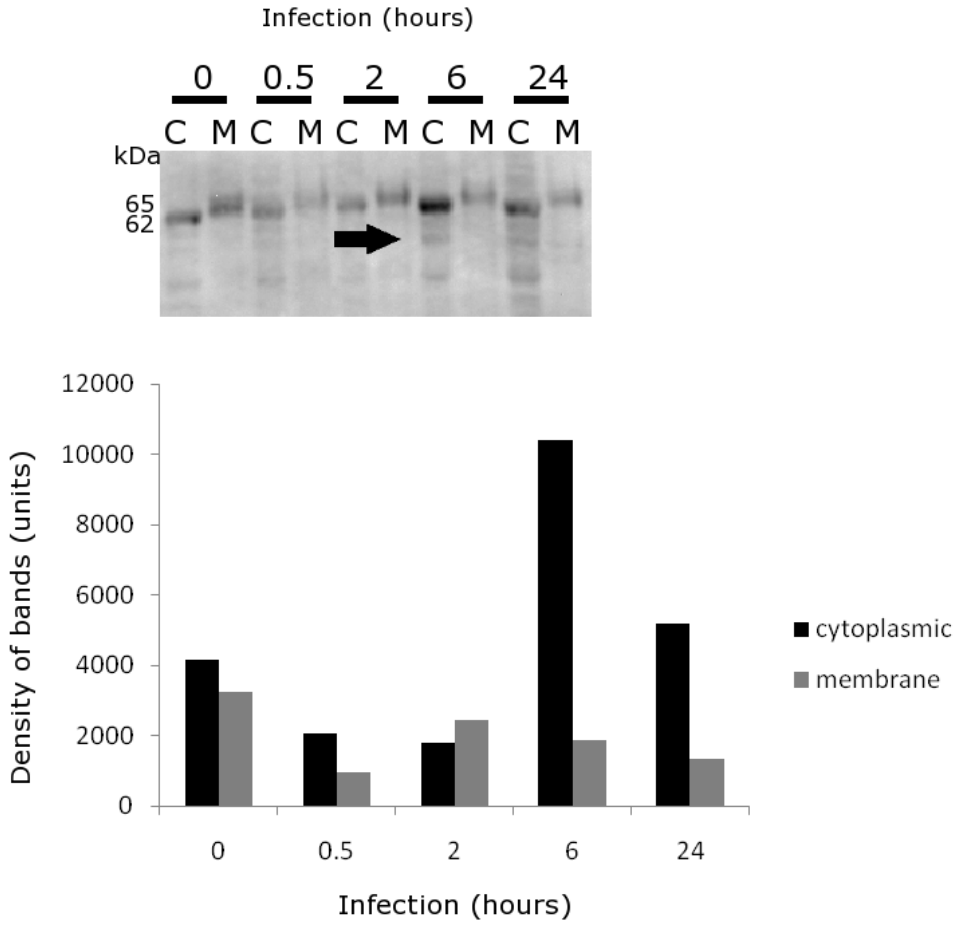

Figure 4.10: Occludin quantification by immunoblotting. Cells cultured on plastic for eight days were infected with *T. gondii* for varying amounts of time. Lysates were processed for SDS-PAGE, loading equal concentrations of protein per lane. One gel was stained with coomassive (for densitometry analysis, conducted by Francis Mulholland) and the other was immunoblotted for occludin (left). Occludin protein bands were normalised by densitometry analysis and quantified using the optical density of band intensity. Cytoplasmic occludin (C, 62kDa) and membrane-associated occludin (M, 65kDa) were compared against the control, where no parasites were added. Arrow points to a degraded or cleavage product of occludin at ≈50kDa. Data represents one of four independent experiments.

ting, an immunoprecipitation of occludin was carried out. Unfortunately, this did not increase the phosphorylation signal. Cell lysates analysed by mass spectrometry revealed a phosphorylated residue within the C-terminus, which indicates that phospho-peptide mapping may prove useful for detecting occludin phosphorylation in future studies (data not shown).

4.2.6 *T. gondii* does not affect other junctional proteins

To determine whether or not other junctional proteins were affected by *T. gondii*, cells were analysed for the expression of claudin 2, claudin 4,

ZO-1 and β catenin. The distribution of these proteins was not altered when compared to cells without *T. gondii* after 2 and 6 hours of infection, although there may be a slight increase in cytoplasmic claudin 2 expression following 6 hours of infection (Figure 4.11, Figure 4.12). This is more likely to be an indirect effect following *T. gondii* infection.

4.2.7 *T. gondii* co-localises with occludin

Having established that occludin was the only tight junction protein affected by *T. gondii*, the parasite was also found to co-localise with the protein (Figure 4.13 and Figure 4.14). After 2 hours of exposure to parasites, occludin (shown in red) appeared to be concentrated at one end of the parasite prior to invasion, suggesting a role in the generation of the moving junction (A - D). After becoming intracellular, the co-localisation with occludin appeared across the surface of the parasite (A - D, G - I).

Although the cells were fixed at the time of imaging, it is possible to speculate a route of parasite movement from images in Figure 4.13. As parasites cluster around the cell edges (E) they co-localise with occludin. Parasite movement between cells, leads to occludin displacement (F), and once the parasite becomes intracellular, occludin is present on the entire surface of the parasite (G). The fate of paracellularly located *T. gondii* was difficult to conclude from fixed samples, but did occur, as confirmed by flow cytometry analysis.

Following 24 hours of infection, the proportion of intracellular occludin and amount of co-localisation with *T. gondii* was far greater than in control cells (Figure 4.14), implying that this association between host and parasite was not just a strategy for entering the cells, but that occludin may have a role in formation and maintenance of the parasitophorous vacuole.

4.2.8 Live imaging of parasite infection in m-IC$_{cl2}$ cells

The ability to track parasite movements in real time provides a solution to the problem of interpreting images from fixed samples to distinguish the routes of entry used by *T. gondii* to infect and transmigrate through cells. Therefore, a live invasion assay was performed. Cells were cultured on a collagen I and fibronectin matrix for 8 days before staining, whilst still alive, for occludin using an antibody that recognises the extracellular domains (red, Figure 4.15), and surface carbohydrates (blue). Parasites were then added to the cells and the dish containing the sample was

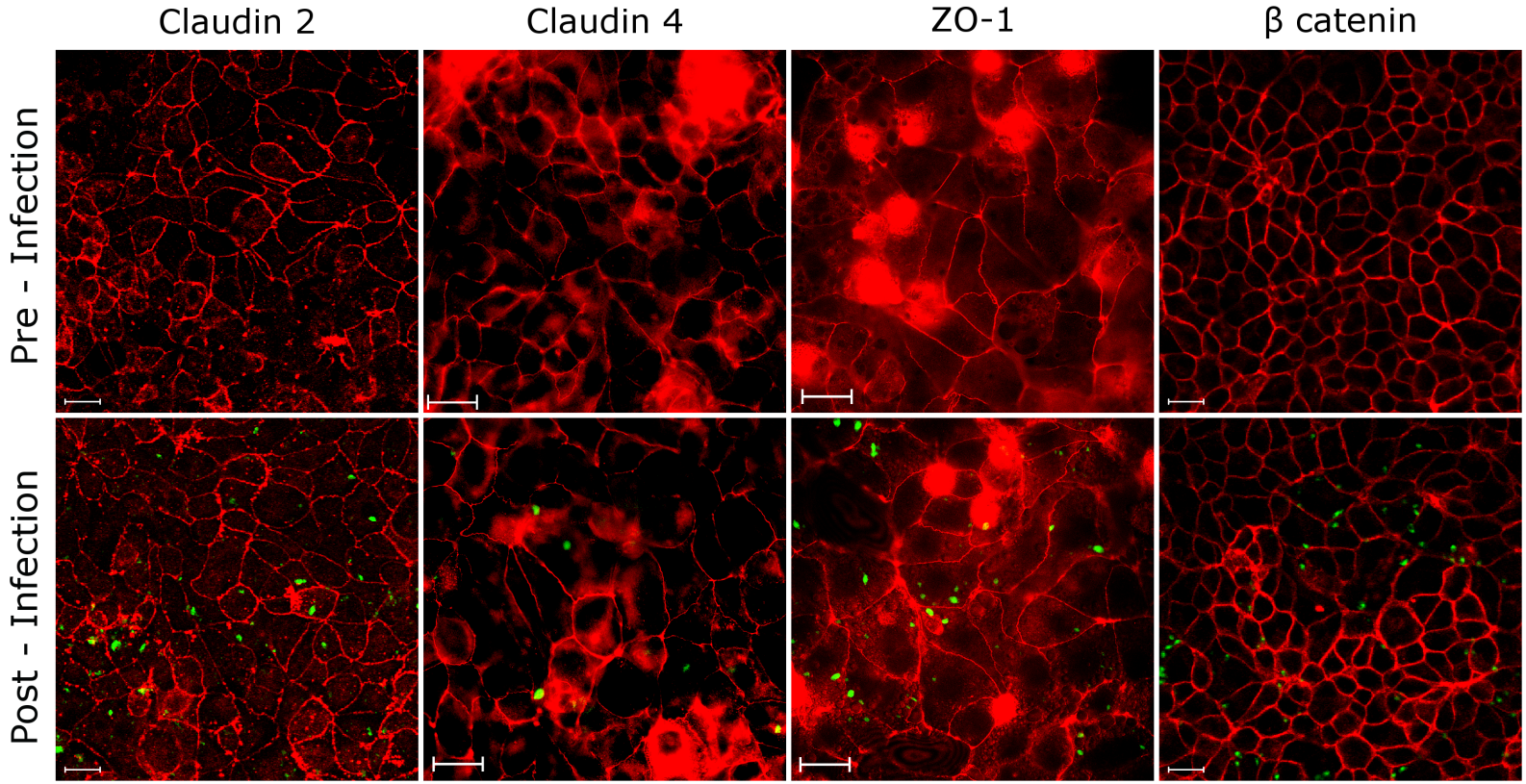

Figure 4.11: Claudin 2, claudin 4, ZO-1 and β catenin are not affected by *T. gondii* 2 hours post infection. Cells on inserts were fixed in 2% PFA and stained for junctional proteins. Images are representative of more than three independent experiments with biological replicates. Scale bar = 20µm. Intense red circular shapes are insert pores (Appendix I).

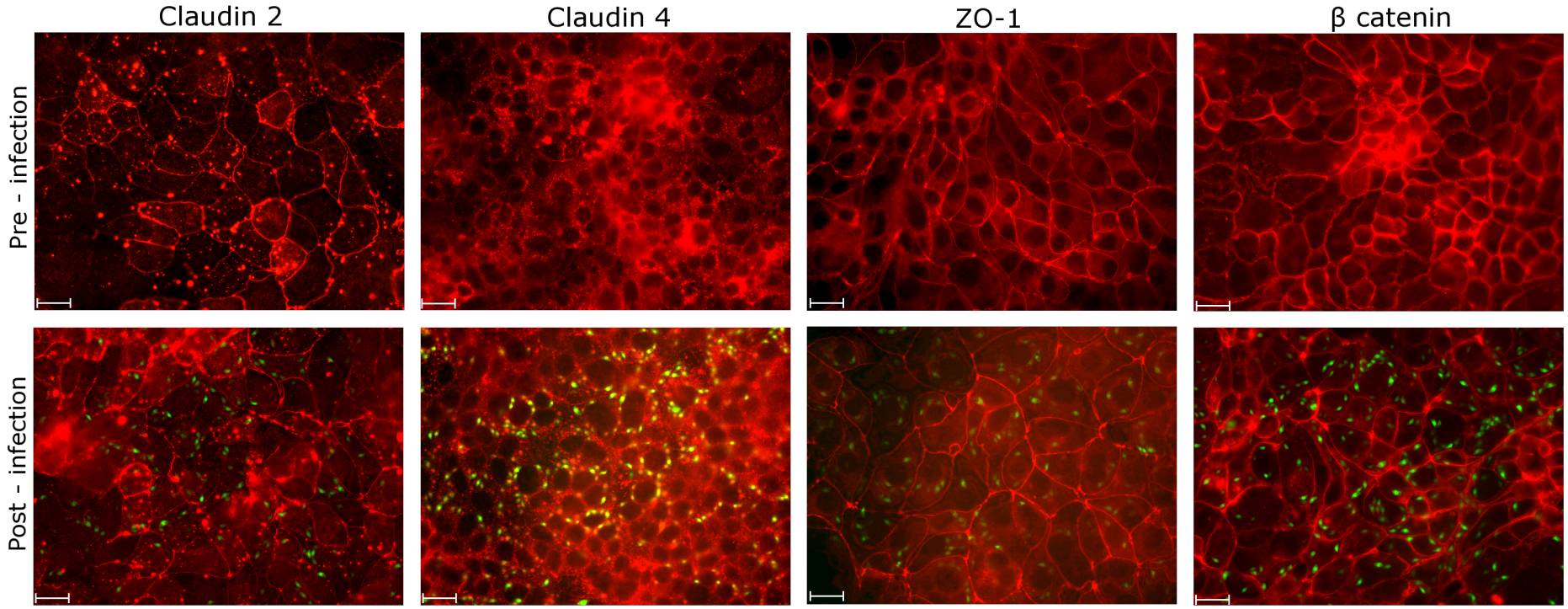

Figure 4.12: Claudin 2, claudin 4, ZO-1 and β catenin were not affected by *T. gondii* 6 hours post-infection. Cells on inserts were fixed with 2% PFA and stained for junctional proteins. Images are representative of more than three independent experiments with biological replicates. Scale bar = 20µm.

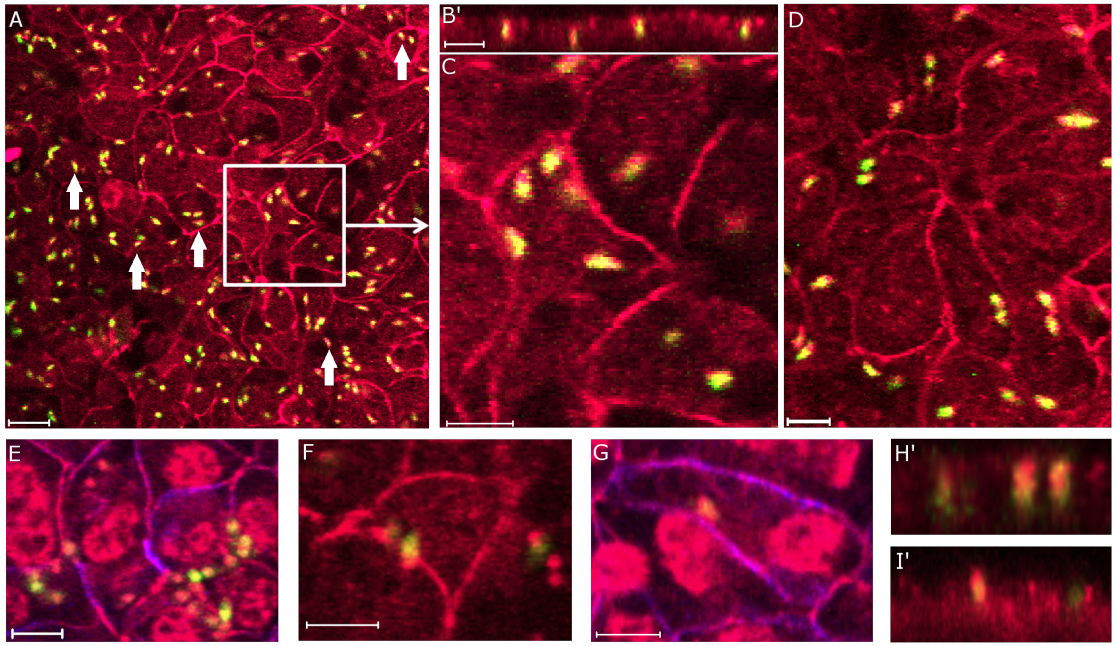

Figure 4.13: Co-localisation with occludin after 2 hours of infection. Cells were infected, fixed with 2% PFA or acetone, and stained for occludin (red) and surface carbohydrates (blue). Parasites are shown in green and co-localisation between occludin and *T. gondii* appear as yellow. (A and C) show polarised co-localisation of occludin on parasites, as highlighted by arrows. The cells within the square have been magnified in (C) to show this polarisation more clearly. (B') shows a typical example of an XZ image to further illustrate this. Parasites cluster around the edge of cells (E), move between (F) and within cells (G). (H' and I') show further examples of parasites coated with occludin. Scale bar is 10μm except for (G) where bar is 20μm. Images are typical of those seen across 10 independent experiments.

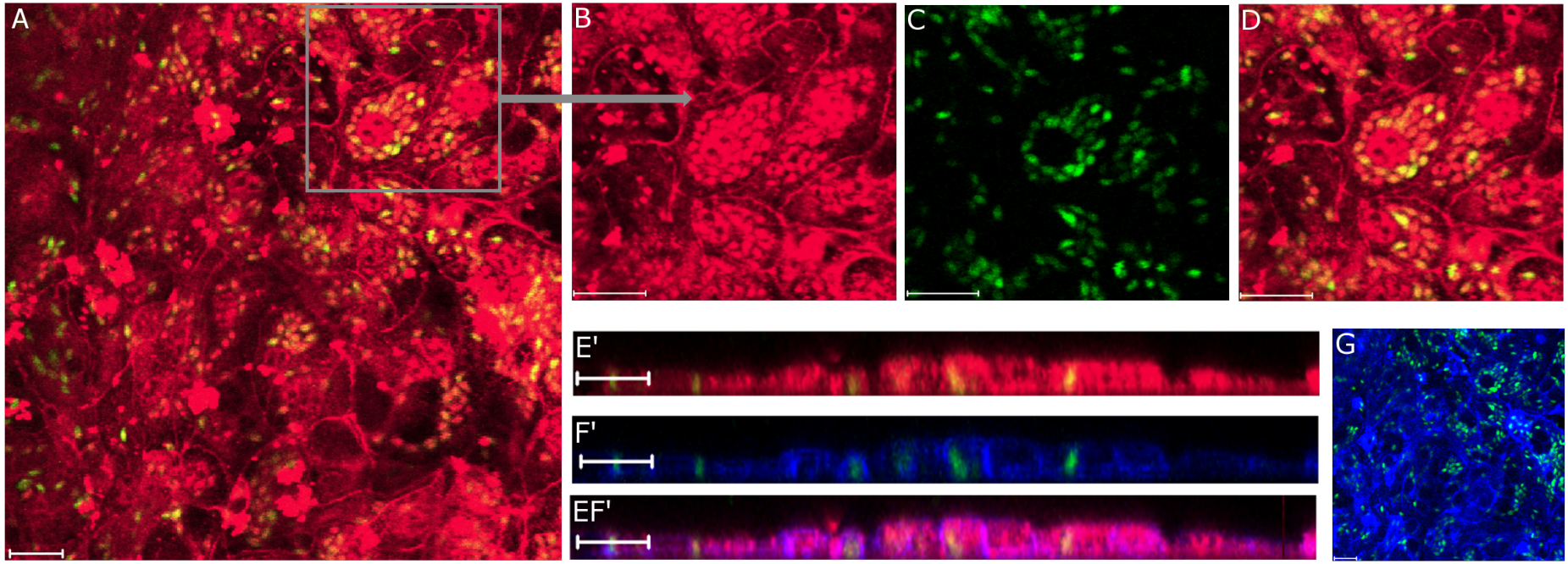

Figure 4.14: Co-localisation of occludin increases over time in the presence of *T. gondii*. After 24 hours of infection, cells were fixed with 2% PFA or acetone and stained for occludin (red) and surface carbohydrates (blue). Parasites are shown in green and co-localisation between occludin and *T. gondii* appear as yellow. (A) highlights one cell infected with multiple parasites which has been magnified in (B - D), where (B) is occludin, (C) shows the parasites and (D) is the merged image. XZ images illustrate that co-localisation is specific to occludin (E') and does not occur with surface carbohydrates (F', G). Merged images are shown in (EF'). Scale bar is 20μm except for (B - D) where bar is 10μm. Images are representative of results from three independent experiments.

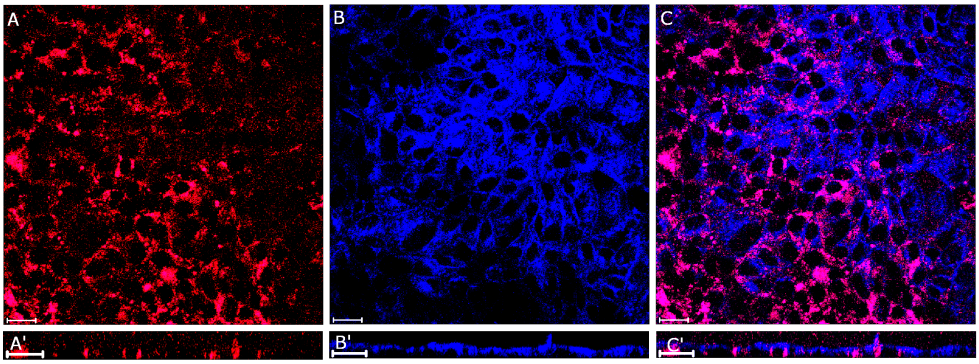

Figure 4.15: Occludin staining in live cells. Cells were grown on a collagen I and fibronectin matrix for 8 days and stained, whilst still alive, for occludin (red, A) and surface carbohydrates (blue, B). Merged images are shown in (C). A - C represent XY images and A' - C' represent XZ images. Scale bar = 20μm.

placed onto a confocal microscopy stage to record the infection in real time. Although it was possible to visualise occludin, the interaction between antibody and protein was not stable as after one hour the levels of immunofluorescence faded and the resolution of occludin-labelled cells decreased. Therefore it was not a useful system to use for identifying the passage of *T. gondii* during infection and requires further optimisation.

However, as the YFP signal from the parasites was stable, it was possible to observe their movements with the cells, as illustrated in Figure 4.16. The images show parasites near the cell edge (A) and the parasites re-orientating themselves after contact with the cells (B), possibly in preparation to invade. There were examples of parasites passing between cells (C) and typical gliding motility of *T. gondii* when interacting with the apical domain was observed, where parasites appeared to move across the cells in a diagonal fashion (D) [Håkansson et al., 1999].

4.2.9 Parasites themselves are required to alter the distribution of occludin

During the invasion of cells, *T. gondii* secretes many proteins. Therefore it was necessary to determine whether parasites were required to affect occludin, or whether a secreted product acted upon occludin. Conditioned media taken from parasite cultures was filtered (0.2μm filter) to remove parasites, and added to the cells. There were no changes in TEER or permeability following addition of conditioned media and more importantly, there were no observed changes in the distribution of occludin (Figure 4.17). This suggests that the parasites themselves are required to alter occludin and that the interactions occur on the surface of the parasite.

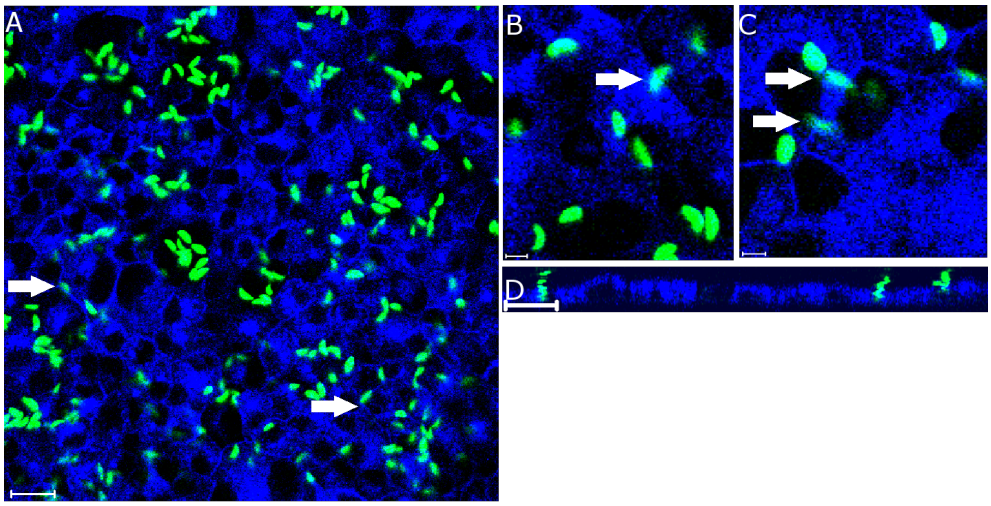

Figure 4.16: Movements of parasites amongst cells. Cells were labelled with surface carbohydrates (blue) and infected with parasites (green) for 2 hours. (A) arrows indicate parasites along cell edges. Images show parasite re-orientation (B), parasite movement between cells (C) and parasite movement along the apical domain (D). Scale bar 10μm (B, C), 20μm (A, D).

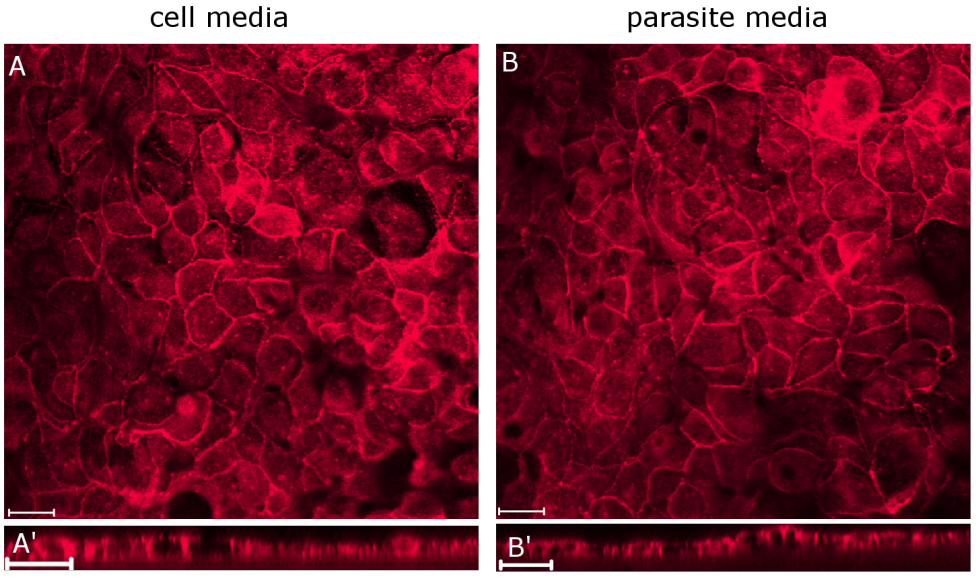

Figure 4.17: Conditioned media does not affect occludin distribution. Cells were incubated with normal cell media or parasite conditioned media for 2 hours before fixing with acetone and staining for occludin. A and B represent XY fields of view, A', and B' represent XZ fields of view. Images are representative of five independent experiments.

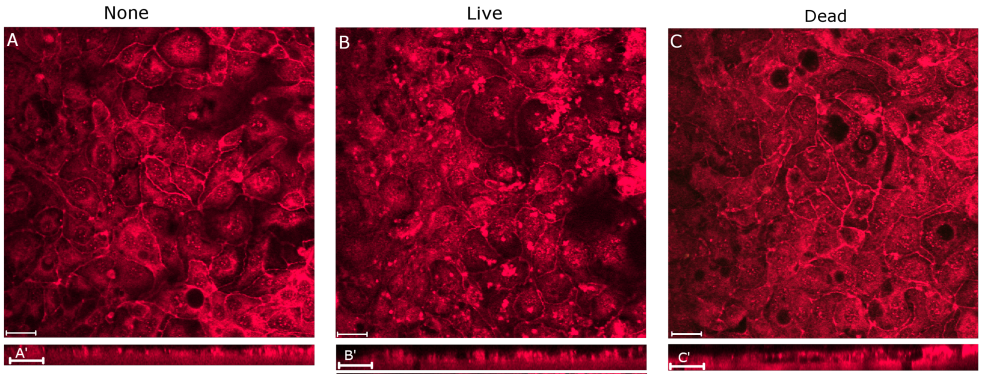

Figure 4.18: Dead parasites have no effect on the distribution of occludin. Cells were exposed to either no parasites (A, A'), live parasites (B, B') or dead parasites (C, C'), (XY, XZ planes). Images are representative of two independent experiments.

4.2.10 Live parasites are required to cause the redistribution of occludin

As conditioned media had no effect on occludin, it was likely that parasites were required to induce alterations of occludin. To determine whether molecules on the surface of *T. gondii* are sufficient to cause occludin redistribution, live or dead parasites were added to cells. Parasites were killed by either freeze-thaw or heat shock method [Koshy et al., 2010]. Parasite death was confirmed by the failure to induce HFF cell lysis after 14 days culture, in parallel to the shift in a YFP positive population seen with flow cytometry (Appendix J).

Following addition of dead parasites to cells, no changes were identified in terms of barrier function, and parasites were not detected in the basal compartment following 2 hours of addition to the apical domain as expected [Barragan et al., 2005; Morisaki et al., 1995]. Furthermore, there was no evidence to suggest that the cellular location of occludin had been drastically altered (Figure 4.18). Therefore it was concluded that live parasites were required for occludin redistribution. This suggests that following attachment with a parasite surface molecule, there is either an increased expression of this/these molecule(s), as a minor change in occludin aggregation was seen with dead parasites (killed by heating), or that a secreted parasite product may then act upon occludin. For example, these could be microneme, rhoptry or dense granule derived proteins which increase in expression following parasite attachment to the cell surface.

4.2.11 Bradyzoites altered permeability and occludin distribution

All the experiments described above were carried out with tachyzoites. However, it is most likely that during a natural infection, bradyzoites will be the life stage of the parasite that comes into contact with the small intestine, although it is known that tachyzoites can survive the acidic stomach to then infect the GI tract [Dalton et al., 2006; Egan et al., 2005; Dubey, 1998b; Camossi et al., 2011]. However, bradyzoites are difficult to maintain in culture as conversion to tachyzoites occurs after 15 - 18 hours of infection *in vitro* and *in vivo* respectively [Dubey, 1997].

To determine whether bradyzoites also affect occludin in the same way as tachyzoites, cells were infected with bradyzoites. Bradyzoites were induced by the pH shock method described by Soete *et al.* 1994, and tested by staining for SAG1 which is expressed only by tachyzoites [Soête et al., 1994]. Also, upon induction, the YFP signal was rapidly photobleached in bradyzoites compared to tachyzoites, and was used as a further indication that the parasite population had been converted.

Cells were infected with either 1.5×10^6 tachyzoites or 2×10^5 bradyzoites and cellular TEER, permeability and parasite transmigration were investigated. Less bradyzoites were added than tachyzoites according to methods published in the literature [Dalton et al., 2006; Dubey, 1998b].

There was no overall difference between tachyzoite and bradyzoite effects on TEER of the monolayer (Figure 4.19), but there was a significant difference in permeability after 2 hours of infection, with the monolayer being more leaky to dextran in the presence of bradyzoites ($P = <0.05$, Figure 4.20). This appeared to be a transient effect, as after 6 hours there were no differences compared to the control (no parasites). It should be noted that these results were collected from only one experiment.

It was difficult to calculate the numbers of bradyzoites that had transmigrated through the monolayer using flow cytometry, because the YFP signal was lost. However, by phase contrast microscopy using a haemocytometer, after 30 minutes of infection, 5 times as many bradyzoites were counted in the basal compartment compared to tachyzoites (Figure 4.21). After 2 hours, the percentage of bradyzoites had not considerably altered, but double the amount of tachyzoites were detected. Following 6 hours of infection, numbers in both populations had appeared to decrease. These results suggest that bradyzoites may transmigrate at a faster rate than tachyzoites, and that maximum numbers of parasites

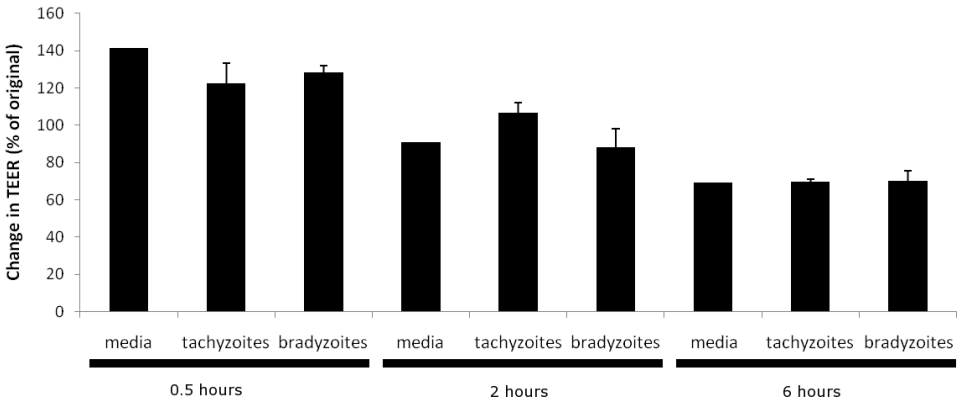

Figure 4.19: TEER was not altered when cells were exposed to bradyzoites. Either media alone, tachyzoites or bradyzoites were added to cells and TEER was recorded after 30 minutes, 2 and 6 hours infection. Data represents an experiment with biological replicates (except for media alone where n = 1).

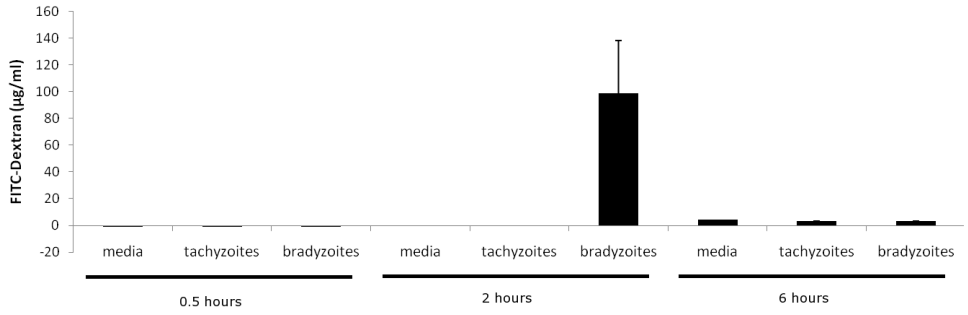

Figure 4.20: Permeability was increased by infection with bradyzoites. Either media alone, tachyzoites or bradyzoites were added to cells and permeability measured after 30 minutes, 2 and 6 hours infection. Data represents an experiment with biological replicates (except for media alone where n = 1).

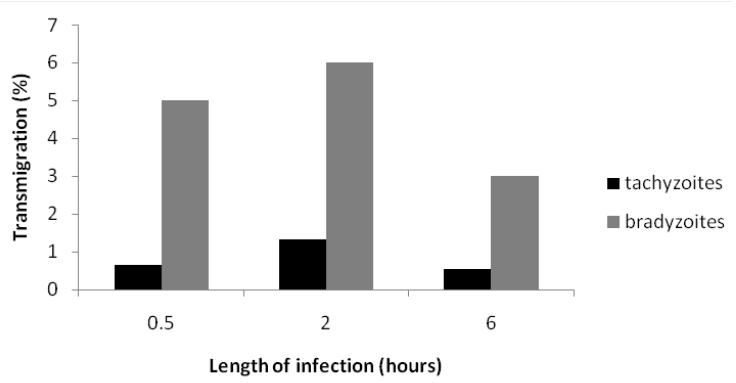

Figure 4.21: Bradyzoites transmigrate at a higher rate compared to tachyzoites. Cells were infected with either bradyzoites or tachyzoites and parasites that had migrated into the basal compartment were counted using a haemocytometer. Data represents one experiment.

transmigrating across the epithelial barrier was achieved within 2 hours. Decreased numbers after 6 hours could be due to parasite lysis or death, invasion through the basal domain, or experimental error.

As tachyzoites affected the cellular distribution of occludin, it was intriguing to see whether or not bradyzoites exerted the same effects. Cells were stained for occludin following infection and Figure 4.22 illustrates that over time, the distribution of occludin became increasingly altered by bradyzoites. Therefore the life stage of the parasite was irrelevant to the effects that the parasite exerts on occludin. The effects on occludin following exposure to bradyzoites after 2 hours appeared to concentrate occludin to the lateral membrane rather than becoming more cytoplasmic as seen with tachyzoites. This may be due to membrane ruffling during bradyzoite invasion [Sasono and Smith, 1998].

4.2.12 Occludin in colonic cells is altered by *T. gondii*

Human colonic cell lines ($CaCo_2$ and C2BBe1) were tested for changes in epithelial barrier function following infection with tachyzoites, and it was found that like m-IC_{cl2} cells, TEER was not altered by the presence of *T. gondii*, but permeability was significantly altered ($P = 0.001$, Figure 4.23). Here, the cells appeared to respond to infection by decreasing the amount of paracellular flux within the monolayer. In terms of transmigrating parasites, less than 0.01% were accounted for in the basal compartment. This was 10 times less compared to the m-IC_{cl2} cells, and supports the decrease found in paracellular permeability. Changes in ionic transport in the colonic cell line HT29/B6, were also reported by Kowalik *et al.* 2004, although they also showed an increase in TEER of

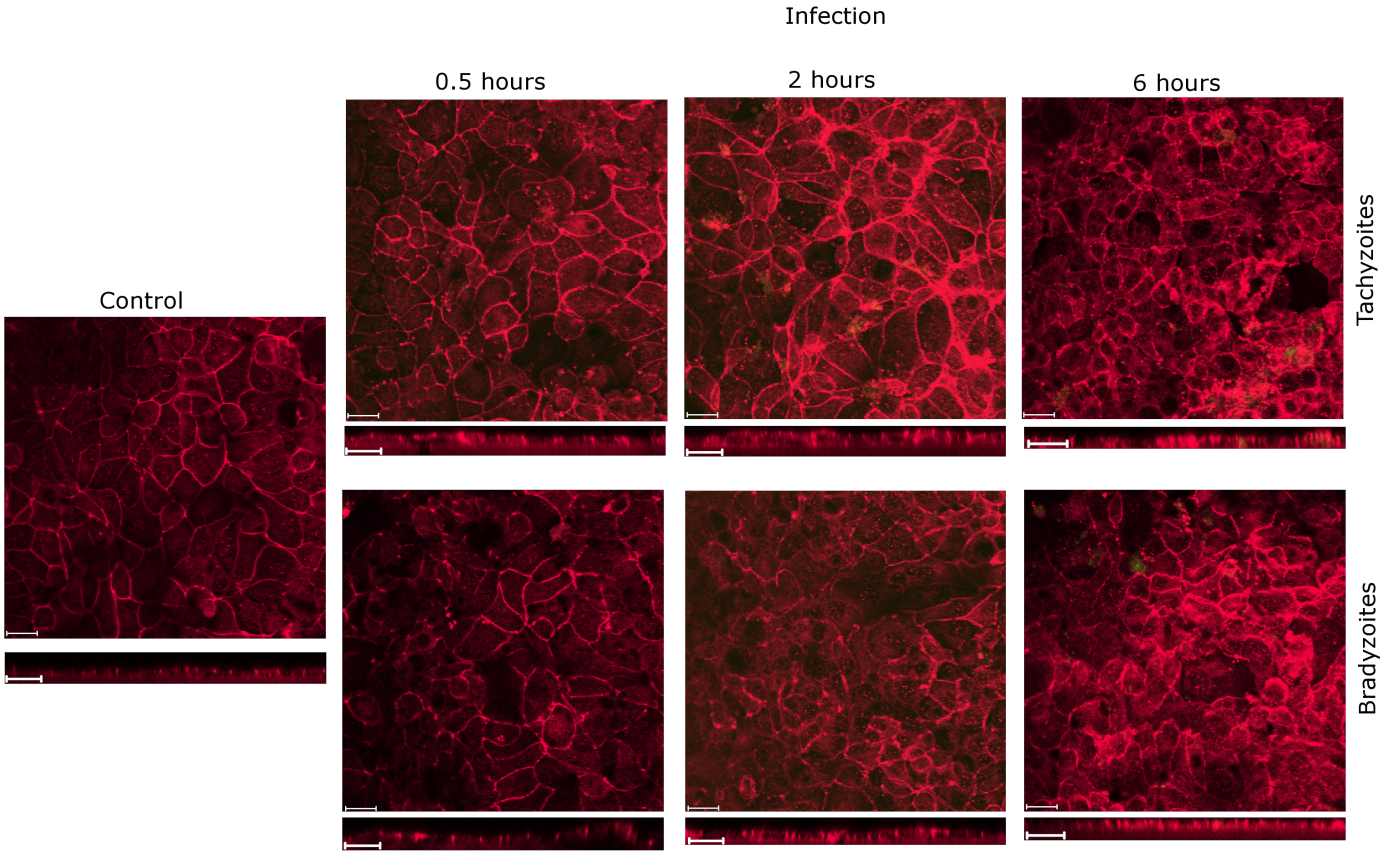

Figure 4.22: Bradyzoites also alter the distribution of occludin. Cells were infected with either nothing (left hand image), tachyzoites (top panel) or bradyzoites (bottom panel) for 30 minutes, 2 hours and 6 hours. After fixing with acetone, cells were stained for occludin. XZ images are shown underneath each XY image. Data shows results from one experiment with biological replicates. Scale bar 20μm.

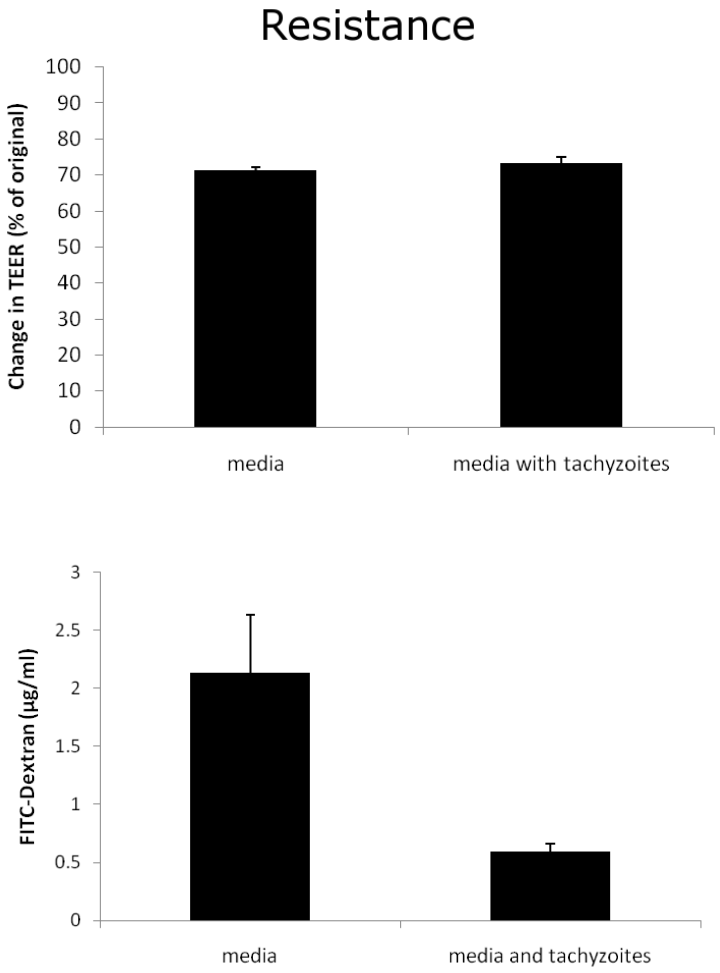

Figure 4.23: Permeability, but not TEER, was altered by *T. gondii* in human colonic C2BBe1 cells. TEER was calculated such that no changes before and after incubation would equal 100%. An increase in TEER would therefore give a value of >100%, and any decreases being shown as <100%. Data represents one experiment with biological replicates. Dextran was measured from the basal compartment of cell inserts.

the monolayer following a 5 hour infection of *T. gondii* [Kowalik et al., 2004].

In colonic cells, occludin was also altered by *T. gondii*, becoming more localised along the apical and lateral membranes, but not increasing in concentration within the cytoplasm (Figure 4.24).

4.3 Discussion

In this chapter, the effects of *T. gondii* infection were analysed by assessing the integrity and functionality of the epithelial barrier by measuring TEER, paracellular permeability and effects on individual tight junction proteins. It was found that the distribution of occludin, but not

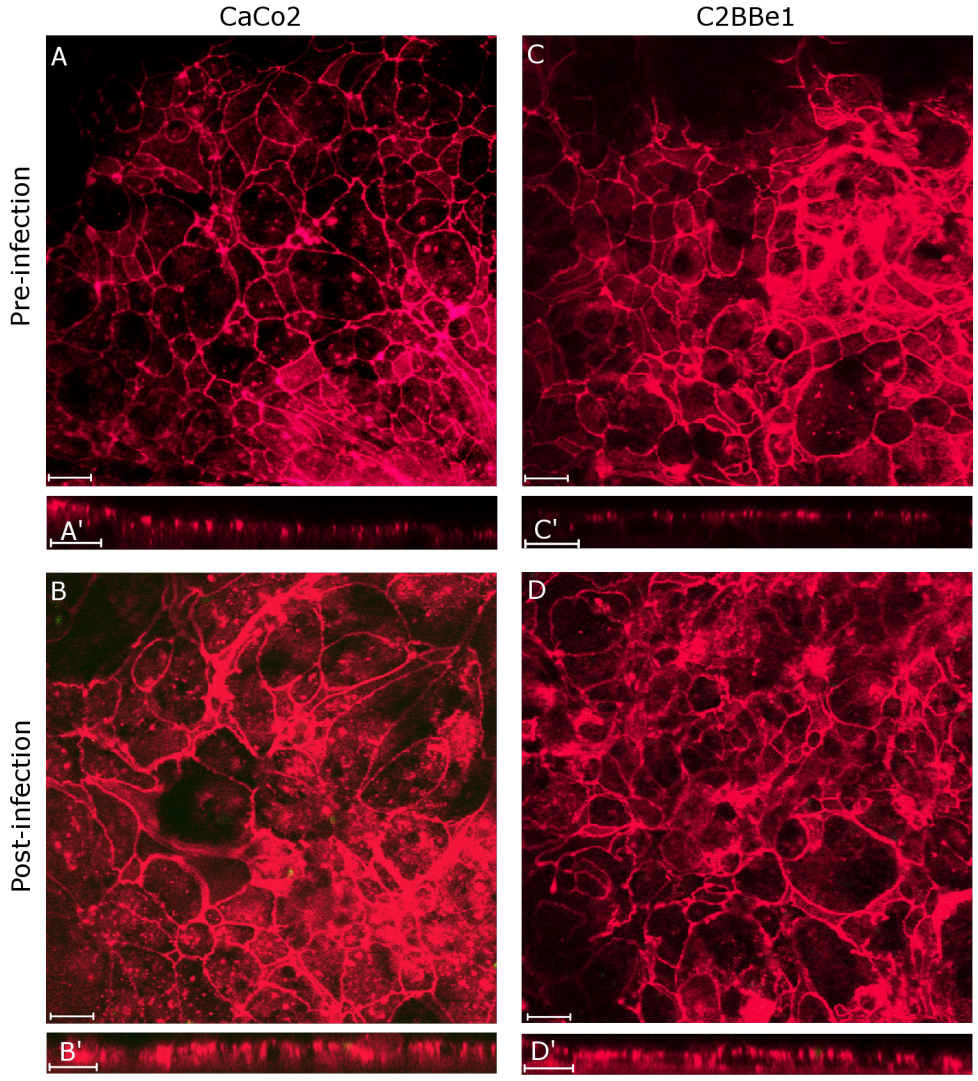

Figure 4.24: Occludin in colonic cell lines was also affected by *T. gondii*. Cells were plated onto inserts and infected with tachyzoites for 2 hours. A - D show XY images of cells stained for occludin (red) and A' - D' show XZ sections. Images represent data from 1 experiment with replicates. Scale bar = 20μm.

other junctional proteins tested, was altered in the presence of *T. gondii* tachyzoites and bradyzoites. There was no change in resistance or permeability of the monolayer suggesting that *T. gondii* tachyzoites do not disrupt the integrity of the barrier function.

4.3.1 Kinetics of *T. gondii* infection in m-IC$_{cl2}$ cells

Data presented in this chapter were obtained using a 5 : 1 ratio of parasites to cells and on average resulted in a 13% infection rate. Similar ratios and infection rates have been used in other studies where *T. gondii* has been chosen for infection of epithelial cells (Table 4.1). Variations in infection rates may be accounted for due to the strain of tachyzoite used, the compactness of the monolayer, or the cell cycle phase of the monolayer [Grimwood et al., 1996; Radke et al., 2001]. In this thesis, it was found that cell number was only 30% of the original number added to the inserts. Additionally, for any given population of *T. gondii*, it was found that 30% were either dead or not expressing YFP (Appendix J), and so it could be that the 5 : 1 ratio of parasites to cells is underestimated. Taking this into account, the ratio may be as high as 8 : 1. This would also affect the percentage of infection and transmigration, which could therefore be higher than calculated.

Parasites (P)	**Cells (C)**	**P : C**	**Infectivity**	**References**
RH	m-IC$_{cl2}$	5 : 1	13%	This thesis
RH	m-IC$_{cl2}$	2 : 1	50%	[Mennechet et al., 2002]
RH	IEC-6	5 : 1	17%	[Dimier and Bout, 1993]
ME49	MODE-K	3 : 1	NR	[Gopal et al., 2011]
BK	HT29/B6	3 : 1	30 - 35%	[Kowalik et al., 2004]

Table 4.1: Infection of *T. gondii* in different cell lines. For every cell, 2 - 5 parasites were added for 2 hours (except BK where infection was for 1 hour). NR - not reported.

In this chapter, it was found that more tachyzoites transmigrated through the monolayer (0.32%) than infected the cells (0.13%), suggesting that the preferred route of entry into the mucosa may be via the paracellular pathway. The cell monolayer was routinely checked and verified for confluency by measuring TEER, assessing permeability and by microscopic examination to rule out the possibility of a breach in integrity before infection. Parasites were often found between cells and beneath an intact monolayer, as assessed by confocal analysis, electron microscopy and flow cytometry.

4.3.2 Cellular responses following exposure to *T. gondii*

Having established that transmigration occurs through the paracellular pathway, changes in epithelial cell barrier were sought. Variations and fluctuations within TEER in non-infected cells can be mainly attributed to experimental error. TEER was measured using an ENDOHM which required each insert to be removed from a well and placed into the device. This will inevitably have altered conductance, but all inserts were treated in the same way and extra measures were taken to ensure as minimal disruption as possible. As in other studies, the TEER and the permeability remained unchanged following exposure to tachyzoites [Barragan et al., 2005], and remained unaltered when using different ratios of parasites to cells, and varying exposure times. Previous studies have illustrated that the stimulation of cells by lipopolysaccharide (LPS) did not lead to the detection of changes in TEER, which was considered to be a result of simultaneous proinflammatory and anti-inflammatory responses [Leonard et al., 2010]. Additionally, changes in ionic conductivity within a few cells would be masked by the overall conductivity of the monolayer. This may explain the variation in TEER fluctuations between experiments presented in this chapter.

However, significant differences were observed with permeability, increasing in the presence of bradyzoites in m-IC_{cl2} cells, and decreasing in the presence of tachyzoites in C2BBe1 cells. These results suggest that bradyzoites do not affect barrier function in the same way as tachyzoites, and that colonic cells are more resistant to infection than small intestinal cells. The increase in lateral localisation of occludin in colonic cells may indicate the role of occludin in regulating macromolecular flux [Al-Sadi et al., 2011]. The data also shows that the assay was responsive to changes in cells following treatment.

It was considered important to check that the small intestinal cells were responding to the presence of parasites in terms of cytokine and chemokine secretion. Although many other cytokines and chemokines are normally secreted following *T. gondii* infection [Hou et al., 2011; Ju et al., 2009], only the levels of KC and MCP-1 were tested in this thesis, both of which were significantly upregulated following infection. This is a well documented response to infection by *T. gondii* and the increased production of KC and MCP-1 in the media following 24 hours infection time was expected [Luangsay et al., 2003]. Luangsay *et al.* 2003, identified the basal secretion of MCP-1 which acted as a chemoattractant

towards the recruitment of IELs. Evidence from Egan *et al.* 2009, suggests that depending on the initial parasite burden, the IELs, in response to MCP-1 interacting with its CCR2 ligand, are capable of influencing the pathogenesis of ileitis [Egan et al., 2009]. Secretion of KC (murine homologue to IL-8 in humans) following *T. gondii* exposure has also been reported by Ju *et al.* 2009, in the human embryonic intestinal epithelial cell line Henle 407, and Denney *et al.* 1999, in human HeLa cells [Ju et al., 2009; Denney et al., 1999]. It is thought that the secretion of these and other molecules from epithelial cells drives the recruitment of immune cells such as IELs to protect the cells from further damage and reduce the numbers of transmigrating parasites [Dalton et al., 2006].

It was interesting to observe that the cells were still responsive to the presence of dead parasites, although not to the same degree as with live parasites. These finding were not in agreement with Denney *et al.* 1999, who confirmed that live parasites were required to elicit a response from epithelial cells to secrete the chemoattractant IL-8 [Denney et al., 1999]. They used fragments of dead *T. gondii* by sonicating parasite lysates, instead of using whole parasites, killed by heating or freezing as described in this chapter, which could explain the differences observed. Dead parasites did not invade the cells and did not transmigrate as they require an active actin-motor complex to infect and move [Morisaki et al., 1995; Håkansson et al., 1999]. They too had no effect on barrier function and did not appear to affect any of the junctional proteins tested, although subtle effects were observed with occludin. This could represent a surface parasite molecule that is upregulated upon attachment to the host cell which then interacts with occludin, inducing changes in expression. As no evidence was found to suggest that the parasites were secreting a product (from studies using conditioned media) that affected occludin, it was concluded that whole live parasites were required to induce these changes. Secretion following attachment may have altered occludin distribution, but was not specifically tested in this thesis.

4.3.3 Effects on tight junctions following *T. gondii* infection by tachyzoites

Dissemination from the gastrointestinal tract is imperative for *T. gondii* to generate a chronic infection within its host. The observation that transmigration was possible led to investigations into interactions between *T. gondii* and the cells. Firstly, it was evident that the parasites clustered around the edges of cells. Observing parasites between cells was not con-

sidered to be entirely due to gravity because live parasites are highly motile [Håkansson et al., 1999]. This was because parasites were seen, by live imaging, to actively sample the monolayer, moving across the cells as they did so. One image taken from a time-lapse video revealed two parasites underneath the apical domain but perpendicular to the junctions, indicating that the parasites are capable of infection through the lateral domain, and has been previously suggested [Velge-Roussel et al., 2001; Barragan et al., 2005].

This phenomenon was predicted to affect tight junction physiology. A decision was taken to look at the following tight junction proteins: occludin, because of original observations made by Dalton *et al.* 2006; claudin 2 and claudin 4, because they had not been previously examined, and ZO-1 because this had been evaluated previously and is an important cytosolic plaque protein of the tight junctional complex [Dalton et al., 2006; Barragan et al., 2005]. The adherens junction protein, β catenin was also tested because levels of the adherens junction protein ICAM-1 have been shown to change in the presence of *T. gondii* [Barragan et al., 2005].

From the results outlined in this chapter, only occludin was altered by *T. gondii*, both by tachyzoites and bradyzoites. The distribution of occludin was drastically modified following infection, with changes identified as early as 30 minutes post-exposure. As originally described by Dalton *et al.* 2006, results in this chapter demonstrate that there was a shift in occludin expression from the tight junctional complex towards a cytoplasmic, apical location after exposure, followed by a substantial increase in concentration within the cytoplasm 24 hours later [Dalton et al., 2006]. This shows that the data collected *in vitro* supports those collected from *in vivo* experiments, justifying the use of m-IC_{cl2} cells as a suitable model for small intestinal epithelial cells.

Following two hours post-infection, not only was it evident that *T. gondii* was co-localising with occludin, but did so in a polarised manner. It can be predicted that as the parasite re-orientates in preparation for infection, the moving junction that forms as the parasite makes contact with the cell involves occludin, a theory which has not yet been proposed or reported in the literature. Co-localisation remains after 24 hours of infection and at this point occludin appears to completely engulf individual parasites, which may be acting as a mask against the cells defence strategies. The parasitophorous vacuole that forms around an intracellular parasite is one that reveals a network of fibrous material between

host and parasite, although identification of interacting proteins has yet to be confirmed [Schatten and Ris, 2004; Mordue et al., 1999]. It may therefore be speculated that occludin and occludin-interacting protein complexes, may be associated with this vacuole.

Degradation products of occludin seen in this study were of a similar size to that seen following metalloproteinase-induced degradation which suggests that *T. gondii* may secrete similar products which regulate occludin [Wachtel et al., 1999]. No changes in cellular distribution of claudin 2, claudin 4, ZO-1 and β catenin were observed following 2 hours of infection by tachyzoites, although after 6 hours a slight increase in cytoplasmic-associated claudin 2 was observed. This could represent a secondary effect following the redistribution of occludin [Raleigh et al., 2011].

To confirm that the changes in occludin were a primary effect from *T. gondii* tachyzoites, rather than a consequence, a live invasion assay was attempted. This would also clarify whether occludin was more important for invasion or transmigration of parasites. Unfortunately this proved unsuccessful by staining live cells with antibodies to occludin. To overcome the technical difficulties of staining live cells for occludin, the production of a cell line expressing a stably fluorescent occludin was initiated. This would provide a method to visualise live cells without the need for immunofluorescent protocols. However, this was also unsuccessful. Alternative approaches could include the use of established fluorescent-occludin cell lines, although there are currently no murine small intestinal cell lines that express this property [Marchiando et al., 2010].

4.3.4 Effects of bradyzoites on epithelial cells

As bradyzoites and sporozoites (the latter of which is not used in this thesis) are the two life stages that naturally infect the host, it was important to consider their infection mechanisms and effects on the small intestinal epithelial barrier. However, as they are difficult to maintain in culture, the experiments described in this thesis were all performed with tachyzoites (with the exception of one experiment), which can also infect the GI tract. However, the tachyzoites are the life stage which disseminate out of the gut and through the body to reside in tissues such as the muscle and brain. As tight junction proteins, especially occludin, are found in a number of different cells, the tachyzoite infection studies are of higher relevance to these cell types and may have implications for

the infiltration of *T. gondii* through the blood-brain and blood-testes barriers.

As previously mentioned, the addition of bradyzoites to cells resulted in the monolayer becoming more permeable to dextran. Further studies could include investigations into the effects on the claudin family of proteins that regulate permeability, following bradyzoite exposure. The results suggested that a higher proportion of bradyzoites transmigrated into the basal compartment and that the rate of transmigration was more rapid, compared to tachyzoites. The percentage of transmigration in this experiment are not comparable to other experiments within this chapter as they were estimated from counting via a haemocytometer, in which autofluorescence was not an issue, and parasites were easily identified, compared to flow cytometry. However, these visual counts are not as accurate as those collected using flow cytometry. Despite this, it was clear from this study that bradyzoites were capable of crossing the epithelial cell barrier via the paracellular pathway.

Bradyzoites affected occludin in a different way to that of tachyzoites as they induced a lateral redistribution of occludin possibly for movement through the paracellular pathway, whereas tachyzoites induce a cytoplasmic redistribution of occludin for invasion of cells. The invasion rates of bradyzoites were not calculated in this study, but may provide information as to which life stage preferentially invades and/or transmigrates in small intestinal epithelial cells. Furthermore, as bradyzoites were not visualised by confocal microscopy due to the lack of YFP fluorescence, antibodies to bradyzoite specific molecules would confirm whether they co-localise with occludin.

4.3.5 Effects of *T. gondii* on colonic epithelial cells

Occludin in human colonic cell lines was also affected by *T. gondii*, but in a slightly different way to that of murine small intestinal cells. Here, occludin appeared more evenly distributed across the lateral membrane compared to non-infected cells. As the permeability was altered following infection, it was conceivable that subtle differences exist in how various cell types respond to infection. The decrease in transmigratory parasites was reflected in the decrease in permeability. As the primary point of contact would be the small intestine *in vivo*, the numbers of invasive and transmigratory parasites was therefore expected to be lower.

4.4 Conclusions

This chapter has provided evidence to show that *Toxoplasma gondii* tachyzoites can alter the distribution and co-localise with occludin, whilst retaining the integrity of the epithelial cell barrier, as measured by TEER and permeability. Bradyzoites also affected occludin in a similar way to tachyzoites, but may have a transient effect on permeability, suggesting that the mechanisms of entry into cells and transmigration between cells could be different between life stages. Additional evidence to support the finding that occludin is an important protein during *T. gondii* infection would be provided by comparing to cells that lack occludin, the results of which are described in Chapter 5. Co-localisation of occludin suggests binding of parasite surface molecules and is discussed in Chapter 6.

Chapter 5

Reduction of occludin expression in m-IC$_{cl2}$ cells

5.1 Introduction

The role of occludin is currently undefined. Previous studies have suggested occludin plays a role in development at both the cellular level and the tissue level [Saitou et al., 2000; Schulzke et al., 2005; Balda et al., 2000]. In order to determine the function of a protein, absence of the protein itself may provide evidence to ascertain various roles. It is possible to suppress a protein by mutating its gene or by eliminating the levels of protein expression using short hairpin RNAs (shRNA) or small interfering RNAs (siRNA). Mice and cells with mutated or deleted occludin have been created and the findings and implications of these were discussed in Chapter 1, Section 1.3.4.

RNA interference is a naturally occurring process in most eukaryotic organisms whereby small RNA transcripts bind to complementary regions in mRNA transcripts causing them to be silenced. This provides a post-transcriptional mechanism to regulate RNA expression within a cell. Double stranded RNA is processed into shorter strands about 20 - 25 nucleotides in length by the RNase III family nuclease enzyme Dicer. These strands are referred to as siRNAs which unwind as they are incorporated into the RNA-induced silencing complex, before binding to the mRNA complementary strand and preventing translation through cleavage [Hannon and Rossi, 2004]. The addition of siRNA is now a routine method and involves transfecting cells with often commercially available siRNA sequences. However, this method only suppresses protein expression transiently as its effect is progressively lost through cell division.

A more stable method is the use of shRNA which can be delivered by

a viral vector that incorporates itself into the DNA of the cell and will therefore be present during all subsequent cell divisions [Paddison et al., 2002; Hannon and Rossi, 2004].

To date only a few studies have been published describing the effects of occludin suppression using RNA interference in epithelial cells. Yu *et al.* 2005, proposed that in the absence of occludin, the actin cytoskeleton is unable to reorganise in response to Rho signalling (a protein involved in cell motility) [Yu et al., 2005]. They also found that occludin may be involved in the apoptotic pathway, observing fewer apoptotic cells being released from the monolayer compared to the control. This was thought to increase the risk of developing a malignant phenotype, a phenomenon which was also described by Saitou *et al.* 1998 [Saitou et al., 1998; Yu et al., 2005]. In fact, Osanai *et al.* 2006, came to the same conclusion, providing evidence that occludin acts as a tumour suppressor gene in cancerous cells [Osanai et al., 2006]. These researchers used epigenetic silencing to prevent occludin expression in a number of carcinoma cell lines [Osanai et al., 2006]. Other studies showed that although epithelial kidney cells appeared to express normal tight junction strands and TEER, there were subtle differences in permeability following occludin suppression, whereby higher amounts of monovalent organic cations were able to pass through the paracellular pathway, and in parallel, identified changes to members of the claudin family [Yu et al., 2005].

To understand the function of occludin in small intestinal epithelial cells, and to investigate further the relationship between *T. gondii* and occludin during infection of m-IC_{cl2} cells, cell lines were developed with reduced amounts of occludin using both siRNA (transient) and shRNA (permanent) approaches. The siRNA approach consisted of three target-specific oligonucleotides from Santa Cruz Biotechnology. The shRNA approach used the retroviral vector pBABEpuro, to deliver the shRNA because of its ability to produce high viral titres [Morgenstern and Land, 1990]. The shRNA in the pBABEpuro vector is under the control of the Moloney murine leukaemia virus (Mo MuLV) Long Terminal Repeat (LTR) promoter, and when incorporated into an env mutated cell line (referred to as the ΨCRE packaging cell line, derived from NIH-3T3 cells), has the ability to produce Mo MuLV virus particles containing the occludin-specific shRNA [Morgenstern and Land, 1990; Danos and Mulligan, 1988]. These could then be delivered into m-IC_{cl2} cells for reduction of occludin expression.

5.2 Results

5.2.1 Transduction of m-IC$_{cl2}$ cells with shRNA virus

In order to generate a stable cell line that would have reduced expression of occludin, a small hairpin RNA (shRNA) was integrated into genomic DNA using a retroviral approach. The shRNA sequence was obtained from Yu *et al.* 2005, and created with *Ngo*MIV and *Bam*H1 restriction enzyme sites at the 5' and 3' termini [Yu et al., 2005]. m-IC$_{cl2}$ cells were transduced with the pBABEpuro shRNA Moloney murine leukaemia virus and positive cells selected by the addition of 3μg/ml puromycin. After seven weeks of culture, there were enough cells to expand the line further. Puromycin selection was maintained throughout the duration of cell culture. Two individual preparations of virus were made and added separately to m-IC$_{cl2}$ cells. For one set of cells (Figure 5.1D), although they replicated, they never reached confluency and instead grew on top of one another. This is not uncommon as although not for transduction, the formation of multi-layered colonies following transfection has previously been reported [Vietor et al., 2001]. However, these cells were not used as the purpose of this study was to investigate *T. gondii* infection within a confluent monolayer of cells. Although they may have represented cells where levels of occludin were reduced, they may have been affected in other ways during transduction. The second set of cells (Figure 5.1C) formed a confluent monolayer after 9 days of culture. This cell preparation was used for the studies outlined below.

5.2.2 Occludin reduction by shRNA was not stable

Transduced cells were analysed for occludin expression by immunoblotting and immunofluorescence. A reduction of 50% was achieved for the cytoplasmic fraction of occludin and a 35% reduction for the membrane-associated fraction, compared to parental cells (Figure 5.2A and Figure 5.3a). The distribution of claudin 2, claudin 4 and β catenin were not significantly altered in shRNA-treated cells (Figure 5.3b and Figure 5.14), although cell morphology was different compared to parental cells.

However, following four successive passages, more occludin was present in the reduced cell line compared to parental cells (Figure 5.2B and Figure 5.4). This analysis shows that the down-regulation of occludin by the pBABEpuro retrovirus was not stable, limiting the number of experiments that could be performed.

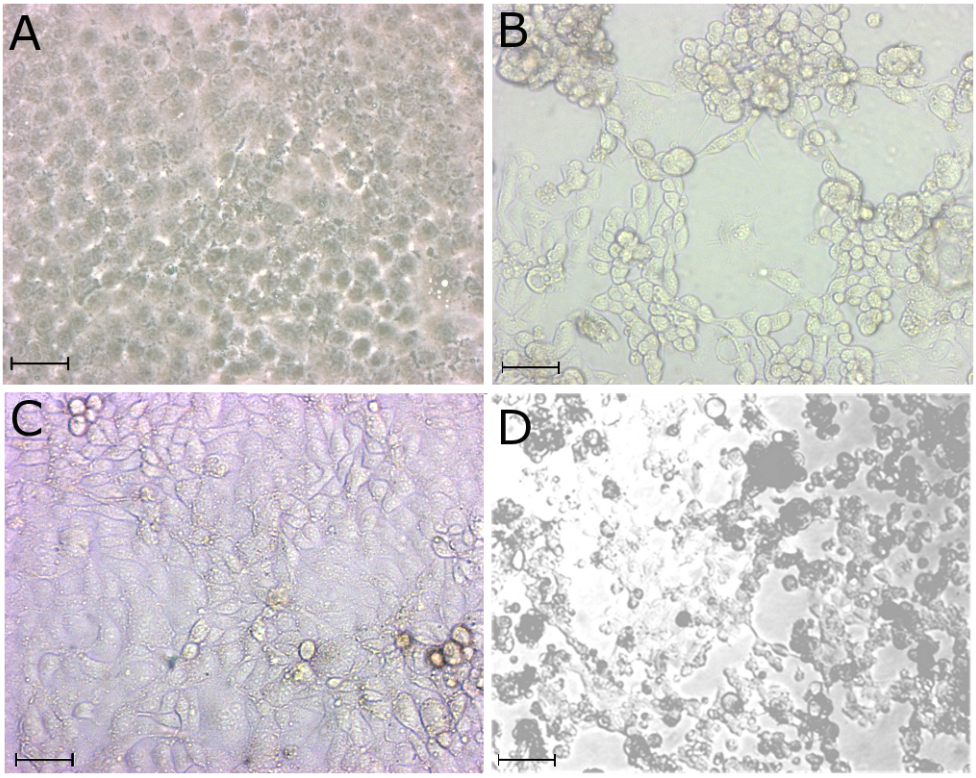

Figure 5.1: shRNA treated cells. m-IC_{cl2} cells containing shRNA-pBABEpuro were grown on 25cm^2 cell culture flasks. Confluent parental cells are shown in (A). shRNA-pBABEpuro cells after 2 days of culture are shown in (B). Images are representative of cells from two separate transduction experiments. (B) After 9 days, only one of these transductions resulted in confluent cells (C), while the other did not (D). Cells shown were of early cultures. Magnification = 20×. Scale bar = 50μm.

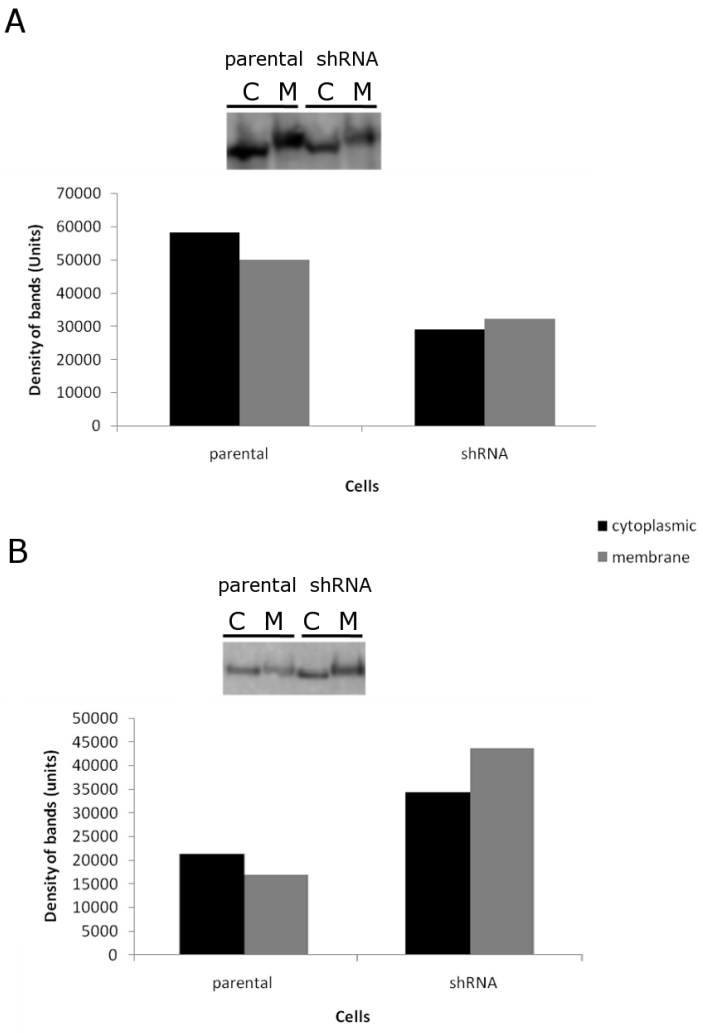

Figure 5.2: Reduced occludin levels in shRNA treated cells. Parental and shRNA-treated cells were grown on 25cm^2 flasks for 8 days and tested for levels of occludin. Early cultures of cells (A) were compared to late cultures of cells (B) by densitometry analysis of immunoblots. Data represents 2 independent experiments for each culture.

All subsequent experiments using the shRNA cells described below were carried out on early cultures which retained a 35 - 50% reduction of occludin, and in parallel, an alternative strategy for RNA interference was adopted to support data obtained from infection of shRNA cells.

5.2.3 Occludin reduction by siRNA was stable

To determine the level of suppression using siRNA, approximately 3 x 10^5 m-IC$_{cl2}$ cells were grown to 80% confluency on 6 well dishes and transfected with either small interfering RNA (siRNA) specific to occludin, non-specific scramble RNA (scRNA, used as a control) or nothing (media alone). Cell lysates were collected and tested for levels of occludin after 48 hours. siRNA decreased the cytoplasmic fraction of occludin by 54%

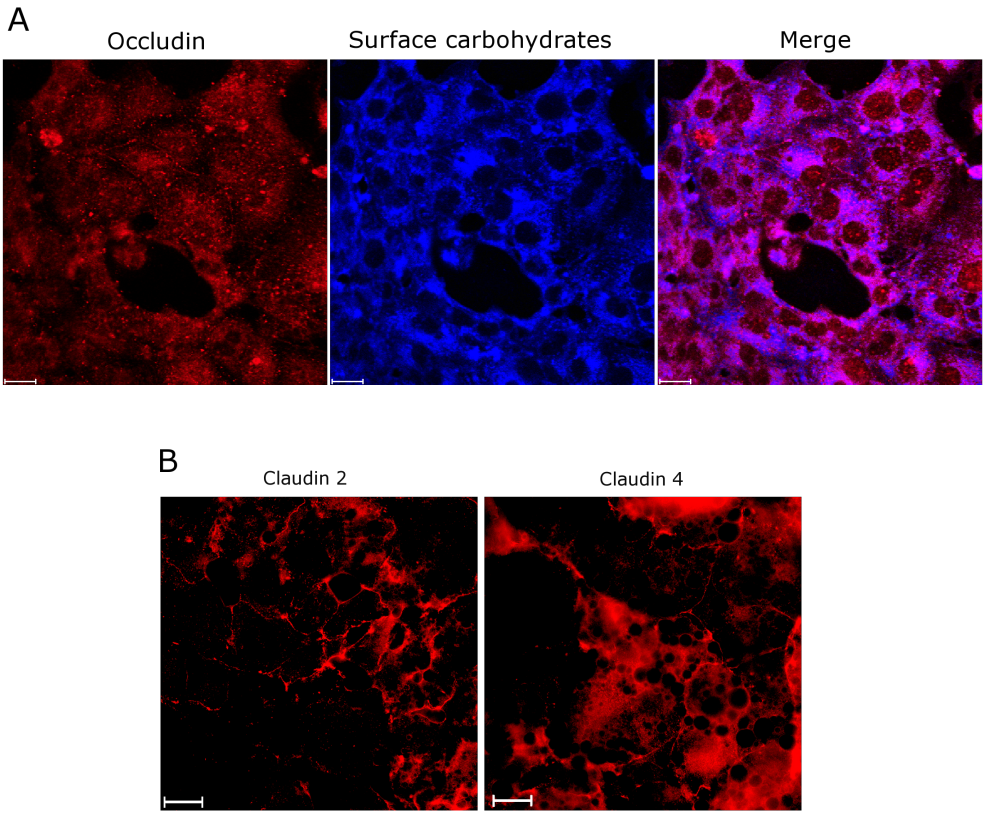

Figure 5.3: Tight junction protein expression in shRNA-treated cells. Cells from early cultures were plated onto coverslips were stained for occludin (red) and surface carbohydrates (blue). Expression levels of occludin are reduced (A) compared to Figure 5.4. (B) Expression of other tight junction proteins was still apparent. Scale bar 20μm.

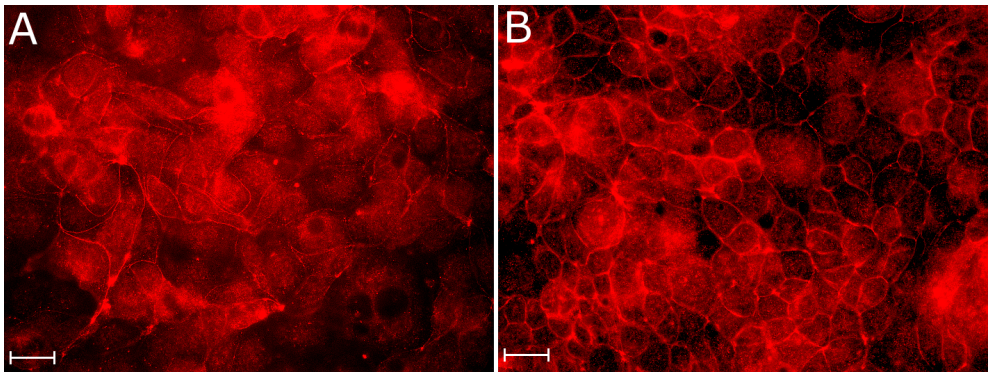

Figure 5.4: shRNA treated cells reverted in progressive cell cultures. Parental cells (A) and late cultures of shRNA-treated cells (B) were stained for occludin. Scale bar 20μm.

compared to the non-transfected cells, whereas for scRNA-transfected cells, levels only changed by <1% (Figure 5.5a). siRNA did not appear to affect the membrane-associated fraction of occludin compared to the control (Figure 5.5b). Occludin reduction was further analysed by immunofluorescence after 2 days of treatment, from cells that had grown on inserts for 11 days. Unlike the immunoblots, it was seen that both the cytoplasmic and membrane-associated fractions were decreased after siRNA treatment compared to control cells.

In a separate experiment, reduction of occludin following transfection was apparent after 6 hours, 3 days and 6 days in the cytoplasmic fraction, being decreased by 61%, 53% and 56% respectively. However, the amount of membrane-associated occludin increased during this time from 29%, 54% to 168% with respect to when media-alone was added as a control.

Together, the data suggested that the siRNA was efficient for reducing occludin levels in m-IC_{cl2} cells.

5.2.4 Barrier function in shRNA but not siRNA-treated cells, was reduced compared to parental cells

To test whether siRNA-treated cells had any effects on barrier function, TEER, permeability and the distribution of other tight junction proteins were analysed.

Confluent cells transduced with shRNA viral particles and transfected with siRNA cells were evaluated for their ability to form a tight and resistant monolayer. siRNA and scRNA were added on day 11 to parent cells and this had no effect on TEER or permeability on subsequent days (Figure 5.6 and Figure 5.8b). The addition of siRNA also made no significant difference to the distribution of claudin 2, claudin 4, ZO-1 or β catenin (Figure 5.13). Therefore, although occludin expression was reduced, there were no apparent effects on barrier function or expression of other tight junctional proteins.

However, the TEER of shRNA-pBABEpuro transduced cells was approximately one third compared to parental and siRNA cells (Figure 5.6). The TEER of these cells did not increase at any time-point after plating and were 400 times more permeable than parental cells (Figure 5.8a), suggesting that they did not completely polarise or differentiate. This was either as a direct result of occludin reduction, or due to the method by which the cell line was generated.

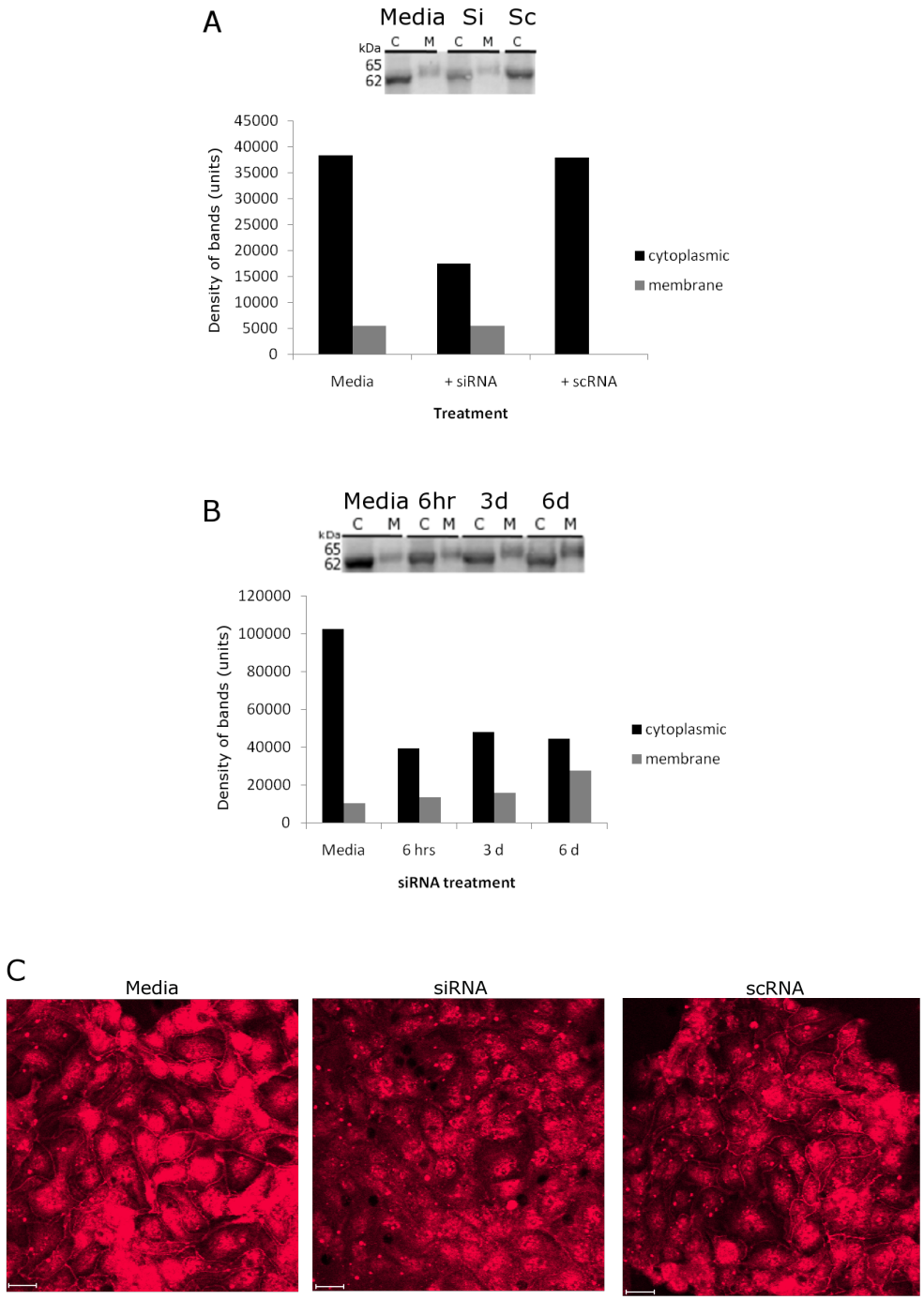

Figure 5.5: Characterisation of siRNA effects in m-IC$_{cl2}$ cells. Either normal media, siRNA or scRNA were added to cells grown on plastic for 6 days and inserts for 11 days. Cells were fixed with 2% PFA and stained for occludin on day 13. Levels of occludin reduction were tested after 2 days of siRNA transfection by immunoblotting and immunofluorescence. Reduction was analysed against occludin expression in parental cells and scRNA-treated cells after 48 hours (A). The reduction was also tested after 6 hours, 3 days and 6 days of treatment (B). Results show densitometry data from one experiment. (C) The distribution of occludin in siRNA treated cells was also visualised by immunofluorescence after 48 hours of treatment. Scale bar = 20μm.

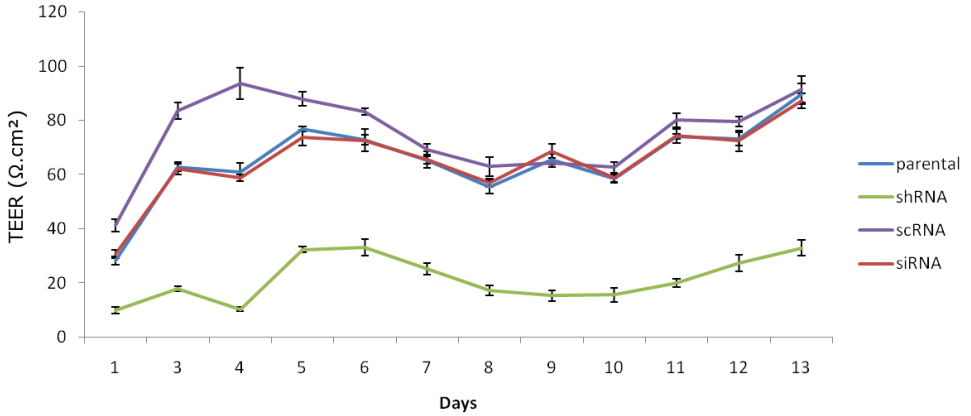

Figure 5.6: Comparison of TEER in parental and occludin-reduced cells. TEER was recorded every 24 hours on cell culture inserts. Data represents an experiment with biological replicates.

5.2.5 Infection of occludin-reduced cells by *T. gondii*

Further understanding of the role that occludin has in maintaining and developing the tight junction complex can be sought by infection studies. In the gastrointestinal tract, it is unclear as to whether or not altered levels of occludin are a cause or a consequence that will ultimately lead to gastrointestinal-associated diseases or disorders [Ciccocioppo et al., 2006; Friswell et al., 2010; Gassler et al., 2001]. Therefore, one method to determine whether or not the decrease in occludin provides a protective mechanism to the barrier, is to use a model organism that is known to infect the small intestine such as *T. gondii*, which has been shown to alter and associate with occludin distribution (Chapter 4 and [Dalton et al., 2006]). The use of a both a permanent (shRNA) and transient (siRNA) system to compare the effects of decreased occludin expression following exposure to *T. gondii,* was employed.

5.2.5.1 TEER was not affected by *T. gondii* in occludin-reduced cells

Having established from data presented in this thesis that *T. gondii* interacts with occludin during infection, an attempt to identify differences in barrier function in the absence of occludin during infection was investigated. On inserts, shRNA cells and siRNA-treated cells were infected for 2 hours with tachyzoites.

TEER was similar between cells prior to the addition of *T. gondii* although over the course of the experiment TEER dropped slightly in all cells, probably due to the disturbances that were caused whilst performing the experiment itself (Figure 5.7b, also described in Chapter 4).

However, the exception was that TEER did not decrease when parental cells were exposed to *T. gondii,* and the difference between the TEER of parental non-infected and infected cells was therefore significant (P = 0.04), indicating that the presence of *T. gondii* may have influenced TEER in some way. There were no significant changes in TEER between infected and non-infected siRNA- and scRNA-treated cells (P = >0.05). This was also true for shRNA cells, although a slight but not significant difference was seen between infected and non-infected cells (Figure 5.7a). Overall, TEER was not altered during exposure to *T. gondii* in occludin reduced cells.

5.2.5.2 Permeability was not affected by *T. gondii* in occludin-reduced cells

Changes in the permeability of both shRNA and siRNA-treated cells were analysed for changes during the presence of *T. gondii.* The amount of FITC-dextran that passed through the shRNA cells was not significantly different in the presence or absence of tachyzoites (P = >0.5, Figure 5.8a). Unlike the shRNA cells, the permeability of the monolayer was not altered by the addition of siRNA or scRNA (P = >0.2), although there was also no change in permeability between infected and non-infected samples (P = >0.6, Figure 5.8b). These results suggest that occludin does not appear to have a major role in the maintenance of epithelial barrier function during infection.

5.2.5.3 Fewer parasites transmigrate through occludin-reduced cells compared to parental cells.

To determine whether or not the number of parasites capable of transmigrating through the cells depended on levels of occludin, parental, shRNA, siRNA and scRNA-treated cells were exposed to parasites for 2 hours. Apical and basal media was collected and analysed by flow cytometry for YFP-positive populations. In shRNA cells, significantly less parasites were present in the basal compartment compared to the wild type cells (P = 0.02, Figure 5.9a). There was no difference in the numbers of parasites within the apical domain (P = 0.05, data not shown).

For siRNA-treated cells, significantly lower numbers of parasites were also detected in the basal compartment compared to parent cells (P = 0.018), even though the numbers of apical parasites were of similar magnitude across all samples (P = >0.3, Figure 5.9b). Together, 70% of

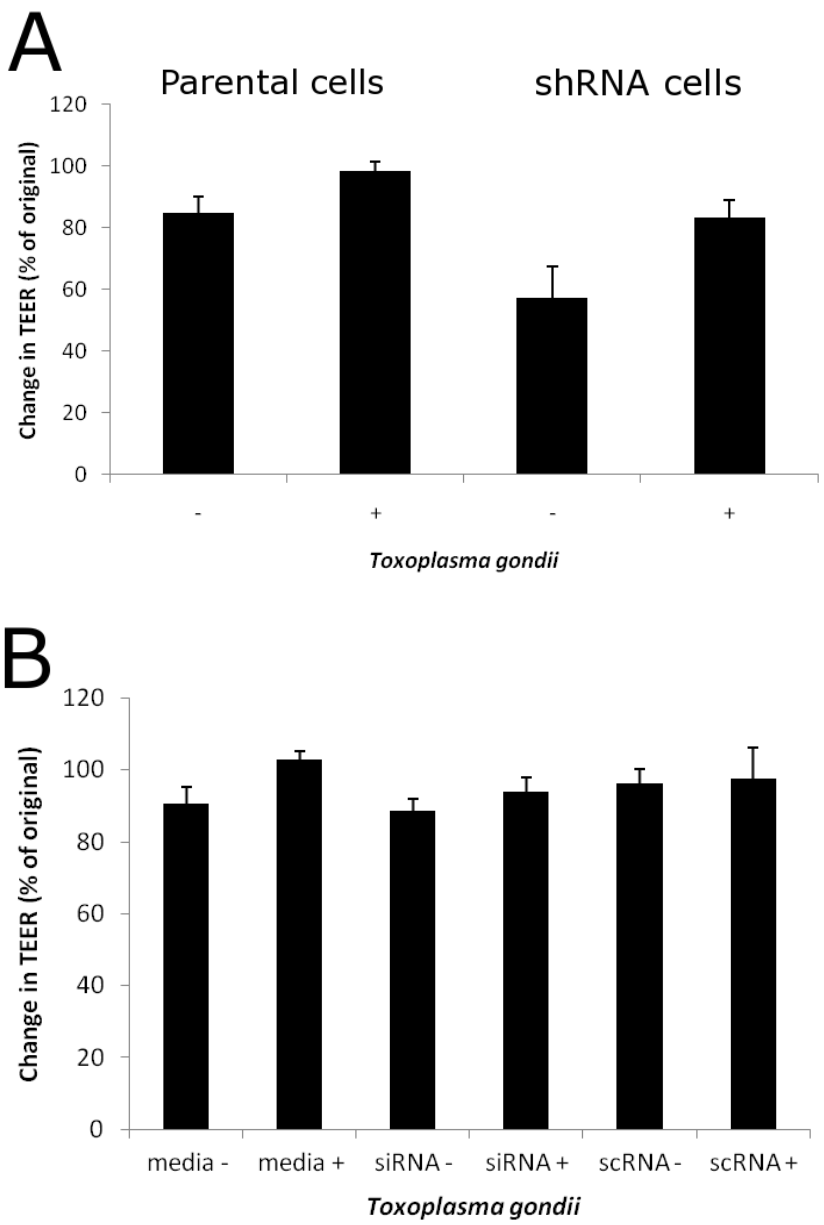

Figure 5.7: TEER was not affected by *T. gondii* in occludin-reduced cells. Parental and shRNA cells were cultured on inserts for 13 days before infecting with tachyzoites for 2 hours (A). Data represents one experiment with biological replicates. (B) Cells were grown on inserts for 11 days before adding treatments. On day 13, parental, siRNA-treated and scRNA-treated cells were infected with tachyzoites for 2 hours. TEER was measured and recorded as a percentage of TEER before *T. gondii* was added, whereby no change in TEER would equal 100%, an increase would appear as >100% and a decrease would appear as <100%. Data represents 3 independent experiments (except scRNA where n = 2).

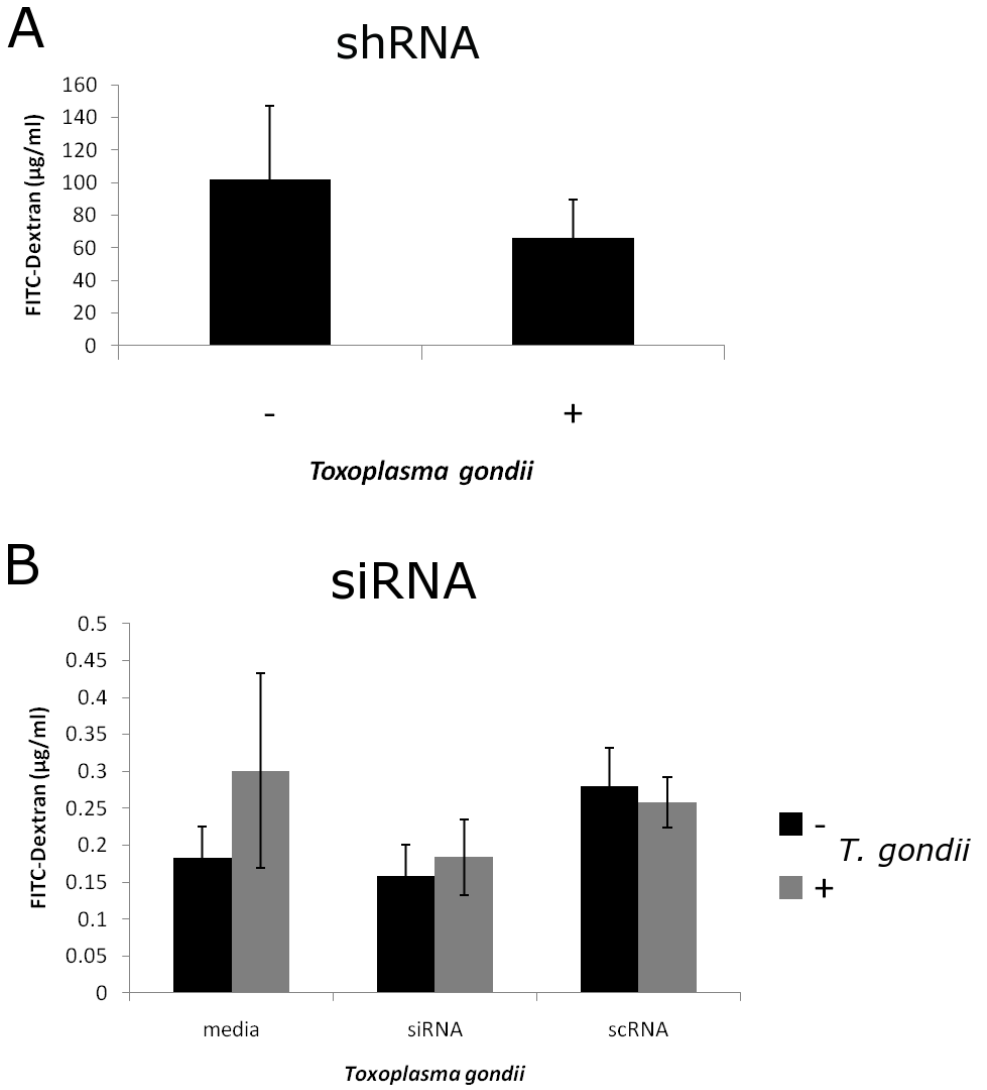

Figure 5.8: Permeability in occludin-reduced cells was not affected by *T. gondii*. Cells were grown on inserts for 13 days (Figure 5.8a) or 11 days before adding siRNA (Figure 5.8b) and infected with *T. gondii* for 2 hours on day 13. Data represents one experiment with replicates for Figure 5.8a, n = 3 for siRNA and n = 2 for scRNA, in Figure 5.8b.

initial parasites added can be accounted for from the apical and basal compartments, suggesting that approximately 30% may be associated with the cell monolayer or the insert membrane. Although more parasites were present in the basal compartment in scRNA-treated cells and less in the apical compartment compared to parent cells, the differences were not significant (P = 0.071, P = >0.3).

5.2.5.4 The percentage of infection is not altered by reduction of occludin in cells

The results from Figure 5.9 suggested that in shRNA and siRNA-treated cells, more parasites were associated with the cell monolayer compared to parent cells, as decreased numbers were found in the basal compartment but no differences were detected in the apical compartment. Therefore, it was necessary to determine whether or not occludin-reduced cells were infected at a higher rate compared to parent cells.

Overall, data collected from two - four independent experiments revealed no differences in the percentage of infection between shRNA and parental cells, and siRNA-treated and parental cells (P = 0.059 and P = 0.055 respectively, Figure 5.10). However results from another experiment did show a significant difference (P = <0.001), where there was increased infection of siRNA-treated cells. Although there was a considerable amount of variation within and between experiments, it was concluded that no detectable differences between parental and occludin-reduced cells were apparent.

5.2.5.5 *T. gondii* altered occludin distribution in occludin-reduced cells

To determine whether or not the parasites were affecting residual occludin in the same way as parent cells, cells were stained for occludin following infection.

For shRNA cells, similar results to those observed in Chapter 4 were seen, whereby following exposure to *T. gondii*, there was both a loss of membrane-associated residual-occludin and co-localisation with the parasite (Figure 5.11).

For siRNA-treated cells, exposure to *T. gondii* also lead to a redistribution of residual occludin, similar to those observed in parent and scRNA-treated cells (Figure 5.12). This suggests that *T. gondii* could still interact with residual occludin implying that the presence of *T.*

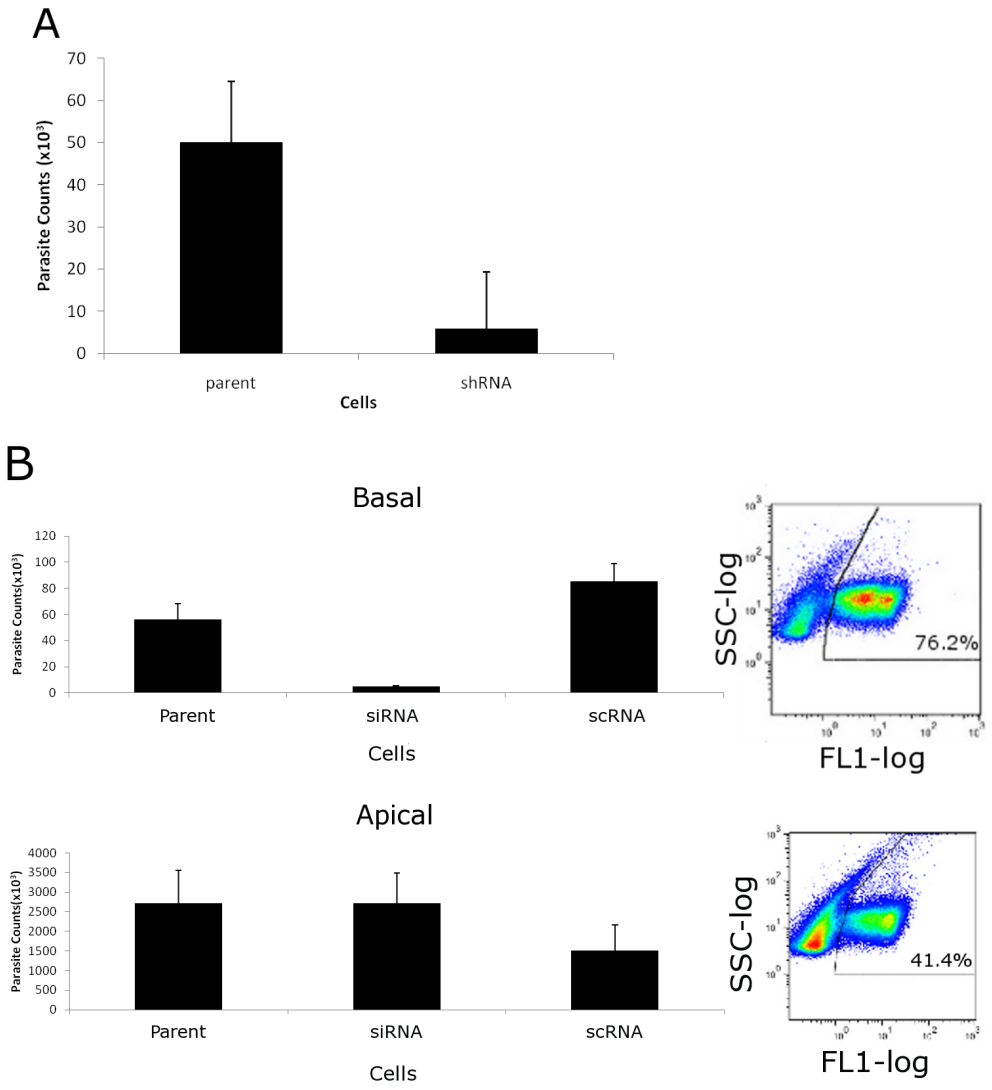

Figure 5.9: Parasite transmigration in occludin-reduced cells was decreased. Parasites were collected from the basal compartment of inserts after 2 hours of addition to the apical domain, and counted using flow cytometry, gating for YFP fluorescence (FL-1 positive populations). Basally collected parasites in shRNA cells are shown in (A), and apical and basally collected parasites in siRNA- and scRNA-treated cells are shown in (B). Data represents one experiment for shRNA and two independent experiments for siRNA and scRNA treatments with replicates.

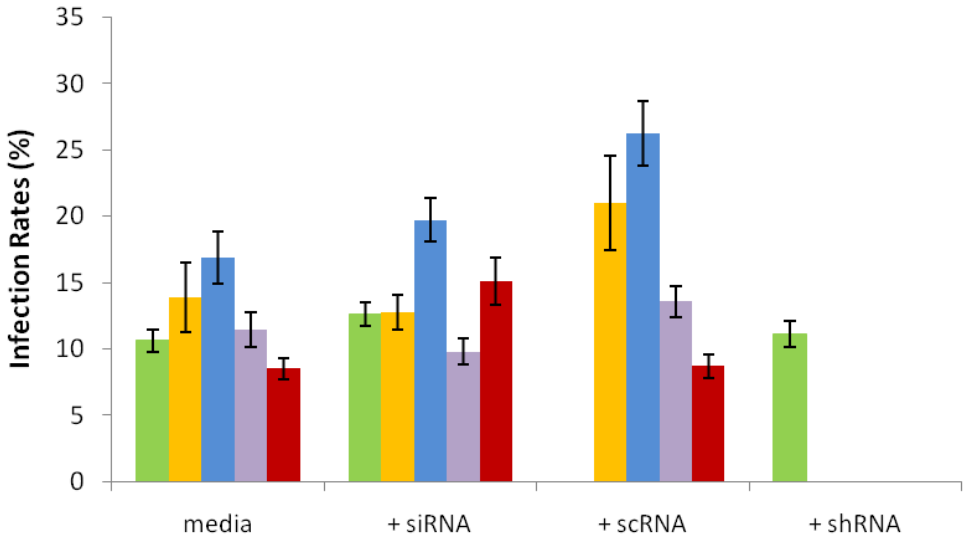

Figure 5.10: *T. gondii* infects parental and occludin-reduced cells to the same degree. Cells were plated onto glass coverslips and cultured for 2 days before adding siRNA or scRNA. Cells were infected with tachyzoites for 2 hours and counter-stained using Haematoxylin and Eosin. Between 48 and 73 fields of view were recorded for each treatment across a data set of three - five independent experiments (shown in different colours), except shRNA where data was from 1 experiment.

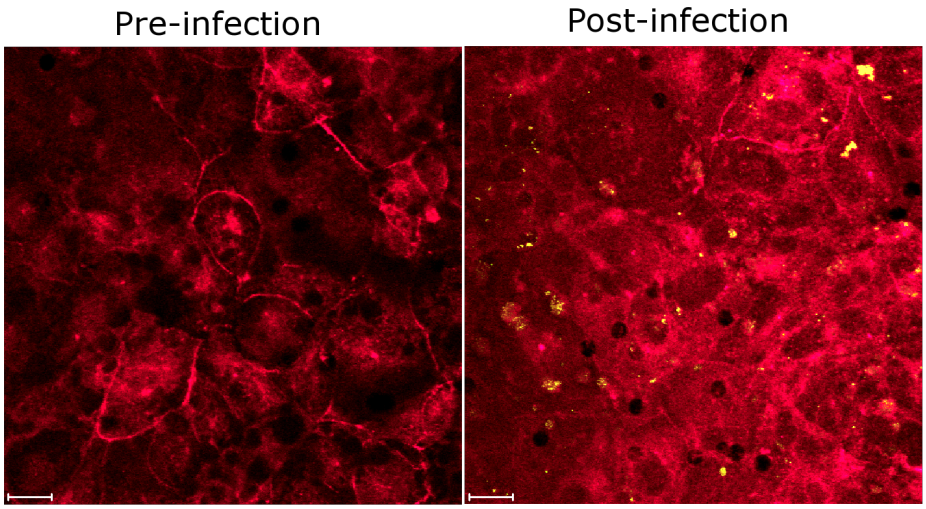

Figure 5.11: Occludin distribution in shRNA cells was altered by *T. gondii*. Cells were stained for occludin (red) following infection. A number of the parasites appear yellow which indicates co-localisation with occludin. Scale bar 20µm.

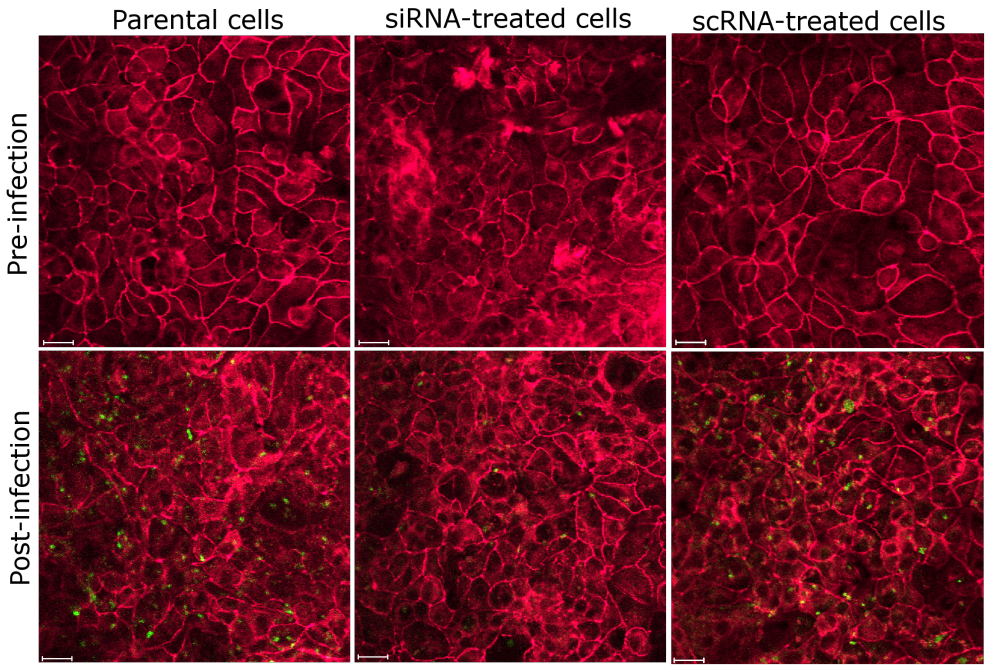

Figure 5.12: Redistribution of occludin by *T. gondii* in siRNA treated cells. Cells were grown on inserts, infected with parasites (green), fixed with acetone and stained for occludin (red). Data is representative of four independent experiments. Scale bar 20μm.

gondii may have increased the amount of membrane-associated occludin in siRNA-treated cells.

5.2.5.6 Other junctional proteins were unaffected in occludin-reduced cells during *T. gondii* infection

Previous work demonstrated that *T. gondii* did not affect other proteins in parent cells (Chapter 4). To confirm that *T. gondii* did not affect other proteins in occludin-reduced cells, the distribution of claudin 2, claudin 4, ZO-1 and β catenin were analysed. As mentioned previously, there were no changes in the distribution of junctional proteins in occludin-reduced cells was observed in non-infected siRNA-treated cells (Figure 5.13). There were also no changes in the distribution of junctional proteins following infection, with the exception of claudin 4, where, following infection in siRNA-treated cells, there was a decrease in expression levels.

The distribution of β catenin within shRNA cells was not also not significantly altered when exposed to *T. gondii* (Figure 5.14).

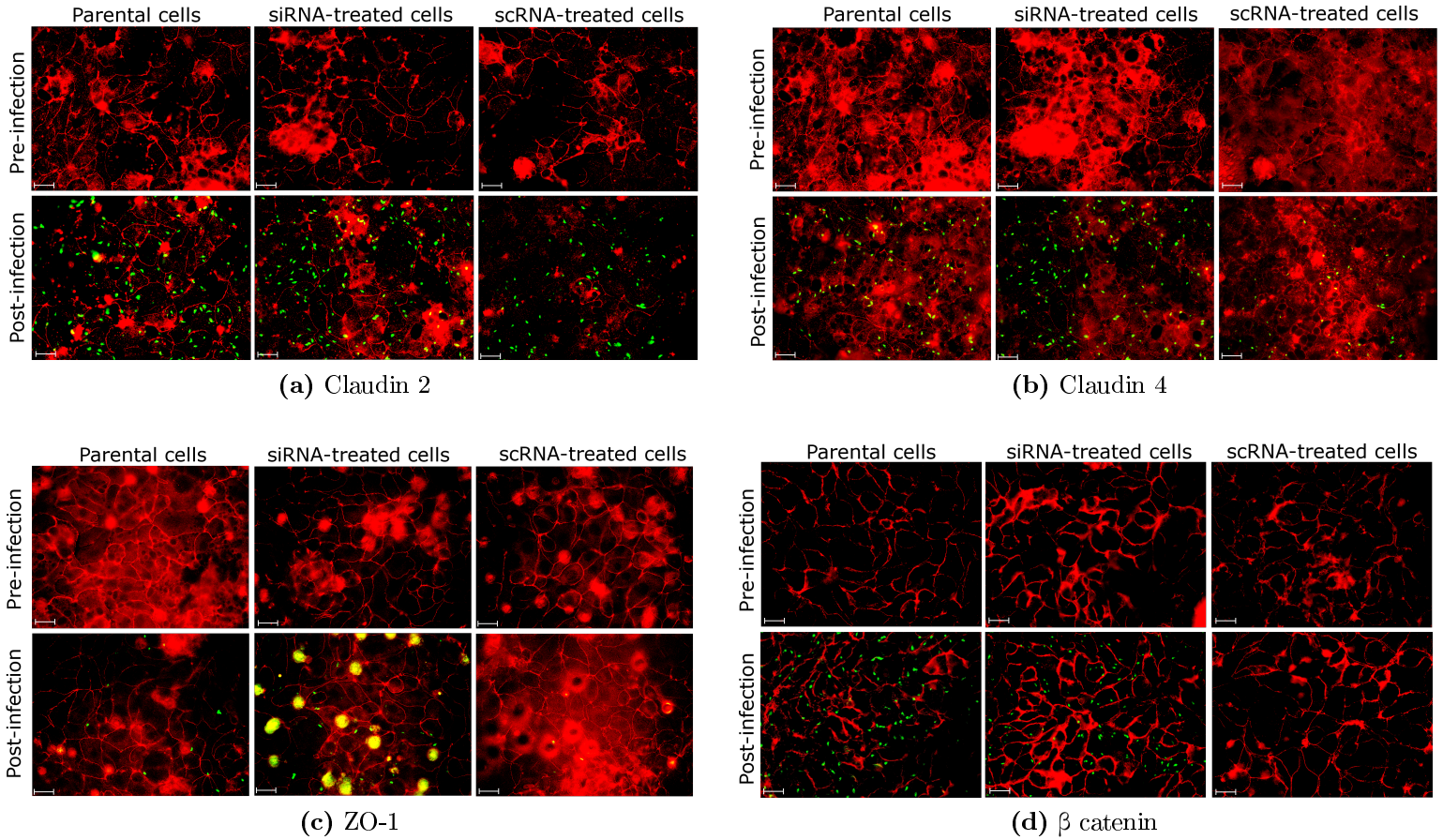

(a) Claudin 2

(b) Claudin 4

(c) ZO-1

(d) β catenin

Figure 5.13: Other junctional proteins were not affected by either the reduction of occludin or *T. gondii*. Cells on inserts were treated with nothing, siRNA or scRNA, fixed with 2% PFA and stained for claudin 2, claudin 4, ZO-1 or β catenin. Images represent data from four independent experiments. Scale bar 20μm.

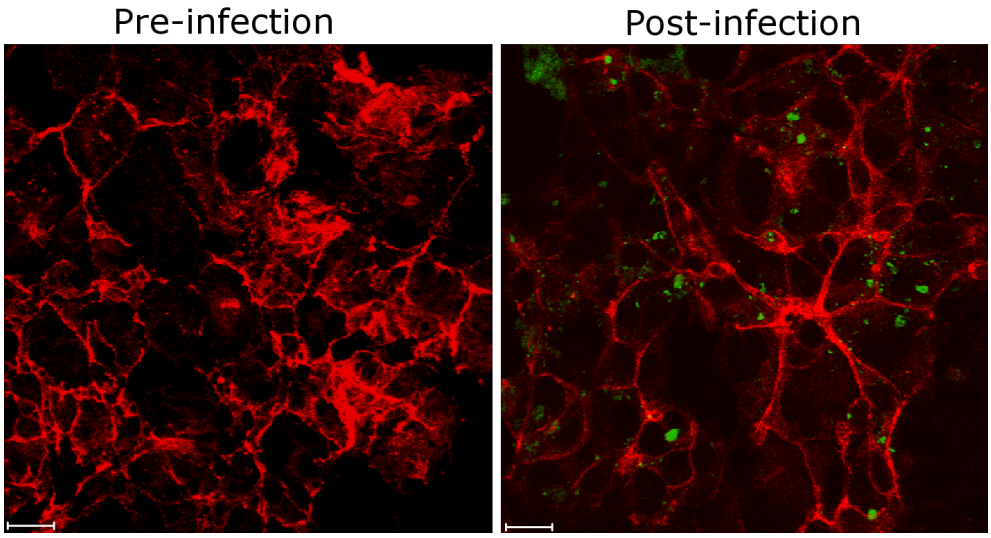

Figure 5.14: β catenin in shRNA cells was not altered by *T. gondii*. Cells with reduced occludin (A) were infected with *T. gondii* (B) and the distribution of β catenin visualised. Scale bar 20μm.

5.3 Discussion

5.3.1 Barrier function in occludin-reduced cells

In this chapter, occludin protein expression was reduced in cells using siRNA and shRNA. To date, there is only one other report where m-IC_{cl2} cells have been transduced with a virus to deliver DNA, showing that this method of delivery can be used in this cell line [Lecollinet et al., 2006]. The infection of cells with reduced occludin resulted in decreased transmigration of *T. gondii*. This could suggest that *T. gondii* uses occludin as a mechanism to enter the basal compartment via the paracellular pathway.

Currently, there are very few publications where occludin expression has been reduced in epithelial cell lines. Saitou *et al.* 1998, used homologous recombination to create occludin deficient embryonic stem cells [Saitou et al., 1998]. They concluded that the cells were still capable of forming tight junction strands and appeared to still function to create an effective barrier, with differentiation and polarisation appearing normal. Itallie *et al.* 2010, also demonstrated no changes in TEER or permeability following knock-down of occludin in MDCK II cells, which did not lead to alterations in the distribution of other junctional proteins [Itallie et al., 2010]. However, Al-Sadi *et al.* 2011, observed an increase in permeability of the monolayer to macromolecules such as 10kDa and 70kDa dextran following occludin suppression [Al-Sadi et al., 2011]. Findings presented in this chapter for siRNA-treated cells, although in a different

cell type, are in agreement with the results published by Saitou *et al.* 1998 and Itallie *et al.* 2010 [Saitou et al., 1998; Itallie et al., 2010].

In this chapter, the siRNA reduction method was not 100% efficient and only had a significant impact on the cytoplasmic fraction of occludin as occludin was still present at the tight junction complex. This may be due to membrane-associated recycling of occludin which would not be affected by the siRNA, or non-silenced mRNA that would still be translated into protein, which may account for the increase in membrane-associated occludin over time. The transient approach was specific to occludin and did not alter the ability of the cells to maintain barrier function, as neither TEER or permeability were altered by the treatment. In addition, the reduction was sustained for a sufficient amount of time to perform infection experiments. However, TEER and permeability in shRNA cells were considerably lower compared to parent cells. In addition, shRNA cells were smaller in depth and not homogeneous in appearance, suggesting that cell polarisation had occurred to a lesser extent. The possibility that occludin may contribute to developing a transepithelial electrical resistance should not be ignored and has been demonstrated in overexpression studies using MDCK cells [Balda et al., 1996].

The shRNA approach proved to not be a viable long-term option, for which there are a number of possible explanations. Transduction rates of m-IC_{cl2} cells with the shRNA was not high, possibly due to a low viral titre or inefficient transduction. Unfortunately, the few cells that survived the puromycin selection took a long time to grow (two months) which may be due to inhibitory effects that puromycin has on cell growth, as others studies suggest that following transduction, cells can be used within three weeks [Osanai et al., 2006]. Attempts to decrease the selective pressure of this treatment were carried out by removing the puromycin for two days and then reintroducing it into the media. This seemed to allow replication to occur as cell colonies started to form.

Noel *et al.* 1994, and Henning *et al.* 1995, reported the use of the IEC-6 rat small intestinal cell line to optimise gene transfer protocols that could be eventually transferred into *in vivo* models [Noel et al., 1994; Henning, 1995]. In these studies, they suggest a number of reasons why transduction efficiency may be low and provide various options to overcome these obstacles. For example, they suggested that the multiple infection of epithelial cells from successive collections of viral culture could increase transfection efficiency. This was not attempted in this thesis, but successive concentrations of viral cultures were added to dif-

ferent transduced cells, although this did not appear to make a significant difference. Noel *et al.* 1994, and Henning *et al.* 1995, also report that undiluted viral culture was inhibitory to transduction efficiency, although in this thesis, it was only the non-diluted viral culture which resulted in a few cells surviving after puromycin selection and hence presumed to be infected with the virus. Noel *et al.* 1994, and Henning *et al.* 1995, suggested the use of β-galactosidase for testing viral titre, as cells that had been transduced could be visualised without exposure to chemicals such as puromycin. If the study was to be repeated, these suggestions could be incorporated into the methodology.

It has been demonstrated that the timing of viral transduction of epithelial cells was crucial to the success of the transduction, in that the cells need to be actively dividing to express the optimum amount of retroviral receptor on their surface, because differentiated cells are known to express reduced levels of the receptor [Henning, 1995; Lecollinet et al., 2006; Miller et al., 1990]. The level of retroviral receptor expression is also known to decrease along the crypt-villus axis [Henning, 1995; Lecollinet et al., 2006]. This makes the m-IC_{cl2} cells an ideal cell line to use for this procedure, as they are derived from cells found in the base of the villus and maintain a crypt-like, partially differentiated phenotype [Bens et al., 1996].

shRNA treated cells that did reach confluency were never completely void of occludin. However, the reduction was not permanent and the cells eventually expressed levels of occludin similar to non-transduced cells. Surprisingly these cells could still survive in the presence of puromycin which suggested several things. Firstly, expression of the pBABEpuro promoter was not strong enough to maintain the dampening of occludin protein expression. Secondly, the integration of DNA into the chromosome did not occur at a suitable place and therefore altered the stability of the cells development and capacity for the DNA to remain intact. Thirdly, some cells may have become resistant to puromycin and replicated. This phenomenon has been reported before and is thought to be due to increases in cell density and reaching the stationary phase of the cell cycle [Cass, 1972]. Puromycin works by inhibiting translation and as the cells became more confluent, the uptake of puromycin may have decreased which in turn may have increased the chances of the cells becoming resistant.

The siRNA transient model was more successful in its ability to reduce occludin and did not have adverse effects on differentiation or po-

larisation, as measured by TEER and permeability. However, further optimisation of the protocol should be considered. For example, addition of the siRNA to cells could be performed at an earlier time point, when cells grown on inserts are not confluent (day 5). This may result in a higher occludin-reduction as non-confluent cells are more easily transfected and there would be sufficient time for occludin already present, to degrade before the cells were used for infection assays. However, as the function of occludin during the development of a confluent monolayer are not defined, it was decided to add siRNA on day 11 of culture, on inserts, to ensure that a monolayer with an effective barrier was established prior to addition of *T. gondii*. However, it would be interesting to determine whether transfection of cells with occludin specific siRNA at earlier time-points had an effect on differentiation and polarisation, as observed when using the shRNA approach. This may shed light on occludin function in small intestinal epithelial cells during polarisation and differentiation.

The expression of claudin 2, claudin 4, ZO-1 and β catenin were similar in siRNA-treated compared to parental cells, and still expressed at the membrane in shRNA cells. This shows that these proteins were functional at the tight junction complex. Following occludin reduction, previous reports have shown an increase in claudin 4 expression [Yu et al., 2005], and an increase in claudin 2 expression [Al-Sadi et al., 2011], suggesting that possible redundancy functions or association with these claudins and occludin [Yu et al., 2005; Balda et al., 2000]. Watson *et al.* 2001, suggested that tight junctions contained proteins that regulate a non-restrictive channel that is permeable to macromolecules and antigens, and a restrictive channel that is permeable to molecules less than 4Å [Watson et al., 2001]. Data from subsequent experiments suggested that occludin may indeed play a role in the non-restrictive channels, while claudins play a role in the restrictive channels [Watson et al., 2001; Yu et al., 2005; Al-Sadi et al., 2011]. Claudin 4 overexpression leads to an increase in TEER through charge selectivity changes in the transcellular pathway whereas claudin 2 has been shown to directly contribute to the number of tight junction pores [Itallie et al., 2001, 2008]. Therefore, had the occludin-reduced cells been cultured for a longer period of time, changes in claudin expression may have been seen, and if not, the discrepancies may be due to experimental differences or functions of individual tight junction proteins in various cell types.

5.3.2 Infection of occludin-reduced cells with *T. gondii*

Despite the limitations mentioned above, cells with experimentally reduced expression of occludin were used to investigate changes in barrier function during infection by *T. gondii*, following on from the observations made in the previous chapter.

In both occludin reduction systems, the presence of *T. gondii* did not alter TEER or permeability. Furthermore, redistribution of residual occludin was still observed following infection, and no other junctional protein was affected, with the exception of claudin 4 whose expression in siRNA-treated cells, were suppressed upon exposure to *T. gondii*. This may represent secondary effects following the reduction of occludin.

However, this chapter revealed that the numbers of transmigrating parasites in the occludin-reduced cells was up to 10 fold lower compared to the parental cells. Considering that occludin was not 100% reduced in either system, this was a surprising result, as it suggests that the parasites are sensitive to changes in the levels of both membrane-associated and cytoplasmic occludin, and that the presence of this protein may play an important role in the ability of the parasite to migrate between cells. In addition, it was not expected that transmigration in shRNA cells would lead to decreased numbers of basal parasites, as the cells were 400 times leakier compared to parental cells. These results strongly suggest that occludin is required for transmigration of *T. gondii*. Previous work carried out in a murine model has shown that intraepithelial lymphocytes (IELs) protect against changes in occludin distribution and decrease the number of disseminating parasites [Dalton et al., 2006]. It could therefore be assumed that in the *in vitro* model, where there are no immune-enterocyte interactions, occludin is available to interact with *T. gondii,* becoming altered in distribution and subsequently providing a gateway that allows the parasite to gain access to the basolateral domain. Further studies should be performed to include a co-culture of immune cells such as iIELs to ascertain whether they are responsible for decreasing the basal parasite burden.

It was intriguing to observe no overall increase in the number of infected cells between parental and siRNA-treated cells. It could be expected that if there was a decreased number of transmigrating parasites, there may be a higher proportion infecting to compensate. However, using the current methodology this was not observed, although the numbers of parasites collected from the apical and basal compartments after 2 hours

was lower in parental cells compared to siRNA-treated cells suggesting that more parasites were associated with the monolayer in parental cells compared to siRNA-treated cells. On reflection, a better method could be employed for further studies in calculating infection, as coverslips do not produce the optimum conditions for cell polarisation and differentiation. Here, the levels of infection were nearly 14 times lower than transmigration for parental cells, and only 4.86 times lower for siRNA treated cells. The low infection rate observed could represent dead parasites, a heterogenous population of *T. gondii* in which given any population of *T. gondii*, only a certain number are capable of infecting cells, unsuitable conditions for infection (cells grown on coverslips), or an underestimate of actual infection. Alternatively, changes within caveolin-dependent lipid rafts as a result of reduced occludin may affect cell surface signalling molecules that are involved in the invasion process by *T. gondii* [Italie et al., 2010]. Overall, the data provides evidence that the preferred route of invasion is through the paracellular pathway and lends further support that tight junction proteins such as occludin may acting as a gateway-transport mechanism for the parasite.

Scramble RNA was used as a control for transfection and unexpectedly, this treatment appeared to slightly increase permeability, numbers of transmigrating parasites, and the percentage of infection by *T. gondii*. Although this unusual result has occurred, it has done so using exactly the same techniques that were employed for delivering the siRNA, making the results following siRNA treatment more convincing towards exerting a real effect on transmigration of *T. gondii*. It follows that any increase in permeability would result in an increased number of parasites counted in the basal compartment, and actually provides an additional test of the systems sensitivity to detect changes. Most importantly, no major changes were detected in other junctional proteins following scRNA, siRNA, or shRNA treatments in the presence or absence of *T. gondii*. This suggested that the siRNA and shRNA were specific and the method of delivery did not significantly alter the expression or location of these proteins.

Finally, the fact that both the transient and permanent suppression of occludin has resulted in the same findings, provides further evidence that both systems were sufficient to use for defining the importance of occludin during *T. gondii* infection.

It should be noted that the data obtained from this study must be interpreted with caution as the levels of occludin were only partially

altered following siRNA and shRNA treatment. Further suppression of occludin may have altered both barrier function and the integrity of the tight junction complex, which may have given rise to differences in results. However, it is also therefore interesting to see that only a partial reduction of occludin has profound effects on transmigration of *T. gondii*.

5.4 Conclusions

Attempts to generate occludin-reduced cells were partially successful but further optimisation is required. Nevertheless, results from these experiments suggest that delivery of siRNA by transfection reagents is the best method for reducing occludin expression in m-IC_{cl2} cells. In differentiated and polarised m-IC_{cl2} cells, the use of siRNA to target occludin did not appear to affect barrier resistance or permeability implying that occludin does not play a key role in maintaining these functions, although the reduction of occludin did impact on the number of transmigrating parasites. However, as the suppression was not 100% effective, it cannot be concluded that occludin has no effect on barrier function. Previous evidence demonstrating co-localisation between occludin and *T. gondii*, and the findings presented in this chapter, suggest that *T. gondii* may harness occludin to facilitate efficient transmigration between epithelial cells. It could be predicted that the over-expression of occludin would increase the numbers of basally located parasites, and it would be interesting to determine the effects of reduced and over-expressed occludin on bradyzoite transmigration levels.

Chapter 6

Occludin interacting proteins within m-IC_{cl2} cells and *T. gondii*

6.1 Introduction

Although it is accepted that *T. gondii* can infect many different cells, molecules on both the parasite surface and host cell surface involved during the process of infection remain to be identified [Lei et al., 2005]. However, they are considered to be present on a wide range of cells and be relatively conserved and abundant proteins, to allow infection of any cell type [Furtado et al., 1992b,a; Dubey et al., 1998; Lei et al., 2005]. To date, the following receptors and ligands have been recognised in this process: in human foreskin fibroblasts and Chinese hamster ovary cells, laminin on *T. gondii* was found to mediate binding to the β1 integrin receptor, α6β1 [Furtado et al., 1992b]; the interactions of microneme proteins to host cells during infection is thought to be important as the surface-associated microneme proteins MIC2 and MIC3 from *T. gondii* can bind to cells [Carruthers et al., 1999; Garcia-Réguet et al., 2000; Huynh et al., 2003]; and Barragan *et al.* 2005, demonstrated that binding of MIC2 could occur through ICAM-1 in MDCK cells [Barragan et al., 2005].

The tachyzoite surface contains glycosylphosphatidylinositol (GPI) 4-anchored proteins [Lekutis et al., 2001] and Debierre-Grockiego *et al.* 2010, provided evidence that galactin-3, which is upregulated during *T. gondii* infection [Bernardes et al., 2006], binds to GPI anchored proteins [Debierre-Grockiego et al., 2010]. Lectins on the surface of the parasite have also been implicated in host cell binding, and have been found to interact with sulfated polysaccharides and sulfated proteoglycans that are commonly found on the surface of cells and are considered important for parasite interactions [Ortega-Barria and Boothroyd, 1999; Lourenço et al., 2001; Carruthers et al., 2000].

Binding partners of occludin that have been identified include ZO-1, ZO-2 and ZO-3 [Furuse et al., 1994; Kale et al., 2003; Li et al., 2005]. Additionally, proteins that co-localise with occludin at the membrane, such as Vesicle-Associated Membrane Protein of 33kDa (VAP-33), Junction-Enriched and Associated Protein (JEAP) and the Coxsackie Adenovirus Receptor-like Membrane protein (CLMP), have also been described [Lapierre et al., 1999; Nishimura et al., 2002; Raschperger et al., 2004]. Other interacting proteins of occludin include kinases and phosphatases such as Phosphatidylinositol 3-Kinase, atypical Protein Kinase C, Casein Kinase 1ε, Casein Kinase 2, Extracellular signal-Related Kinase (ERK), Protein Phosphatase 2A and Protein Phosphatase 1 [Basuroy et al., 2006; Du et al., 2010; Seth et al., 2007; Clarke et al., 2000; McKenzie et al., 2006; Andreeva et al., 2001].

In this thesis, evidence has been presented to show that occludin may be involved during the process of *T. gondii* transmigration of epithelial cells. Not only was the cellular expression of occludin altered, but parasite co-localisation suggests that *T. gondii* may bind occludin, which could also play a role in the formation and maintenance of the parasitophorous vacuole. Therefore, recombinant occludin fragments were generated to test *T. gondii* interactions and infected cell lysates were analysed for the identification of interacting molecules.

6.2 Results

6.2.1 *T. gondii* binds to the extracellular loops of occludin

Using a flow cytometry based assay, recombinant occludin fragments were generated and incubated with parasites to confirm binding.

6.2.1.1 Generation of recombinant occludin fragments

As the extracellular loops (ECLs) of occludin bind each other on adjacent cells ([Gorodeski, 2006; McCaffrey et al., 2008]), it was thought that this part of the molecule is most likely to be in contact and therefore interact with *T. gondii.* Therefore, a fragment was generated that included the sequence from ECL1 to the end of the ECL2 (referred to as ECL1-ECL2).

The DNA sequence was amplified from FLAG-tagged occludin within a pBABEpuro plasmid vector, using the pECL1F and pECL2R primers (see Appendix D). DNA was inserted into a pET3a plasmid vector and recombinant protein produced from large scale cultures of BL21 *E.coli.*

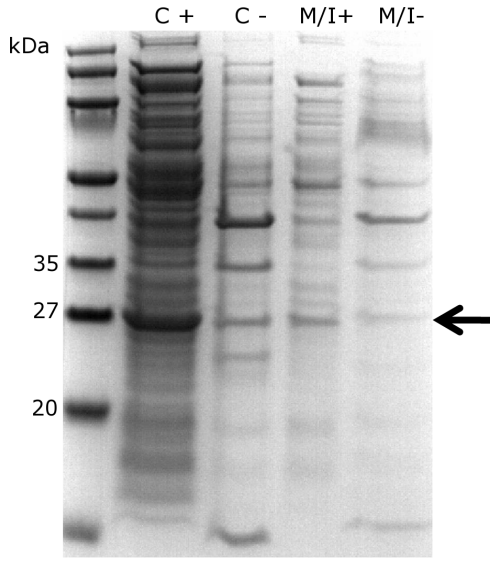

Figure 6.1: Recombinant ECL1-ECL2 was found in the cytoplasm of bacterial cultures. Induced or non-induced bacteria cultures, using 4mM IPTG were lysed and analysed for the production of recombinant protein on coomassie-stained gels. The lysates were separated into cytoplasmic fractions (C) and membrane-associated and inclusion body fractions (M/I), with (+) or without (-) IPTG induction.

Recombinant ECL1-ECL2 was highly expressed in the cytoplasmic fraction from BL21 *E.coli* lysates (Figure 6.1). Protein was also present in the membrane-associated and inclusion body fraction in the absence of IPTG induction, although to a lesser extent compared to the cytoplasmic fraction. Therefore, the soluble fraction was used as a source of recombinant protein.

After protein purification, recombinant fragments were immunoblotted to confirm reactivity with anti-occludin antibodies recognising the extracellular loops of occludin, specifically the ECL2 region. Recombinant ECL1-ECL2 was 27kDa in size and possible dimerisation may have occurred as protein bands were also found at 35kDa (Figure 6.2).

6.2.1.2 Binding assay with *T. gondii* and recombinant ECL1-ECL2

To test whether or not ECL1-ECL2 and *T. gondii* interact, a binding experiment was performed. Using a flow cytometry based assay, parasites fixed with 2% PFA were incubated with recombinant protein and fluorescently-labelled secondary antibodies were added to detect parasite-protein complexes. As controls, parasites were incubated with either protein or antibodies alone. Non-specific binding was reduced by adding 1% BSA to the parasite suspension.

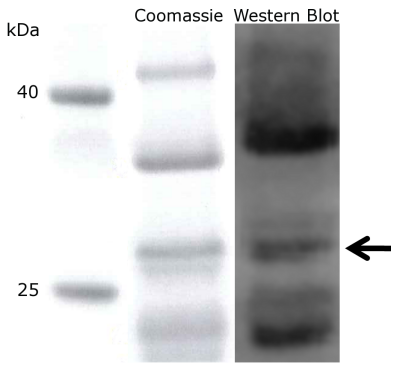

Figure 6.2: Recombinant ECL1-ECL2. Purified recombinant protein was resolved using a 4 - 12% SDS-PAGE gel and either stained with Coommassie Brilliant Blue (left) or immunoblotted and probed with an anti-occludin antibody that recognises the extracellular loops of occludin (right). The monomeric protein was detectable at 27kDa (arrow). Potential dimers were also detected at 35kDa, and possibly a degraded, cleaved or partial-protein product at 15kDa. The protein molecular marker is shown on the left hand side.

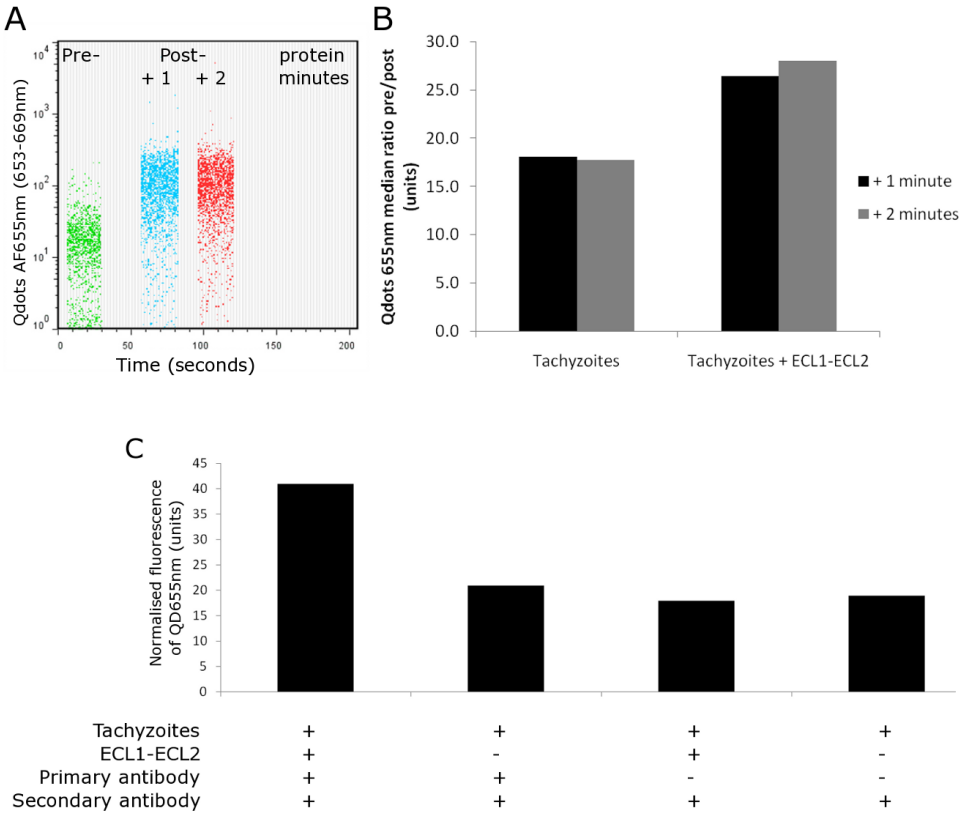

Figure 6.3: *T. gondii* binds to the extracellular loops of occludin. Approximately 5.5 x 10^5 fixed parasites were incubated in PBS supplemented with 1% BSA for 15 minutes, before adding recombinant ECL1-ECL2 fragments (8µg/ml). An anti-occludin antibody was added to the mixture, followed by secondary antibody (Quantum dots conjugated to Alexa Fluor 655nm, Invitrogen). After one minute, and two minutes, samples were acquired by flow cytometry (A). The increase in fluorescence detected upon ECL1-ECL2 addition is depicted in (B). Controls showed that the shift in fluorescence was due to binding of the protein and not to the antibodies (C). Data was corrected for background fluorescence of Quantum dots Alexa Fluor 655nm. This experiment was performed and analysed by Roy Bongaerts (Institute of Food Research, Norwich, UK).

The presence of recombinant ECL1-ECL2 occludin increased fluorescence following incubation with an antibody-complex (Figure 6.3). After two minutes of incubation, the specific fluorescent signal increased further, consistent with a continuation of binding events. A fluorescent signal was not observed with *T. gondii* in the absence of protein nor with incubation with antibodies alone. Due to technical reasons, it was only possible to perform this experiment once in the time available. Although only a preliminary experiment, the data suggests that *T. gondii* can bind to the extracellular loops of occludin. Separate ECL-1 and ECL-2 occludin fragments have been generated and will be used to determine which extracellular loop governs the binding to *T. gondii.*

6.2.2 Immunoprecipitation

To identify molecules that bind and interact with occludin during *T. gondii* infection, immunoprecipitations (IP) and bioinformatic searches were performed.

6.2.2.1 Immunoprecipitation following *T. gondii* infection

To find potential cellular and parasite-derived binding partners of occludin, anti-occludin IPs of *T. gondii* infected (2 hours and 6 hours) and non-infected cells were performed. Protein bands of between 55 - 230kDa were extracted from SYPRO Ruby stained gels (Figure 6.4), and prepared for sequence identification by mass spectrometry analysis (performed by Francis Mulholland, Institute of Food Research, Norwich, UK).

The molecules listed from MASCOT software following mass spectrometry analysis were condensed according to the following criteria: only molecules that had two or more peptide matches and molecules over the 95% probability for significance value were included (indicated by the peptide score and calculated within MASCOT) and peptides which recognised heavy and light chain regions of antibodies were ignored as these most likely came from the antibody used for the IP.

Molecules were categorised into those associated with the cytoskeleton such as myosin, actin and keratin and microtubule-related proteins such as tubulin; protein regulators for example kinases, ubiquitination proteins, chaperones, protein folding-associated molecules; general proteins involved in cell metabolism such as ATPases, glycolysis-associated proteins; molecules involved in stress responses like heat shock proteins and protein disulphide isomerases; *T. gondii* derived proteins and un-

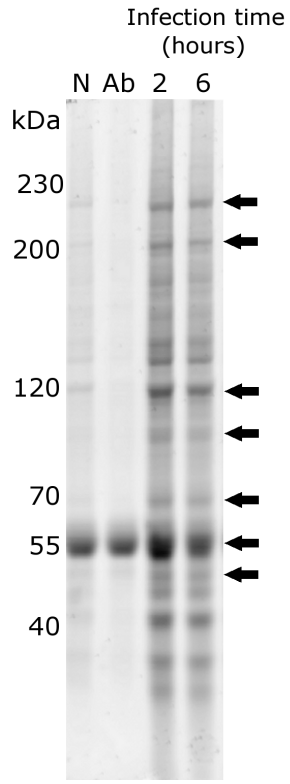

Figure 6.4: Protein identification following an occludin IP from infected cell lysates. Occludin was precipitated from cell lysates that were non-infected (N) or infected with *T. gondii* (for 2 or 6 hours), using an anti-occludin antibody and resolved by SDS-PAGE. Precipitate containing antibody alone (no cell lysates) was used as a control (Ab). The large SYPRO Ruby stained band at 55kDa included the antibody and the band at 70kDa contained occludin. Other protein bands were extracted for identification of possible binding partners (arrows). The experiment was repeated twice.

characterised proteins (those without database annotations).

Within these criteria, molecules were then listed according to how significant they were in terms of peptide coverage over the entire sequence and prevalence within the sample. The higher the score, the more likely the identified molecule was a true result. A selection of molecules that were identified are shown in Table 6.1, with the full list provided in Appendix K. Molecules associated with ATP, glycolysis and general cell metabolism have not been included for analysis within this chapter. Table 6.1 lists molecules from highest to lowest numbers of peptide hits within functional categories and length of infection.

Molecules in Table 6.1 are of interest for further study as functions consistent with occludin regulation was found. Although not all peptides were checked against the *T. gondii* genome, it was assumed that the majority of molecules listed were derived from murine cells. However, six *T. gondii* derived proteins were identified from cells infected for 2 hours, which are considered as key findings. These were a protein disulphide isomerase (TGME49_011680), Rhoptry protein 18 (TGME49_005250), a subtilase family protein (TGME49_004050), a CELF protein (named after CUG-binding protein and Embryonically lethal abnormal vision (ELAV)-type RNA binding protein 3 [Ladd et al., 2001]) (TGME49_121500), HSP70 (TGME49_051780) and HSP90 (TGME49_08830).

The implications of specific molecules on occludin regulation during infection by *T. gondii*, are discussed in Section 6.3.

6.2.3 Bioinformatics

6.2.3.1 Potential binding partners of occludin from *T. gondii*

Using a complementary approach to find potential molecules that interact with occludin, the sequence of murine occludin was BLASTed against the *T. gondii* genome [1]. This database is designed such that sequence homology to a molecule is initially searched within the ME49 strain of *T. gondii*, and if none are found, the GT1 and VEG strains are searched. For every profile within the database, homologues are given for the other strains, but are generally not reported in this thesis.

As *T. gondii* was shown to bind to the extracellular loops of occludin, it was assumed that the interacting protein on the parasite surface may possess a degree of sequence similarity. Therefore, the occludin sequence from ECL1-ECL2 was BLASTed. This search revealed seven *T. gondii*

[1] http://www.toxodb.org

Function	Accession Number	Annotation	Infection (hours)	Peptide hits	Protein Score	Pred. Size (kDa)	Obs. Size (kDa)
CM	Q4FJZ2	Karyopherin (Importin) α 6	0	2	66	60.31	70
CM	Q1PG84	pBK1	2	3	92	52.25	70
CM	Q3U517	Apoptosis inhibitor 5	2	2	45	57.09	70
CM	D3Z0M9	Dead box helicase family	6	2	41	95.78	120
CR	P63038	60 kDa heat shock protein, mitochondrial	0	3	138	61.09	70
CR	P27773	Protein disulfide-isomerase A3	0	3	47	57.10	70
CR	P63017	Heat shock 70 kDa protein	2	10	220	71.06	70
CR	B6KDQ4	Heat shock protein 70	2	10	213	73.29	70
CR	B6K8N0	Heat shock protein 70	2	8	185	73.38	70
CR	A2AUF6	Heat shock 70kD protein 5 (Glucose-regulated protein)	2	6	200	72.49	70
CR	P27773	Protein disulfide-isomerase A3	2	6	181	57.10	70
CR	P63038	60 kDa heat shock protein, mitochondrial	2	4	169	61.09	70
CR	Q71LX8	Heat shock protein 90 α	2	3	55	83.57	100
CR	Q71LX8	Heat shock protein 90 α	6	15	284	83.57	100
CR	P07901	Heat shock protein 90 α	6	14	243	85.13	100
CR	A4QPD6	Phospholipase A2, activating protein	6	4	112	88.59	100
CR	B6KKA5	Heat shock protein 90	6	3	76	82.28	100
CY	B6KJM2	Membrane skeletal protein IMC1	2	7	87	70.35	100
CY	B6KM69	Myosin A	2	3	44	93.89	100
CY	Q62418	Drebrin-like protein	2	2	76	48.96	55
CY	B2RRX1	β actin	2	2	67	42.05	70
CY	B2RRX1	β actin	2	2	67	42.05	55
CY	Q3TWG5	Dynein cytoplasmic 1 light intermediate chain 1	2	2	65	56.86	70
CY	Q8VDD5	Myosin-9 Cellular myosin heavy chain, type A	6	22	697	227.43	230
CY	Q8VDD5	Myosin-9 Cellular myosin heavy chain, type A	6	21	544	227.43	200
CY	Q7TPR4	α-actinin-1	6	19	561	103.63	120
CY	P57780	α-actinin-4 F-actin cross-linking protein	6	15	385	105.37	120
CY	Q8VDD5	Myosin-9 Cellular myosin heavy chain, type A	6	9	265	227.43	120
CY	P21271	Myosin-Vb	6	7	180	212.09	230
CY	Q3UH59	Myosin, heavy polypeptide 10, non-muscle	6	6	125	234.33	200
CY	Q8VDD5	Myosin-9 Cellular myosin heavy chain, type A	6	5	128	227.43	100
CY	B8JK03	Myosin Va	6	2	92	216.70	230
CY	B2RRX1	β actin	6	2	84	42.05	100
CY	B2RRX1	β actin	6	2	73	42.05	120
CY	B1AQZ2	Kinesin family member 3A	6	2	61	82.98	100
CY	B2RRE2	Myosin 19 Protein	6	2	51	233.02	200
PR	P80315	T-complex protein 1 subunit δ	0	3	62	58.54	70
PR	B1AT36	Proteasome (Prosome, macropain) 26S subunit, non-ATPase	0	2	68	50.94	55
PR	O55222	Integrin-linked protein kinase	0	2	55	51.85	55
PR	Q542X7	Chaperonin subunit 2 (β)	2	5	159	57.78	55
PR	P11983	T-complex protein 1 subunit α	2	5	157	60.87	70
PR	Q3TII3	Elongation factor 1-α	2	4	175	50.41	55
PR	Q9WVM1	Rac GTPase-activating protein 1	2	4	145	70.86	70
PR	Q3TII0	T-complex protein 1 subunit δ	2	4	117	58.56	70
PR	Q5NCU1	Ras-GTPase-activating protein SH3-domain binding protein 1	2	4	50	51.85	70
PR	P50396	Rab GDP dissociation inhibitor α	2	3	53	51.06	55
PR	B6KJR5	Ubiquitin associated domain-containing protein	2	2	121	208.30	100
PR	Q9JMA1	Ubiquitin carboxyl-terminal hydrolase 14	2	2	88	56.42	70
PR	Q542X7	Chaperonin subunit 2 (β)	2	2	71	57.78	55
PR	A2BH28	Ubiquitin-like 1 (Sentrin) activating enzyme E1B	2	2	48	71.21	100
PR	Q3TML6	Eukaryotic translation initiation factor 2, subunit 3	2	2	42	51.60	55
PR	B2MWM9	Calreticulin	2	2	33	48.14	55
PR	Q5SXR6	Clathrin, heavy polypeptide (Hc)	6	24	784	193.63	200
PR	Q6PEE6	Adaptor protein complex AP-2, α 2 subunit	6	5	115	104.85	120
PR	Q3T9Y4	Coatomer protein complex, subunit β 1	6	5	102	108.14	120
PR	Q5SXR6	Clathrin, heavy polypeptide (Hc)	6	4	120	193.63	120
PR	A2BH28	Ubiquitin-like 1 (Sentrin) activating enzyme E1B	6	3	116	71.21	100
PR	B1ASH6	Rho guanine nucleotide exchange factor (GEF) 16	6	3	108	80.67	100
PR	Q8CIJ3	Eukaryotic translation initiation factor 3 subunit B	6	3	71	110.11	120
PR	B1AXN9	Ribosomal protein S6 kinase polypeptide 3	6	2	88	80.96	100
PR	O55029	Coatomer subunit β	6	2	55	103.24	120
PR	Q5SWR1	Adaptor-related protein complex 2, β 1 subunit	6	2	40	106.57	120
PR	A5XDA7	ROCK2 splice variant	6	2	37	167.80	200
TG	B6KKA5	Heat shock protein 90	2	6	156	82.28	100
TG	B6KHU4	Heat shock protein 70	2	6	139	78.54	70
TG	B9PU53	Subtilase family protein	2	4	82	85.79	100
TG	Q2PAY2	Rhoptry protein 18	2	3	92	62.70	55
TG	B9Q331	CELF family protein	2	2	36	50.94	55
TG	B6KTXO	Protein disulfide isomerase	2	2	33	52.80	55

Table 6.1: Selected proteins identified by Mass Spectrometry following IPs. Non-infected and infected cell lysates were precipitated for occludin and resolved by gel electrophoresis. Murine and *T. gondii* databases were searched by Alex Jones (Sainsbury Laboratory, Norwich, UK) using a peptide mass tolerance of 15ppm and a fragment mass tolerance of 0.6Da within MASCOT (Matrix Science) software. Numbers of peptide matches are shown along with peptide scores (only significant proteins are shown, and scores indicate logarithmic probabilities towards identity or extensive homology to known proteins). Predicted sizes are based on database searches and observed sizes represent the molecular weight according to the SYPRO Ruby stained gel. CM - cell metabolism, CR - cell response proteins, CY - cytoskeletal and microtubule-related, PR - protein regulators, TG - *T. gondii* derived. Proteins include data obtained from two independent IPs.

proteins (Table 6.2). As it is currently unknown if both extracellular loops are involved in binding with *T. gondii*, separate BLAST searches against ECL1 and ECL2 were performed. These revealed five proteins for each ECL, all of which were different from those found from the combined ECL1-ECL2 search. It was concluded in Chapter 4 that conditioned parasite media containing secreted proteins had no effect on occludin and that live parasites were required to induce effects on occludin. This is consistent with a transmembrane-domain containing molecule being involved in binding to occludin. Of the 17 proteins revealed from these searches, 8 were transmembrane domain-containing proteins. These proteins were then aligned with occludin (Table 6.3).

Multiple products from *T. gondii* may interact with occludin, especially following infection where the C-terminus of occludin would also be accessible to the parasite and its secreted products. Therefore, further BLAST searches were performed, this time against the C-terminus, as well as the full length sequence of murine occludin. This search revealed 19 proteins of which five aligned to residues within ECL2, and one within the intracellular loop (Table 6.2). Eight proteins were annotated as conserved hypothetical proteins and were therefore grouped together.

On average, *T. gondii* proteins against full length occludin were approximately 17% identical and 33% similar to occludin. These similarities were mainly within the C-terminus of occludin, although the zinc finger FYVE domain-containing protein, myosin F (TgMyoF), the Hsc70/Hsp90-organising protein and the dense granule protein 5 precursor aligned to residues within ECL2 (Figure 6.3). The DEAD/DEAH box helicase protein aligned to residues within the whole sequence length of occludin and was also identified from the IPs. This suggests that the criteria used to search for potential interacting partners using bioinformatics were valid.

BLASTing *T. gondii* against ECL1 resulted in five *T. gondii* proteins that aligned with a higher sequence identity and similarity compared to the other searches. The alignments were concentrated around, but not exclusive to, the repetitive glycine-tyrosine residues of occludin. For example, one protein aligned with residues WDR-YG at the beginning of ECL1. This protein also aligned with ECL2 sequences (YLY-Y) which is a highly conserved sequence in mammals, and Blaschuk *et al.* 2002, have described the motif as an occludin cell-adhesion recognition (CAR) sequence [Blaschuk et al., 2002].

BLASTing with ECL2 highlighted a vesicle-associated membrane pro-

Occludin homology	ID number	Annotation of protein	TMD	Length aa	MW kDa	Sequence Identity (%)	Sequence Similarity (%)
C terminus	many	conserved hypothetical proteins	0	-	-	~15	~30
C terminus	056060	nucleosome assembly protein	0	812	89.5	16	31
C terminus	012880	M protein repeat, viral A type inclusion protein	0	4817	560.1	17	32
C terminus	021500	dual specificity protein phosphatase, catalytic domain	0	982	109.1	16	28
C terminus	031170	chromosome condensation protein	0	1640	183.4	16	30
C terminus	039970	merozoite surface protein	0	191	21.7	19	32
IEL - C terminus	GT1_037870	dense granule protein 5 precursor	0	120	13.0	17	31
ECL2 - C terminus	VEG_041710	zinc finger FYVE domain containing protein	0	538	59.2	18	33
ECL2 - C terminus	052220	Hsc70/Hsp90-organising protein	0	565	63.3	18	32
ECL2 - C terminus	078870	myosin F (TgMyoF) protein	0	1953	216.4	15	26
whole protein	GT1_049520	DEAD/DEAH box helicase	0	1454	156.9	17	29
ECL1	**081590**	**conserved hypothetical protein**	**2**	**116**	**13.9**	**39**	**44**
ECL1	**116550**	**conserved hypothetical protein**	**2**	**116**	**13.0**	**37**	**47**
ECL1	064610	heterogeneous nuclear ribonucleoprotein A3	0	430	45.0	42	47
ECL1	GT1_062610	phenylalanyl tRNA synthetase isoform	0	525	59.3	37	42
ECL1	039500	proteasome subunit alpha type 4	0	252	27.9	22	24
ECL2	096020	hypothetical protein	0	157	17.4	26	39
ECL2	**091300**	**endoplasmic reticulum retrieval protein 1 (RER1)**	**2**	**222**	**25.4**	**18**	**36**
ECL2	GT1_088810	tRNA isopentenyl transferase	0	741	80.3	21	33
ECL2	**VEG_025150**	**Vesicle associated membrane protein -7 (VAMP7)**	**3**	**221**	**25.0**	**16**	**24**
ECL2	093010	tRNA val	0	136	15.2	29	35
ECL1+ECL2	GT1_027340	phosphatidylinositol-4-phosphate 5-kinase	0	2148	233.0	18	28
ECL1+ECL2	**090870**	**patched family domain containing protein**	**12**	**1178**	**130.6**	**20**	**38**
ECL1+ECL2	**020390**	**conserved hypothetical protein**	**4**	**258**	**27.5**	**18**	**33**
ECL1+ECL2	031110	conserved hypothetical protein	0	1106	118.5	21	38
ECL1+ECL2	**049760**	**vitamin K epoxide reductase subunit 1**	**3**	**136**	**14.5**	**20**	**31**
ECL1+ECL2	GT1_073250	conserved hypothetical protein	0	120	13.9	22	32
ECL1+ECL2	**GT1_005760**	**conserved hypothetical protein**	**2**	**116**	**13.8**	**36**	**41**

Table 6.2: BLASTing the *T. gondii* genome for occludin homologues revealed 35 molecules. Searches against different parts of the occludin molecule were searched for *T. gondii* homologues. Protein annotations were according to these provided in the database. All proteins are preceded with 'ME49_' unless stated otherwise. Proteins that have transmembrane domains are highlighted, and numbers of domains are listed (TMD). Length of proteins in terms of the number of amino acids are shown and the molecular weight (MW) in kDa. Identical residues and similar residues (where the amino acid changes without affecting charge or hydrophobicity) are represented as a percentage of total sequence identity or similarity.

tein similar to a protein identified from immunoprecipitates as this protein has been annotated as VAMP in the VEG strain, but a disulphide isomerase within GT1 strain.

The putative vitamin K epoxide reductase subunit 1 protein was the only protein that aligned with the two cysteine residues within ECL2. This protein could interact with occludin through disulphide bonds.

Although there was not enough time or resources to investigate these findings in further details, the results from the searches offer a starting point for future work.

6.3 Discussion

Results presented in this thesis have illustrated that *T. gondii* appears to co-localise with occludin. In this chapter, evidence has been provided to confirm these interactions by illustrating binding to the extracellular loops of occludin.

To search for occludin binding partners two complementary approaches were used which revealed a number of potential candidates molecules that were both cellular and parasite derived.

6.3.1 Immunoprecipitation

To identify cellular proteins that might interact with and regulate occludin, IPs were performed to both concentrate the protein and detect occludin-protein complexes. Gel electrophoresis of cell lysates revealed a number of protein species ranging from 50 - 230kDa. Although occludin was detected within a 70kDa species, it was not present in large quantities, although previous studies have shown that occludin does not efficiently stain with SYPRO Ruby which may explain its relatively low appearance within the analysis [Li et al., 2005]. However, as samples were immunoblotted in parallel to those sent for mass spectrometry analysis, confirmation that the IP extracted occludin from the lysates was provided. Future experiments would involve entire gel lane digestion, or a sample solution digest using multi-dimensional protein identification technology (MudPIT) for Mass Spectrometry analysis. To rule out non-specific binding of proteins, an immunoprecipitation of cell lysates and magnetic beads, in the absence of anti-occludin antibody, should be included in future experiments.

ID	Sequence from ECL1-ECL2 of murine occludin
	TLAWDRGYGTGLFGGSLNYPYSGFGYGGGYGGGYGGYGYGYGGYTDPRAAKGFLLAMAAFCFIASLVIFVTSVIRSGMSRTRRYYLIVIIVSAILGIMVFIATIVYIMGVNPTAQASGSMYGSQIYMICNQFYTPGGTGLYVDQYLYHYCVVDPQE
CHP	----DRGYG----G----YPYSG-GYG--YG-GY-GY-YGYG-Y----------
CHP	---W--GYG----G----YPY-G--YG-GYG--YG-Y-YGYGGY----------
CHP	-----RGYG----G----YPYSG-GYG--YG-GY-GY-YGYG-Y----------
RER1	----------Y----YM----F----G-G-Y----L------DP--
VAMP7	----------PTAQ-----Y----Y---------------DQY--HY-VV----
PFD	T-A----Y--G-FG----------Y---R----------C-----V---TSV--S--S-T-T--L------A--------A--VY--GV--T--A----------I-N----------Y---Y----P-E
CHP	----------F---L--P---F-Y----------Y-------P----------AF-F---L-IF---VI-SG-SR-----L-V-------G---FI-T------VN----------GS---M------TP--T----------Y-----Q-
VKER1	----------G--------AA-G-L----A-----S-VI--T--IRSG---T--YL-----V----------A------G----------C--FYT---T--Y----LY--CVV----
CHP	----------P-------L-M-A-CF-AS-------V--S--SR---Y----------LG----------QASGS-YG-------N-FY-PG----------VD-Q-
HNR A3	---W----G-G--GG---Y-----GYGGG-G--YG-YGYGYGGY--P--A----------

Table 6.3: Eight transmembrane domain proteins from *T. gondii* align within the extracellular loops of occludin. ECL1 and ECL2 of occludin were BLASTed against the *T. gondii* genome. Proteins containing transmembrane domains were aligned (using EMBOSS) with occludin against the relevant proportion of sequence from *T. gondii* protein. Only identical amino acids are shown. ECL1 and ECL2 sequences of murine occludin are shown in blue and the transmembrane domains and intracellular loop (ICL) in black. Two proteins that matched the ECL loops but did not contain transmembrane domains are included at the bottom of the table to illustrate that high sequence identity can occur in other proteins. Molecules shown are derived from Table 6.2. CHP - conserved hypothetical protein, RER1 - endoplasmic reticulum retrieval protein 1, VAMP7 - vesicle-associated membrane protein 7, PFD - patched family domain containing protein, VKER1 - vitamin K epoxide reductase subunit 1, HNR A3 - heterogeneous nuclear ribonucleoprotein A3.

6.3.1.1 Products from *T. gondii*

Following two hours of infection, six *T. gondii* proteins were detected from the immunoprecipitates. These were a subtilase family protein, CELF protein, a disulphide isomerase, rhoptry protein 18 (ROP18), and two heat shock proteins.

Subtilase family protein Subtilases are serine proteases important for protein-processing during infection. TgSUB1 is a GPI-anchored protein found in the micronemes that localises at the parasite surface after microneme secretion, whereas TgSUB2 is a rhoptry protein maturase [Lagal et al., 2010; Miller et al., 2003]. The presence of this protein in the lysates suggests that a serine protease subtilase complex may interact with occludin. This interaction may lead to degradation of occludin, such as that observed in Figure 4.10, and could be caused by a molecule such as a serine protease subtilase [Wachtel et al., 1999].

CELF protein CELF proteins contain RNA recognition-motif domains that are involved in the regulation of alternative splicing, but little is known about *T. gondii* derived CELF [Ladd et al., 2001].

Disulphide isomerases Protein disulphide isomerases catalyse, reduce and isomerise disulphide bonds between cysteine residues during protein folding. The formation of disulphide bonds via cysteine residues has been reported to play a role in the invasion of epithelial cells by other pathogens [Davis et al., 2002]. In addition to this role, studies have shown that disulphide isomerases may represent important cell-parasite interactions during infection by *Neospora caninum* and have been observed to be present on cell surfaces [Naguleswaran et al., 2005; Turano et al., 2002]. Antibodies to *T. gondii* specific disulphide isomerase have been detected in human tears, revealing a role in the immune response to the pathogen [Meek et al., 2002a,b]. This could be an important molecule for affecting occludin during *T. gondii* invasion and further investigations into the interactions between occludin and disulphide isomerase are required. This could be achieved using recombinant occludin fragments to perform IPs with lysates from *T. gondii*. Fluorescent microscopy could also confirm the expression profile of disulphide isomerases during infection to see if co-localisation occurs with occludin.

ROP18 Occludin is a protein that can be hyperphosphorylated on serine/threonine residues [Wong, 1997]. ROP18 is present on the surface of the parasitophorous vacuole and has serine/threonine kinase activity [Hajj et al., 2007]. A primary function of ROP18 is to increase the multiplication rate of *T. gondii* once invasion has taken place and therefore may be an important virulence factor [Saeij et al., 2006; Taylor et al., 2006]. As occludin was shown to remain associated with *T. gondii* up to 24 hours after infection (Figure 4.14), ROP18 may bind to occludin as part of the parasite moving junction, and continue to interact with it after the parasitophorous vacuole has formed. Confocal microscopy could confirm this and phosphorylation of occludin by recombinant ROP18 would confirm whether or not ROP18 plays a role in the regulation of occludin.

Heat shock proteins Heat shock proteins 70 (HSP70) and HSP90 proteins from the immunoprecipitates were derived from both the cells and the parasites. HSP70 from *T. gondii* is an anti-apoptotic chaperone that is considered to be a danger signal, inhibiting the production of nitric oxide from macrophages and increasing parasite replication ([Mun et al., 2000; Hwang et al., 2010]), while HSP90 is important for invasion and intracellular proliferation of *T. gondii* [Ahn et al., 2003]. Both HSP70 and HSP90 are involved in stage conversion [Echeverria et al., 2005; Weiss et al., 1998]. There presence suggests that occludin interactions with *T. gondii* may play a role in parasite survival.

6.3.1.2 Other molecules

Kinases Within the immunoprecipitates, integrin-linked protein kinase (non-infected cells), ribosomal protein S6 kinase and Rho-associated, coiled-coil containing protein kinase 2 (ROCK2) were detected. Integrin protein kinases are serine/threonine kinases involved in regulating cell adhesion to the extracellular matrix [Wu et al., 1998]. Ribosomal protein S6 kinase has a wide range of functions including cell cycle regulation, regulating gene and protein expression, phosphorylating small GTPases and acting as a substrate for ERK [Frödin and Gammeltoft, 1999]. ERK has been shown to bind to the C-terminus of occludin, preventing its disruption within the tight junction and ribosomal S6 kinase may therefore be part of a complex which affects the function of occludin following stress signals [Basuroy et al., 2006]. ROCK2 can regulate the activity of ribosomal S6 kinase, phosphorylate myosin light chain kinase, and bind to RhoA and RhoC [Pelosi et al., 2007; Riento and Ridley,

2003]. This suggests that through binding to RhoA, ROCK2 may influence the phosphorylation state of occludin. Furthermore, ROCK2 leads to the suppression of Rac1 activation that induces lamellipodia formation and cell migration, in which occludin also plays a role [Marchiando et al., 2011]. These results indicate that ROCK2 may be involved in an occludin protein complex which following infection, may be upregulated to support plasma membrane changes to accommodate the formation of the moving junction.

Cytoskeletal molecules Other proteins which are known to regulate tight junctions and interact with occludin include the Rho guanine nucleotide exchange factor 16 and Rac/Rab/Ras GTPases that were also identified from the IPs [Jou et al., 1998]. Associated with the cytoskeleton, many myosins, actins and keratins were found as well as microtubule and microfilament derived proteins such as tubulin, debrin and dynein. This provides evidence to suggest that an increased level of occludin may be present at the tight junction complex and therefore associated with the cytoskeleton following infection.

Cellular response molecules Anti-apoptotic signal pathways may be activated by *T. gondii* during infection and upregulate proteins such as anti-apoptotic inhibitor 5 (Api5), a molecule of which was identified from the IPs [Morris et al., 2006].

Protein disulphide isomerases can be found on the cell surface as well as in the endoplasmic reticulum where they assist in protein synthesis and correct folding [Mandel et al., 1993; Gilbert, 1997]. Inside the endoplasmic reticulum, protein disulphide isomerases act as chaperones to TAP (transporter associated with antigen processing)-translocated peptides that bind to MHC-1 molecules [Lammert et al., 1997]. On the cell surface, they can contribute to thiol redox stability, influencing the ability of nitric oxide to diffuse into a cell [Zai et al., 1999]. Thiol disulphide exchange within occludin oligomers has been documented and therefore could influence occludin dynamics and movement within the tight junction complex [McCaffrey et al., 2008].

HSP70 is also involved in antigen presentation in immune cells, transporting MHC class 1 associated peptides to the surface for T cell recognition [Castelli et al., 2001]. This could indicate that occludin has a role in antigen recognition pathways perhaps by stabilising interactions between the plasma membrane and the cytoskeleton. Furthermore, the induction

of heat stress has previously been found to increase the levels of occludin expression both at the mRNA and the protein level and are thought to protect against breaches within the intestinal barrier [Dokladny et al., 2008]. This would provide a mechanism by which *T. gondii* crosses the epithelial barrier without affecting its integrity, suggesting that upregulation of occludin may function to buffer transient changes within the paracellular pathway. As dendritic cells, which express occludin [Rescigno et al., 2001], can pass freely between cells moving from a basal to apical direction, it could be that *T. gondii* has developed a similar technique to move from the apical to the basal domain of cells, and activates pathways such as heat stress to achieve this strategy.

Recycling molecules A number of recycling, endocytic-related and degradation-mediated molecules were found in the immunoprecipitates, indicating occludin turnover has been altered during infection by *T. gondii*. Examples of molecules found include chaperones and protein assembly molecules such as HSP70 and HSP90, and actinin 4 which is known to recruit occludin to the tight junction complex via MICAL-L2 [Nakatsuji et al., 2008]. This implies that new or recycled occludin could be transported to the membrane during infection. In addition, clathrin, coatomer subunits, adaptor protein complexes and phospholipase A2 were also detected from the precipitates which are involved in endocytosis and recycling of proteins [de Figueiredo et al., 1998]. Consistent with these findings, the presence of a degraded species of occludin was found in immunoblots of infected cells (Figure 4.10) could have been caused by ubiquitination, possible from ubiquitin-like 1 enzymes that were also found in the IPs.

6.3.2 *T. gondii* binds to occludin

Initial contact with occludin is likely to be via the extracellular loops and as confirmed in this chapter, *T. gondii* can bind to this region of occludin. Following attachment and interaction with occludin, other proteins may be secreted from the parasite such as those found in the immunoprecipitates. However, *T. gondii* may also be acting on occludin via the intracellular N- and C-termini. In addition to the extracellular domains, BLAST searches against the C-terminus of occludin were also performed and revealed a dual specificity protein phosphatase and dense granule protein 5, which may regulate occludin once invasion has occurred.

6.3.3 Bioinformatics

To limit the search for *T. gondii* derived molecules that could potentially bind to occludin, a bioinformatics approach was used.

The occludin sequence is most conserved within the coiled-coil region of the C-terminus and extracellular loop 2 [Ando-Akatsuka et al., 1996]. Occludin can form dimers and oligomers both at the C-terminus and the extracellular loops, via disulphide bonds generated by cysteine residues [McCaffrey et al., 2007, 2008; Blasig et al., 2006; Nusrat et al., 2000, 2005; Itallie and Anderson, 1997]. Therefore an assumption was made to suggest that pathogen proteins may have similar residue sequences and consequently a similar structure to that of occludin for binding to occur.

The structure of occludin has only been described within the distal part of the C-terminus and a predicted structure for ECL2 can be made using software such as ESyPred3D [Li et al., 2005]. Within the *T. gondii* genome there are many uncharacterised proteins of unknown structures. For these reasons, the analyses of potential binding candidate proteins was based on sequence similarity alone.

6.3.3.1 Homology to full length occludin

Searching the genome for proteins that aligned with full length occludin revealed a *T. gondii* nucleosome assembly protein (NAP), a chromosome condensation protein and an Hsc70/HSP90 organising protein which acts as a chaperone for other proteins [Echeverria et al., 2010]. NAP is highly conserved across species and is known to bind histones during nucleosome assembly, regulates transcription, regulates the cell cycle by controlling mitotic events, and interacts with the importin family protein karyopherin [Altman and Kellogg, 1997; Shikama et al., 2000; Miyaji-Yamaguchi et al., 2003].

Also identified was an M protein repeat, viral A type inclusion protein which is involved in parasite replication and virulence [Gubbels et al., 2006], and a dual specificity protein phosphatase that could potentially alter the phosphorylation status of occludin. These proteins are plausible candidates for interacting with occludin.

The FYVE zinc finger domain-containing protein showed similarity to parts of the ECL2-C-terminus of occludin. FYVE domains bind to zinc and are themselves rich in cysteine residues [Gillooly et al., 2001]. The function of mammalian FYVE proteins have not been described, but they are thought to be involved in membrane trafficking to and from

endosomes, signal transduction, regulation of the cytoskeleton, and some phosphatases contain FYVE domains [Gillooly et al., 2001]. Therefore it is feasible that in *T. gondii,* these proteins may alter cytoskeletal properties of the cell via interactions with occludin. As the FYVE proteins express cysteine residues which are accessible for binding, this protein may interact with the cysteine residues on ECL2 of occludin and compete with the disulphide bonds between occludin on adjacent cells. This could be tested by co-precipitating recombinant occludin and *T. gondii.*

6.3.3.2 Homology to the extracellular loops of occludin

It was assumed that the proteins from *T. gondii* would initially interact with external residues of occludin and would therefore be surface proteins themselves. This was confirmed using a recombinant ECL1-ECL2 fragment, *T. gondii* bound to the extracellular loops of occludin. Homology to ECL1 was highest in all searches although alignment with cysteine residues within ECL2 suggests that both loops may be important in the binding of occludin to *T. gondii.*

A proteosome subunit α type 4 protein partially aligned with ECL1 and ECL2. The YLYHY motif has been described previously as a CAR sequence whereby peptides blocked aggregation in occludin expressing fibroblasts and increased permeability [Blaschuk et al., 2002]. Additionally, the protein aligns with the second cysteine residue on ECL2 which is thought to be involved in occludin dimerisation [McCaffrey et al., 2008], providing further support that this protein may interact with occludin, by possibly inducing endocytic recycling and/or degradation.

Vesicle-associated membrane protein (VAMP) aligned with ECL2. VAP-33 has been shown to co-localise with occludin at the tight junction complex and may play a role in the delivery of occludin to the membrane [Lapierre et al., 1999]. This protein is therefore a candidate for an occludin-interacting protein and was found within the IPs from the VEG strain. However, the equivalent protein within the GT1 strain is annotated as a disulphide isomerase (and in the ME49 strain is annotated as a hypothetical protein). This is of particular interest as disulphide isomerases from both *T. gondii* and cells were detected in IPs. This lends further support to the validity of the criteria used to conduct the bioinformatic searches.

One protein that aligned against sequences within ECL1-ECL2 possesses hedgehog receptor activity. Activation of the hedgehog pathway leads to increased expression of the transcription factor Snail, another

zinc finger domain containing protein [Li et al., 2006]. This is known to decrease expression of claudin 1, occludin, ZO-1 and E-cadherin suggesting that this is another feasible candidate molecule for interacting with occludin [Ohkubo and Ozawa, 2004].

6.3.3.3 Transmembrane domain containing molecules from *T. gondii* that have homology to occludin

Having identified 17 proteins from *T. gondii* against a BLAST of the extracellular domains of occludin, the search was narrowed down to include only transmembrane domain-containing proteins. This identified seven proteins: four conserved hypothetical proteins with either two or four transmembrane domains; a patched family-containing protein; a retrieval endoplasmic reticulin 1 protein, and a putative vitamin K epoxide reductase subunit 1 protein (VKERs1). VKERs1 aligned to both of the cysteines found in ECL2 as well as one cysteine residue in ECL1. VKER reduces vitamin K after oxidation of glutamic acid, is involved in maintaining an anti-oxidative state to promote cell survival and has a role in angiogenesis [Westhofen et al., 2011; Goodstadt and Ponting, 2004; Wang et al., 2005]. As *T. gondii* is known to minimise the amount of oxidative stress during infection, expression of an anti-oxidant such as VKER could be a potential candidate protein for this pathway [Choi et al., 2011]. Four cysteines and either a serine or threonine residue has been implicated as the active site of this protein which acts by reducing disulphide bonds [Goodstadt and Ponting, 2004]. The binding of cysteine residues on occludin dimers may therefore be disrupted by this reductase. This could alter the functionality of occludin, as multiple domains of occludin have various roles which alter its presence at the tight junction complex [Balda et al., 2000; Nusrat et al., 2005]. Again, co-IPs and binding assays with recombinant proteins could be performed to confirm any interactions. It is possible that this protein may possess other functions and properties that have not yet been identified that could influence changes within occludin.

6.3.4 Future work

The generation of separate ECL1 and ECL2 proteins would reveal which ECL is responsible for *T. gondii* binding. A recombinant occludin C-terminus fragment could also be used to look at cytoplasmic protein interactions following incubation with *T. gondii*. Further evidence for

binding could involve the addition of recombinant occludin fragments to cell media along with the parasites. This would show if competitive inhibition between parasites and recombinant occludin prevents changes in the distribution of cellular occludin, in a similar way as seen in the presence of IELs [Inagaki-Ohara et al., 2006; Dalton et al., 2006].

As a complementary approach, recombinant occludin fragments could be used to co-IP *T. gondii* lysates. This experiment would allow only *T. gondii* interacting proteins to be analysed for binding partners of occludin. From these results, proteins identified from the mass spectrometer could be purified and added to recombinant occludin fragments to confirm interactions. Individual residues that govern binding could be identified by the introduction of site-specific mutations within the recombinant proteins.

The proteins identified from the bioinformatic searches that match the results from the IP could be purified and incubated with recombinant occludin fragments to test for binding ability. Their expression profile within *T. gondii* during infection would also provide valuable information to determine whether they are important for extracellular binding to occludin or following invasion of a cell.

To examine potential candidate occludin binding proteins, priority could be given to those identified in both experimental approaches that are *T. gondii* derived proteins. These were disulphide isomerases (parasite and cell derived), HSPs, myosins, ribonucleoproteins, DEAD box helicases and tRNA-derived molecules (Table 6.4).

Cellular-derived kinases such as ROCK2 could be investigated for their ability to directly phosphorylate occludin. Occludin turnover and recycling pathways could be investigated to determine how *T. gondii* affects the half-life of occludin. Proteins containing transmembrane domains that were identified from the bioinformatic searches could be analysed for interactions with the extracellular loops of occludin and proteins without transmembrane domains could be analysed for interactions within the C-terminus. This would provide information on primary and secondary effects on occludin which could also shed light on occludin regulation pathways. Site directed mutations within *T. gondii* products or parasites deficient in candidate interacting molecules would confirm binding to occludin and identify any effects in transmigration and/or invasion. However, it is recognised that limiting searches to include only sequence similarity will not identify all molecules involved in the disruption of occludin by *T. gondii.*

Molecules identified from Immunoprecipitations	Molecules identified from Bioinformatics
Protein disulphide isomerase	Vesicle-Associated Membrane Protein (also known as a PDI)
HSP70/HSP90	HSC70/HSP90
Myosin A	Myosin F
DEAD box helicase family	DEAD/DEAH box helicase
tRNA synthetase	tRNA val/tRNA transferase/tRNA synthetase
Nuclear ribonucleoprotein K	nucleosome assembly protein/nuclear ribonucleoprotein A3
Subtilase family protein	
Rhoptry protein 18	
CELF family protein	
	merozoite surface protein
	M protein repeat viral A type inclusion protein
	Dense granule protein 5
	Vitamin K epoxide reductase
	endoplasmic reticulum retrieval protein 1
	dual specificity protein phosphatase
	proteosome subunit
	chromosome condensation protein
	zinc finger FYVE domain containing protein
	patched family domain containing protein
	phosphatidylinositol-4-phosphate 5-kinase

Table 6.4: *T. gondii*-derived molecules from the bioinformatics and IPs. Following the search for occludin-binding partners, it was found that molecules of both a similar and different nature were present using the two approaches.

6.4 Conclusions

T. gondii binds to the extracellular loops of occludin and six *T. gondii*-derived proteins have been identified that may interact with occludin following IP analysis. Additional proteins have been proposed that could interact with occludin from bioinformatic searches which leaves scope for further work to test these proteins by purification, binding experiments and co-IPs with cells and recombinant occludin fragments. These techniques would all provide a more comprehensive answer than analyses based on sequence identity alone from bioinformatic searches. The proteins identified from this work may be used in research for the development of therapeutic targets for preventing *T. gondii* invasion.

Chapter 7

Discussion

In this thesis, data has been provided to illustrate that *Toxoplasma gondii* interacts with epithelial tight junction complexes via the extracellular loops of occludin and that these interactions are important for the dissemination of *T. gondii*. Co-localisation with intracellular occludin during infection may represent occludin as a host cell receptor for invasion and formation of the moving junction.

7.1 The impact of *T. gondii* on m-IC$_{cl2}$ cells

T. gondii is thought to infect the host by dissemination from the GI tract via the paracellular pathway [Barragan et al., 2005]. In this thesis, infection of m-IC$_{cl2}$ cells with *T. gondii* was analysed using cell culture inserts which allow epithelial barrier function to be assessed and transmigrating parasites to be detected and quantified. It was found that cells were polarised with fully formed tight junctions by day 13 (Chapter 3) and all subsequent infections on inserts were carried out at this time point, which is similar to previously described reports using these cells [Bahi et al., 2002; Mennechet et al., 2002].

Exposure of cells to tachyzoites revealed that neither TEER nor permeability to 3kDa dextran were affected, showing that the integrity of the epithelial barrier remained intact despite parasites clustering around the edges of cells. Additionally, the distribution of junctional proteins claudin 4, ZO-1 and β catenin were unaltered although slight variations in claudin 2 distribution were observed six hours post-infection. Tachyzoites are highly replicating and invasive but it is the bradyzoites, the slow cyst-forming stage, which have been mostly associated with natural infections [Black and Boothroyd, 2000]. Unlike tachyzoites, a change in permeability was detected with bradyzoites, but TEER remained unaltered (Chapter 4). Although this experiment was only performed once, it sup-

ports suggestions that the mechanisms of infection between tachyzoites and bradyzoites may be different [Tomavo et al., 1991]. Changes in permeability can result from changes within the claudin family of proteins [Takehara et al., 2009], but have not yet been investigated during bradyzoite infection, with the exception of a report by Dalton *et al.* 2006, who observed a decrease in claudin 3 expression in mice lacking the TCR-V$\gamma 7^{+}$ subset of IELs [Dalton et al., 2006]. However, tachyzoites of *Neospora caninum* (*N. caninum*) have been shown to infect cells at a faster rate compared to bradyzoites [Vonlaufen et al., 2004], although a comparison between different life stages on transmigration rates have not been reported. Bradyzoites contain different surface antigens to tachyzoites and because the parasites are capable of infecting any nucleated cell, it is probable that there are multiple antigens and proteins the parasites use to infect different cells, as demonstrated by Vonlaufen *et al.* 2004, with *N. caninum* [Vonlaufen et al., 2004].

In m-IC_{cl2} cells, numbers of transmigrating tachyzoites were more than 2.5 fold higher compared to the number of intracellular parasites following two hours of infection. This suggests that the favoured route of infection is via the paracellular pathway, although it remains to be seen as to whether the parasites can also infect from the basal domain as well as the apical or lateral domains.

7.2 Effects on the distribution of occludin by *T. gondii*

Data presented in this thesis suggests that occludin does not play a role in maintaining the integrity of the epithelial barrier when small intestinal epithelial cells were challenged with *T. gondii.* In cells where occludin expression had been experimentally reduced, no changes in TEER or permeability were detected compared to infected and non-infected cells (Chapter 5). However, the cellular expression of occludin was dramatically affected by both tachyzoites and bradyzoites (Chapter 4). Occludin appeared more aggregated and less specific to the tight junction complex with exposure to tachyzoites, although with bradyzoites, occludin appeared more concentrated at the lateral membrane. This may represent different routes of infection, where bradyzoites are more migratory than tachyzoites, which supports the preliminary data that suggests transmigration occurs five fold more with bradyzoites compared to tachyzoites (Chapter 4). The effects on occludin appeared to be primary rather than secondary because the parasites were seen to co-localise and bind to the

protein (Chapter 4 and Chapter 6). Additional evidence for primary effects would be through identification of changes in occludin phosphorylation, which can be observed within 15 minutes post treatment [Antonetti et al., 1999], but this was difficult to test with m-IC_{cl2} cells. Secondary effects as a result of other proteins affected within the actin cytoskeleton in response to pathogenic stimuli, would cause a cascade of disruption through the tight junction complex that might affect occludin, but co-localisation may not occur [Nusrat et al., 2001; Canil et al., 1993; Francis et al., 1992; Jepson et al., 1995].

Changes in the expression profile of occludin in cells following exposure to *T. gondii* did not correlate with the proportion of infected cells, demonstrating that infected cells may secrete a substance that acts upon neighbouring cells (paracrine signalling). This has has been reported in cells exposed for example, to *Listeria monocytogenes*, *Shigella flexneri* and *T. gondii* [Kasper et al., 2010; Dolowschiak et al., 2010]. Possible secreted products include cytokines such as TNFα, IL-1α and IL-1β and chemokines such as IL-8 and colony stimulating factor-1 [Molestina et al., 2003; Denney et al., 1999; Corre et al., 1999]. In support of this theory MCP-1 and IL-8 were secreted by cells exposed to both live and dead parasites (Chapter 4).

Alternatively, *T. gondii* secretes products that may trigger signalling cascades from neighbouring cells. Although conditioned media had no effect on occludin, attachment with the parasite itself may be necessary for secreted products such as microneme and rhoptry-derived proteins, to act upon occludin. Discrepancies between occludin expression from immunofluorescence and immunoblotting data could also be explained by this phenomena, whereby immunofluorescence shows whether individual and neighbouring cells are affected by *T. gondii,* but immunoblotting results would mask these localised effects, especially as only 13% of cells were found to be infected. Additionally, as dephosphorylation of hyperphosphorylated occludin may remain in the membrane-associated fraction of cell lysates, this difference would be masked using immunoblotting techniques. Using phospho-peptide mapping techniques, mass spectrometry would be able to confirm levels of, and residues that are, phosphorylated.

T. gondii has mechanisms to prevent cell death upon infection, enabling it to replicate and eventually disperse within the host [Goebel et al., 2001]. After 24 hours of infection *in vitro*, cells contained multiple parasites, that often clustered around the nucleus (Chapter 4). Interest-

ingly, the parasites appeared to remain associated with occludin. Upon entering cells, a parasitophorous vacuole (PPV) forms and eventually host proteins are excluded from the PPV membrane, although currently unidentified host fibrous material may remain [Mordue et al., 1999; Schatten and Ris, 2004]. Based on results presented in this thesis, occludin could be one such PPV protein and may represent a method that *T. gondii* uses to manipulate host cell metabolism, particularly as occludin plays a role in apoptosis [Yu et al., 2005]. Control of host molecules at the PPV membrane have also been described for IκB which increases NFκB-induced activation of anti-apoptotic molecules [Molestina et al., 2003]. Furthermore, data presented in Chapter 6 shows the presence of both cellular and parasite derived HSP70 following immunoprecipitation of occludin from lysates of infected cells. HSP70-mediated anti-apoptosis following *T. gondii* infection leads to upregulation of Bcl-2 but also TLR4-dependent phospholipase A2 production [Hwang et al., 2010; Fang et al., 2008]. Phospholipase A2 was also found in the IPs and functions to hydrolyse bonds between arachidonic acid and lysophospholipids. Arachidonic acid is a precursor of inflammatory mediators such as prostaglandins and platelet activating factor [Fang et al., 2008].

The evidence presented in Chapter 6 suggests that *T. gondii* binds to the extracellular loops of occludin. *In vivo,* this interaction may compete with iIELs as they express occludin and therefore possibly bind to cellular occludin, providing a protective function against infection by maintaining barrier integrity and decreasing dissemination of pathogens such as *T. gondii* [Dalton et al., 2006; Lepage et al., 1998; Alexander et al., 1998]. In their absence, parasites would be free to bind occludin and move between cells, as seen *in vitro.* A similar hypothesis was presented by Inagaki-Ohara *et al.* 2006, for *Eimeria vermiformis* where the authors suggested that during infection, disruption of occludin and E-cadherin were only seen in epithelial cells and not IELs [Inagaki-Ohara et al., 2006]. Subsequent experiments to visualise invasion and transmigration using real time imaging with cells that express fluorescently-labelled occludin and co-cultured in the presence of IELs should confirm the direct interactions with occludin and answer these questions.

Live imaging would also confirm the route of entry into cells as *T. gondii* may be able to invade both from the apical and basolateral domains. *Shigella flexneri* and reovirus infect epithelial cells from the basolateral membrane via prior invasion of M cells, but can also penetrate the tight junction complex to gain access to the lateral domain

[Mounier et al., 1992; Sakaguchi et al., 2002; Barton et al., 2001]. In doing so, occludin, claudins and ZO-1 are disrupted resulting in breaches in barrier function [Sakaguchi et al., 2002].

Overall, this thesis implies that occludin is more important for transmigration of *T. gondii* than for invasion of cells, and evidence to support this was presented in Chapter 5 whereby the reduction of cellular occludin following siRNA/shRNA treatment decreased transmigration 10 fold without affecting the numbers of infected cells. As the levels of occludin were only decreased by 50% following siRNA treatment, this was a surprising result because it was expected that half the concentration of occludin would result in half (or 2 fold) the number of transmigrating parasites. This suggests that the presence of occludin at the tight junction complex plays a role in the dissemination of the parasite into the mucosal layer by using occludin in a trojan horse manner. Alternatively, the reduced occludin levels in siRNA/shRNA treated cells could have affected the structure of the tight junction complex in terms of paracellular macromolecular flux, which is in part regulated by occludin, and thereby affecting transmigration rates, but was not tested in this thesis [Al-Sadi et al., 2011].

The absence of altered proportions of infected cells where occludin had been reduced was also intriguing because intracellular *T. gondii* remained associated with residual occludin in these cells, further supporting suggestions that it plays a role in the generation and maintenance of PPV signalling pathways. Occludin may require N-linked glycosylation to traffic to the membrane, and could become glypiated, allowing the molecule to remain associated with a PPV that gradually excludes host proteins but retains GPI-anchored proteins [Gut et al., 1998; Mordue et al., 1999]. The change in transmigration, but not the infection rate of occludin-reduced cells, does not rule out the possibility that *T. gondii* binds to occludin in order to infect cells, as it is generally accepted that multiple proteins and receptors govern this process [Furtado et al., 1992b,a; Carruthers et al., 2000; Mineo et al., 1993]. Moreover, the similarity of tricellulin and MarvelD3 could suggest that *T. gondii* uses multiple occludin-family proteins to enter cells [Raleigh et al., 2010].

7.3 Disruption of occludin following *T. gondii* infection

Changes observed in occludin levels following exposure to *T. gondii* may be due to altered transcription, translation and/or endocytic/recycling pathways. Alterations in mRNA stability or changes in ribosomal recruitment rates may account for mRNA disruption, although previous studies have found that occludin expression is controlled by translation and turnover rates more so than by mRNA levels [Raleigh et al., 2010]. Further work using real time-polymerase chain reaction (RT-PCR) would be required to confirm any effects on mRNA. Other pathogens have been shown to alter occludin mRNA, such as the related pathogens *Eimeria vermiformis* and *Plasmodium falciparum*, which suggests that *T. gondii* could also regulate the mRNA of tight junction proteins [Susomboon et al., 2006; Inagaki-Ohara et al., 2006].

A detrimental effect on occludin mRNA has also been demonstrated by rotavirus infection in $CaCo_2$ cells [Beau et al., 2007]. Rotavirus also induced a decrease in the amount of non-phosphorylated occludin which was concluded to be dependent on Protein Kinase A signalling [Beau et al., 2007]. Rotavirus surface protein VP8 affects TEER and permeability in MDCK cells, resulting in localisation of occludin on the lateral membrane. As the VP8 protein expresses a degree of similarity to that of the extracellular loops of occludin and claudins, the authors postulated that rotavirus could be using occludin to enter the cells. Data obtained from infection with *T. gondii* in this thesis and other experimental work using recombinant occludin peptides supports this hypothesis, where binding to extracellular loops causes internalisation of occludin, and possibly other interacting proteins [Nava et al., 2004; Lacaz-Vieira et al., 1999].

Alternatively, *T. gondii* could affect the rate of occludin endocytosis and recycling. Vesicle-associated proteins (clathrin, GTPases), chaperones and ubiquitin-associated proteins as well as myosins and actin related molecules were identified from the occludin immunoprecipitates following infection (Chapter 6). These molecules favour the endocytosis hypothesis, but others identified from the IPs such as RhoGEF16, HSP60 and T-complex protein subunits suggest recycling and synthesis of occludin may occur in parallel. Previous studies have shown that peptides of ECL1 and ECL2 increase the rate of occludin turnover and as *T. gondii* was found to bind the extracellular loops (Chapter 6), it is possible that endocytosis of occludin may occur following interactions with

the parasite [Wong and Gumbiner, 1997; Lacaz-Vieira et al., 1999]. This could also explain why after 24 hours of infection, the concentration of cellular occludin was higher compared to non-infected cells (Chapter 4). Previous studies report that the integrity of the microtubules and microfilaments are important in maintaining occludin motility, and therefore the presence of myosins, ROCK2 and clathrin molecular complexes (which are also found in cell shedding and wound healing pathways) in occludin immunoprecipitates, could represent protective mechanisms such as the expulsion of infected cells [Subramanian et al., 2007; Marchiando et al., 2011; Yin and Yu, 2008]. Myosin 9 (also called non-muscle heavy chain IIA) and myosin 10 (also called non-muscle heavy chain IIB) function to connect the acto-myosin cytoskeleton with microtubules (via kinesin) to stabilise cell migratory capacity [Even-Ram et al., 2007]. As myosin 9 and kinesin were found in the IPs, it is probable that occludin plays a role in these pathways. Together, this indicates a possible homeostatic role of occludin in preventing changes to tight junction complexes in the GI tract, which *T. gondii* may manipulate. Furthermore, HSP90 (also detected from IPs of infected cells) inhibition leads to decreased leukocyte adhesion, inhibition of proinflammatory cytokines, barrier breakdown and decreased tyrosine phosphorylation of occludin and ZO-1 [Poulaki et al., 2007; Kale et al., 2003; Elias et al., 2009]. This suggests that internalisation of occludin following infection by *T. gondii* may be caused by increased tyrosine phosphorylation. As previously mentioned, phospho-analysis of m-IC_{cl2} cells proved difficult but through concentrating occludin using an IP technique, this may be possible in future studies.

An increased rate of recycling is thought to be a common mechanism in pathogen invasion [Veiga et al., 2007]. For example, Hepatitis C virus enters hepatocytes by binding to claudin 6, claudin 9, the first extracellular loop of claudin 1 and the second extracellular loop of occludin, which caused endocytosis of occludin in a dynamin II dependent mechanism [Liu et al., 2010; Zheng et al., 2007; Evans et al., 2007]. Dynamin is a GTPase which plays a role in clathrin dependent endocytosis [Caldas et al., 2009]. The critical motif within the second extracellular loop of occludin contains two conserved cysteine residues that are thought to form disulphide bridges [Michta et al., 2010]. Binding of pathogen-derived molecules to ECL2 may disrupt these bonds and therefore providing a mechanism of entry into the cell. The identification of parasite-derived Vitamin K epoxide reductase and protein disulphide isomerases from the

bioinformatic searches and IPs strongly suggests that disulphide bonds may be involved in this interaction.

Studies have shown that occludin, ZO-1, JAM-A, β catenin, N-cadherin and β actin co-immunoprecipitate with dynamin II in the blood testes barrier and in hepatocytes [Lie et al., 2006; Liu et al., 2010]. The authors suggested that dynamin II facilitates dis-engagement of the tight junction complex with the adherens junctional complex to avoid disruption of the barrier during cell movement [Lie et al., 2006]. This mechanism may explain how *T. gondii* avoids alterations in barrier integrity as parasite-derived dynamin is known to be involved in the invasion of cells which may include interactions with occludin and ICAM-1 [Caldas et al., 2009; Barragan et al., 2005].

The upregulation of ICAM-1 on MDCK II cells following infection from *T. gondii* supports the notion that the parasites are transmigrating through the paracellular pathway [Barragan et al., 2005; Ikenouchi et al., 2008]. Although no changes within the adherens junctional protein β catenin was detected following infection (Chapter 4), it suggests that *T. gondii* can affect specific proteins within specific junctions in order to cross the epithelium. ICAM-1 is expressed on leukocytes and endothelial cells and binding to its ligand (leukocyte function-associated antigen-1) activates leukocyte transmigration via actin-cytoskeletal rearrangements [Etienne-Manneville et al., 2000; Marlin and Springer, 1987]. It could be predicted that *T. gondii* uses occludin to enter the paracellular pathway and then recruits adherens molecules such as ICAM-1 to the surface to continue movement through the paracellular space. In doing so, this would initiate signalling cascades to recruit lymphocytes providing the parasites with an opportunity to infect immune cells and use them as a transport vehicle for reaching the lymph nodes. This mechanism would not require changes in the epithelial barrier function and so the integrity of the monolayer remains intact.

Other pathogens such as the Coxsackie virus can enter epithelial cells via a caveolar and macropinocytosis mechanism, and appears to require occludin to be present for invasion to occur [Coyne et al., 2007]. This is interesting as although no differences in numbers of cells infected were identified in occludin-reduced cells, transmigration was decreased, further supporting evidence to suggest that occludin is required for transmigration, but possibly supplementary for invasion.

7.4 A range of junctional proteins are affected by pathogens

During infection many pathogens exert multiple effects on cells making it difficult to identify roles that individual proteins play in maintaining the epithelial barrier (Table 7.1). Permeability and TEER are often altered (although not observed in *T. gondii* infection), probably due to reorganisations of the actin cytoskeleton, which indirectly affect tight junction proteins. As there are over 50 proteins involved in the tight junction complex, redundancy probably exists and each protein may have multiple functions. For example, occludin expression is required in order to expel apoptotic cells from the monolayer but is also important for driving protein polarity complexes during cell migration [Yu et al., 2005; Du et al., 2010]. Pathogens could exploit these mechanisms by targeting occludin to induce changes in cell survival and migration to gain access to the basolateral domain [Beeman et al., 2009].

There are a number of pathogens that induce occludin redistribution and degradation (Table 7.1). Astrovirus, *Campylobacter jejuni* and Enteropathogenic *Escherichia coli* (EPEC) affect membrane-associated occludin, in addition to inducing changes within the actin cytoskeleton which increases permeability and decreases TEER [Beltinger et al., 2008; Chen et al., 2006; Moser et al., 2007; Simonovic et al., 2000]. In addition to affecting occludin, *Campylobacter jejuni* infection also alters other junctional proteins, increasing claudin 1 expression and decreasing JAM1 expression [Beltinger et al., 2008; Chen et al., 2006], while EPEC affects the interactions between occludin, ZO-1 and claudin 1 [Muza-Moons et al., 2004]. EPEC was also seen to induce dephosphorylation of occludin by a serine/threonine phosphatase [Muza-Moons et al., 2004].

Salmonella enterica serovar Typhimurium causes a redistribution of ZO-1 and occludin without affecting total cellular concentration of occludin [Boyle et al., 2006; Jepson et al., 1995]. Secreted effectors of *S.* Typhimurium such as SopB, SopE, SopE2, SipA, were found to affect the tight junctions via Rho family GTPase activation, causing a decrease in TEER and increase in permeability [Boyle et al., 2006; Jepson et al., 1995]. The Rho family of proteins are small GTP binding proteins and are cytoplasmic plaque proteins of the tight junctions [Benais-Pont et al., 2003; Hall, 1998]. They are activated by guanylate exchange factors and can alter the actin cytoskeleton [Yu et al., 2005; Benais-Pont et al., 2003]. They have also been implicated in the regulation of occludin

Pathogen	Junction proteins affected	References
Campylobacter jejuni	Occludin, claudin 1, JAM-1	[Beltinger et al., 2008; Chen et al., 2006]
Enteropathogenic *Escherichia coli*	Occludin, claudin 1, ZO-1	[Muza-Moons et al., 2004; Simonovic et al., 2000]
Salmonella Typhimurium	Occludin, ZO-1	[Jepson et al., 1995; Dalton et al., 2006; Boyle et al., 2006]
Shigella flexneri	Occludin, claudin 1, ZO-1, ZO-2, E-cadherin	[Sakaguchi et al., 2002]
Vibrio cholerae	Occludin, ZO-1	[Wu et al., 1996, 2000]
Helicobacter plyori	Occludin	[Lytton et al., 2005]
Listeria monocytogenes	E-cadherin	[Pentecost et al., 2006; Bonazzi et al., 2008]
Clostridium difficile	Occludin, ZO-1, ZO-2	[Nusrat et al., 2001]
Clostridium perfringens	Occludin, claudin3, claudin 4	[Singh et al., 2000; Sonoda et al., 1999]
Astrovirus	Occludin	[Moser et al., 2007]
Rotavirus	Occludin, claudin 3, ZO-1	[Nava et al., 2004; Beau et al., 2007]
Coxsackie Virus	Occludin	[Coyne et al., 2007]
Hepatitis C virus	Occludin, claudin 1, claudin 6, claudin 9	[Evans et al., 2007; Liu et al., 2010; Zheng et al., 2007]
Reovirus	JAM	[Barton et al., 2001]
Eimeria vermiformis	E-cadherin	[Inagaki-Ohara et al., 2006]
Plasmodium falciparum	Occludin, ZO-1, vinulin, ICAM-1, VCAM, E-selectin	[Susomboon et al., 2006]
Toxoplasma gondii	Occludin, claudin 2, claudin 3, ZO-1, ICAM-1	This thesis, [Barragan et al., 2005; Dalton et al., 2006]
Trichinella spiralis	Occludin	[McDermott et al., 2003]

Table 7.1: Pathogens that alter junctional proteins.

whereby occludin phosphorylation is dependent on Rho signalling and in the absence of occludin, Rho signalling cascades are impaired [Yamamoto et al., 2008; Yu et al., 2005; Gopalakrishnan et al., 1998]. Rho guanine nucleotide exchange factor 16 was identified from immunoprecipitates in Chapter 6, further supporting existing evidence of interactions between occludin and the Rho protein family, and suggesting that *T. gondii* may also affect cellular GTPase activity.

Clostridium difficile toxin affects occludin, ZO-1 and ZO-2 [Nusrat et al., 2001]. This was again associated with a decrease in TEER, increased permeability and rearrangements within the actin cytoskeleton. Occludin was found to be linked to caveolin-1 raft-like domains, which also suggests Rho protein involvement [Nusrat et al., 2001]. *Clostridium perfringens* enterotoxin bound to the extracellular loop of claudin 3, degraded both claudin 3 and claudin 4 and complexed with occludin [Singh et al., 2000; Sonoda et al., 1999; Fujita et al., 2000]. The fact that *Clostridium perfringens* can bind to claudin 3 and results in its degradation, and that *T. gondii* binds to occludin and results in a degradation product (as presented in Chapter 4), suggests that similar mechanisms exist between some pathogens in targeting tight junction proteins for methods of infection.

7.5 Degradation of occludin by pathogens

Metalloproteinases (MMPs) are endopeptidases that degrade extracellular matrix proteins and cleave cell surface receptors. MMP-mediated degradation of occludin resulting in a 50kDa fragment has been previously reported and the redistribution of occludin is similar to that observed in this thesis following exposure to *T. gondii* [Wachtel et al., 1999]. In addition, after six hours of infection, a ≈45kDa occludin product was observed in the cytoplasmic fraction by SDS-PAGE (Chapter 4), and similar products have been observed with exposure to other pathogens. This suggests that *T. gondii* may produce metalloproteinases such as MMP2 and MMP9 that degrade occludin [Muñoz et al., 2009].

Occludin degradation has been observed in mast cells and epithelial cells following infection by various pathogens for example, *Helicobacter pylori*, *Trichinella spiralis* and *Vibrio cholerae* [McDermott et al., 2003; Wu et al., 1996, 2000; Lytton et al., 2005]. A serine or cysteine protease was responsible for the degradation caused by *Trichinella spiralis*, and a zinc-containing metalloprotease (cytotoxin haemagglutinin/protease) was responsible for the degradation seen in *Vibrio cholerae* infection [Mc-

Dermott et al., 2003; Wu et al., 1996, 2000]. Previous protease-induced degradation has been shown to occur with the dust mite allergen Der p 1 cysteine peptidase [Wan et al., 2000], highlighting the importance of studying cysteine proteases in future studies with *T. gondii* as they may be important virulence factors. It was therefore interesting to find a subtilase serine protease protein within the immunoprecipitates of infected cells which may warrant further investigation (Chapter 6).

Following *Vibrio cholerae* infection, degradation of occludin extracellular domains was observed [Wu et al., 2000]. It was speculated by Wu *et al.* 1996 and 2000, that changes within the extracellular domains could cause conformational changes within the protein, leading to intracellular signal transduction, affecting ZO-1 binding and therefore indirectly altering the organisation of the actin cytoskeleton [Wu et al., 1996, 2000]. Lytton *et al.* 2005, provided evidence to show that degraded occludin, following infection by *Helicobacter pylori,* was a product of protease cleavage and suggested that occludin recycling was disrupted [Lytton et al., 2005]. Additionally, the authors observed that degraded occludin was only seen within the epithelial cells and not in immune cells (Jurkat T cells). This finding is in agreement with other reports stating that immune cells expressing tight junction proteins are unaltered by pathogenic stimuli, and further supporting the hypothesis of their protective function [Dalton et al., 2006; Lepage et al., 1998; Inagaki-Ohara et al., 2006]. Therefore, it is possible that *T. gondii* also causes a degradation of occludin from epithelial cells, through protease cleavage. The involvement of cysteine and serine proteases during *T. gondii* infection has been previously implicated in microneme and rhoptry secretion, gliding motility and cellular invasion [Teo et al., 2007; Conseil et al., 1999; Que et al., 2002; Miller et al., 2003]. The presence of a subtilase family protein within occludin immunoprecipitates therefore supports evidence that *T. gondii* may cleave occludin upon invasion.

A more comprehensive analysis of products present within immunoprecipitates of infected cells may have revealed the presence of other proteases. Additionally, it would be useful to evaluate the potential of specific protease inhibitors to target both attachment and penetration of the cell during infection, to ascertain the effects on occludin degradation products.

7.6 Potential binding partners of occludin from *T. gondii*-derived proteins

The rhoptry proteins are considered crucial for achieving invasion, as demonstrated recently in studies with RON8 [Straub et al., 2011]. The moving junction that forms during invasion is heavily dependent on these proteins and because occludin is associated with the parasite both extracellularly and intracellularly, it was speculated that rhoptry proteins may drive this interaction. Consistent with this, ROP18 was found within the immunoprecipitates, as reported in Chapter 6. ROP18 is a serine/threonine kinase that could alter phosphorylation levels, and therefore the cellular expression of occludin. ROP18 binds to immunity-related GTPases, and acts within an anti-apoptotic pathway to prevent parasite clearance in macrophages [Fentress et al., 2010]. Further work to confirm the interactions between ROP18 and occludin would involve investigating the effects on invasion and transmigration in parasites with specific rhoptry protein deletions or mutations, and analyses of immunoprecipitates that are designed to favour the detection of *T. gondii* associated proteins instead of host proteins. For example, this could be achieved by using recombinant occludin fragments such as ECL1-ECL2. It would also be interesting to see whether or not the differing levels of ROP18 between parasite strains correlates to differences in occludin redistribution [Taylor et al., 2006].

Following bioinformatics, where the *T. gondii* database was searched for sequence similarity to the extracellular loops of occludin, alignments were made with 22 molecules. Potential candidates were based on the presence of disulphide bonds within the extracellular loops of occludin, which provides a mechanism for like-to-like binding. Vitamin K epoxide reductase aligned to residues within the extracellular loops of occludin, which provides a candidate protein for these interactions. As occludin was associated with intracellular *T. gondii*, endocytosis and recycling pathways were predicted to play a role in the redistribution of occludin. It was therefore interesting to detect vesicle-associated membrane protein 7 and endoplasmic reticulum retrieval protein 1 from the bioinformatic searches. In addition, of the proteins known to be secreted during *T. gondii* infection (micronemes, rhoptries, dense granules), dense granule protein 5 was detected.

However, as occludin was associated with *T. gondii* following invasion, interactions with the N- and C-termini may also occur, although sequence

similarity is less likely to be an effective method of screening in this case. Nevertheless, bioinformatic searches did reveal a dual specificity protein phosphatase which may act upon serine/threonine or tyrosine residues within the C-terminus of occludin (PhospMotif_finder [1]).

Overlapping results from the bioinformatic searches and data obtained from the IP studies, in addition to information from the literature, suggests that the theoretical searches were valid and may prove useful in focussing the search for identification of *T.gondii* binding partners to occludin.

7.7 Proposed model of infection by *T. gondii* in m-IC$_{cl2}$ cells

Based on the results presented in thesis, the following model of infection is proposed (Figure 7.1).

Tight junction complexes include transmembrane proteins (occludin and claudins) and cytoplasmic plaque proteins (ZO-1) which link to the cytoskeleton. Occludin is represented as a 4-transmembrane domain-containing protein with 2 extracellular loops, a short N-terminus and longer C-terminus [2]. It is not currently known whether ECLs bind like-to-like or if ECL1 binds to ECL2. Adherens junctions are also present on the lateral domain (β catenin). There is a pool of junctional proteins within the cytoplasm and as the cells become polarised, the nucleus is situated toward the basal domain.

(A) *T. gondii* infection commences with cellular contact and adhesion. As the parasites move paracellularly, surface proteins are altered and a polarised anterior forms (dark brown).

(B) An occludin binding molecule, represented by a hypothetical 6 transmembrane domain protein with 3 extracellular loops, is upregulated on the parasite surface (light brown). This has been drawn differently to occludin to highlight that the *T. gondii* interacting molecule(s) may not be identical in size or shape.

(C) Occludin dimers are disrupted by the presence of *T. gondii*, possibly by disulphide isomerases, causing neighbouring occludin interactions on adjacent cells, to break. Extracellular loops are then free to bind to an interacting molecule on the parasite surface. Changes in conformation or phosphorylation status of occludin may send intracellular signals

[1] `http://www.hprd.org`
[2] `http://www.zonapse.net/occludin`

to recruit additional occludin to the membrane, induce/destroy oligomerisation, and lead to endocytosis and recycling (by clathrin-mediated vesicles, or vesicle-associated membrane proteins for example). At this point, parasites either transmigrate (D) or infect the cell (E).

(D) Transmigration initiates intracellular signalling cascades to recruit host occludin to the membrane which assists in parasite binding and movement. This may be through changes at the mRNA and/or translation level. As the parasites move through the paracellular pathway, occludin molecules detach and are degraded (by ubiquitin-like enzymes, black arrows) or disordered (blue arrows, by disulphide isomerases or Vitamin K epoxide reductase for example). As a consequence, dimers and oligomers disassemble within the cytoplasm causing an apical aggregation of the protein (occludin becomes apically located within the cytoplasm such that it appears underneath microvilli on the cell surface, also depicted in (E)). Endocytic and/or recycling processes to occludin would be activated and the cytoskeleton may be altered (for example through myosin 9, myosin 10, GTPase disturbances). The upregulation of adherens junctional proteins such as ICAM-1 may also assist in lateral migration of *T. gondii*.

(E) Invasion of cells forms a moving junction and a parasitophorous vacuole (purple). Occludin may represent a receptor for parasite entry and assist in microneme (subtilase family proteins) and rhoptry protein (ROP18) secretion into the cell.

Occludin (and possibly the corresponding binding molecules of *T. gondii*) may be eliminated from the PPV as the parasite surface changes in protein/antigen expression (for example HSP70, HSP90) to promote survival. This would also result in higher than normal concentrations of cytoplasmic occludin, which may include degraded occludin fragments. Alternatively, occludin remains associated with the PPV and provides a communication channel between the host and parasite for nutrients and metabolites, or prevents cellular-driven occludin signalling pathways that may result in apoptosis. Following invasion, the presence of occludin at the tight junction complex may increase over time as recycling pathways are activated.

7.8 Unanswered questions

What are the cellular molecules that regulate occludin?

Kinases were identified from the immunoprecipitates that may be

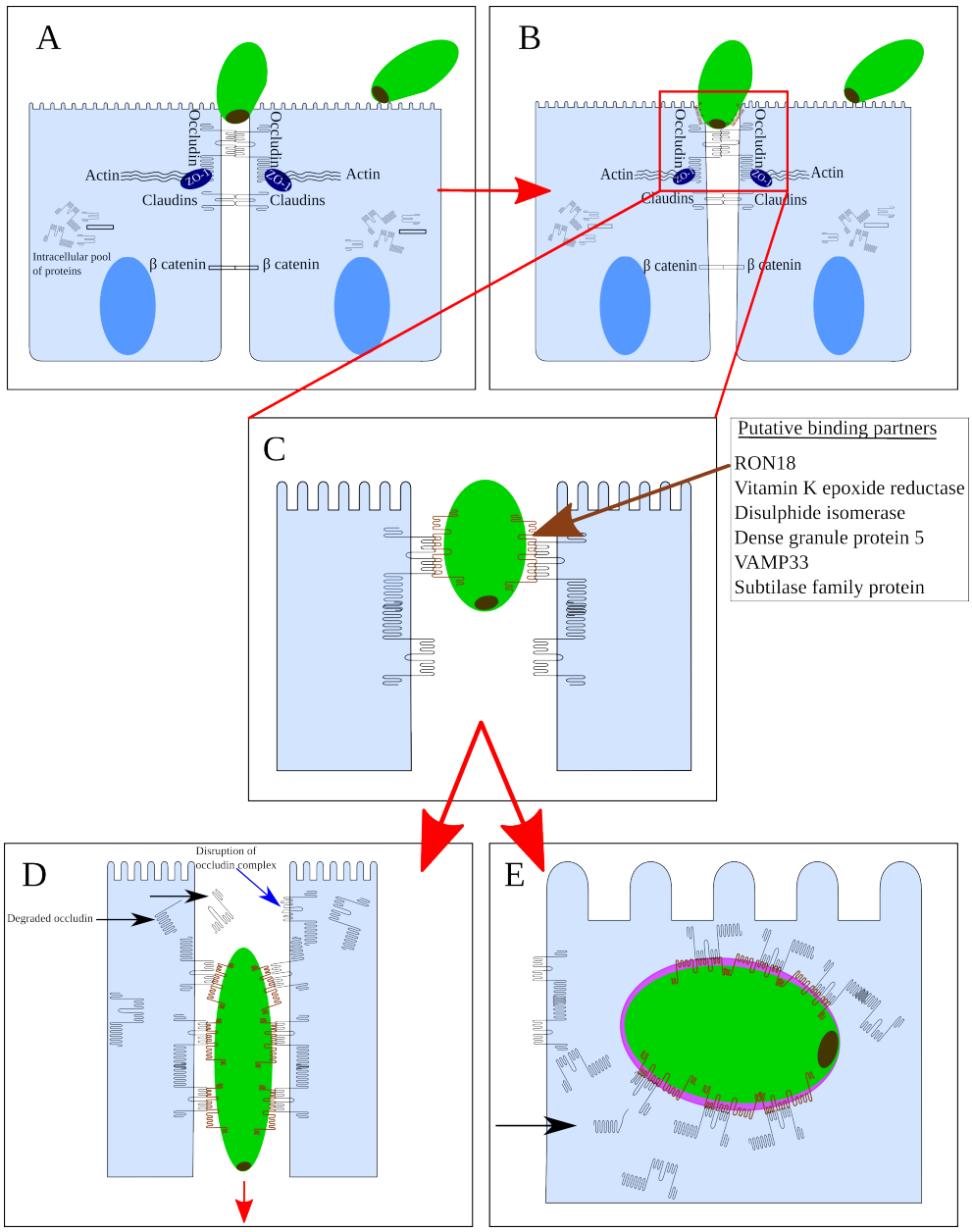

Figure 7.1: Invasion of small intestinal epithelial cells by *T. gondii*. (A) Tight junction complexes before infection. (B) *T. gondii* adheres to the apical domain and associates with the paracellular pathway. (C) *T. gondii* interacts with occludin. (D) Parasites use occludin to move between cells. (E) *T. gondii* is coated with occludin upon cell entry. Blue arrows indicate disruption to occludin complexes and black arrows represent degradation of occludin molecules. *T. gondii* interacting molecules to cellular occludin (black) are shown in brown and the parasitophorous vacuole in purple.

involved in the regulation of occludin including ROCK2, which phosphorylates serine/threonine residues and represents a candidate kinase to investigate in more detail. This kinase is found in *T. gondii* as well as murine cells and could alter the phosphorylation status of occludin. To determine this, *in vitro* kinase assays with recombinant occludin fragments could be performed, measuring ATP/GTP consumption or ADP/GDP accumulation, or via radio-labelling of ATP/GTP. A dual specificity protein phosphatase was identified from bioinformatic searches and could regulate occludin by dephosphorylating the hyperphosphorylated species at the tight junctions. To determine which specific residues are phosphorylated or dephosphorylated in the presence of kinases or phosphatases, mass spectrometry analysis could be employed using peptide mass fingerprinting techniques in a similar manner described by Smales *et al.* 2003, when they identified casein kinase 2 as an occludin kinase [Smales et al., 2003].

Changes in the expression of molecules that immunoprecipitate with occludin following infection over time would be interesting to analyse. For example α actinin 1 and 4, detected from the immunoprecipitates in Chapter 6, could be involved in recycling of occludin from the membrane, possibly as a result of occludin dephosphorylation. Parallel changes in expression between proteins may indicate complexes and pathways that are involved. However, conformational changes within occludin could also account for these differences [McKenzie et al., 2006]. The binding of occludin to *T. gondii* might be predicted to induce conformational changes within the C-terminus of occludin, which would initiate cascades of signal transduction that result in the internalisation of a parasite-protein multi-complex. In order to test this, mutations or truncations of residues and peptides within the C-terminus of occludin could be generated, that would inhibit intracellular signalling pathways, following infection.

Which residues within occludin are crucial for T. gondii *binding*?

This thesis has shown that *T. gondii* binds to the extracellular loops of occludin. Separate recombinant ECL-1 and ECL-2 fragments would address which loops govern these interactions and site-directed mutagenesis within the recombinant fragments would identify the residues important for binding. This may also focus the search for potential *T. gondii*-derived molecules that interact with occludin that are based on sequence similarity, or conserved residues within a binding motif. Additionally, recombinant C-terminus occludin fragments could be used to

investigate interacting partners once the parasite has become internalised within the cell, as the presence of ROP18 and subtilase-like proteins from the IPs suggests that additional binding proteins may be acting upon occludin.

Further experiments to confirm that occludin is essential during *T. gondii* infection would involve the incubation of occludin recombinant fragments to the cell media upon infection in competitive inhibition experiments. It could be predicted that cellular occludin would be altered to a lesser degree, perhaps resulting in decreased transmigration. On the contrary, the overexpression of occludin in cells would be predicted to cause an increased number of transmigrating parasites detected in the basal compartment, although from the current results it is difficult to predict how this may affect the proportion of cellular invasion by *T. gondii*.

As the disruption of occludin did not result in a change in epithelial barrier function through *T. gondii* binding, it could be possible to use peptides against the same sequence of occludin as a target for therapeutic intervention. This possibility stems from previous suggestions using occludin and claudin mimetic peptides to temporarily disrupt the barrier for drug delivery [Mrsny et al., 2008; Tavelin et al., 2003]. This may be less toxic to cells than conventional methods and has been reviewed by Deli, 2009 [Deli, 2009].

Which products in T. gondii *bind and act upon occludin?*

To identify binding partners of occludin it would be necessary to look at molecular expression profiles on the surface of *T. gondii* during infection. Any products identified could then be imaged by fluorescent microscopy using specifically raised antibodies to determine localisation within the parasite. It was suggested that the initial interacting molecule is probably not secreted by the parasite and it was predicted that they are most likely surface molecules that are upregulated during infection as in the presence of dead parasites, only slight changes in occludin distribution were observed. A number of candidate proteins were identified from the bioinformatic searches and further work could include investigations into the potential of these proteins to interact with occludin. Proteins highlighted from the search contained cysteine residues which may interact with the conserved cysteine residues on the ECL2 of occludin. Additionally, some proteins were highlighted that are already known to associate with occludin. A protein disulphide isomerase/VAMP molecule

was detected from the infected immunoprecipitates and as *T. gondii* expresses these proteins, it is possible that the isomerase could act upon the extracellular domains of occludin to form a complex between itself and cellular occludin, via disulphide bonds. This would allow the parasite to attach to the host cell surface. Mutations and deletions of *T. gondii* candidate molecules would confirm whether they are crucial in transmigration and/or invasion of cells.

Immunoprecipitations between *T. gondii* and recombinant occludin fragments may also reveal binding partners[3] although physical attachment to cells may be required for occludin binding molecules to become upregulated.

The effects on kinases and phosphatases during infection could reveal important information on the mechanisms of occludin regulation and assist in defining a function for the protein. Kinase assays and kinome analyses could be performed to assess this.

Are there differences between parasites that infect versus parasites that transmigrate epithelial cells in terms of surface protein expression?

It would be interesting to determine whether or not within a population of parasites, different receptors, surface antigens and proteins are expressed upon contact with cells. Are there parasites within a population that can only invade cells or only transmigrate? It could be predicted that the parasites which infect cells, replicate, cause cell lysis and consequently spread to other cells within the GI tract, sustain only an acute infection. However, it is the parasites that disseminate via the paracellular pathway and are rapidly transported to lymph nodes and out of the GI tract, which establish a chronic infection. A comparison of protein expression from immunoprecipitations of parasites that infect versus those that transmigrate would reveal potential candidates to investigate further. This study may also illustrate differences between strains of *T. gondii* and could highlight novel virulence factors. Furthermore, microarrays and RT-PCR may be carried out to detect changes at the mRNA level.

Is the degree of bradyzoite transmigration affected in occludin-reduced cells?

[3]New data obtained after submission of this thesis reveals the presence of MIC3, type 1 rhoptry protein 5B and GRA6 following *T. gondii* incubation with cells or recombinant ECL1-ECL2 occludin.

As the host is most likely to be infected by bradyzoites or sporozoites, it would be necessary to determine whether bradyzoites co-localise with occludin. As a higher proportion of bradyzoites were detected in the basal compartment compared to tachyzoites, it would be expected that in occludin-reduced cells, transmigration would also be impaired. This could confirm the importance of occludin for parasite dissemination from the GI tract. In addition, confirmation that the binding partners of occludin from *T. gondii* are expressed in all three life stages of the parasite would provide information on the importance of and conservation of the interactions. It is accepted that *T. gondii* probably interacts with multiple proteins to infect virtually all cell types and so it is plausible to conclude that mechanisms of infection and therefore the binding molecules on bradyzoites and sporozoites may be different to that of tachyzoites.

Are there differences in the interactions of occludin between parasite strains?

Differences in expression profiles of occludin interacting molecules may be apparent between strains of *T. gondii* which may relate to virulence and degree of dissemination within the host. It could be predicted that virulent strains which disseminate at a faster rate compared to avirulent strains, may express higher concentrations of occludin interacting molecules on their surface compared to avirulent strains.

7.9 Concluding remarks

In summary, this thesis has demonstrated that occludin is directly affected by *T. gondii* exposure and that binding of the extracellular loops to the parasite could govern the redistribution of occludin observed in small intestinal epithelial cells. It is proposed that *T. gondii* uses occludin as a mechanism to transmigrate through the paracellular pathway, without impinging on the integrity of the epithelial cell barrier. Potential candidate proteins from *T. gondii* that may interact with occludin have been identified following immunoprecipitations of infected cell lysates and from bioinformatic searches. These experiments also revealed cellular candidate proteins that may play a role in the regulation of occludin during infection. In addition, occludin could represent a *T. gondii* receptor for cell invasion which is important in the formation and survival of *T. gondii* within the parasitophorous vacuole.

Therefore, occludin has been shown to play an important role in the transmigration of *T. gondii* and may also assist in the invasion and intracellular survival of *T. gondii*.

Appendix A

Commercial Suppliers

Abcam
330 Cambridge Science Park
Cambridge
CB4 0FL
UK

Agar Scientific Limited
Unit 7, M11 Buisness Link
Parsonage Lane
Stansted
Essex
CM24 8GF

American Type Tissue Collection
PO Box 1549
Manassas VA 20108

Applied Biosystems
Lingley House
120 Birthwood Boulevard
Warrington
WA3 7QH

BD Biosciences
The Danby Building
Edmund Halley Road
Oxford Science Park
Oxford
OX4 4DQ

BDH Laboratory Supplies
Poole
Dorset
BH15 1TD

Bio-Rad
BioRad House
Maxted Road
Hemel Hempstead
Hertfordshire
HP2 7DX

Biosera
1 Acorn House
The Broyle
Ringmer
East Sussex BN8 5NN

Bitplane Scientific Solutions
Bitplane AG
Badenerstrasse 682
CH-8048
Zurich
Switzerland

BMG Labtech Ltd
PO BOX 73
Aylesbury
Bucks
HP20 2QJ

Carl Zeiss Ltd
PO Box 78
Woodfield Road
Welwyn Garden City
Hertfordshire
AL7 1LU

Caltag Medsystems
Whiteleaf Business Centre
11 Little Balmer
Buckingham
MK18 1TF

Cell Signalling Technology Inc
3 Trask Lane
Danvers
MA 01923

Danahar Corporation
2099 Pennysylvania Avenue NW
Washington DC 20006
Dako UK Ltd
Cambridge House
St Thomas Place, Ely
Cambridgeshire
CB7 4EX

Eppendorf UK Limited
Endurance House Vision Park
Histon
Cambridge
CB24 9ZR

Expedeon Ltd
Unit 1A Button End
Harston
Cambridgeshire
CB22 7GX

Fermentas GmbH
Opelstrasse 9
68789 St. Leon Rot
Germany

FisherScientific
Bishop Meadow Road
Loughborough
Leistershire
LE11 5RG

GE Healthcare UK Ltd
(Amersham Biosciences)
Amersham Place
Little Chalfont
Buckinghamshire
HP7 9NA

Greiner BioOne
Unit 5
Stroudwater Buisness Park
Brunel Way
Stonehouse
Gloucesteshire
GL10 3SX

Health Protection Agency
7th Floor
Holborn Gate
330 High Holborn
London
WC1V 7PP

IBIDI GmbH
Am Klopferspitz 19
D-82152 Martinsried (Munchen)
Germany

Insight Biotechnology Ltd
2nd Floor Titan Court
3 Bishop Square
Hatfield
AL10 9NA

Invitrogen Ltd
Inchinnan Buisness Park
3 Foundation Drive
Paisley
PA4 9RF

JacksonImmunoResearch
(via Statech Scientific Ltd)
7 Acorn Buisness Centre
Oaksdrive
Newmarket
Suffolk
CB8 7SY

Labequip Ltd
170 Shields Court
Unit 2
Markham
Ontario
Canada
L3R 9T5

London Resin Co Ltd
273-287 Regent Street London
London
W1B 2HA

Lonza Group Ltd
Muenchensteinerstrasse 38
CH - 4002 Basel
Switzerland

Matrix Corporation Technology
Deanway Buisness Centre
Wilmslow Road
Wilmslow
Cheshire
SK9 3HW

Molecular Devices
1311 Orleans Drive
Sunnyvale
CA 94089-1136
USA

New England Biolabs (UK) Ltd
75/77 Knowl Piece
Wilbury Way
Hitchin
Hertfordshire
SG4 0TY

Nunc
(supplied through ThermoScientific)

Oxoid Ltd
Wade Road
Basingstoke
Hampshire
RG24 8PW

PerkinElmer Ltd
940 Winter Street
Waltham
Massachusetts
02451, USA

Pierce Chemical Company
(ThermoFisherScientific)
Perbio Science UK Ltd
Unit 9
Ately Way
North Nelson Industrial Estate
Cramlington
Northumberland
NE23 1WA

Promega Ltd
Delta House
Southampton Science Park
Hampshire
Southampton
SO16 7NS

Qiagen
Qiagen House
Fleming Way
Crawley
West Sussex
RH10 9NQ

Reichert Microscope Services
3362 Walden Ave
Depew
New York
14043, USA

Sartorius AG
Weender Landstrasse 94-108
D-37075
Goettingen
Germany

SantaCruz Biotechnology
2145 Delaware Avenue
SantaCruz
CA-95060
USA

Sarstedt Ltd
68 Boston Road
Beaumont Leys
Leicester
LE4 1AW

Scientific Laboratory Supplies Ltd (Whatmann)
Wilford Industrial Estate
Ruddington Lane
Nottingham
NG11 7EP

Sigma Aldrich
The Old Brickyard
New Road
Gillingham
Dorset
SP8 4XT

Vector Laboratories Ltd
2 Accent Park
Bakewell Road
Orton Southgate
Peterborough
PE2 6XS

VWR International Ltd
Hunter Boulevard
Magna Park
Lutterworth
Leicestershire
LE17 4XN

World Precision Instruments Ltd
Astonbury Farm Business Centre
Stevenage
Hertfordshire
SG2 7EG

Appendix B

List of Antibodies used for Immunofluorescence

Primary Antibody	**Secondary and Tertiary Antibody**
10µg/ml Rabbit anti-occludin (Zymed, Invitrogen, Paisley, UK)	20µg/ml biotin-XX goat anti-rabbit IgG; 1µg/ml Streptavidin pacific blue conjugate (Invitrogen)
0.5µg/ml Mouse anti-β catenin (BD Biosciences)	3µg/ml Cy5 conjugated goat anti-mouse IgG (Jackson Immunoresearch (Suffolk, UK))
5µg/ml Mouse anti-claudin 2 (Zymed, Invitrogen)	3µg/ml Cy5 conjugated goat anti-mouse IgG (Jackson ImmunoResearch)
5µg/ml Mouse anti claudin 4 conjugated to Alexa Fluor 594 (Invitrogen)	
2µg/ml Rat anti-ZO-1 (Santa Cruz)	2µg/ml goat anti-rat texas red (Caltag (Buckingham, UK))
20µg/ml each of Rhodamine Wheat Germ and Peanut Agglutinin (Vector Labs)	
10µg/ml Rabbit IgG (Vector Labs)	
0.5µg/ml or 5µg/ml Mouse IgG Tricolour (Caltag)	
2µg/ml Rat IgG2a conjugated to FITC (Caltag)	

Appendix C

Densitometry

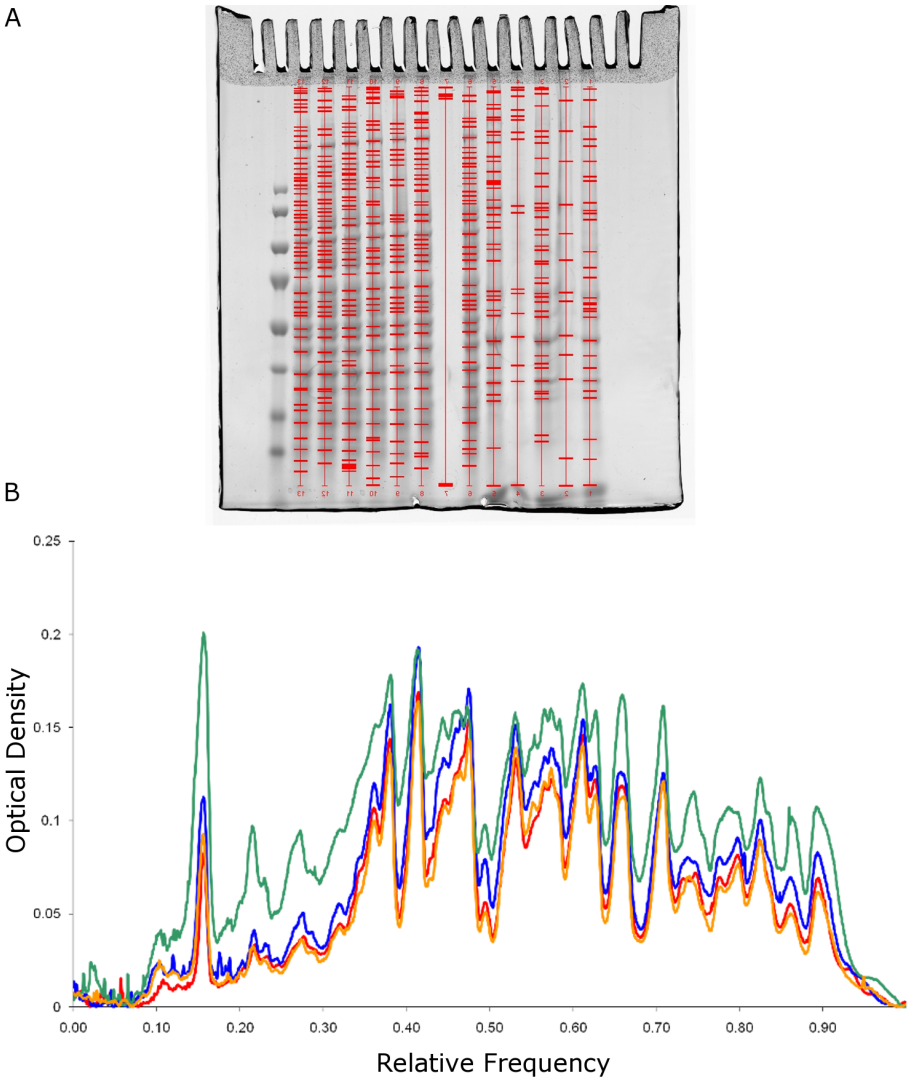

Figure C.1: An example of protein bands on an SDS-PAGE gel that were analysed using densitometry. (A) Cell lysates were subjected to gel electrophoresis, the gel stained with Coomassie Brilliant Blue and protein bands were detected and aligned between lanes using QuantityOne software (performed by Francis Mulholland, Institute of Food Research, Norwich, UK). Optical density was plotted such that corresponding bands across lanes overlapped in relative frequency (B).

Appendix D

List of primers

Description	Name	Sequence of primer
pBABE shRNA and FLAG-occludin sequencing	Set 1 Forward (F)	CCTCCGCCTCCTCTTCTTCC
pBABE FLAG-occludin sequencing	Set 1 Reverse (R)	CCGCCGATACCTCCGATACC
pBABE FLAG-occludin sequencing	Set 2 F	GGGCTCTTTGGAGGAAGCC
pBABE FLAG-occludin sequencing	Set 2 R	CCGTTTCACTTACCGTTCGC
pBABE FLAG-occludin sequencing	Set 3 F	CCCCAATGTTGAAGAGTGGG
pBABE FLAG-occludin sequencing	Set 3 R	GGGGTCGTCCGTCTTCATACG
pBABE shRNA sequencing	Set 3 Rb	GGAACTGGGCGGAGTTAGGGG
ECL 1 occludin	pECL1 F	GGACATCATATGGCTTCCACACTTGCTTGGGACAGAG
ECL 2 occludin	pECL2 R	CCAGTAGGATCCCTACTCCTGGGGATCAACCAC
PET3a-occludin sequencing	T7 F	TAATACGACTCACTATAGGG
PET3a-occludin sequencing	T7 R	GCTAGTTATTGCTCAGCGG

Table D.1: List of primers used for generating PCR products and sequencing

Appendix E

Plasmid Map for pBABEpuro plasmid vector containing FLAG-tagged occludin

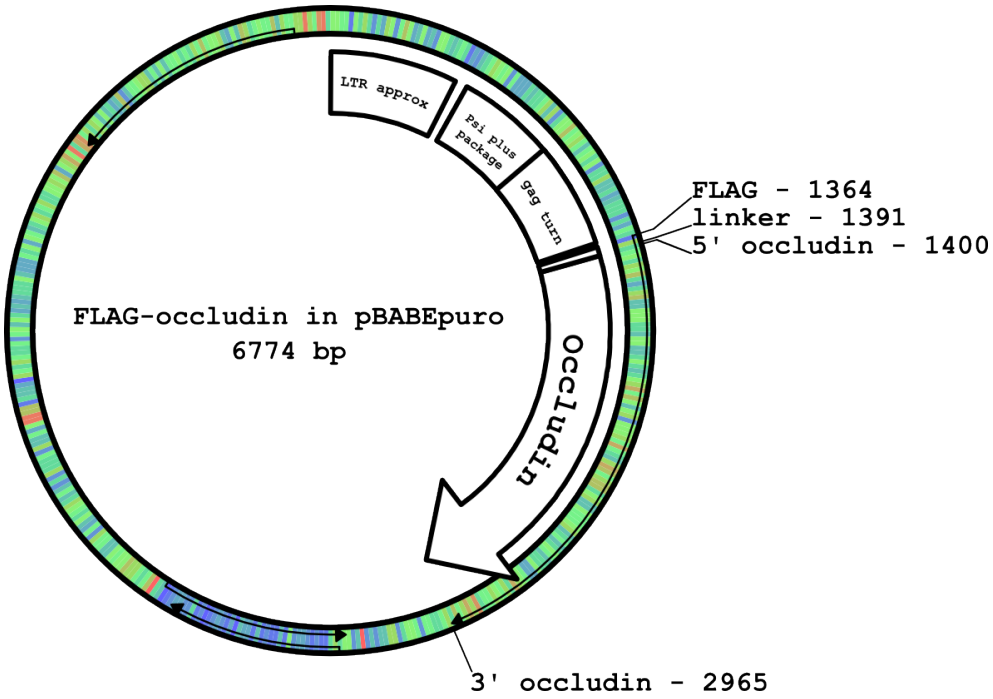

Figure E.1: Plasmid map of FLAG-tagged occludin in the pBABEpuro vector

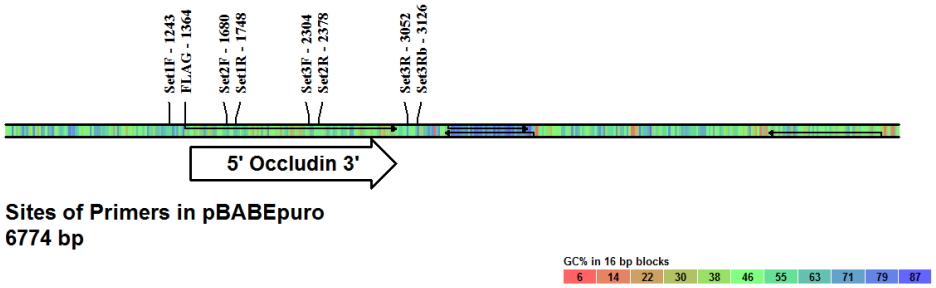

Figure E.2: Primers used for sequencing of FLAG-tagged occludin in pBABEpuro

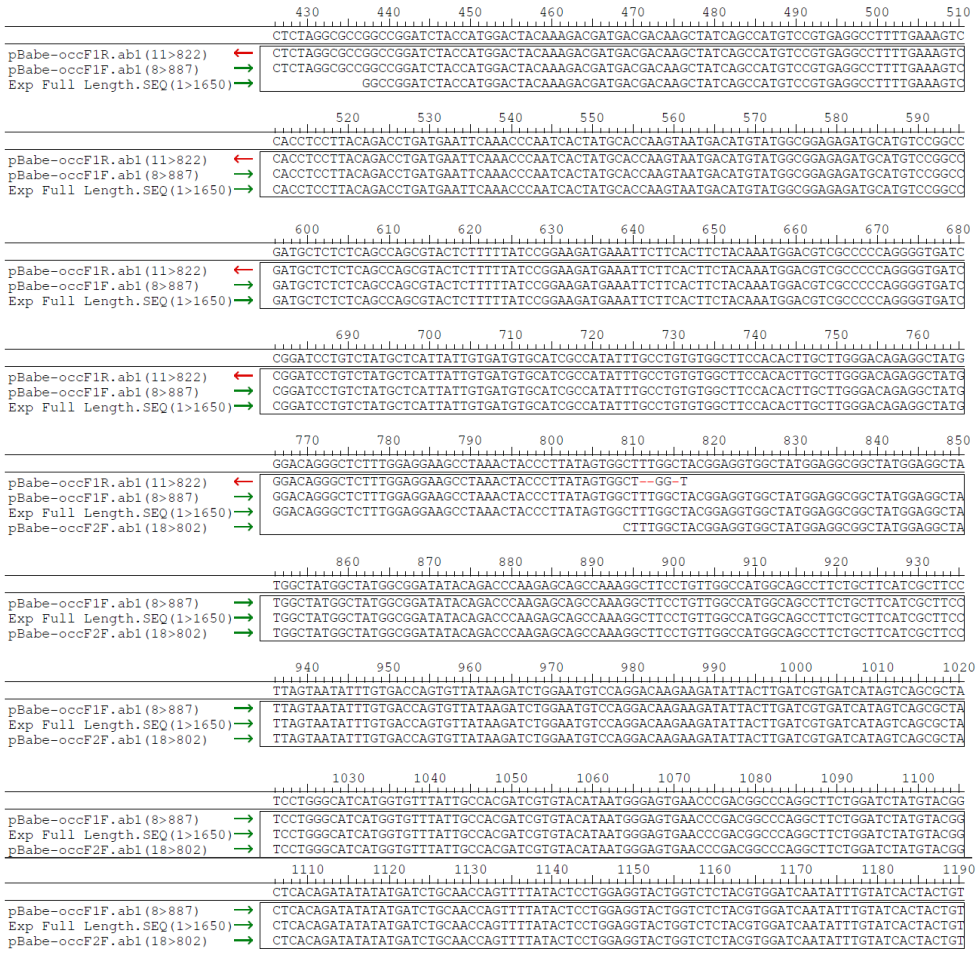

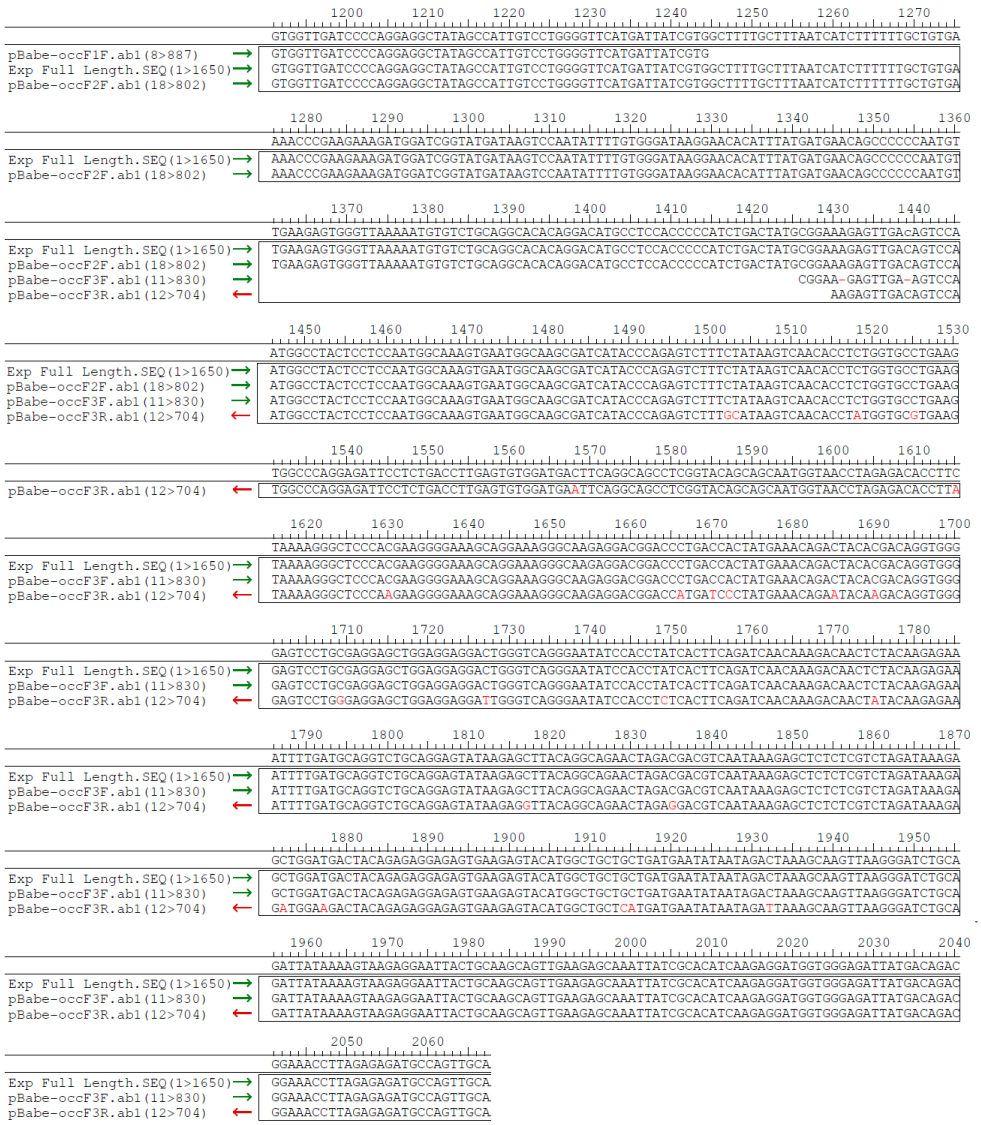

Figure E.3: Sequence of FLAG-tagged occludin in pBABEpuro. DNA sequences were prepared and sent to TGAC for sequencing. The expected sequence was aligned to the sequence obtained from the plasmid vector DNA (top lines) using the primers shown. Differences are highlighted in red.

Appendix F

Recombinant occludin fragments

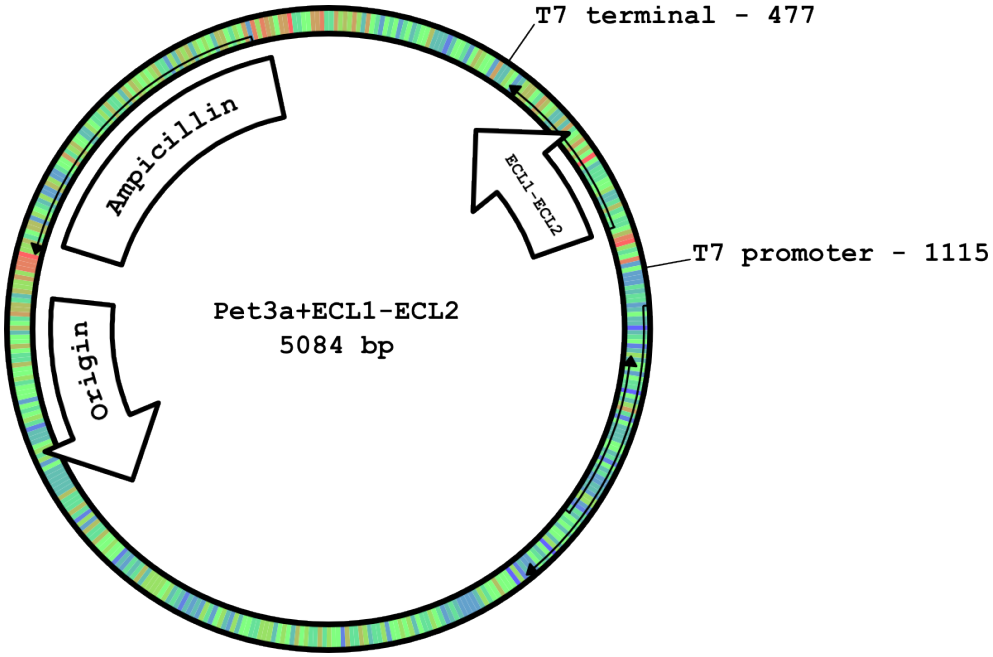

Figure F.1: Pet3a+ECL1-ECL2 plasmid map

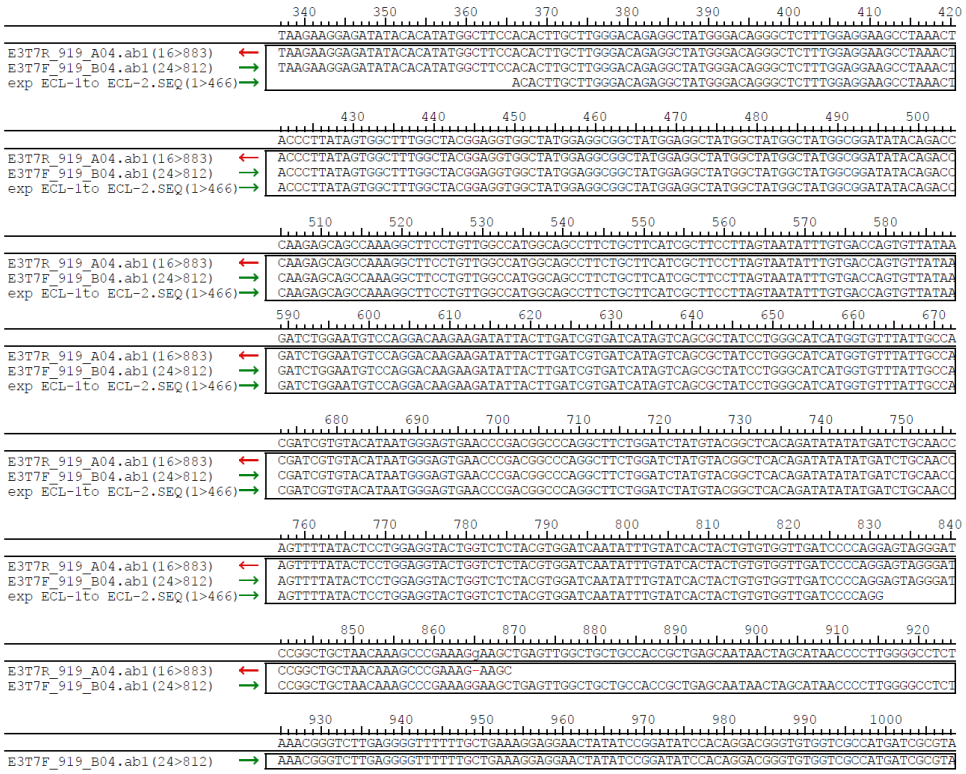

Figure F.2: Sequence of ECL1+ECL2. The DNA sequence of ECL1-ECL2 was amplified from the FLAG-tagged occludin pBABEpuro vector and inserted into a Pet3a plasmid vector. The sequence was verified at TGAC and confirmed a 100% identity match between observed (top and middle) and expected (bottom) sequences, using T7F and T7R primers.

Appendix G

Plasmid Map for pBABEpuro plasmid vector containing shRNA

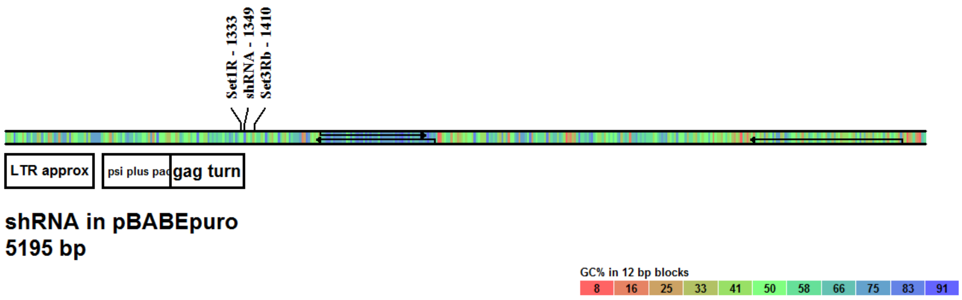

(a) Primers for shRNA

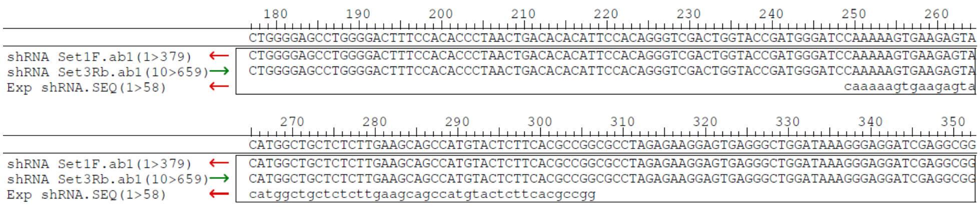

(b) Sequence of shRNA in pBABEpuro. The expected sequence was aligned to the sequence obtained from the plasmid vector (top lines) using the primers shown.

Figure G.1: shRNA in pBABEpuro

Appendix H

Comparison between fixation methods

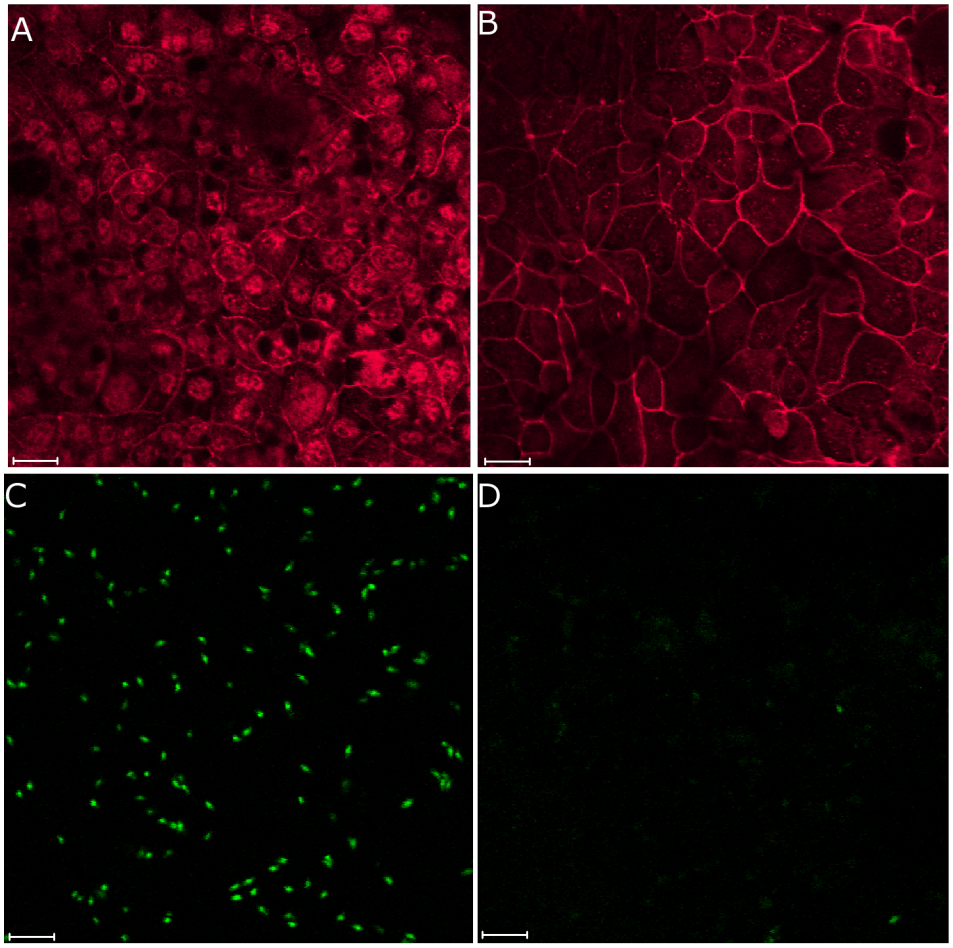

Figure H.1: Comparison between fixation with 2% PFA and acetone. Cells and parasites were fixed with either 2% paraformaldehyde (A and C) or acetone (B and D). Cells were stained for occludin (red) and YFP *T.gondii* are shown in green. PFA shows a higher background of occludin staining which is also present in the nucleus, and the parasites are also clear to see. Acetone emphasises the membrane bound occludin staining, but destroys the ability to visualise the parasites. The images are from different inserts within an experiment. Scale bar represents 20μm. Magnification 40×.

Appendix I

Cell culture inserts

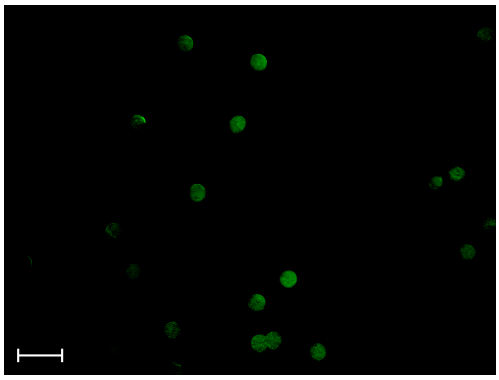

Figure I.1: FITC-dextran stained pores on the cell culture insert. Pores can be seen as green circles on the membrane. The green staining could be FITC-dextran which has become associated with the pores. Tests were carried out to confirm that this did not make a difference to TEER measurements from the cells.

Appendix J

Comparisons between live and dead parasites

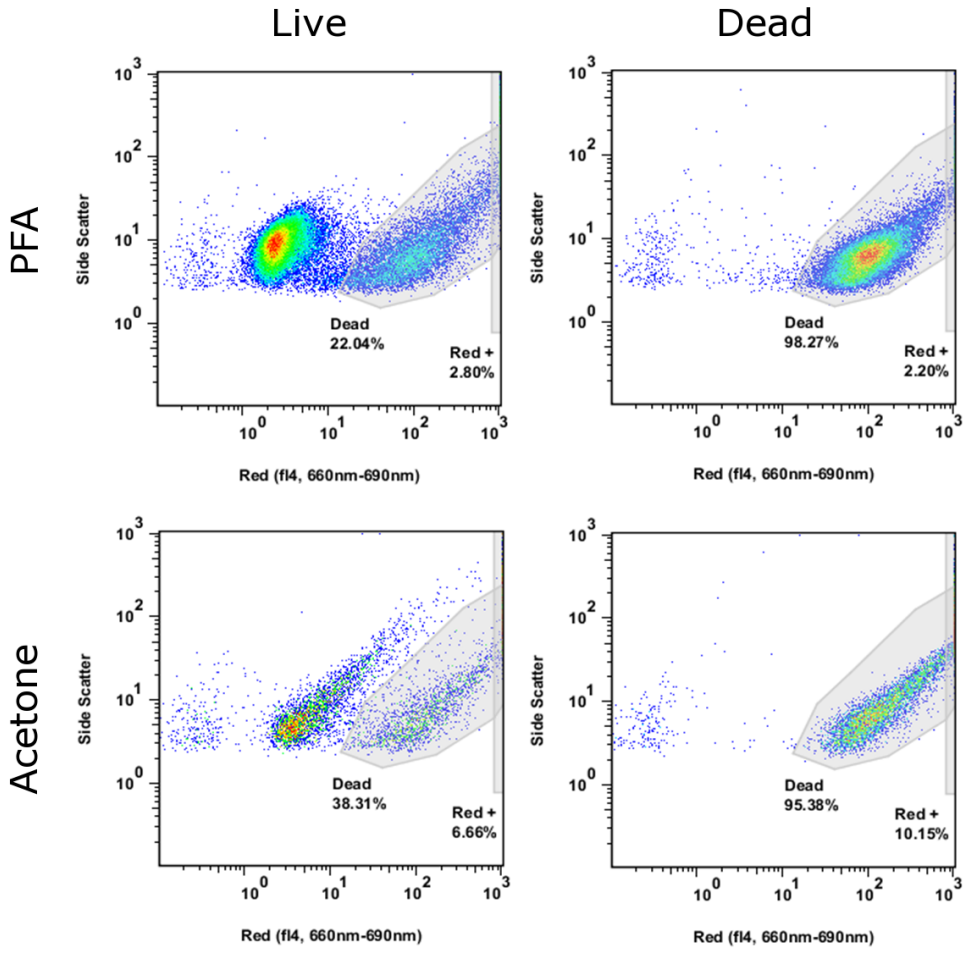

Figure J.1: Comparison between fixation methods and composition of a parasite population. A live/dead fixable red dye was added to live or dead parasites for 10 minutes. The parasites were fixed in either 2% PFA or acetone. The results confirm that the parasites were killed by freezing and heating, and that in any given population $\approx$ 70% of parasites are alive. Red gating shows aggregates of parasites. Data represents 1 of 2 independent experiments.

Appendix K

Mass spectrometry data

Non infected and infected cell lysates were precipitated for occludin and subjected to gel electrophoresis. Murine and *T. gondii* databases were searched by Alex Jones (Sainsbury Laboratory, Norwich, UK) using a peptide mass tolerance of 15ppm and a fragment mass tolerance of 0.6 Da within MASCOT (Matrix Science) software. Number of peptide matches are shown along with peptide scores (only significant proteins are shown, and scores indicate logarithmic probablilites towards identity or extensive homology to known proteins). CM - cell metabolism, CR - cell response proteins, CY - cytoskeletal and microtubule-related, PR - protein regulators, TG - *T. gondii* derived. Proteins include data obtained from two independent immunoprecipitations.

Function	Accession Number	Annotation	Infection (hours)	Protein Score	Peptide Hits	Pred. Size (kDa)	Obs. Size (kDa)
CM	Q03265	ATP synthase subunit alpha, mitochondrial	0	235	9	59.83	55
CM	P52480	Pyruvate kinase isozymes M1/M2	0	187	9	58.378	70
CM	P56480	ATP synthase subunit beta, mitochondrial	0	217	6	56.265	55
CM	Q61753	D-3-phosphoglycerate dehydrogenase	0	172	5	57.347	55
CM	B2M1R6	Heterogeneous nuclear ribonucleoprotein K	0	87	4	48.76	70
CM	B1AXW8	Aldehyde dehydrogenase 4 family, member A1	0	82	3	62.258	70
CM	Q03265	ATP synthase subunit alpha, mitochondrial	0	74	3	59.83	55
CM	Q2TPA8	Hydroxysteroid dehydrogenase-like protein 2	0	65	3	54.516	70
CM	Q4FJZ2	Karyopherin (Importin) alpha 6 Kpna6 protein	0	66	2	60.307	70
CM	P17563	Selenium-binding protein 1	0	64	2	53.051	55
CR	P63038	60 kDa heat shock protein, mitochondrial	0	138	3	61.088	70
CR	P27773	Protein disulfide-isomerase A3	0	47	3	57.099	70
CY	P68372	Tubulin beta-2C chain	0	146	6	50.255	55
CY	P05213	Tubulin alpha-1B chain	0	114	4	50.804	55
CY	P68368	Tubulin alpha-4A	0	136	3	50.634	55
CY	P11679	Keratin, type II cytoskeletal 8	0	103	3	54.531	55
CY	B6KLA1	Tubulin beta chain	0	108	2	50.554	55
CY	B2RTP7	Keratin 2 protein	0	85	2	71.336	70
CY	Q9DCV7	Keratin, type II cytoskeletal 7	0	55	2	50.678	55
PR	Q3UA81	Elongation factor 1-alpha	0	199	6	50.423	55
PR	P11983	T-complex protein 1 subunit alpha	0	137	3	60.867	70
PR	P80315	T-complex protein 1 subunit delta	0	62	3	58.543	70
PR	B1AT36	Proteasome (Prosome, macropain) 26S subunit	0	68	2	50.936	55

PR	O55222	Integrin-linked protein kinase	0	55	2	51.853	55
UN	Q3U6X6	Uncharacterised protein	0	156	7	61.616	70
UN	Q3TET0	Uncharacterised protein	0	94	4	60.159	70
UN	Q3U4S9	Uncharacterised protein	0	71	3	57.577	70
UN	Q3UKQ2	Uncharacterised protein	0	91	2	60.089	70
UN	Q3T9A1	Uncharacterised protein	0	64	2	56.572	70
UN	Q3TWV0	Uncharacterised protein	0	46	2	53.69	55
CM	Q03265	ATP synthase subunit alpha, mitochondrial	2	396	14	59.83	55
CM	B2RUB9	Thymopoietin	2	347	14	75.807	100
CM	P52480	Pyruvate kinase isozymes M1/M2	2	311	14	58.378	70
CM	Q03265	ATP synthase subunit alpha, mitochondrial	2	298	8	59.83	55
CM	Q8CAQ8	Mitochondrial inner membrane protein Mitofilin	2	247	8	84.247	100
CM	P56480	ATP synthase subunit beta, mitochondrial	2	215	8	56.265	55
CM	Q03265	ATP synthase subunit alpha, mitochondrial	2	232	7	59.83	55
CM	Q3UGE3	Phosphoglucomutase 2	2	221	7	61.665	70
CM	P17563	Selenium-binding protein 1	2	184	6	53.051	55
CM	P62814	Vacuolar proton pump subunit B 2	2	149	6	56.857	55
CM	P56480	ATP synthase subunit beta, mitochondrial	2	172	5	56.265	55
CM	P17563	Selenium-binding protein 1 56 kDa	2	144	5	53.051	55
CM	B2M1R6	Heterogeneous nuclear ribonucleoprotein K	2	138	5	48.76	70
CM	Q8BMS1	Long chain 3-hydroxyacyl-CoA dehydrogenase	2	119	5	83.302	100
CM	Q2TPA8	Hydroxysteroid dehydrogenase-like protein 2	2	127	4	54.516	70
CM	P52480	Pyruvate kinase isozymes M1/M2	2	116	4	58.378	55
CM	Q8C2Q3	RNA-binding protein 14	2	103	4	69.577	70
CM	B8JK32	Heterogeneous nuclear ribonucleoprotein M	2	99	4	72.25	70
CM	P56480	ATP synthase subunit beta, mitochondrial	2	95	4	56.265	55

CM	B6KI67	ATP synthase subunit alpha	2	88	4	61.472	55
CM	Q61753	D-3-phosphoglycerate dehydrogenase	2	189	3	57.347	55
CM	P06745	Glucose-6-phosphate isomerase	2	135	3	62.955	55
CM	Q1PG84	pBK1	2	92	3	52.245	70
CM	B6KAW2	Glycyl-tRNA synthetase	2	83	3	87.118	100
CM	A2AKD8	Syntrophin acidic 1	2	76	3	54.088	70
CM	Q03265	ATP synthase subunit alpha, mitochondrial	2	75	3	59.83	55
CM	B6KBY3	ATP synthase subunit beta	2	70	3	60.107	55
CM	P56480	ATP synthase subunit beta, mitochondrial	2	63	3	56.265	55
CM	P06745	Glucose-6-phosphate isomerase	2	57	3	62.955	70
CM	B9EIA2	DNA segment, Chr 1, Pasteur Institute 1	2	47	3	73.494	70
CM	Q3TC53	Adenylyl cyclase-associated protein	2	42	3	51.915	55
CM	Q4FJZ2	Karyopherin (Importin) alpha 6 Kpna6 protein	2	155	2	60.307	70
CM	B6KTX0	Protein disulfide isomerase	2	144	2	53.054	55
CM	B1AXY3	Smu-1 suppressor of mec-8 and unc-52 homolog (C. elegans)	2	102	2	58.134	55
CM	P26443	Glutamate dehydrogenase 1, mitochondrial	2	116	2	61.64	55
CM	B3RH23	Lamin A	2	99	2	74.478	70
CM	B6KEK5	ATP-dependent RNA helicase	2	88	2	78.943	100
CM	Q61753	D-3-phosphoglycerate dehydrogenase	2	86	2	57.347	55
CM	B6KDM4	Eukaryotic translation initiation factor 3 subunit 6 interacting protein	2	81	2	75.596	70
CM	Q99KA3	Atp6v1b1 protein (Proton pump)	2	80	2	44.878	55
CM	B6KAT9	Pyruvate kinase	2	78	2	58.12	70
CM	Q8BVE3	V-type proton ATPase subunit H	2	77	2	56.275	55
CM	Q9DBL7	Bifunctional coenzyme A synthase	2	73	2	62.213	70
CM	Q5SX74	Proline 4-hydroxylasE	2	66	2	61.116	70
CM	Q8VDX7	Phosphofructokinase, liver, B-type	2	65	2	86.104	100

CM	Q1JSB7	RNA binding protein, putative	2	62	2	51.148	55
CM	B6KI67	ATP synthase subunit alpha	2	59	2	61.472	70
CM	B6KIF7	Lysyl-tRNA synthetase	2	52	2	75.031	70
CM	B6KBY3	ATP synthase subunit beta	2	48	2	60.107	55
CM	Q3U517	Apoptosis inhibitor 5	2	45	2	57.092	70
CR	P63017	Heat shock 70 kDa protein	2	220	10	71.055	70
CR	B6KDQ4	Heat shock protein 70, putative	2	213	10	73.291	70
CR	B6K8N0	Heat shock protein 70, putative	2	185	8	73.379	70
CR	A2AUF6	Heat shock 70kD protein 5 (Glucose-regulated protein)	2	200	6	72.492	70
CR	P27773	Protein disulfide-isomerase A3	2	181	6	57.099	70
CR	P63038	60 kDa heat shock protein, mitochondrial	2	169	4	61.088	70
CR	Q71LX8	Heat shock protein 90 alpha	2	55	3	83.571	100
CY	B6KJM2	Membrane skeletal protein IMC1	2	87	7	70.351	100
CY	P11679	Keratin, type II cytoskeletal 8	2	160	6	54.531	55
CY	P11679	Keratin, type II cytoskeletal 8	2	107	5	54.531	55
CY	P11679	Keratin, type II cytoskeletal 8	2	97	4	54.531	55
CY	B2RRE8	CD2-associated protein	2	83	3	70.56	100
CY	Q9DCV7	Keratin, type II cytoskeletal 7	2	76	3	50.678	55
CY	B6KM69	Myosin A	2	44	3	93.887	100
CY	Q62418	Drebrin-like protein	2	76	2	48.955	55
CY	B2RRX1	Actin, beta	2	67	2	42.052	70
CY	B2RRX1	Actin, beta	2	67	2	42.052	55
CY	Q9DCV7	Keratin, type II cytoskeletal 7	2	46	2	50.678	55
MT	B2RSN3	MCG1395 Tubulin, beta 2B	2	161	4	50.377	55
MT	P68368	Tubulin alpha-4A chain	2	131	4	50.634	55
MT	P05213	Tubulin alpha-1B chain	2	111	4	50.804	55

MT	B6K9T3	Tubulin alpha chain	2	123	3	50.823	55
MT	B6KLA1	Tubulin beta chain	2	118	3	50.554	55
MT	Q3TWG5	Dynein cytoplasmic 1 light intermediate chain 1	2	65	2	56.864	70
PR	Q3TII3	Elongation factor 1-alpha	2	249	6	50.414	55
PR	B6KN45	Elongation factor 1-alpha	2	217	5	49.316	55
PR	Q542X7	Chaperonin subunit 2 (Beta)	2	159	5	57.783	55
PR	P11983	T-complex protein 1 subunit alpha	2	157	5	60.867	70
PR	Q3TII3	Elongation factor 1-alpha	2	175	4	50.414	55
PR	Q9WVM1	Rac GTPase-activating protein 1	2	145	4	70.856	70
PR	Q3TII0	T-complex protein 1 subunit delta	2	117	4	58.561	70
PR	Q5NCU1	Ras-GTPase-activating protein SH3-domain binding protein 1	2	50	4	51.854	70
PR	B6KN45	Elongation factor 1-alpha	2	127	3	49.316	55
PR	B6KN45	Elongation factor 1-alpha	2	119	3	49.316	55
PR	P50396	Rab GDP dissociation inhibitor alpha	2	53	3	51.059	55
PR	B6KJR5	Ubiquitin associated domain-containing protein	2	121	2	208.295	100
PR	Q9JMA1	Ubiquitin carboxyl-terminal hydrolase 14	2	88	2	56.422	70
PR	Q542X7	Chaperonin subunit 2 (Beta)	2	71	2	57.783	55
PR	A2BH28	Ubiquitin-like 1 (Sentrin) activating enzyme E1B	2	48	2	71.209	100
PR	Q3TML6	Eukaryotic translation initiation factor 2, subunit 3	2	42	2	51.603	55
PR	B2MWM9	Calreticulin	2	33	2	48.136	55
TG	B6KKA5	Heat shock protein 90	2	156	6	82.281	100
TG	B6KHU4	Heat shock protein 70, putative	2	139	6	78.544	70
TG	B9PU53	Subtilase family protein	2	82	4	85.785	100
TG	Q2PAY2	Rhoptry protein 18	2	92	3	62.702	55
TG	B9Q331	CELF family protein, putative	2	36	2	50.94	55
TG	B6KTXO	Protein disulfide isomerase	2	33	2	52.8	55

UN	Q3TET0	Uncharacterised protein	2	180	9	60.159	70
UN	Q3TFD9	Uncharacterised protein	2	161	7	53.713	55
UN	Q3UKQ2	Uncharacterised protein	2	237	6	60.089	70
UN	Q3TWV0	Uncharacterised protein	2	144	6	53.69	55
UN	Q3TF87	Uncharacterised protein	2	134	6	57.58	55
UN	Q3TWV0	Uncharacterised protein	2	133	6	53.69	55
UN	E9PZV5	Uncharacterised protein	2	118	6	52.227	55
UN	E0CZE0	Uncharacterised protein	2	69	6	58.04	70
UN	Q3TW93	Uncharacterised protein	2	150	5	73.731	70
UN	Q3TZK4	Uncharacterised protein	2	142	5	27.929	100
UN	Q3TFD9	Uncharacterised protein	2	130	5	53.713	55
UN	Q3TF72	Uncharacterised protein	2	151	4	57.452	55
UN	Q3UGJ3	Uncharacterised protein	2	110	4	54.47	55
UN	Q3TIZ0	Uncharacterised protein	2	90	4	50.592	55
UN	Q3TWV0	Uncharacterised protein	2	85	4	53.69	55
UN	D3Z3F7	Uncharacterised protein	2	82	3	48.008	55
UN	Q3TLX1	Uncharacterised protein	2	79	3	55.714	55
UN	Q3U6U7	Uncharacterised protein	2	79	3	54.063	55
UN	Q3UWV5	Uncharacterised protein	2	74	3	67.824	100
UN	Q3T9A1	Uncharacterised protein	2	69	3	56.572	70
UN	Q3U8U8	Uncharacterised protein	2	69	3	70.824	70
UN	Q3U7C0	Uncharacterised protein	2	50	3	89.932	100
UN	Q3U4S9	Uncharacterised protein	2	100	2	57.577	70
UN	Q3TNH0	Uncharacterised protein	2	86	2	46.079	55
UN	Q3U9U3	Uncharacterised protein	2	77	2	42.526	55
UN	Q3U548	Uncharacterised protein	2	75	2	55.852	55

UN	Q3U122	Uncharacterised protein	2	68	2	42.367	55
UN	Q3TMB8	Uncharacterised protein	2	68	2	55.571	55
UN	Q3U6U7	Uncharacterised protein	2	66	2	54.063	55
UN	Q3TN28	Uncharacterised protein	2	63	2	69.305	100
UN	Q3TJ01	Uncharacterised protein	2	60	2	55.731	70
UN	Q3U122	Uncharacterised protein	2	56	2	42.367	70
UN	Q3TIZ0	Uncharacterised protein	2	49	2	50.592	55
UN	Q3TK29	Uncharacterised protein	2	48	2	80.487	70
UN	Q3TMC5	Uncharacterised protein	2	47	2	57.601	55
UN	B6KDR3	Uncharacterised protein	2	46	2	68.731	100
UN	D3Z3F7	Uncharacterised protein	2	46	2	48.008	55
UN	E9Q1R3	Uncharacterised protein	2	36	2	37.593	70
UN	Q3U548	Uncharacterised protein	2	35	2	55.852	55
CM	Q8CAQ8	Mitochondrial inner membrane protein Mitofilin	6	194	9	84.247	100
CM	Q8CGC7	Bifunctional aminoacyl-tRNA synthetase	6	166	7	171.713	200
CM	A4QPD6	Phospholipase A2, activating protein	6	112	4	88.591	100
CM	Q99K08	Phosphofructokinase, muscle	6	106	4	86.104	100
CM	Q99KI0	Aconitate hydratase, mitochondrial	6	70	4	86.151	100
CM	A2A5S1	Chromosome segregation 1-like (S. cerevisiae)	6	65	3	111.183	120
CM	Q5DTI2	ATPase, Ca++ transporting, cardiac muscle, slow twitch 2	6	108	2	118.178	120
CM	Q8K3H0	DCC-interacting protein 13-alpha	6	77	2	79.963	100
CM	Q6P5E4	UDP-glucose:glycoprotein glucosyltransferase 1	6	45	2	177.006	200
CM	Q76LL6	FH1/FH2 domain-containing protein 3	6	35	2	176.63	200
CM	Q14CH7	Alanyl-tRNA synthetase, mitochondrial	6	42	2	107.743	120
CM	D3Z0M9	Dead box helicase family	6	41	2	95.778	120
CR	Q71LX8	Heat shock protein 90 alpha	6	284	15	83.571	100

CR	P07901	Heat shock protein HSP 90-alpha	6	243	14	85.134	100
CR	B6KKA5	Heat shock protein 90	6	76	3	82.281	100
MT	B1AQZ2	Kinesin family member 3A	6	61	2	82.981	100
CY	Q8VDD5	Myosin-9 Cellular myosin heavy chain, type A	6	697	22	227.429	230
CY	Q8VDD5	Myosin-9 Cellular myosin heavy chain, type A	6	544	21	227.429	200
CY	Q7TPR4	Alpha-actinin-1	6	561	19	103.631	120
CY	P57780	Alpha-actinin-4 F-actin cross-linking protein	6	385	15	105.368	120
CY	Q8VDD5	Myosin-9 Cellular myosin heavy chain, type A	6	265	9	227.429	120
CY	P21271	Myosin-Vb	6	180	7	212.092	230
CY	Q3UH59	Myosin, heavy polypeptide 10, non-muscle	6	125	6	234.332	200
CY	Q8VDD5	Myosin-9 Cellular myosin heavy chain, type A	6	128	5	227.429	100
CY	B8JK03	Myosin Va	6	92	2	216.697	230
CY	B2RRX1	Actin, beta	6	84	2	42.052	100
CY	B2RRX1	Actin, beta	6	73	2	42.052	120
CY	B2RRE2	Myosin 19 Protein	6	51	2	233.021	200
PR	Q5SXR6	Clathrin, heavy polypeptide (Hc)	6	784	24	193.631	200
PR	Q6PEE6	Adaptor protein complex AP-2, alpha 2 subunit	6	115	5	104.849	120
PR	Q3T9Y4	Coatomer protein complex, subunit beta 1	6	102	5	108.138	120
PR	Q5SXR6	Clathrin, heavy polypeptide (Hc)	6	120	4	193.631	120
PR	A2BH28	Ubiquitin-like 1 (Sentrin) activating enzyme E1B	6	116	3	71.209	100
PR	B1ASH6	Arhgef16 protein Rho guanine nucleotide exchange factor (GEF) 16	6	108	3	80.673	100
PR	B1AXN9	Ribosomal protein S6 kinase polypeptide 3	6	88	2	80.961	100
PR	Q8CIJ3	Eif3b protein	6	71	3	110.111	120
PR	O55029	Coatomer subunit beta	6	55	2	103.24	120
PR	Q5SWR1	Adaptor-related protein complex 2, beta 1 subunit	6	40	2	106.567	120
PR	A5XDA7	ROCK2 splice variant	6	37	2	167.796	200

UN	E9QN72	Uncharacterised protein	6	258	9	140.297	200
UN	Q3TGJ9	Uncharacterised protein	6	141	7	81.084	100
UN	Q3TXF9	Uncharacterised protein	6	165	6	114.222	120
UN	Q3U630	Uncharacterised protein	6	121	5	84.256	100
UN	E9QPE7	Uncharacterised protein	6	83	5	224.074	230
UN	Q3THX5	Uncharacterised protein	6	114	4	96.984	120
UN	Q3UI30	Uncharacterised protein	6	114	3	68.818	100
UN	Q3TGN5	Uncharacterised protein	6	101	3	77.152	120
UN	E9QQ50	Uncharacterised protein	6	94	3	162.237	200
UN	Q3TVN4	Uncharacterised protein	6	84	3	104.638	120
UN	E9PVU0	Uncharacterised protein	6	88	2	147.64	200
UN	Q3UGW8	Uncharacterised protein	6	77	2	77.415	100
UN	Q3TW74	Uncharacterised protein	6	73	2	101.79	120
UN	Q3UT19	Uncharacterised protein	6	61	2	77.388	100
UN	Q3TB79	Uncharacterised protein	6	59	2	81.012	100
UN	Q3V2D0	Uncharacterised protein	6	57	2	106.98	120
UN	E9Q039	Uncharacterised protein	6	53	2	100.749	120
UN	Q3UPJ3	Uncharacterised protein	6	47	2	115.368	230
UN	E9Q5P4	Uncharacterised protein	6	46	2	99.15	120
UN	Q3TGQ3	Uncharacterised protein	6	46	2	100.698	120
UN	E0CXD1	Uncharacterised protein	6	44	2	79.169	100
UN	E9Q0U7	Uncharacterised protein	6	41	2	92.532	120
UN	E9PX59	Uncharacterised protein	6	37	2	183.964	200
UN	E9Q5B5	Uncharacterised protein	6	35	2	100.576	120

Bibliography

Aberle H, Bauer A, Stappert J, Kispert A, Kemler R (1997) beta-catenin is a target for the ubiquitin-proteasome pathway. *EMBO J* 16:3797–3804.

Ahn HJ, Kim S, Nam HW (2003) Molecular cloning of the 82-kDa heat shock protein (HSP90) of Toxoplasma gondii associated with the entry into and growth in host cells. *Biochem Biophys Res Commun* 311:654–659.

Al-Sadi R, Khatib K, Guo S, Ye D, Youssef M, Ma TY (2011) Occludin Regulates Macromolecule Flux across the Intestinal Epithelial Tight Junction Barrier. *Am J Physiol Gastrointest Liver Physiol* .

Al-Sadi R, Ye D, Dokladny K, Ma TY (2008) Mechanism of IL-1beta-induced increase in intestinal epithelial tight junction permeability. *J Immunol* 180:5653–5661.

Al-Sadi RM, Ma TY (2007) IL-1beta causes an increase in intestinal epithelial tight junction permeability. *J Immunol* 178:4641–4649.

Alexander DL, Mital J, Ward GE, Bradley P, Boothroyd JC (2005) Identification of the moving junction complex of Toxoplasma gondii: a collaboration between distinct secretory organelles. *PLoS Pathog* 1:e17.

Alexander JS, Dayton T, Davis C, Hill S, Jackson TH, Blaschuk O, Symonds M, Okayama N, Kevil CG, Laroux FS, Berney SM, Kimpel D (1998) Activated T-lymphocytes express occludin, a component of tight junctions. *Inflammation* 22:573–582.

Aliberti J, Hieny S, e Sousa CR, Serhan CN, Sher A (2002) Lipoxin-mediated inhibition of IL-12 production by DCs: a mechanism for regulation of microbial immunity. *Nat Immunol* 3:76–82.

Aliberti J, Valenzuela JG, Carruthers VB, Hieny S, Andersen J, Charest H, e Sousa CR, Fairlamb A, Ribeiro JM, Sher A (2003) Molecular mimicry of a CCR5 binding-domain in the microbial activation of dendritic cells. *Nat Immunol* 4:485–490.

Altman R, Kellogg D (1997) Control of mitotic events by Nap1 and the Gin4 kinase. *J Cell Biol* 138:119–130.

Amano M, Ito M, Kimura K, Fukata Y, Chihara K, Nakano T, Matsuura Y, Kaibuchi K (1996) Phosphorylation and activation of myosin by Rho-associated kinase (Rho-kinase). *J Biol Chem* 271:20246–20249.

Amasheh S, Meiri N, Gitter AH, Schöneberg T, Mankertz J, Schulzke JD, Fromm M (2002) Claudin-2 expression induces cation-selective channels in tight junctions of epithelial cells. *J Cell Sci* 115:4969–4976.

Amoli MM, Carthy D, Platt H, Ollier WER (2008) EBV Immortalization of human B lymphocytes separated from small volumes of cryopreserved whole blood. *Int J Epidemiol* 37 Suppl 1:i41–i45.

Anderson JM (2001) Molecular structure of tight junctions and their role in epithelial transport. *News Physiol Sci* 16:126–130.

Anderson JM, Itallie CMV (2009) Physiology and function of the tight junction. *Cold Spring Harb Perspect Biol* 1:a002584.

Ando-Akatsuka Y, Saitou M, Hirase T, Kishi M, Sakakibara A, Itoh M, Yonemura S, Furuse M, Tsukita S (1996) Interspecies diversity of the occludin sequence: cDNA cloning of human, mouse, dog, and rat-kangaroo homologues. *J Cell Biol* 133:43–47.

Andreeva AY, Krause E, Müller EC, Blasig IE, Utepbergenov DI (2001) Protein kinase C regulates the phosphorylation and cellular localization of occludin. *J Biol Chem* 276:38480–38486.

Antonetti DA, Barber AJ, Hollinger LA, Wolpert EB, Gardner TW (1999) Vascular endothelial growth factor induces rapid phosphorylation of tight junction proteins occludin and zonula occluden 1. A potential mechanism for vascular permeability in diabetic retinopathy and tumors. *J Biol Chem* 274:23463–23467.

Aoki N, Ito K, Ito M (1997) Isolation and characterization of mouse high-glycine/tyrosine proteins. *J Biol Chem* 272:30512–30518.

Arques JL, Hautefort I, Ivory K, Bertelli E, Regoli M, Clare S, Hinton JCD, Nicoletti C (2009) Salmonella induces flagellin- and MyD88-dependent migration of bacteria-capturing dendritic cells into the gut lumen. *Gastroenterology* 137:579–87, 587.e1–2.

Bachmann A, Schneider M, Theilenberg E, Grawe F, Knust E (2001) Drosophila Stardust is a partner of Crumbs in the control of epithelial cell polarity. *Nature* 414:638–643.

Bahi SE, Caliot E, Bens M, Bogdanova A, Kernéis S, Kahn A, Vandewalle A, Pringault E (2002) Lymphoepithelial interactions trigger specific regulation of gene expression in the M cell-containing follicle-associated epithelium of Peyer's patches. *J Immunol* 168:3713–3720.

Balda MS, Flores-Maldonado C, Cereijido M, Matter K (2000) Multiple domains of occludin are involved in the regulation of paracellular permeability. *J Cell Biochem* 78:85–96.

Balda MS, Whitney JA, Flores C, González S, Cereijido M, Matter K (1996) Functional dissociation of paracellular permeability and transepithelial electrical resistance and disruption of the apical-basolateral intramembrane diffusion barrier by expression of a mutant tight junction membrane protein. *J Cell Biol* 134:1031–1049.

Balda MS, Garrett MD, Matter K (2003) The ZO-1-associated Y-box factor ZONAB regulates epithelial cell proliferation and cell density. *J Cell Biol* 160:423–432.

Bamforth SD, Kniesel U, Wolburg H, Engelhardt B, Risau W (1999) A dominant mutant of occludin disrupts tight junction structure and function. *J Cell Sci* 112 (Pt 12):1879–1888.

Banga SS, Kim S, Hubbard K, Dasgupta T, Jha KK, Patsalis P, Hauptschein R, Gamberi B, Dalla-Favera R, Kraemer P, Ozer HL (1997) SEN6, a locus for SV40-mediated immortalization of human cells, maps to 6q26-27. *Oncogene* 14:313–321.

Banks MR, Farthing MJG, Robberecht P, Burleigh DE (2005) Antisecretory actions of a novel vasoactive intestinal polypeptide (VIP) antagonist in human and rat small intestine. *Br J Pharmacol* 144:994–1001.

Barragan A, Brossier F, Sibley LD (2005) Transepithelial migration of Toxoplasma gondii involves an interaction of intercellular adhesion molecule 1 (ICAM-1) with the parasite adhesin MIC2. *Cell Microbiol* 7:561–568.

Barragan A, Sibley LD (2002) Transepithelial migration of Toxoplasma gondii is linked to parasite motility and virulence. *J Exp Med* 195:1625–1633.

Barrios-Rodiles M, Brown KR, Ozdamar B, Bose R, Liu Z, Donovan RS, Shinjo F, Liu Y, Dembowy J, Taylor IW, Luga V, Przulj N, Robinson M, Suzuki H, Hayashizaki Y, Jurisica I, Wrana JL (2005) High-throughput mapping of a dynamic signaling network in mammalian cells. *Science* 307:1621–1625.

Barton ES, Forrest JC, Connolly JL, Chappell JD, Liu Y, Schnell FJ, Nusrat A, Parkos CA, Dermody TS (2001) Junction adhesion molecule is a receptor for reovirus. *Cell* 104:441–451.

Basuroy S, Seth A, Elias B, Naren AP, Rao R (2006) MAPK interacts with occludin and mediates EGF-induced prevention of tight junction disruption by hydrogen peroxide. *Biochem J* 393:69–77.

Bazzoni G, Martinez-Estrada OM, Mueller F, Nelboeck P, Schmid G, Bartfai T, Dejana E, Brockhaus M (2000a) Homophilic interaction of junctional adhesion molecule. *J Biol Chem* 275:30970–30976.

Bazzoni G, Martinez-Estrada OM, Orsenigo F, Cordenonsi M, Citi S, Dejana E (2000b) Interaction of junctional adhesion molecule with the tight junction components ZO-1, cingulin, and occludin. *J Biol Chem* 275:20520–20526.

Beau I, Cotte-Laffitte J, Amsellem R, Servin AL (2007) A protein kinase A-dependent mechanism by which rotavirus affects the distribution and mRNA level of the functional tight junction-associated protein, occludin, in human differentiated intestinal Caco-2 cells. *J Virol* 81:8579–8586.

Beaulieu JF, Nichols B, Quaroni A (1989) Posttranslational regulation of sucrase-isomaltase expression in intestinal crypt and villus cells. *J Biol Chem* 264:20000–20011.

Bedin M, Gaben AM, Saucier C, Mester J (2004) Geldanamycin, an inhibitor of the chaperone activity of HSP90, induces MAPK-independent cell cycle arrest. *Int J Cancer* 109:643–652.

Beeman NE, Baumgartner HK, Webb PG, Schaack JB, Neville MC (2009) Disruption of occludin function in polarized epithelial cells activates the extrinsic pathway of apoptosis leading to cell extrusion without loss of transepithelial resistance. *BMC Cell Biol* 10:85.

Beltinger J, del Buono J, Skelly MM, Thornley J, Spiller RC, Stack WA, Hawkey CJ (2008) Disruption of colonic barrier function and induction of mediator release by strains of Campylobacter jejuni that invade epithelial cells. *World J Gastroenterol* 14:7345–7352.

Benais-Pont G, Punn A, Flores-Maldonado C, Eckert J, Raposo G, Fleming TP, Cereijido M, Balda MS, Matter K (2003) Identification of a tight junction-associated guanine nucleotide exchange factor that activates Rho and regulates paracellular permeability. *J Cell Biol* 160:729–740.

Bennouna S, Bliss SK, Curiel TJ, Denkers EY (2003) Cross-talk in the innate immune system: neutrophils instruct recruitment and activation of dendritic cells during microbial infection. *J Immunol* 171:6052–6058.

Bens M, Bogdanova A, Cluzeaud F, Miquerol L, Kerneis S, Kraehenbuhl JP, Kahn A, Pringault E, Vandewalle A (1996) Transimmortalized mouse intestinal cells (m-ICc12) that maintain a crypt phenotype. *Am J Physiol* 270:C1666–C1674.

Berdoy M, Webster JP, Macdonald DW (2000) Fatal attraction in rats infected with Toxoplasma gondii. *Proc Biol Sci* 267:1591–1594.

Bernardes ES, Silva NM, Ruas LP, Mineo JR, Loyola AM, Hsu DK, Liu FT, Chammas R, Roque-Barreira MC (2006) Toxoplasma gondii infection reveals a novel regulatory role for galectin-3 in the interface of innate and adaptive immunity. *Am J Pathol* 168:1910–1920.

Bhadra R, Guan H, Khan IA (2010) Absence of both IL-7 and IL-15 severely impairs the development of CD8 T cell response against Toxoplasma gondii. *PLoS One* 5:e10842.

Bhopale GM (2003) Development of a vaccine for toxoplasmosis: current status. *Microbes Infect* 5:457–462.

Bierly AL, Shufesky WJ, Sukhumavasi W, Morelli AE, Denkers EY (2008) Dendritic cells expressing plasmacytoid marker PDCA-1 are Trojan horses during Toxoplasma gondii infection. *J Immunol* 181:8485–8491.

Black MW, Boothroyd JC (2000) Lytic cycle of Toxoplasma gondii. *Microbiol Mol Biol Rev* 64:607–623.

Blaschuk OW, Oshima T, Gour BJ, Symonds JM, Park JH, Kevil CG, Trocha SD, Michaud S, Okayama N, Elrod JW, Alexander JS, Sasaki M (2002) Identification of an occludin cell adhesion recognition sequence. *Inflammation* 26:193–198.

Blasig IE, Winkler L, Lassowski B, Mueller SL, Zuleger N, Krause E, Krause G, Gast K, Kolbe M, Piontek J (2006) On the self-association potential of transmembrane tight junction proteins. *Cell Mol Life Sci* 63:505–514.

Bohne W, Heesemann J, Gross U (1993) Induction of bradyzoite-specific Toxoplasma gondii antigens in gamma interferon-treated mouse macrophages. *Infect Immun* 61:1141–1145.

Bohne W, Heesemann J, Gross U (1994) Reduced replication of Toxoplasma gondii is necessary for induction of bradyzoite-specific antigens: a possible role for nitric oxide in triggering stage conversion. *Infect Immun* 62:1761–1767.

Boivin MA, Roy PK, Bradley A, Kennedy JC, Rihani T, Ma TY (2009) Mechanism of interferon-gamma-induced increase in T84 intestinal epithelial tight junction. *J Interferon Cytokine Res* 29:45–54.

Bojarski C, Weiske J, Schöneberg T, Schröder W, Mankertz J, Schulzke JD, Florian P, Fromm M, Tauber R, Huber O (2004) The specific fates of tight junction proteins in apoptotic epithelial cells. *J Cell Sci* 117:2097–2107.

Bonazzi M, Veiga E, Pizarro-Cerdá J, Cossart P (2008) Successive post-translational modifications of E-cadherin are required for InlA-mediated internalization of Listeria monocytogenes. *Cell Microbiol* 10:2208–2222.

Bornholdt J, Friis S, Godiksen S, Poulsen SS, Santoni-Rugiu E, Bisgaard HC, Lothe IM, Ikdahl T, Tveit KM, Johnson E, Kure EH, Vogel LK (2011) The level of claudin-7 is reduced as an early event in colorectal carcinogenesis. *BMC Cancer* 11:65.

Boyle EC, Brown NF, Finlay BB (2006) Salmonella enterica serovar Typhimurium effectors SopB, SopE, SopE2 and SipA disrupt tight junction structure and function. *Cell Microbiol* 8:1946–1957.

Bradley PJ, Ward C, Cheng SJ, Alexander DL, Coller S, Coombs GH, Dunn JD, Ferguson DJ, Sanderson SJ, Wastling JM, Boothroyd JC (2005) Proteomic analysis of rhoptry organelles reveals many novel constituents for host-parasite interactions in Toxoplasma gondii. *J Biol Chem* 280:34245–34258.

Brattain MG, Strobel-Stevens J, Fine D, Webb M, Sarrif AM (1980) Establishment of mouse colonic carcinoma cell lines with different metastatic properties. *Cancer Res* 40:2142–2146.

Brecht S, Carruthers VB, Ferguson DJ, Giddings OK, Wang G, Jakle U, Harper JM, Sibley LD, Soldati D (2001) The toxoplasma micronemal protein MIC4 is an adhesin composed of six conserved apple domains. *J Biol Chem* 276:4119–4127.

Bruewer M, Utech M, Ivanov AI, Hopkins AM, Parkos CA, Nusrat A (2005) Interferon-gamma induces internalization of epithelial tight junction proteins via a macropinocytosis-like process. *FASEB J* 19:923–933.

Bullen TF, Forrest S, Campbell F, Dodson AR, Hershman MJ, Pritchard DM, Turner JR, Montrose MH, Watson AJM (2006) Characterization of epithelial cell shedding from human small intestine. *Lab Invest* 86:1052–1063.

Burg JL, Perelman D, Kasper LH, Ware PL, Boothroyd JC (1988) Molecular analysis of the gene encoding the major surface antigen of Toxoplasma gondii. *J Immunol* 141:3584–3591.

Burnette DT, Manley S, Sengupta P, Sougrat R, Davidson MW, Kachar B, Lippincott-Schwartz J (2011) A role for actin arcs in the leading-edge advance of migrating cells. *Nat Cell Biol* 13:371–382.

Butcher BA, Kim L, Johnson PF, Denkers EY (2001) Toxoplasma gondii tachyzoites inhibit proinflammatory cytokine induction in infected macrophages by preventing nuclear translocation of the transcription factor NF-kappa B. *J Immunol* 167:2193–2201.

Butcher BA, Denkers EY (2002) Mechanism of entry determines the ability of Toxoplasma gondii to inhibit macrophage proinflammatory cytokine production. *Infect Immun* 70:5216–5224.

Buxton D, Innes EA (1995) A commercial vaccine for ovine toxoplasmosis. *Parasitology* 110 Suppl:S11–S16.

Buzoni-Gatel D, Debbabi H, Mennechet FJ, Martin V, Lepage AC, Schwartzman JD, Kasper LH (2001) Murine ileitis after intracellular parasite infection is controlled by TGF-beta-producing intraepithelial lymphocytes. *Gastroenterology* 120:914–924.

Buzoni-Gatel D, Debbabi H, Moretto M, Dimier-Poisson IH, Lepage AC, Bout DT, Kasper LH (1999) Intraepithelial lymphocytes traffic to the intestine and enhance resistance to Toxoplasma gondii oral infection. *J Immunol* 162:5846–5852.

Buzoni-Gatel D, Lepage AC, Dimier-Poisson IH, Bout DT, Kasper LH (1997) Adoptive transfer of gut intraepithelial lymphocytes protects against murine infection with Toxoplasma gondii. *J Immunol* 158:5883–5889.

Caldas LA, Attias M, de Souza W (2009) Dynamin inhibitor impairs Toxoplasma gondii invasion. *FEMS Microbiol Lett* 301:103–108.

Camossi LG, Greca-Júnior H, Corrêa APFL, Richini-Pereira VB, Silva RC, Silva AVD, Langoni H (2011) Detection of Toxoplasma gondii DNA in the milk of naturally infected ewes. *Vet Parasitol* 177:256–261.

Canil C, Rosenshine I, Ruschkowski S, Donnenberg MS, Kaper JB, Finlay BB (1993) Enteropathogenic Escherichia coli decreases the transepithelial electrical resistance of polarized epithelial monolayers. *Infect Immun* 61:2755–2762.

Carruthers VB, Giddings OK, Sibley LD (1999) Secretion of micronemal proteins is associated with toxoplasma invasion of host cells. *Cell Microbiol* 1:225–235.

Carruthers VB, Håkansson S, Giddings OK, Sibley LD (2000) Toxoplasma gondii uses sulfated proteoglycans for substrate and host cell attachment. *Infect Immun* 68:4005–4011.

Carruthers VB, Sibley LD (1999) Mobilization of intracellular calcium stimulates microneme discharge in Toxoplasma gondii. *Mol Microbiol* 31:421–428.

Carruthers V, Boothroyd JC (2007) Pulling together: an integrated model of Toxoplasma cell invasion. *Curr Opin Microbiol* 10:83–89.

Cass CE (1972) Density-dependent resistance to puromycin in cell cultures. *J Cell Physiol* 79:139–146.

Castelli C, Ciupitu AM, Rini F, Rivoltini L, Mazzocchi A, Kiessling R, Parmiani G (2001) Human heat shock protein 70 peptide complexes specifically activate antimelanoma T cells. *Cancer Res* 61:222–227.

Chen ML, Ge Z, Fox JG, Schauer DB (2006) Disruption of tight junctions and induction of proinflammatory cytokine responses in colonic epithelial cells by Campylobacter jejuni. *Infect Immun* 74:6581–6589.

Chen X, Macara IG (2006) Par-3 mediates the inhibition of LIM kinase 2 to regulate cofilin phosphorylation and tight junction assembly. *J Cell Biol* 172:671–678.

Chen Y, Lu Q, Schneeberger EE, Goodenough DA (2000) Restoration of tight junction structure and barrier function by down-regulation of the mitogen-activated protein kinase pathway in ras-transformed Madin-Darby canine kidney cells. *Mol Biol Cell* 11:849–862.

Chen Y, Merzdorf C, Paul DL, Goodenough DA (1997) COOH terminus of occludin is required for tight junction barrier function in early Xenopus embryos. *J Cell Biol* 138:891–899.

Chen YH, Lu Q, Goodenough DA, Jeansonne B (2002a) Nonreceptor tyrosine kinase c-Yes interacts with occludin during tight junction formation in canine kidney epithelial cells. *Mol Biol Cell* 13:1227–1237.

Chen Y, Chou K, Fuchs E, Havran WL, Boismenu R (2002b) Protection of the intestinal mucosa by intraepithelial gamma delta T cells. *Proc Natl Acad Sci U S A* 99:14338–14343.

Chiba H, Osanai M, Murata M, Kojima T, Sawada N (2008) Transmembrane proteins of tight junctions. *Biochim Biophys Acta* 1778:588–600.

Chin AC, Lee WY, Nusrat A, Vergnolle N, Parkos CA (2008) Neutrophil-mediated activation of epithelial protease-activated receptors-1 and -2 regulates barrier function and transepithelial migration. *J Immunol* 181:5702–5710.

Choi SH, Park SJ, Cha GH, Quan JH, Chang NS, Ahn MH, Shin DW, Lee YH (2011) Toxoplasma gondii protects against H(2) O(2) -induced apoptosis in ARPE-19 cells through the transcriptional regulation of apoptotic elements and downregulation of the p38 MAPK pathway. *Acta Ophthalmol* .

Chou CH, Lieu AS, Wu CH, Chang LK, Loh JK, Lin RC, Chen WJ, Liao HD, Fu WS, Chang CS, Lin CC, Hsu CM, Chio CC, Howng SL, Hong YR (2010) Differential expression of hedgehog signaling components and Snail/E-cadherin in human brain tumors. *Oncol Rep* 24:1225–1232.

Ciccocioppo R, Finamore A, Ara C, Sabatino AD, Mengheri E, Corazza GR (2006) Altered expression, localization, and phosphorylation of epithelial junctional proteins in celiac disease. *Am J Clin Pathol* 125:502–511.

Clarke H, Soler AP, Mullin JM (2000) Protein kinase C activation leads to dephosphorylation of occludin and tight junction permeability increase in LLC-PK1 epithelial cell sheets. *J Cell Sci* 113 (Pt 18):3187–3196.

Claude P, Goodenough DA (1973) Fracture faces of zonulae occludentes from "tight" and "leaky" epithelia. *J Cell Biol* 58:390–400.

Cohen CJ, Shieh JT, Pickles RJ, Okegawa T, Hsieh JT, Bergelson JM (2001) The coxsackievirus and adenovirus receptor is a transmembrane component of the tight junction. *Proc Natl Acad Sci U S A* 98:15191–15196.

Colgan SP, Parkos CA, Delp C, Arnaout MA, Madara JL (1993) Neutrophil migration across cultured intestinal epithelial monolayers is modulated by epithelial exposure to IFN-gamma in a highly polarized fashion. *J Cell Biol* 120:785–798.

Conseil V, Soête M, Dubremetz JF (1999) Serine protease inhibitors block invasion of host cells by Toxoplasma gondii. *Antimicrob Agents Chemother* 43:1358–1361.

Coppens I, Dunn JD, Romano JD, Pypaert M, Zhang H, Boothroyd JC, Joiner KA (2006) Toxoplasma gondii sequesters lysosomes from mammalian hosts in the vacuolar space. *Cell* 125:261–274.

Cordenonsi M, Turco F, D'atri F, Hammar E, Martinucci G, Meggio F, Citi S (1999) Xenopus laevis occludin. Identification of in vitro phosphorylation sites by protein kinase CK2 and association with cingulin. *Eur J Biochem* 264:374–384.

Corr SC, Gahan CCGM, Hill C (2008) M-cells: origin, morphology and role in mucosal immunity and microbial pathogenesis. *FEMS Immunol Med Microbiol* 52:2–12.

Corre I, Pineau D, Hermouet S (1999) Interleukin-8: an autocrine/paracrine growth factor for human hematopoietic progenitors acting in synergy with colony stimulating factor-1 to promote monocyte-macrophage growth and differentiation. *Exp Hematol* 27:28–36.

Cosnes J, Gower-Rousseau C, Seksik P, Cortot A (2011) Epidemiology and natural history of inflammatory bowel diseases. *Gastroenterology* 140:1785–1794.e4.

Couesnon A, Pereira Y, Popoff MR (2008) Receptor-mediated transcytosis of botulinum neurotoxin A through intestinal cell monolayers. *Cell Microbiol* 10:375–387.

Courret N, Darche S, Sonigo P, Milon G, Buzoni-Gâtel D, Tardieux I (2006) CD11c- and CD11b-expressing mouse leukocytes transport single Toxoplasma gondii tachyzoites to the brain. *Blood* 107:309–316.

Coyne CB, Shen L, Turner JR, Bergelson JM (2007) Coxsackievirus entry across epithelial tight junctions requires occludin and the small GTPases Rab34 and Rab5. *Cell Host Microbe* 2:181–192.

Coëffier M, Gloro R, Boukhettala N, Aziz M, Lecleire S, Vandaele N, Antonietti M, Savoye G, Bôle-Feysot C, Déchelotte P, Reimund JM, Ducrotté P (2010) Increased proteasome-mediated degradation of occludin in irritable bowel syndrome. *Am J Gastroenterol* 105:1181–1188.

Dalton JE, Cruickshank SM, Egan CE, Mears R, Newton DJ, Andrew EM, Lawrence B, Howell G, Else KJ, Gubbels MJ, Striepen B, Smith

JE, White SJ, Carding SR (2006) Intraepithelial gammadelta+ lymphocytes maintain the integrity of intestinal epithelial tight junctions in response to infection. *Gastroenterology* 131:818–829.

Danos O, Mulligan RC (1988) Safe and efficient generation of recombinant retroviruses with amphotropic and ecotropic host ranges. *Proc Natl Acad Sci U S A* 85:6460–6464.

Darido C, Buchert M, Pannequin J, Bastide P, Zalzali H, Mantamadiotis T, Bourgaux JF, Garambois V, Jay P, Blache P, Joubert D, Hollande F (2008) Defective claudin-7 regulation by Tcf-4 and Sox-9 disrupts the polarity and increases the tumorigenicity of colorectal cancer cells. *Cancer Res* 68:4258–4268.

Davis CH, Raulston JE, Wyrick PB (2002) Protein disulfide isomerase, a component of the estrogen receptor complex, is associated with Chlamydia trachomatis serovar E attached to human endometrial epithelial cells. *Infect Immun* 70:3413–3418.

de Figueiredo P, Drecktrah D, Katzenellenbogen JA, Strang M, Brown WJ (1998) Evidence that phospholipase A2 activity is required for Golgi complex and trans Golgi network membrane tubulation. *Proc Natl Acad Sci U S A* 95:8642–8647.

Debierre-Grockiego F, Niehus S, Coddeville B, Elass E, Poirier F, Weingart R, Schmidt RR, Mazurier J, Guérardel Y, Schwarz RT (2010) Binding of Toxoplasma gondii glycosylphosphatidylinositols to galectin-3 is required for their recognition by macrophages. *J Biol Chem* 285:32744–32750.

Deli MA (2009) Potential use of tight junction modulators to reversibly open membranous barriers and improve drug delivery. *Biochim Biophys Acta* 1788:892–910.

Delorme V, Garcia A, Cayla X, Tardieux I (2002) A role for Toxoplasma gondii type 1 ser/thr protein phosphatase in host cell invasion. *Microbes Infect* 4:271–278.

Denney CF, Eckmann L, Reed SL (1999) Chemokine secretion of human cells in response to Toxoplasma gondii infection. *Infect Immun* 67:1547–1552.

Derouin F, Pelloux H, on Clinical Parasitology ESCMIDSG (2008) Prevention of toxoplasmosis in transplant patients. *Clin Microbiol Infect* 14:1089–1101.

Dimier IH, Bout DT (1993) Rat intestinal epithelial cell line IEC-6 is activated by recombinant interferon-gamma to inhibit replication of the coccidian Toxoplasma gondii. *Eur J Immunol* 23:981–983.

Dimier-Poisson I, Aline F, Mévélec MN, Beauvillain C, Buzoni-Gatel D, Bout D (2003) Protective mucosal Th2 immune response against Toxoplasma gondii by murine mesenteric lymph node dendritic cells. *Infect Immun* 71:5254–5265.

Dobrowolski JM, Carruthers VB, Sibley LD (1997) Participation of myosin in gliding motility and host cell invasion by Toxoplasma gondii. *Mol Microbiol* 26:163–173.

Dobrowolski JM, Sibley LD (1996) Toxoplasma invasion of mammalian cells is powered by the actin cytoskeleton of the parasite. *Cell* 84:933–939.

Dokladny K, Ye D, Kennedy JC, Moseley PL, Ma TY (2008) Cellular and molecular mechanisms of heat stress-induced up-regulation of occludin protein expression: regulatory role of heat shock factor-1. *Am J Pathol* 172:659–670.

Dolowschiak T, Chassin C, Mkaddem SB, Fuchs TM, Weiss S, Vandewalle A, Hornef MW (2010) Potentiation of epithelial innate host responses by intercellular communication. *PLoS Pathog* 6:e1001194.

Drees F, Pokutta S, Yamada S, Nelson WJ, Weis WI (2005) Alpha-catenin is a molecular switch that binds E-cadherin-beta-catenin and regulates actin-filament assembly. *Cell* 123:903–915.

D'Souza T, Agarwal R, Morin PJ (2005) Phosphorylation of claudin-3 at threonine 192 by cAMP-dependent protein kinase regulates tight junction barrier function in ovarian cancer cells. *J Biol Chem* 280:26233–26240.

D'Souza T, Indig FE, Morin PJ (2007) Phosphorylation of claudin-4 by PKCepsilon regulates tight junction barrier function in ovarian cancer cells. *Exp Cell Res* 313:3364–3375.

Du D, Xu F, Yu L, Zhang C, Lu X, Yuan H, Huang Q, Zhang F, Bao H, Jia L, Wu X, Zhu X, Zhang X, Zhang Z, Chen Z (2010) The tight junction protein, occludin, regulates the directional migration of epithelial cells. *Dev Cell* 18:52–63.

Dubey JP (1997) Bradyzoite-induced murine toxoplasmosis: stage conversion, pathogenesis, and tissue cyst formation in mice fed bradyzoites of different strains of Toxoplasma gondii. *J Eukaryot Microbiol* 44:592–602.

Dubey JP (1998a) Advances in the life cycle of Toxoplasma gondii. *Int J Parasitol* 28:1019–1024.

Dubey JP (1998b) Re-examination of resistance of Toxoplasma gondii tachyzoites and bradyzoites to pepsin and trypsin digestion. *Parasitology* 116 (Pt 1):43–50.

Dubey JP (2009) Toxoplasmosis in sheep–the last 20 years. *Vet Parasitol* 163:1–14.

Dubey JP, Lindsay DS, Speer CA (1998) Structures of Toxoplasma gondii tachyzoites, bradyzoites, and sporozoites and biology and development of tissue cysts. *Clin Microbiol Rev* 11:267–299.

Dubey JP, Velmurugan GV, Rajendran C, Yabsley MJ, Thomas NJ, Beckmen KB, Sinnett D, Ruid D, Hart J, Fair PA, McFee WE, Shearn-Bochsler V, Kwok OCH, Ferreira LR, Choudhary S, Faria EB, Zhou H, Felix TA, Su C (2011) Genetic characterisation of Toxoplasma gondii in wildlife from North America revealed widespread and high prevalence of the fourth clonal type. *Int J Parasitol* .

Dunn JD, Ravindran S, Kim SK, Boothroyd JC (2008) The Toxoplasma gondii dense granule protein GRA7 is phosphorylated upon invasion and forms an unexpected association with the rhoptry proteins ROP2 and ROP4. *Infect Immun* 76:5853–5861.

Dzierszinski F, Nishi M, Ouko L, Roos DS (2004) Dynamics of Toxoplasma gondii differentiation. *Eukaryot Cell* 3:992–1003.

Ebnet K, Schulz CU, Brickwedde MKMZ, Pendl GG, Vestweber D (2000) Junctional adhesion molecule interacts with the PDZ domain-containing proteins AF-6 and ZO-1. *J Biol Chem* 275:27979–27988.

Ebnet K, Suzuki A, Horikoshi Y, Hirose T, Brickwedde MKMZ, Ohno S, Vestweber D (2001) The cell polarity protein ASIP/PAR-3 directly associates with junctional adhesion molecule (JAM). *EMBO J* 20:3738–3748.

Echeverria PC, Figueras MJ, Vogler M, Kriehuber T, de Miguel N, Deng B, Dalmasso MC, Matthews DE, Matrajt M, Haslbeck M, Buchner J, Angel SO (2010) The Hsp90 co-chaperone p23 of Toxoplasma gondii: Identification, functional analysis and dynamic interactome determination. *Mol Biochem Parasitol* 172:129–140.

Echeverria PC, Matrajt M, Harb OS, Zappia MP, Costas MA, Roos DS, Dubremetz JF, Angel SO (2005) Toxoplasma gondii Hsp90 is a potential drug target whose expression and subcellular localization are developmentally regulated. *J Mol Biol* 350:723–734.

Egan CE, Craven MD, Leng J, Mack M, Simpson KW, Denkers EY (2009) CCR2-dependent intraepithelial lymphocytes mediate inflammatory gut pathology during Toxoplasma gondii infection. *Mucosal Immunol* 2:527–535.

Egan CE, Dalton JE, Andrew EM, Smith JE, Gubbels MJ, Striepen B, Carding SR (2005) A requirement for the Vgamma1+ subset of peripheral gammadelta T cells in the control of the systemic growth of Toxoplasma gondii and infection-induced pathology. *J Immunol* 175:8191–8199.

Elias BC, Suzuki T, Seth A, Giorgianni F, Kale G, Shen L, Turner JR, Naren A, Desiderio DM, Rao R (2009) Phosphorylation of Tyr-398 and Tyr-402 in occludin prevents its interaction with ZO-1 and destabilizes its assembly at the tight junctions. *J Biol Chem* 284:1559–1569.

Elmore SA, Jones JL, Conrad PA, Patton S, Lindsay DS, Dubey JP (2010) Toxoplasma gondii: epidemiology, feline clinical aspects, and prevention. *Trends Parasitol* 26:190–196.

Escaffit F, Boudreau F, Beaulieu JF (2005) Differential expression of claudin-2 along the human intestine: Implication of GATA-4 in the maintenance of claudin-2 in differentiating cells. *J Cell Physiol* 203:15–26.

Etienne-Manneville S, Manneville JB, Adamson P, Wilbourn B, Greenwood J, Couraud PO (2000) ICAM-1-coupled cytoskeletal rearrangements and transendothelial lymphocyte migration involve intracellular calcium signaling in brain endothelial cell lines. *J Immunol* 165:3375–3383.

Evans MJ, von Hahn T, Tscherne DM, Syder AJ, Panis M, Wölk B, Hatziioannou T, McKeating JA, Bieniasz PD, Rice CM (2007) Claudin-1 is a hepatitis C virus co-receptor required for a late step in entry. *Nature* 446:801–805.

Even-Ram S, Doyle AD, Conti MA, Matsumoto K, Adelstein RS, Yamada KM (2007) Myosin IIA regulates cell motility and actomyosin-microtubule crosstalk. *Nat Cell Biol* 9:299–309.

Fang H, Mun HS, Kikumura A, Sayama Y, Norose K, Yano A, Aosai F (2008) Toxoplasma gondii-derived heat shock protein 70 induces lethal anaphylactic reaction through activation of cytosolic phospholipase A2 and platelet-activating factor via Toll-like receptor 4/myeloid differentiation factor 88. *Microbiol Immunol* 52:366–374.

Farquhar MG, Palade GE (1963) Junctional complexes in various epithelia. *J Cell Biol* 17:375–412.

Farshori P, Kachar B (1999) Redistribution and phosphorylation of occludin during opening and resealing of tight junctions in cultured epithelial cells. *J Membr Biol* 170:147–156.

Fendrich V, Waldmann J, Esni F, Ramaswamy A, Mullendore M, Buchholz M, Maitra A, Feldmann G (2007) Snail and Sonic Hedgehog activation in neuroendocrine tumors of the ileum. *Endocr Relat Cancer* 14:865–874.

Fentress SJ, Behnke MS, Dunay IR, Mashayekhi M, Rommereim LM, Fox BA, Bzik DJ, Taylor GA, Turk BE, Lichti CF, Townsend RR, Qiu W, Hui R, Beatty WL, Sibley LD (2010) Phosphorylation of immunity-related GTPases by a Toxoplasma gondii-secreted kinase promotes macrophage survival and virulence. *Cell Host Microbe* 8:484–495.

Fihn BM, Sjöqvist A, Jodal M (2000) Permeability of the rat small intestinal epithelium along the villus-crypt axis: effects of glucose transport. *Gastroenterology* 119:1029–1036.

Flegr J (2007) Effects of toxoplasma on human behavior. *Schizophr Bull* 33:757–760.

Flegr J, Havlícek J, Kodym P, Malý M, Smahel Z (2002) Increased risk of traffic accidents in subjects with latent toxoplasmosis: a retrospective case-control study. *BMC Infect Dis* 2:11.

Fourmaux MN, Achbarou A, Mercereau-Puijalon O, Biderre C, Briche I, Loyens A, Odberg-Ferragut C, Camus D, Dubremetz JF (1996) The MIC1 microneme protein of Toxoplasma gondii contains a duplicated receptor-like domain and binds to host cell surface. *Mol Biochem Parasitol* 83:201–210.

Fox BA, Falla A, Rommereim LM, Tomita T, Gigley JP, Mercier C, Cesbron-Delauw MF, Weiss LM, Bzik DJ (2011) Type II Toxoplasma gondii KU80 Knockout Strains Enable Functional Analysis of Genes Required for Cyst Development and Latent Infection. *Eukaryot Cell* .

Francis CL, Starnbach MN, Falkow S (1992) Morphological and cytoskeletal changes in epithelial cells occur immediately upon interaction with Salmonella typhimurium grown under low-oxygen conditions. *Mol Microbiol* 6:3077–3087.

Frank DN, Amand ALS, Feldman RA, Boedeker EC, Harpaz N, Pace NR (2007) Molecular-phylogenetic characterization of microbial community imbalances in human inflammatory bowel diseases. *Proc Natl Acad Sci U S A* 104:13780–13785.

Frenkel JK, Pfefferkorn ER, Smith DD, Fishback JL (1991) Prospective vaccine prepared from a new mutant of Toxoplasma gondii for use in cats. *Am J Vet Res* 52:759–763.

Friswell M, Campbell B, Rhodes J (2010) The role of bacteria in the pathogenesis of inflammatory bowel disease. *Gut Liver* 4:295–306.

Frizzell RA, Schultz SG (1972) Ionic conductances of extracellular shunt pathway in rabbit ileum. Influence of shunt on transmural sodium transport and electrical potential differences. *J Gen Physiol* 59:318–346.

Frödin M, Gammeltoft S (1999) Role and regulation of 90 kDa ribosomal S6 kinase (RSK) in signal transduction. *Mol Cell Endocrinol* 151:65–77.

Fuchs SY, Fried VA, Ronai Z (1998) Stress-activated kinases regulate protein stability. *Oncogene* 17:1483–1490.

Fujita H, Chiba H, Yokozaki H, Sakai N, Sugimoto K, Wada T, Kojima T, Yamashita T, Sawada N (2006) Differential expression and subcellular localization of claudin-7, -8, -12, -13, and -15 along the mouse intestine. *J Histochem Cytochem* 54:933–944.

Fujita K, Katahira J, Horiguchi Y, Sonoda N, Furuse M, Tsukita S (2000) Clostridium perfringens enterotoxin binds to the second extracellular loop of claudin-3, a tight junction integral membrane protein. *FEBS Lett* 476:258–261.

Furtado GC, Cao Y, Joiner KA (1992b) Laminin on Toxoplasma gondii mediates parasite binding to the beta 1 integrin receptor alpha 6 beta 1 on human foreskin fibroblasts and Chinese hamster ovary cells. *Infect Immun* 60:4925–4931.

Furtado GC, Slowik M, Kleinman HK, Joiner KA (1992a) Laminin enhances binding of Toxoplasma gondii tachyzoites to J774 murine macrophage cells. *Infect Immun* 60:2337–2342.

Furuse M, Fujimoto K, Sato N, Hirase T, Tsukita S, Tsukita S (1996) Overexpression of occludin, a tight junction-associated integral membrane protein, induces the formation of intracellular multilamellar bodies bearing tight junction-like structures. *J Cell Sci* 109 (Pt 2):429–435.

Furuse M, Furuse K, Sasaki H, Tsukita S (2001) Conversion of zonulae occludentes from tight to leaky strand type by introducing claudin-2 into Madin-Darby canine kidney I cells. *J Cell Biol* 153:263–272.

Furuse M, Hirase T, Itoh M, Nagafuchi A, Yonemura S, Tsukita S, Tsukita S (1993) Occludin: a novel integral membrane protein localizing at tight junctions. *J Cell Biol* 123:1777–1788.

Furuse M, Itoh M, Hirase T, Nagafuchi A, Yonemura S, Tsukita S, Tsukita S (1994) Direct association of occludin with ZO-1 and its possible involvement in the localization of occludin at tight junctions. *J Cell Biol* 127:1617–1626.

Furuse M, Sasaki H, Fujimoto K, Tsukita S (1998) A single gene product, claudin-1 or -2, reconstitutes tight junction strands and recruits occludin in fibroblasts. *J Cell Biol* 143:391–401.

Furuse M, Sasaki H, Tsukita S (1999) Manner of interaction of heterogeneous claudin species within and between tight junction strands. *J Cell Biol* 147:891–903.

Furuse M (2009) Knockout animals and natural mutations as experimental and diagnostic tool for studying tight junction functions in vivo. *Biochim Biophys Acta* 1788:813–819.

Gagné D, Groulx JF, Benoit YD, Basora N, Herring E, Vachon PH, Beaulieu JF (2010) Integrin-linked kinase regulates migration and proliferation of human intestinal cells under a fibronectin-dependent mechanism. *J Cell Physiol* 222:387–400.

Garcia-Réguet N, Lebrun M, Fourmaux MN, Mercereau-Puijalon O, Mann T, Beckers CJ, Samyn B, Beeumen JV, Bout D, Dubremetz JF (2000) The microneme protein MIC3 of Toxoplasma gondii is a secretory adhesin that binds to both the surface of the host cells and the surface of the parasite. *Cell Microbiol* 2:353–364.

Garrard SM, Capaldo CT, Gao L, Rosen MK, Macara IG, Tomchick DR (2003) Structure of Cdc42 in a complex with the GTPase-binding domain of the cell polarity protein, Par6. *EMBO J* 22:1125–1133.

Gassler N, Rohr C, Schneider A, Kartenbeck J, Bach A, Obermüller N, Otto HF, Autschbach F (2001) Inflammatory bowel disease is associated with changes of enterocytic junctions. *Am J Physiol Gastrointest Liver Physiol* 281:G216–G228.

Ghassemifar MR, Sheth B, Papenbrock T, Leese HJ, Houghton FD, Fleming TP (2002) Occludin TM4(-): an isoform of the tight junction protein present in primates lacking the fourth transmembrane domain. *J Cell Sci* 115:3171–3180.

Gilbert HF (1997) Protein disulfide isomerase and assisted protein folding. *J Biol Chem* 272:29399–29402.

Gilbert LA, Ravindran S, Turetzky JM, Boothroyd JC, Bradley PJ (2007) Toxoplasma gondii targets a protein phosphatase 2C to the nuclei of infected host cells. *Eukaryot Cell* 6:73–83.

Gillooly DJ, Simonsen A, Stenmark H (2001) Cellular functions of phosphatidylinositol 3-phosphate and FYVE domain proteins. *Biochem J* 355:249–258.

Gluzman Y (1981) SV40-transformed simian cells support the replication of early SV40 mutants. *Cell* 23:175–182.

Goebel S, Gross U, Lüder CG (2001) Inhibition of host cell apoptosis by Toxoplasma gondii is accompanied by reduced activation of the caspase cascade and alterations of poly(ADP-ribose) polymerase expression. *J Cell Sci* 114:3495–3505.

Gonzalez V, Combe A, David V, Malmquist NA, Delorme V, Leroy C, Blazquez S, Ménard R, Tardieux I (2009) Host cell entry by apicomplexa parasites requires actin polymerization in the host cell. *Cell Host Microbe* 5:259–272.

Gonzalez-Mariscal L, de Ramírez BC, Cereijido M (1985) Tight junction formation in cultured epithelial cells (MDCK). *J Membr Biol* 86:113–125.

González-Mariscal L, Betanzos A, Avila-Flores A (2000) MAGUK proteins: structure and role in the tight junction. *Semin Cell Dev Biol* 11:315–324.

Goodstadt L, Ponting CP (2004) Vitamin K epoxide reductase: homology, active site and catalytic mechanism. *Trends Biochem Sci* 29:289–292.

Gopal R, Birdsell D, Monroy FP (2011) Regulation of chemokine responses in intestinal epithelial cells by stress and Toxoplasma gondii infection. *Parasite Immunol* 33:12–24.

Gopalakrishnan S, Raman N, Atkinson SJ, Marrs JA (1998) Rho GTPase signaling regulates tight junction assembly and protects tight junctions during ATP depletion. *Am J Physiol* 275:C798–C809.

Gordon JI, Hermiston ML (1994) Differentiation and self-renewal in the mouse gastrointestinal epithelium. *Curr Opin Cell Biol* 6:795–803.

Gorodeski GI (2006) A new model occludin regulation of tight-junctional resistance in low-resistance epithelia. *Medical Hypotheses and Research* 3:769–784.

Green KJ, Jones JC (1996) Desmosomes and hemidesmosomes: structure and function of molecular components. *FASEB J* 10:871–881.

Grimwood J, Mineo JR, Kasper LH (1996) Attachment of Toxoplasma gondii to host cells is host cell cycle dependent. *Infect Immun* 64:4099–4104.

Gu JM, Lim SO, Park YM, Jung G (2008) A novel splice variant of occludin deleted in exon 9 and its role in cell apoptosis and invasion. *FEBS J* 275:3145–3156.

Guan H, Moretto M, Bzik DJ, Gigley J, Khan IA (2007) NK cells enhance dendritic cell response against parasite antigens via NKG2D pathway. *J Immunol* 179:590–596.

Gubbels MJ, Li C, Striepen B (2003) High-throughput growth assay for Toxoplasma gondii using yellow fluorescent protein. *Antimicrob Agents Chemother* 47:309–316.

Gubbels MJ, Striepen B, Shastri N, Turkoz M, Robey EA (2005) Class I major histocompatibility complex presentation of antigens that escape from the parasitophorous vacuole of Toxoplasma gondii. *Infect Immun* 73:703–711.

Gubbels MJ, Vaishnava S, Boot N, Dubremetz JF, Striepen B (2006) A MORN-repeat protein is a dynamic component of the Toxoplasma gondii cell division apparatus. *J Cell Sci* 119:2236–2245.

Guillermo LVC, DaMatta RA (2004) Nitric oxide inhibition after Toxoplasma gondii infection of chicken macrophage cell lines. *Poult Sci* 83:776–782.

Guo X, Rao JN, Liu L, Zou T, Keledjian KM, Boneva D, Marasa BS, Wang JY (2005) Polyamines are necessary for synthesis and stability of occludin protein in intestinal epithelial cells. *Am J Physiol Gastrointest Liver Physiol* 288:G1159–G1169.

Gut A, Kappeler F, Hyka N, Balda MS, Hauri HP, Matter K (1998) Carbohydrate-mediated Golgi to cell surface transport and apical targeting of membrane proteins. *EMBO J* 17:1919–1929.

Guy-Grand D, Cerf-Bensussan N, Malissen B, Malassis-Seris M, Briottet C, Vassalli P (1991) Two gut intraepithelial CD8+ lymphocyte populations with different T cell receptors: a role for the gut epithelium in T cell differentiation. *J Exp Med* 173:471–481.

Hahn U, Cho A, Schuppan D, Hahn EG, Merker HJ, Riecken EO (1987a) Intestinal epithelial cells preferentially attach to a biomatrix derived from human intestinal mucosa. *Gut* 28 Suppl:153–158.

Hahn U, Schuppan D, Hahn EG, Merker HJ, Riecken EO (1987b) Intestinal cells produce basement membrane proteins in vitro. *Gut* 28 Suppl:143–151.

Hajj HE, Lebrun M, Arold ST, Vial H, Labesse G, Dubremetz JF (2007) ROP18 is a rhoptry kinase controlling the intracellular proliferation of Toxoplasma gondii. *PLoS Pathog* 3:e14.

Haley PJ (2003) Species differences in the structure and function of the immune system. *Toxicology* 188:49–71.

Hall A (1998) Rho GTPases and the actin cytoskeleton. *Science* 279:509–514.

Halonen SK, Weidner E (1994) Overcoating of Toxoplasma parasitophorous vacuoles with host cell vimentin type intermediate filaments. *J Eukaryot Microbiol* 41:65–71.

Hannon GJ, Rossi JJ (2004) Unlocking the potential of the human genome with RNA interference. *Nature* 431:371–378.

Hara T, Honda K, Shitashige M, Ono M, Matsuyama H, Naito K, Hirohashi S, Yamada T (2007) Mass spectrometry analysis of the native protein complex containing actinin-4 in prostate cancer cells. *Mol Cell Proteomics* 6:479–491.

Haskins J, Gu L, Wittchen ES, Hibbard J, Stevenson BR (1998) ZO-3, a novel member of the MAGUK protein family found at the tight junction, interacts with ZO-1 and occludin. *J Cell Biol* 141:199–208.

He Y, Chu SH, Walker WA (1993) Nucleotide supplements alter proliferation and differentiation of cultured human (Caco-2) and rat (IEC-6) intestinal epithelial cells. *J Nutr* 123:1017–1027.

Henning SJ (1995) Gene transfer into the intestinal epithelium. *Advanced Drug Delivery Reviews* 17:341–347.

Hill D, Dubey JP (2002) Toxoplasma gondii: transmission, diagnosis and prevention. *Clin Microbiol Infect* 8:634–640.

Hinck L, Näthke IS, Papkoff J, Nelson WJ (1994) Dynamics of cadherin/catenin complex formation: novel protein interactions and pathways of complex assembly. *J Cell Biol* 125:1327–1340.

Hirai K, Hirato K, Yanagawa R (1966) A cinematographic study of the penetration of cultured cells by Toxoplasma gondii. *Jpn J Vet Res* 14:81–90.

Holmes JL, Itallie CMV, Rasmussen JE, Anderson JM (2006) Claudin profiling in the mouse during postnatal intestinal development and along the gastrointestinal tract reveals complex expression patterns. *Gene Expr Patterns* 6:581–588.

Hooper LV, Macpherson AJ (2010) Immune adaptations that maintain homeostasis with the intestinal microbiota. *Nat Rev Immunol* 10:159–169.

Hornef MW, Normark BH, Vandewalle A, Normark S (2003) Intracellular recognition of lipopolysaccharide by toll-like receptor 4 in intestinal epithelial cells. *J Exp Med* 198:1225–1235.

Hou B, Benson A, Kuzmich L, DeFranco AL, Yarovinsky F (2011) Critical coordination of innate immune defense against Toxoplasma gondii by dendritic cells responding via their Toll-like receptors. *Proc Natl Acad Sci U S A* 108:278–283.

Howe DK, Honoré S, Derouin F, Sibley LD (1997) Determination of genotypes of Toxoplasma gondii strains isolated from patients with toxoplasmosis. *J Clin Microbiol* 35:1411–1414.

Hu K, Roos DS, Murray JM (2002) A novel polymer of tubulin forms the conoid of Toxoplasma gondii. *J Cell Biol* 156:1039–1050.

Huber D, Balda MS, Matter K (2000) Occludin modulates transepithelial migration of neutrophils. *J Biol Chem* 275:5773–5778.

Huynh MH, Carruthers VB (2006) Toxoplasma MIC2 is a major determinant of invasion and virulence. *PLoS Pathog* 2:e84.

Huynh MH, Rabenau KE, Harper JM, Beatty WL, Sibley LD, Carruthers VB (2003) Rapid invasion of host cells by Toxoplasma requires secretion of the MIC2-M2AP adhesive protein complex. *EMBO J* 22:2082–2090.

Hwang IY, Quan JH, Ahn MH, Ahmed HAH, Cha GH, Shin DW, Lee YH (2010) Toxoplasma gondii infection inhibits the mitochondrial apoptosis through induction of Bcl-2 and HSP70. *Parasitol Res* 107:1313–1321.

Håkansson S, Morisaki H, Heuser J, Sibley LD (1999) Time-lapse video microscopy of gliding motility in Toxoplasma gondii reveals a novel, biphasic mechanism of cell locomotion. *Mol Biol Cell* 10:3539–3547.

Hölttä-Vuori M, Tanhuanpää K, Möbius W, Somerharju P, Ikonen E (2002) Modulation of cellular cholesterol transport and homeostasis by Rab11. *Mol Biol Cell* 13:3107–3122.

Ikenouchi J, Furuse M, Furuse K, Sasaki H, Tsukita S, Tsukita S (2005) Tricellulin constitutes a novel barrier at tricellular contacts of epithelial cells. *J Cell Biol* 171:939–945.

Ikenouchi J, Sasaki H, Tsukita S, Furuse M, Tsukita S (2008) Loss of occludin affects tricellular localization of tricellulin. *Mol Biol Cell* 19:4687–4693.

Inagaki-Ohara K, Dewi FN, Hisaeda H, Smith AL, Jimi F, Miyahira M, Abdel-Aleem ASF, Horii Y, Nawa Y (2006) Intestinal intraepithelial lymphocytes sustain the epithelial barrier function against Eimeria vermiformis infection. *Infect Immun* 74:5292–5301.

Inagaki-Ohara K, Sawaguchi A, Suganuma T, Matsuzaki G, Nawa Y (2005) Intraepithelial lymphocytes express junctional molecules in murine small intestine. *Biochem Biophys Res Commun* 331:977–983.

Ismael AB, Sekkai D, Collin C, Bout D, Mévélec MN (2003) The MIC3 gene of Toxoplasma gondii is a novel potent vaccine candidate against toxoplasmosis. *Infect Immun* 71:6222–6228.

Ismail AS, Behrendt CL, Hooper LV (2009) Reciprocal interactions between commensal bacteria and gamma delta intraepithelial lymphocytes during mucosal injury. *J Immunol* 182:3047–3054.

Itallie CMV, Anderson JM (1997) Occludin confers adhesiveness when expressed in fibroblasts. *J Cell Sci* 110 (Pt 9):1113–1121.

Itallie CV, Rahner C, Anderson JM (2001) Regulated expression of claudin-4 decreases paracellular conductance through a selective decrease in sodium permeability. *J Clin Invest* 107:1319–1327.

Itallie CMV, Fanning AS, Bridges A, Anderson JM (2009) ZO-1 stabilizes the tight junction solute barrier through coupling to the perijunctional cytoskeleton. *Mol Biol Cell* 20:3930–3940.

Itallie CMV, Fanning AS, Holmes J, Anderson JM (2010) Occludin is required for cytokine-induced regulation of tight junction barriers. *J Cell Sci* 123:2844–2852.

Itallie CMV, Holmes J, Bridges A, Gookin JL, Coccaro MR, Proctor W, Colegio OR, Anderson JM (2008) The density of small tight junction pores varies among cell types and is increased by expression of claudin-2. *J Cell Sci* 121:298–305.

Itallie CMV, Mitic LL, Anderson JM (2011) Claudin-2 forms homodimers and is a component of a high molecular weight protein complex. *J Biol Chem* 286:3442–3450.

Itoh M, Furuse M, Morita K, Kubota K, Saitou M, Tsukita S (1999) Direct binding of three tight junction-associated MAGUKs, ZO-1, ZO-2, and ZO-3, with the COOH termini of claudins. *J Cell Biol* 147:1351–1363.

Itoh M, Morita K, Tsukita S (1999) Characterization of ZO-2 as a MAGUK family member associated with tight as well as adherens junctions with a binding affinity to occludin and alpha catenin. *J Biol Chem* 274:5981–5986.

Ivanov AI, Nusrat A, Parkos CA (2004) Endocytosis of epithelial apical junctional proteins by a clathrin-mediated pathway into a unique storage compartment. *Mol Biol Cell* 15:176–188.

Jacquet A, Coulon L, Nève JD, Daminet V, Haumont M, Garcia L, Bollen A, Jurado M, Biemans R (2001) The surface antigen SAG3 mediates the attachment of Toxoplasma gondii to cell-surface proteoglycans. *Mol Biochem Parasitol* 116:35–44.

Jain S, Suzuki T, Seth A, Samak G, Rao R (2011) PKCzeta phosphorylates occludin and promotes assembly of epithelial tight junctions. *Biochem J* .

Jan G, Delorme V, Saksouk N, Abrivard M, Gonzalez V, Cayla X, Hakimi MA, Tardieux I (2009) A Toxoplasma type 2C serine-threonine phosphatase is involved in parasite growth in the mammalian host cell. *Microbes Infect* 11:935–945.

Jepson MA, Collares-Buzato CB, Clark MA, Hirst BH, Simmons NL (1995) Rapid disruption of epithelial barrier function by Salmonella typhimurium is associated with structural modification of intercellular junctions. *Infect Immun* 63:356–359.

Jerome ME, Radke JR, Bohne W, Roos DS, White MW (1998) Toxoplasma gondii bradyzoites form spontaneously during sporozoite-initiated development. *Infect Immun* 66:4838–4844.

Johansson MEV, Phillipson M, Petersson J, Velcich A, Holm L, Hansson GC (2008) The inner of the two Muc2 mucin-dependent mucus layers in colon is devoid of bacteria. *Proc Natl Acad Sci U S A* 105:15064–15069.

Jongert E, Melkebeek V, Craeye SD, Dewit J, Verhelst D, Cox E (2008) An enhanced GRA1-GRA7 cocktail DNA vaccine primes anti-Toxoplasma immune responses in pigs. *Vaccine* 26:1025–1031.

Jou TS, Schneeberger EE, Nelson WJ (1998) Structural and functional regulation of tight junctions by RhoA and Rac1 small GTPases. *J Cell Biol* 142:101–115.

Ju CH, Chockalingam A, Leifer CA (2009) Early response of mucosal epithelial cells during Toxoplasma gondii infection. *J Immunol* 183:7420–7427.

Kafsack BFC, Pena JDO, Coppens I, Ravindran S, Boothroyd JC, Carruthers VB (2009) Rapid membrane disruption by a perforin-like protein facilitates parasite exit from host cells. *Science* 323:530–533.

Kale G, Naren AP, Sheth P, Rao RK (2003) Tyrosine phosphorylation of occludin attenuates its interactions with ZO-1, ZO-2, and ZO-3. *Biochem Biophys Res Commun* 302:324–329.

Kanaya T, Miyazawa K, Takakura I, Itani W, Watanabe K, Ohwada S, Kitazawa H, Rose MT, McConochie HR, Okano H, Yamaguchi T, Aso H (2008) Differentiation of a murine intestinal epithelial cell line (MIE) toward the M cell lineage. *Am J Physiol Gastrointest Liver Physiol* 295:G273–G284.

Kasper CA, Sorg I, Schmutz C, Tschon T, Wischnewski H, Kim ML, Arrieumerlou C (2010) Cell-cell propagation of NF-κB transcription factor and MAP kinase activation amplifies innate immunity against bacterial infection. *Immunity* 33:804–816.

Kedinger M, Duluc I, Fritsch C, Lorentz O, Plateroti M, Freund JN (1998) Intestinal epithelial-mesenchymal cell interactions. *Ann N Y Acad Sci* 859:1–17.

Kelly MN, Kolls JK, Happel K, Schwartzman JD, Schwarzenberger P, Combe C, Moretto M, Khan IA (2005) Interleukin-17/interleukin-17 receptor-mediated signaling is important for generation of an optimal polymorphonuclear response against Toxoplasma gondii infection. *Infect Immun* 73:617–621.

Kernéis S, Bogdanova A, Kraehenbuhl JP, Pringault E (1997) Conversion by Peyer's patch lymphocytes of human enterocytes into M cells that transport bacteria. *Science* 277:949–952.

Khan IA, Thomas SY, Moretto MM, Lee FS, Islam SA, Combe C, Schwartzman JD, Luster AD (2006) CCR5 is essential for NK cell trafficking and host survival following Toxoplasma gondii infection. *PLoS Pathog* 2:e49.

Kijlstra A, Jongert E (2008) Control of the risk of human toxoplasmosis transmitted by meat. *Int J Parasitol* 38:1359–1370.

Kim SH, Li Z, Sacks DB (2000) E-cadherin-mediated cell-cell attachment activates Cdc42. *J Biol Chem* 275:36999–37005.

Kim YS, Ho SB (2010) Intestinal goblet cells and mucins in health and disease: recent insights and progress. *Curr Gastroenterol Rep* 12:319–330.

Kimura Y, Shiozaki H, Hirao M, Maeno Y, Doki Y, Inoue M, Monden T, Ando-Akatsuka Y, Furuse M, Tsukita S, Monden M (1997) Expression of occludin, tight-junction-associated protein, in human digestive tract. *Am J Pathol* 151:45–54.

Knudsen KA, Wheelock MJ (1992) Plakoglobin, or an 83-kD homologue distinct from beta-catenin, interacts with E-cadherin and N-cadherin. *J Cell Biol* 118:671–679.

Kojima T, Sawada N, Chiba H, Kokai Y, Yamamoto M, Urban M, Lee GH, Hertzberg EL, Mochizuki Y, Spray DC (1999) Induction of tight junctions in human connexin 32 (hCx32)-transfected mouse hepatocytes: connexin 32 interacts with occludin. *Biochem Biophys Res Commun* 266:222–229.

Kojima T, ichi Takano K, Yamamoto T, Murata M, Son S, Imamura M, Yamaguchi H, Osanai M, Chiba H, Himi T, Sawada N (2008) Transforming growth factor-beta induces epithelial to mesenchymal transition by down-regulation of claudin-1 expression and the fence function in adult rat hepatocytes. *Liver Int* 28:534–545.

Komano H, Fujiura Y, Kawaguchi M, Matsumoto S, Hashimoto Y, Obana S, Mombaerts P, Tonegawa S, Yamamoto H, Itohara S (1995) Homeostatic regulation of intestinal epithelia by intraepithelial gamma delta T cells. *Proc Natl Acad Sci U S A* 92:6147–6151.

Koshy AA, Fouts AE, Lodoen MB, Alkan O, Blau HM, Boothroyd JC (2010) Toxoplasma secreting Cre recombinase for analysis of host-parasite interactions. *Nat Methods* 7:307–309.

Kowalik S, Clauss W, Zahner H (2004) Toxoplasma gondii: changes of transepithelial ion transport in infected HT29/B6 cell monolayers. *Parasitol Res* 92:152–158.

Krug SM, Amasheh S, Richter JF, Milatz S, Günzel D, Westphal JK, Huber O, Schulzke JD, Fromm M (2009) Tricellulin forms a barrier to macromolecules in tricellular tight junctions without affecting ion permeability. *Mol Biol Cell* 20:3713–3724.

Kucharzik T, Walsh SV, Chen J, Parkos CA, Nusrat A (2001) Neutrophil transmigration in inflammatory bowel disease is associated with differential expression of epithelial intercellular junction proteins. *Am J Pathol* 159:2001–2009.

Kumar NM, Gilula NB (1996) The gap junction communication channel. *Cell* 84:381–388.

Kurrey NK, K A, Bapat SA (2005) Snail and Slug are major determinants of ovarian cancer invasiveness at the transcription level. *Gynecol Oncol* 97:155–165.

Lacaz-Vieira F, Jaeger MM, Farshori P, Kachar B (1999) Small synthetic peptides homologous to segments of the first external loop of occludin impair tight junction resealing. *J Membr Biol* 168:289–297.

Ladd AN, Charlet N, Cooper TA (2001) The CELF family of RNA binding proteins is implicated in cell-specific and developmentally regulated alternative splicing. *Mol Cell Biol* 21:1285–1296.

Lafferty KD (2006) Can the common brain parasite, Toxoplasma gondii, influence human culture? *Proc Biol Sci* 273:2749–2755.

Laffont S, Powrie F (2009) Immunology: Dendritic-cell genealogy. *Nature* 462:732–733.

Lagal V, Binder EM, Huynh MH, Kafsack BFC, Harris PK, Diez R, Chen D, Cole RN, Carruthers VB, Kim K (2010) Toxoplasma gondii protease TgSUB1 is required for cell surface processing of micronemal adhesive complexes and efficient adhesion of tachyzoites. *Cell Microbiol* 12:1792–1808.

Lam SK (1993) Epidemiology and genetics of peptic ulcer. *Gastroenterol Jpn* 28 Suppl 5:145–157.

Lamarque M, Besteiro S, Papoin J, Roques M, Normand BVL, Morlon-Guyot J, Dubremetz JF, Fauquenoy S, Tomavo S, Faber BW, Kocken CH, Thomas AW, Boulanger MJ, Bentley GA, Lebrun M (2011) The RON2-AMA1 interaction is a critical step in moving junction-dependent invasion by apicomplexan parasites. *PLoS Pathog* 7:e1001276.

Lambert H, Hitziger N, Dellacasa I, Svensson M, Barragan A (2006) Induction of dendritic cell migration upon Toxoplasma gondii infection potentiates parasite dissemination. *Cell Microbiol* 8:1611–1623.

Lambert H, Vutova PP, Adams WC, Loré K, Barragan A (2009) The Toxoplasma gondii-shuttling function of dendritic cells is linked to the parasite genotype. *Infect Immun* 77:1679–1688.

Lammert E, Stevanović S, Brunner J, Rammensee HG, Schild H (1997) Protein disulfide isomerase is the dominant acceptor for peptides translocated into the endoplasmic reticulum. *Eur J Immunol* 27:1685–1690.

Lapierre LA, Tuma PL, Navarre J, Goldenring JR, Anderson JM (1999) VAP-33 localizes to both an intracellular vesicle population and with occludin at the tight junction. *J Cell Sci* 112 (Pt 21):3723–3732.

Lau C, Lytle C, Straus DS, DeFea KA (2011) Apical and basolateral pools of proteinase-activated receptor-2 direct distinct signaling events in the intestinal epithelium. *Am J Physiol Cell Physiol* 300:C113–C123.

Lecollinet S, Gavard F, Havenga MJE, Spiller OB, Lemckert A, Goudsmit J, Eloit M, Richardson J (2006) Improved gene delivery to intestinal mucosa by adenoviral vectors bearing subgroup B and d fibers. *J Virol* 80:2747–2759.

Lee YH, Ely KH, Lepage A, Kasper LH (1999) Interleukin-15 enhances host protection against acute Toxoplasma gondii infection in T-cell receptor alpha-/-deficient mice. *Parasite Immunol* 21:299–306.

Lefrançois-Martinez AM, Diaz-Guerra MJ, Vallet V, Kahn A, Antoine B (1994) Glucose-dependent regulation of the L-pyruvate kinase gene in a hepatoma cell line is independent of insulin and cyclic AMP. *FASEB J* 8:89–96.

Lei Y, Davey M, Ellis JT (2005) Attachment and invasion of Toxoplasma gondii and Neospora caninum to epithelial and fibroblast cell lines in vitro. *Parasitology* 131:583–590.

Lekutis C, Ferguson DJ, Grigg ME, Camps M, Boothroyd JC (2001) Surface antigens of Toxoplasma gondii: variations on a theme. *Int J Parasitol* 31:1285–1292.

Lemmers C, Michel D, Lane-Guermonprez L, Delgrossi MH, Médina E, Arsanto JP, Bivic AL (2004) CRB3 binds directly to Par6 and regulates the morphogenesis of the tight junctions in mammalian epithelial cells. *Mol Biol Cell* 15:1324–1333.

Leonard F, Collnot EM, Lehr CM (2010) A three-dimensional coculture of enterocytes, monocytes and dendritic cells to model inflamed intestinal mucosa in vitro. *Mol Pharm* 7:2103–2119.

Lepage AC, Buzoni-Gatel D, Bout DT, Kasper LH (1998) Gut-derived intraepithelial lymphocytes induce long term immunity against Toxoplasma gondii. *J Immunol* 161:4902–4908.

Li X, Deng W, Nail CD, Bailey SK, Kraus MH, Ruppert JM, Lobo-Ruppert SM (2006) Snail induction is an early response to Gli1 that determines the efficiency of epithelial transformation. *Oncogene* 25:609–621.

Li Y, Fanning AS, Anderson JM, Lavie A (2005) Structure of the conserved cytoplasmic C-terminal domain of occludin: identification of the ZO-1 binding surface. *J Mol Biol* 352:151–164.

Lie PPY, Xia W, Wang CQF, Mruk DD, Yan HHN, hang Wong C, Lee WM, Cheng CY (2006) Dynamin II interacts with the cadherin- and occludin-based protein complexes at the blood-testis barrier in adult rat testes. *J Endocrinol* 191:571–586.

Lindström I, Sundar N, Lindh J, Kironde F, Kabasa JD, Kwok OCH, Dubey JP, Smith JE (2008) Isolation and genotyping of Toxoplasma gondii from Ugandan chickens reveals frequent multiple infections. *Parasitology* 135:39–45.

Liu S, Kuo W, Yang W, Liu W, Gibson GA, Dorko K, Watkins SC, Strom SC, Wang T (2010) The second extracellular loop dictates Occludin-mediated HCV entry. *Virology* 407:160–170.

Lourenço EV, Pereira SR, Faça VM, Coelho-Castelo AA, Mineo JR, Roque-Barreira MC, Greene LJ, Panunto-Castelo A (2001) Toxoplasma gondii micronemal protein MIC1 is a lactose-binding lectin. *Glycobiology* 11:541–547.

Lourenço EV, Bernardes ES, Silva NM, Mineo JR, Panunto-Castelo A, Roque-Barreira MC (2006) Immunization with MIC1 and MIC4 induces protective immunity against Toxoplasma gondii. *Microbes Infect* 8:1244–1251.

Lovett JL, Sibley LD (2003) Intracellular calcium stores in Toxoplasma gondii govern invasion of host cells. *J Cell Sci* 116:3009–3016.

Luangsay S, Kasper LH, Rachinel N, Minns LA, Mennechet FJD, Vandewalle A, Buzoni-Gatel D (2003) CCR5 mediates specific migration of Toxoplasma gondii-primed CD8 lymphocytes to inflammatory intestinal epithelial cells. *Gastroenterology* 125:491–500.

Lui WY, Lee WM (2005) cAMP perturbs inter-Sertoli tight junction permeability barrier in vitro via its effect on proteasome-sensitive ubiquitination of occludin. *J Cell Physiol* 203:564–572.

Lytton SD, Fischer W, Nagel W, Haas R, Beck FX (2005) Production of ammonium by Helicobacter pylori mediates occludin processing and disruption of tight junctions in Caco-2 cells. *Microbiology* 151:3267–3276.

Ma TY, Iwamoto GK, Hoa NT, Akotia V, Pedram A, Boivin MA, Said HM (2004) TNF-alpha-induced increase in intestinal epithelial tight junction permeability requires NF-kappa B activation. *Am J Physiol Gastrointest Liver Physiol* 286:G367–G376.

Macartney KK, Baumgart DC, Carding SR, Brubaker JO, Offit PA (2000) Primary murine small intestinal epithelial cells, maintained in long-term culture, are susceptible to rotavirus infection. *J Virol* 74:5597–5603.

MacDonald TT (2003) The mucosal immune system. *Parasite Immunol* 25:235–246.

Macpherson AJ, Gatto D, Sainsbury E, Harriman GR, Hengartner H, Zinkernagel RM (2000) A primitive T cell-independent mechanism of intestinal mucosal IgA responses to commensal bacteria. *Science* 288:2222–2226.

Macpherson AJ, Harris NL (2004) Interactions between commensal intestinal bacteria and the immune system. *Nat Rev Immunol* 4:478–485.

Madara JL (1990) Maintenance of the macromolecular barrier at cell extrusion sites in intestinal epithelium: physiological rearrangement of tight junctions. *J Membr Biol* 116:177–184.

Madara JL, Dharmsathaphorn K (1985) Occluding junction structure-function relationships in a cultured epithelial monolayer. *J Cell Biol* 101:2124–2133.

Makarova O, Roh MH, Liu CJ, Laurinec S, Margolis B (2003) Mammalian Crumbs3 is a small transmembrane protein linked to protein associated with Lin-7 (Pals1). *Gene* 302:21–29.

Mandel R, Ryser HJ, Ghani F, Wu M, Peak D (1993) Inhibition of a reductive function of the plasma membrane by bacitracin and antibodies against protein disulfide-isomerase. *Proc Natl Acad Sci U S A* 90:4112–4116.

Manger ID, Hehl AB, Boothroyd JC (1998) The surface of Toxoplasma tachyzoites is dominated by a family of glycosylphosphatidylinositol-anchored antigens related to SAG1. *Infect Immun* 66:2237–2244.

Mankertz J, Tavalali S, Schmitz H, Mankertz A, Riecken EO, Fromm M, Schulzke JD (2000) Expression from the human occludin promoter is affected by tumor necrosis factor alpha and interferon gamma. *J Cell Sci* 113 (Pt 11):2085–2090.

Mankertz J, Waller JS, Hillenbrand B, Tavalali S, Florian P, Schöneberg T, Fromm M, Schulzke JD (2002) Gene expression of the tight junction protein occludin includes differential splicing and alternative promoter usage. *Biochem Biophys Res Commun* 298:657–666.

Marchiando AM, Shen L, Graham WV, Edelblum KL, Duckworth CA, Guan Y, Montrose MH, Turner JR, Watson AJM (2011) The epithelial barrier is maintained by in vivo tight junction expansion during pathologic intestinal epithelial shedding. *Gastroenterology* 140:1208–1218.e2.

Marchiando AM, Shen L, Graham WV, Weber CR, Schwarz BT, Austin JR, Raleigh DR, Guan Y, Watson AJM, Montrose MH, Turner JR (2010) Caveolin-1-dependent occludin endocytosis is required for TNF-induced tight junction regulation in vivo. *J Cell Biol* 189:111–126.

Marlin SD, Springer TA (1987) Purified intercellular adhesion molecule-1 (ICAM-1) is a ligand for lymphocyte function-associated antigen 1 (LFA-1). *Cell* 51:813–819.

Marshman E, Booth C, Potten CS (2002) The intestinal epithelial stem cell. *Bioessays* 24:91–98.

Martin AM, Liu T, Lynn BC, Sinai AP (2007) The Toxoplasma gondii parasitophorous vacuole membrane: transactions across the border. *J Eukaryot Microbiol* 54:25–28.

Martin V, Supanitsky A, Echeverria PC, Litwin S, Tanos T, Roodt ARD, Guarnera EA, Angel SO (2004) Recombinant GRA4 or ROP2 protein combined with alum or the gra4 gene provides partial protection in chronic murine models of toxoplasmosis. *Clin Diagn Lab Immunol* 11:704–710.

Martìn-Padura I, Lostaglio S, Schneemann M, Williams L, Romano M, Fruscella P, Panzeri C, Stoppacciaro A, Ruco L, Villa A, Simmons D, Dejana E (1998) Junctional adhesion molecule, a novel member of the immunoglobulin superfamily that distributes at intercellular junctions and modulates monocyte transmigration. *J Cell Biol* 142:117–127.

Massey-Harroche D (2000) Epithelial cell polarity as reflected in enterocytes. *Microsc Res Tech* 49:353–362.

Matsuda M, Kubo A, Furuse M, Tsukita S (2004) A peculiar internalization of claudins, tight junction-specific adhesion molecules, during the intercellular movement of epithelial cells. *J Cell Sci* 117:1247–1257.

Matter K, Balda MS (1998) Biogenesis of tight junctions: the C-terminal domain of occludin mediates basolateral targeting. *J Cell Sci* 111 (Pt 4):511–519.

Matter K, Balda MS (2003) Functional analysis of tight junctions. *Methods* 30:228–234.

McCaffrey G, Seelbach MJ, Staatz WD, Nametz N, Quigley C, Campos CR, Brooks TA, Davis TP (2008) Occludin oligomeric assembly at tight junctions of the blood-brain barrier is disrupted by peripheral inflammatory hyperalgesia. *J Neurochem* 106:2395–2409.

McCaffrey G, Staatz WD, Quigley CA, Nametz N, Seelbach MJ, Campos CR, Brooks TA, Egleton RD, Davis TP (2007) Tight junctions contain oligomeric protein assembly critical for maintaining blood-brain barrier integrity in vivo. *J Neurochem* .

McCaffrey G, Willis CL, Staatz WD, Nametz N, Quigley CA, Hom S, Lochhead JJ, Davis TP (2009) Occludin oligomeric assemblies at tight junctions of the blood-brain barrier are altered by hypoxia and reoxygenation stress. *J Neurochem* 110:58–71.

McCarthy KM, Skare IB, Stankewich MC, Furuse M, Tsukita S, Rogers RA, Lynch RD, Schneeberger EE (1996) Occludin is a functional component of the tight junction. *J Cell Sci* 109 (Pt 9):2287–2298.

McDermott JR, Bartram RE, Knight PA, Miller HRP, Garrod DR, Grencis RK (2003) Mast cells disrupt epithelial barrier function during enteric nematode infection. *Proc Natl Acad Sci U S A* 100:7761–7766.

McKee AS, Dzierszinski F, Boes M, Roos DS, Pearce EJ (2004) Functional inactivation of immature dendritic cells by the intracellular parasite Toxoplasma gondii. *J Immunol* 173:2632–2640.

McKenzie JAG, Riento K, Ridley AJ (2006) Casein kinase I epsilon associates with and phosphorylates the tight junction protein occludin. *FEBS Lett* 580:2388–2394.

McNeil E, Capaldo CT, Macara IG (2006) Zonula occludens-1 function in the assembly of tight junctions in Madin-Darby canine kidney epithelial cells. *Mol Biol Cell* 17:1922–1932.

Medina R, Rahner C, Mitic LL, Anderson JM, Itallie CMV (2000) Occludin localization at the tight junction requires the second extracellular loop. *J Membr Biol* 178:235–247.

Meek B, Back JW, Klaren VNA, Speijer D, Peek R (2002a) Conserved regions of protein disulfide isomerase are targeted by natural IgA antibodies in humans. *Int Immunol* 14:1291–1301.

Meek B, Back JW, Klaren VNA, Speijer D, Peek R (2002b) Protein disulfide isomerase of Toxoplasma gondii is targeted by mucosal IgA antibodies in humans. *FEBS Lett* 522:104–108.

Meissner M, Reiss M, Viebig N, Carruthers VB, Toursel C, Tomavo S, Ajioka JW, Soldati D (2002) A family of transmembrane microneme proteins of Toxoplasma gondii contain EGF-like domains and function as escorters. *J Cell Sci* 115:563–574.

Mellitzer G, Beucher A, Lobstein V, Michel P, Robine S, Kedinger M, Gradwohl G (2010) Loss of enteroendocrine cells in mice alters lipid absorption and glucose homeostasis and impairs postnatal survival. *J Clin Invest* 120:1708–1721.

Mennechet FJD, Kasper LH, Rachinel N, Li W, Vandewalle A, Buzoni-Gatel D (2002) Lamina propria CD4+ T lymphocytes synergize with murine intestinal epithelial cells to enhance proinflammatory response against an intracellular pathogen. *J Immunol* 168:2988–2996.

Mestas J, Hughes CCW (2004) Of Mice and Not Men: Differences between Mouse and Human Immunology. *The Journal of Immunology* 172:2731–2738.

Michta ML, Hopcraft SE, Narbus CM, Kratovac Z, Israelow B, Sourisseau M, Evans MJ (2010) Species-specific regions of occludin required by hepatitis C virus for cell entry. *J Virol* 84:11696–11708.

Miller CM, Boulter NR, Ikin RJ, Smith NC (2009) The immunobiology of the innate response to Toxoplasma gondii. *Int J Parasitol* 39:23–39.

Miller DG, Adam MA, Miller AD (1990) Gene transfer by retrovirus vectors occurs only in cells that are actively replicating at the time of infection. *Mol Cell Biol* 10:4239–4242.

Miller H, Zhang J, Kuolee R, Patel GB, Chen W (2007) Intestinal M cells: the fallible sentinels? *World J Gastroenterol* 13:1477–1486.

Miller SA, Thathy V, Ajioka JW, Blackman MJ, Kim K (2003) TgSUB2 is a Toxoplasma gondii rhoptry organelle processing proteinase. *Mol Microbiol* 49:883–894.

Mineo JR, McLeod R, Mack D, Smith J, Khan IA, Ely KH, Kasper LH (1993) Antibodies to Toxoplasma gondii major surface protein (SAG-1, P30) inhibit infection of host cells and are produced in murine intestine after peroral infection. *J Immunol* 150:3951–3964.

Minns LA, Menard LC, Foureau DM, Darche S, Ronet C, Mielcarz DW, Buzoni-Gatel D, Kasper LH (2006) TLR9 is required for the gut-associated lymphoid tissue response following oral infection of Toxoplasma gondii. *J Immunol* 176:7589–7597.

Miyaji-Yamaguchi M, Kato K, Nakano R, Akashi T, Kikuchi A, Nagata K (2003) Involvement of nucleocytoplasmic shuttling of yeast Nap1 in mitotic progression. *Mol Cell Biol* 23:6672–6684.

Molestina RE, El-Guendy N, Sinai AP (2008) Infection with Toxoplasma gondii results in dysregulation of the host cell cycle. *Cell Microbiol* 10:1153–1165.

Molestina RE, Payne TM, Coppens I, Sinai AP (2003) Activation of NF-kappaB by Toxoplasma gondii correlates with increased expression of antiapoptotic genes and localization of phosphorylated IkappaB to the parasitophorous vacuole membrane. *J Cell Sci* 116:4359–4371.

Monteiro VG, Soares CP, de Souza W (1998) Host cell surface sialic acid residues are involved on the process of penetration of Toxoplasma gondii into mammalian cells. *FEMS Microbiol Lett* 164:323–327.

Mordue DG, Desai N, Dustin M, Sibley LD (1999) Invasion by Toxoplasma gondii establishes a moving junction that selectively excludes host cell plasma membrane proteins on the basis of their membrane anchoring. *J Exp Med* 190:1783–1792.

Moretto MM, Weiss LM, Combe CL, Khan IA (2007) IFN-gamma-producing dendritic cells are important for priming of gut intraepithelial lymphocyte response against intracellular parasitic infection. *J Immunol* 179:2485–2492.

Morgan L, Shah B, Rivers LE, Barden L, Groom AJ, Chung R, Higazi D, Desmond H, Smith T, Staddon JM (2007) Inflammation and dephosphorylation of the tight junction protein occludin in an experimental model of multiple sclerosis. *Neuroscience* 147:664–673.

Morgenstern JP, Land H (1990) Advanced mammalian gene transfer: high titre retroviral vectors with multiple drug selection markers and a complementary helper-free packaging cell line. *Nucleic Acids Res* 18:3587–3596.

Morimoto S, Nishimura N, Terai T, Manabe S, Yamamoto Y, Shinahara W, Miyake H, Tashiro S, Shimada M, Sasaki T (2005) Rab13 mediates the continuous endocytic recycling of occludin to the cell surface. *J Biol Chem* 280:2220–2228.

Morisaki JH, Heuser JE, Sibley LD (1995) Invasion of Toxoplasma gondii occurs by active penetration of the host cell. *J Cell Sci* 108 (Pt 6):2457–2464.

Morita K, Furuse M, Fujimoto K, Tsukita S (1999) Claudin multigene family encoding four-transmembrane domain protein components of tight junction strands. *Proc Natl Acad Sci U S A* 96:511–516.

Morris EJ, Michaud WA, Ji JY, Moon NS, Rocco JW, Dyson NJ (2006) Functional identification of Api5 as a suppressor of E2F-dependent apoptosis in vivo. *PLoS Genet* 2:e196.

Moser LA, Carter M, Schultz-Cherry S (2007) Astrovirus increases epithelial barrier permeability independently of viral replication. *J Virol* 81:11937–11945.

Moudy R, Manning TJ, Beckers CJ (2001) The loss of cytoplasmic potassium upon host cell breakdown triggers egress of Toxoplasma gondii. *J Biol Chem* 276:41492–41501.

Mounier J, Vasselon T, Hellio R, Lesourd M, Sansonetti PJ (1992) Shigella flexneri enters human colonic Caco-2 epithelial cells through the basolateral pole. *Infect Immun* 60:237–248.

Mrsny RJ, Brown GT, Gerner-Smidt K, Buret AG, Meddings JB, Quan C, Koval M, Nusrat A (2008) A key claudin extracellular loop domain is critical for epithelial barrier integrity. *Am J Pathol* 172:905–915.

Mun HS, Aosai F, Norose K, Chen M, Hata H, Tagawa YI, Iwakura Y, Byun DS, Yano A (2000) Toxoplasma gondii Hsp70 as a danger signal in toxoplasma gondii-infected mice. *Cell Stress Chaperones* 5:328–335.

Mun HS, Aosai F, Norose K, Chen M, Piao LX, Takeuchi O, Akira S, Ishikura H, Yano A (2003) TLR2 as an essential molecule for protective immunity against Toxoplasma gondii infection. *Int Immunol* 15:1081–1087.

Murakami T, Felinski EA, Antonetti DA (2009) Occludin phosphorylation and ubiquitination regulate tight junction trafficking and vascular endothelial growth factor-induced permeability. *J Biol Chem* 284:21036–21046.

Muresan Z, Paul DL, Goodenough DA (2000) Occludin 1B, a variant of the tight junction protein occludin. *Mol Biol Cell* 11:627–634.

Musil LS, Le AC, VanSlyke JK, Roberts LM (2000) Regulation of connexin degradation as a mechanism to increase gap junction assembly and function. *J Biol Chem* 275:25207–25215.

Muza-Moons MM, Schneeberger EE, Hecht GA (2004) Enteropathogenic Escherichia coli infection leads to appearance of aberrant tight junctions strands in the lateral membrane of intestinal epithelial cells. *Cell Microbiol* 6:783–793.

Muñoz M, Heimesaat MM, Danker K, Struck D, Lohmann U, Plickert R, Bereswill S, Fischer A, Dunay IR, Wolk K, Loddenkemper C, Krell HW, Libert C, Lund LR, Frey O, Hölscher C, Iwakura Y, Ghilardi N, Ouyang W, Kamradt T, Sabat R, Liesenfeld O (2009) Interleukin (IL)-23 mediates Toxoplasma gondii-induced immunopathology in the gut via matrixmetalloproteinase-2 and IL-22 but independent of IL-17. *J Exp Med* 206:3047–3059.

Mévélec MN, Ducournau C, Ismael AB, Olivier M, Sèche E, Lebrun M, Bout D, Dimier-Poisson I (2010) Mic1-3 Knockout Toxoplasma gondii is a good candidate for a vaccine against T. gondii-induced abortion in sheep. *Vet Res* 41:49.

Müller SL, Portwich M, Schmidt A, Utepbergenov DI, Huber O, Blasig IE, Krause G (2005) The tight junction protein occludin and the adherens junction protein alpha-catenin share a common interaction mechanism with ZO-1. *J Biol Chem* 280:3747–3756.

Naguleswaran A, Alaeddine F, Guionaud C, Vonlaufen N, Sonda S, Jenoe P, Mevissen M, Hemphill A (2005) Neospora caninum protein disulfide isomerase is involved in tachyzoite-host cell interaction. *Int J Parasitol* 35:1459–1472.

Nakatsuji H, Nishimura N, Yamamura R, Kanayama HO, Sasaki T (2008) Involvement of actinin-4 in the recruitment of JRAB/MICAL-L2 to cell-cell junctions and the formation of functional tight junctions. *Mol Cell Biol* 28:3324–3335.

Nam HW (2009) GRA proteins of Toxoplasma gondii: maintenance of host-parasite interactions across the parasitophorous vacuolar membrane. *Korean J Parasitol* 47 Suppl:S29–S37.

Nash S, Stafford J, Madara JL (1987) Effects of polymorphonuclear leukocyte transmigration on the barrier function of cultured intestinal epithelial monolayers. *J Clin Invest* 80:1104–1113.

Nava P, López S, Arias CF, Islas S, González-Mariscal L (2004) The rotavirus surface protein VP8 modulates the gate and fence function of tight junctions in epithelial cells. *J Cell Sci* 117:5509–5519.

Nigam SK, Rodriguez-Boulan E, Silver RB (1992) Changes in intracellular calcium during the development of epithelial polarity and junctions. *Proc Natl Acad Sci U S A* 89:6162–6166.

Ning Y, Manegold PC, Hong YK, Zhang W, Pohl A, Lurje G, Winder T, Yang D, Labonte MJ, Wilson PM, Ladner RD, Lenz HJ (2010) Interleukin-8 is associated with proliferation, migration, angiogenesis

and chemosensitivity in vitro and in vivo in colon cancer cell line models. *Int J Cancer* .

Nishimura M, Kakizaki M, Ono Y, Morimoto K, Takeuchi M, Inoue Y, Imai T, Takai Y (2002) JEAP, a novel component of tight junctions in exocrine cells. *J Biol Chem* 277:5583–5587.

Nissapatorn V (2009) Toxoplasmosis in HIV/AIDS: a living legacy. *Southeast Asian J Trop Med Public Health* 40:1158–1178.

Noel RA, Shukla P, Henning SJ (1994) Optimization of gene transfer into intestinal epithelial cells using a retroviral vector. *J Pediatr Gastroenterol Nutr* 19:43–49.

Nunbhakdi-Craig V, Machleidt T, Ogris E, Bellotto D, White CL, Sontag E (2002) Protein phosphatase 2A associates with and regulates atypical PKC and the epithelial tight junction complex. *J Cell Biol* 158:967–978.

Nusrat A, Chen JA, Foley CS, Liang TW, Tom J, Cromwell M, Quan C, Mrsny RJ (2000) The coiled-coil domain of occludin can act to organize structural and functional elements of the epithelial tight junction. *J Biol Chem* 275:29816–29822.

Nusrat A, von Eichel-Streiber C, Turner JR, Verkade P, Madara JL, Parkos CA (2001) Clostridium difficile toxins disrupt epithelial barrier function by altering membrane microdomain localization of tight junction proteins. *Infect Immun* 69:1329–1336.

Nusrat A, Brown GT, Tom J, Drake A, Bui TTT, Quan C, Mrsny RJ (2005) Multiple protein interactions involving proposed extracellular loop domains of the tight junction protein occludin. *Mol Biol Cell* 16:1725–1734.

Ogura Y, Bonen DK, Inohara N, Nicolae DL, Chen FF, Ramos R, Britton H, Moran T, Karaliuskas R, Duerr RH, Achkar JP, Brant SR, Bayless TM, Kirschner BS, Hanauer SB, Nuñez G, Cho JH (2001) A frameshift mutation in NOD2 associated with susceptibility to Crohn's disease. *Nature* 411:603–606.

O'Hara AM, Shanahan F (2006) The gut flora as a forgotten organ. *EMBO Rep* 7:688–693.

Ohkubo T, Ozawa M (2004) The transcription factor Snail downregulates the tight junction components independently of E-cadherin downregulation. *J Cell Sci* 117:1675–1685.

Ortega-Barria E, Boothroyd JC (1999) A Toxoplasma lectin-like activity specific for sulfated polysaccharides is involved in host cell infection. *J Biol Chem* 274:1267–1276.

Osanai M, Murata M, Nishikiori N, Chiba H, Kojima T, Sawada N (2006) Epigenetic silencing of occludin promotes tumorigenic and metastatic properties of cancer cells via modulations of unique sets of apoptosis-associated genes. *Cancer Res* 66:9125–9133.

Ouellette AJ (2010) Paneth cells and innate mucosal immunity. *Curr Opin Gastroenterol* 26:547–553.

Pacheco-Soares C, Souza WD (1998) Redistribution of parasite and host cell membrane components during Toxoplasma gondii invasion. *Cell Struct Funct* 23:159–168.

Paddison PJ, Caudy AA, Bernstein E, Hannon GJ, Conklin DS (2002) Short hairpin RNAs (shRNAs) induce sequence-specific silencing in mammalian cells. *Genes Dev* 16:948–958.

Pageot LP, Perreault N, Basora N, Francoeur C, Magny P, Beaulieu JF (2000) Human cell models to study small intestinal functions: recapitulation of the crypt-villus axis. *Microsc Res Tech* 49:394–406.

Parker SJ, Roberts CW, Alexander J (1991) CD8+ T cells are the major lymphocyte subpopulation involved in the protective immune response to Toxoplasma gondii in mice. *Clin Exp Immunol* 84:207–212.

Passos ST, Silver JS, O'Hara AC, Sehy D, Stumhofer JS, Hunter CA (2010) IL-6 promotes NK cell production of IL-17 during toxoplasmosis. *J Immunol* 184:1776–1783.

Patrick DM, Leone AK, Shellenberger JJ, Dudowicz KA, King JM (2006) Proinflammatory cytokines tumor necrosis factor-alpha and interferon-gamma modulate epithelial barrier function in Madin-Darby canine kidney cells through mitogen activated protein kinase signaling. *BMC Physiol* 6:2.

Paul EC, Hochman J, Quaroni A (1993) Conditionally immortalized intestinal epithelial cells: novel approach for study of differentiated enterocytes. *Am J Physiol* 265:C266–C278.

Pelosi M, Marampon F, Zani BM, Prudente S, Perlas E, Caputo V, Cianetti L, Berno V, Narumiya S, Kang SW, Musarò A, Rosenthal N (2007) ROCK2 and its alternatively spliced isoform ROCK2m positively control the maturation of the myogenic program. *Mol Cell Biol* 27:6163–6176.

Peng J, He F, Zhang C, Deng X, Yin F (2011) Protein kinase C-a signals P115 RhoGEF phosphorylation and RhoA activation in TNF-a-induced mouse brain microvascular endothelial cell barrier dysfunction. *J Neuroinflammation* 8:28.

Pentecost M, Otto G, Theriot JA, Amieva MR (2006) Listeria monocytogenes invades the epithelial junctions at sites of cell extrusion. *PLoS Pathog* 2:e3.

Persson CM, Lambert H, Vutova PP, Dellacasa-Lindberg I, Nederby J, Yagita H, Ljunggren HG, Grandien A, Barragan A, Chambers BJ (2009) Transmission of Toxoplasma gondii from infected dendritic cells to natural killer cells. *Infect Immun* 77:970–976.

Persson EK, Agnarson AM, Lambert H, Hitziger N, Yagita H, Chambers BJ, Barragan A, Grandien A (2007) Death receptor ligation or exposure to perforin trigger rapid egress of the intracellular parasite Toxoplasma gondii. *J Immunol* 179:8357–8365.

Petersen E, Nielsen HV, Christiansen L, Spenter J (1998) Immunization with E. coli produced recombinant T. gondii SAG1 with alum as adjuvant protect mice against lethal infection with Toxoplasma gondii. *Vaccine* 16:1283–1289.

Peterson MD, Mooseker MS (1992) Characterization of the enterocyte-like brush border cytoskeleton of the C2BBe clones of the human intestinal cell line, Caco-2. *J Cell Sci* 102 (Pt 3):581–600.

Pezzella-D'Alessandro N, Moal HL, Bonhomme A, Valere A, Klein C, Gomez-Marin J, Pinon JM (2001) Calmodulin distribution and the actomyosin cytoskeleton in Toxoplasma gondii. *J Histochem Cytochem* 49:445–454.

Pfefferkorn ER (1984) Interferon gamma blocks the growth of Toxoplasma gondii in human fibroblasts by inducing the host cells to degrade tryptophan. *Proc Natl Acad Sci U S A* 81:908–912.

Pifer R, Benson A, Sturge CR, Yarovinsky F (2011) UNC93B1 is essential for TLR11 activation and IL-12-dependent host resistance to Toxoplasma gondii. *J Biol Chem* 286:3307–3314.

Potten CS, Loeffler M (1990) Stem cells: attributes, cycles, spirals, pitfalls and uncertainties. Lessons for and from the crypt. *Development* 110:1001–1020.

Poulaki V, Iliaki E, Mitsiades N, Mitsiades CS, Paulus YN, Bula DV, Gragoudas ES, Miller JW (2007) Inhibition of Hsp90 attenuates inflammation in endotoxin-induced uveitis. *FASEB J* 21:2113–2123.

Poupel O, Boleti H, Axisa S, Couture-Tosi E, Tardieux I (2000) Toxofilin, a novel actin-binding protein from Toxoplasma gondii, sequesters actin monomers and caps actin filaments. *Mol Biol Cell* 11:355–368.

Quaroni A, Tian JQ, Göke M, Podolsky DK (1999) Glucocorticoids have pleiotropic effects on small intestinal crypt cells. *Am J Physiol* 277:G1027–G1040.

Quaroni A, Wands J, Trelstad RL, Isselbacher KJ (1979) Epithelioid cell cultures from rat small intestine. Characterization by morphologic and immunologic criteria. *J Cell Biol* 80:248–265.

Que X, Ngo H, Lawton J, Gray M, Liu Q, Engel J, Brinen L, Ghosh P, Joiner KA, Reed SL (2002) The cathepsin B of Toxoplasma gondii, toxopain-1, is critical for parasite invasion and rhoptry protein processing. *J Biol Chem* 277:25791–25797.

Rachinel N, Buzoni-Gatel D, Dutta C, Mennechet FJD, Luangsay S, Minns LA, Grigg ME, Tomavo S, Boothroyd JC, Kasper LH (2004) The induction of acute ileitis by a single microbial antigen of Toxoplasma gondii. *J Immunol* 173:2725–2735.

Radke JR, Striepen B, Guerini MN, Jerome ME, Roos DS, White MW (2001) Defining the cell cycle for the tachyzoite stage of Toxoplasma gondii. *Mol Biochem Parasitol* 115:165–175.

Rahner C, Mitic LL, Anderson JM (2001) Heterogeneity in expression and subcellular localization of claudins 2, 3, 4, and 5 in the rat liver, pancreas, and gut. *Gastroenterology* 120:411–422.

Raikwar NS, Vandewalle A, Thomas CP (2010) Nedd4-2 interacts with occludin to inhibit tight junction formation and enhance paracellular conductance in collecting duct epithelia. *Am J Physiol Renal Physiol* 299:F436–F444.

Rajasekaran SA, Barwe SP, Gopal J, Ryazantsev S, Schneeberger EE, Rajasekaran AK (2007) Na-K-ATPase regulates tight junction permeability through occludin phosphorylation in pancreatic epithelial cells. *Am J Physiol Gastrointest Liver Physiol* 292:G124–G133.

Raleigh DR, Boe DM, Yu D, Weber CR, Marchiando AM, Bradford EM, Wang Y, Wu L, Schneeberger EE, Shen L, Turner JR (2011) Occludin S408 phosphorylation regulates tight junction protein interactions and barrier function. *J Cell Biol* 193:565–582.

Raleigh DR, Marchiando AM, Zhang Y, Shen L, Sasaki H, Wang Y, Long M, Turner JR (2010) Tight junction-associated MARVEL proteins marveld3, tricellulin, and occludin have distinct but overlapping functions. *Mol Biol Cell* 21:1200–1213.

Ranaldi G, Islam K, Sambuy Y (1992) Epithelial cells in culture as a model for the intestinal transport of antimicrobial agents. *Antimicrob Agents Chemother* 36:1374–1381.

Rao JN, Li J, Li L, Bass BL, Wang JY (1999) Differentiated intestinal epithelial cells exhibit increased migration through polyamines and myosin II. *Am J Physiol* 277:G1149–G1158.

Raschperger E, Engstrom U, Pettersson RF, Fuxe J (2004) CLMP, a novel member of the CTX family and a new component of epithelial tight junctions. *J Biol Chem* 279:796–804.

Rescigno M, Urbano M, Valzasina B, Francolini M, Rotta G, Bonasio R, Granucci F, Kraehenbuhl JP, Ricciardi-Castagnoli P (2001) Dendritic cells express tight junction proteins and penetrate gut epithelial monolayers to sample bacteria. *Nat Immunol* 2:361–367.

Resnick-Silverman L, Pang Z, Li G, Jha KK, Ozer HL (1991) Retinoblastoma protein and simian virus 40-dependent immortalization of human fibroblasts. *J Virol* 65:2845–2852.

Revel JP, Karnovsky MJ (1967) Hexagonal array of subunits in intercellular junctions of the mouse heart and liver. *J Cell Biol* 33:C7–C12.

Riazuddin S, Ahmed ZM, Fanning AS, Lagziel A, ichiro Kitajiri S, Ramzan K, Khan SN, Chattaraj P, Friedman PL, Anderson JM, Belyantseva IA, Forge A, Riazuddin S, Friedman TB (2006) Tricellulin is a tight-junction protein necessary for hearing. *Am J Hum Genet* 79:1040–1051.

Riento K, Ridley AJ (2003) Rocks: multifunctional kinases in cell behaviour. *Nat Rev Mol Cell Biol* 4:446–456.

Riesen FK, Rothen-Rutishauser B, Wunderli-Allenspach H (2002) A ZO1-GFP fusion protein to study the dynamics of tight junctions in living cells. *Histochem Cell Biol* 117:307–315.

Rimoldi M, Chieppa M, Vulcano M, Allavena P, Rescigno M (2004) Intestinal epithelial cells control dendritic cell function. *Ann N Y Acad Sci* 1029:66–74.

Roberts CW, Alexander J (1992) Studies on a murine model of congenital toxoplasmosis: vertical disease transmission only occurs in BALB/c mice infected for the first time during pregnancy. *Parasitology* 104 Pt 1:19–23.

Roberts CL, Keita AV, Duncan SH, O'Kennedy N, Söderholm JD, Rhodes JM, Campbell BJ (2010) Translocation of Crohn's disease Escherichia coli across M-cells: contrasting effects of soluble plant fibres and emulsifiers. *Gut* 59:1331–1339.

Roh MH, Fan S, Liu CJ, Margolis B (2003) The Crumbs3-Pals1 complex participates in the establishment of polarity in mammalian epithelial cells. *J Cell Sci* 116:2895–2906.

Roh MH, Liu CJ, Laurinec S, Margolis B (2002) The carboxyl terminus of zona occludens-3 binds and recruits a mammalian homologue of discs lost to tight junctions. *J Biol Chem* 277:27501–27509.

Ronet C, Darche S, de Moraes ML, Miyake S, Yamamura T, Louis JA, Kasper LH, Buzoni-Gatel D (2005) NKT cells are critical for the initiation of an inflammatory bowel response against Toxoplasma gondii. *J Immunol* 175:899–908.

Rosowski EE, Lu D, Julien L, Rodda L, Gaiser RA, Jensen KDC, Saeij JPJ (2011) Strain-specific activation of the NF-kappaB pathway by GRA15, a novel Toxoplasma gondii dense granule protein. *J Exp Med* 208:195–212.

Rothen-Rutishauser B, Braun A, Günthert M, Wunderli-Allenspach H (2000) Formation of multilayers in the caco-2 cell culture model: a confocal laser scanning microscopy study. *Pharm Res* 17:460–465.

Ryan MJ, Johnson G, Kirk J, Fuerstenberg SM, Zager RA, Torok-Storb B (1994) HK-2: an immortalized proximal tubule epithelial cell line from normal adult human kidney. *Kidney Int* 45:48–57.

Saeij JPJ, Boyle JP, Coller S, Taylor S, Sibley LD, Brooke-Powell ET, Ajioka JW, Boothroyd JC (2006) Polymorphic secreted kinases are key virulence factors in toxoplasmosis. *Science* 314:1780–1783.

Saeij JPJ, Coller S, Boyle JP, Jerome ME, White MW, Boothroyd JC (2007) Toxoplasma co-opts host gene expression by injection of a polymorphic kinase homologue. *Nature* 445:324–327.

Saeij JPJ, Boyle JP, Boothroyd JC (2005) Differences among the three major strains of Toxoplasma gondii and their specific interactions with the infected host. *Trends Parasitol* 21:476–481.

Saitou M, Fujimoto K, Doi Y, Itoh M, Fujimoto T, Furuse M, Takano H, Noda T, Tsukita S (1998) Occludin-deficient embryonic stem cells can differentiate into polarized epithelial cells bearing tight junctions. *J Cell Biol* 141:397–408.

Saitou M, Furuse M, Sasaki H, Schulzke JD, Fromm M, Takano H, Noda T, Tsukita S (2000) Complex phenotype of mice lacking occludin, a component of tight junction strands. *Mol Biol Cell* 11:4131–4142.

Sakaguchi T, Köhler H, Gu X, McCormick BA, Reinecker HC (2002) Shigella flexneri regulates tight junction-associated proteins in human intestinal epithelial cells. *Cell Microbiol* 4:367–381.

Sakakibara A, Furuse M, Saitou M, Ando-Akatsuka Y, Tsukita S (1997) Possible involvement of phosphorylation of occludin in tight junction formation. *J Cell Biol* 137:1393–1401.

Samarin SN, Ivanov AI, Flatau G, Parkos CA, Nusrat A (2007) Rho/Rho-associated kinase-II signaling mediates disassembly of epithelial apical junctions. *Mol Biol Cell* 18:3429–3439.

Sanders MA, Basson MD (2000) Collagen IV-dependent ERK activation in human Caco-2 intestinal epithelial cells requires focal adhesion kinase. *J Biol Chem* 275:38040–38047.

Saouros S, Edwards-Jones B, Reiss M, Sawmynaden K, Cota E, Simpson P, Dowse TJ, Jäkle U, Ramboarina S, Shivarattan T, Matthews S,

Soldati-Favre D (2005) A novel galectin-like domain from Toxoplasma gondii micronemal protein 1 assists the folding, assembly, and transport of a cell adhesion complex. *J Biol Chem* 280:38583–38591.

Sasono PM, Smith JE (1998) Toxoplasma gondii: an ultrastructural study of host-cell invasion by the bradyzoite stage. *Parasitol Res* 84:640–645.

Savage DC, Siegel JE, Snellen JE, Whitt DD (1981) Transit time of epithelial cells in the small intestines of germfree mice and ex-germfree mice associated with indigenous microorganisms. *Appl Environ Microbiol* 42:996–1001.

Saxonov S, Berg P, Brutlag DL (2006) A genome-wide analysis of CpG dinucleotides in the human genome distinguishes two distinct classes of promoters. *Proc Natl Acad Sci U S A* 103:1412–1417.

Scharton-Kersten TM, Wynn TA, Denkers EY, Bala S, Grunvald E, Hieny S, Gazzinelli RT, Sher A (1996) In the absence of endogenous IFN-gamma, mice develop unimpaired IL-12 responses to Toxoplasma gondii while failing to control acute infection. *J Immunol* 157:4045–4054.

Schatten H, Ris H (2004) Three-Dimensional Imaging of Toxoplasma gondii - Host Cell Interactions within the Parasitophorous Vacuole. *Microscopy and Microanalysis* 10:580–585.

Schmidt A, Utepbergenov DI, Mueller SL, Beyermann M, Schneider-Mergener J, Krause G, Blasig IE (2004) Occludin binds to the SH3-hinge-GuK unit of zonula occludens protein 1: potential mechanism of tight junction regulation. *Cell Mol Life Sci* 61:1354–1365.

Schulzke JD, Gitter AH, Mankertz J, Spiegel S, Seidler U, Amasheh S, Saitou M, Tsukita S, Fromm M (2005) Epithelial transport and barrier function in occludin-deficient mice. *Biochim Biophys Acta* 1669:34–42.

Schwab JC, Beckers CJ, Joiner KA (1994) The parasitophorous vacuole membrane surrounding intracellular Toxoplasma gondii functions as a molecular sieve. *Proc Natl Acad Sci U S A* 91:509–513.

Senes A, Ubarretxena-Belandia I, Engelman DM (2001) The Calpha —H...O hydrogen bond: a determinant of stability and specificity in transmembrane helix interactions. *Proc Natl Acad Sci U S A* 98:9056–9061.

Seth A, Sheth P, Elias BC, Rao R (2007) Protein phosphatases 2A and 1 interact with occludin and negatively regulate the assembly of tight junctions in the CACO-2 cell monolayer. *J Biol Chem* 282:11487–11498.

Shaw MH, Reimer T, Sánchez-Valdepeñas C, Warner N, Kim YG, Fresno M, Nuñez G (2009) T cell-intrinsic role of Nod2 in promoting type 1 immunity to Toxoplasma gondii. *Nat Immunol* 10:1267–1274.

Shaw SK, Hermanowski-Vosatka A, Shibahara T, McCormick BA, Parkos CA, Carlson SL, Ebert EC, Brenner MB, Madara JL (1998) Migration of intestinal intraepithelial lymphocytes into a polarized epithelial monolayer. *Am J Physiol* 275:G584–G591.

Sheffield HG, Melton ML (1968) The fine structure and reproduction of Toxoplasma gondii. *J Parasitol* 54:209–226.

Shen L, Turner JR (2005) Actin depolymerization disrupts tight junctions via caveolae-mediated endocytosis. *Mol Biol Cell* 16:3919–3936.

Shen L, Weber CR, Turner JR (2008) The tight junction protein complex undergoes rapid and continuous molecular remodeling at steady state. *J Cell Biol* 181:683–695.

Sheth B, Moran B, Anderson JM, Fleming TP (2000) Post-translational control of occludin membrane assembly in mouse trophectoderm: a mechanism to regulate timing of tight junction biogenesis and blastocyst formation. *Development* 127:831–840.

Sheth P, Basuroy S, Li C, Naren AP, Rao RK (2003) Role of phosphatidylinositol 3-kinase in oxidative stress-induced disruption of tight junctions. *J Biol Chem* 278:49239–49245.

Shikama N, Chan HM, Krstic-Demonacos M, Smith L, Lee CW, Cairns W, Thangue NBL (2000) Functional interaction between nucleosome assembly proteins and p300/CREB-binding protein family coactivators. *Mol Cell Biol* 20:8933–8943.

Shirahata T, Muroya N, Ohta C, Goto H, Nakane A (1992) Correlation between increased susceptibility to primary Toxoplasma gondii infection and depressed production of gamma interferon in pregnant mice. *Microbiol Immunol* 36:81–91.

Sibley LD, Khan A, Ajioka JW, Rosenthal BM (2009) Genetic diversity of Toxoplasma gondii in animals and humans. *Philos Trans R Soc Lond B Biol Sci* 364:2749–2761.

Siliciano JD, Goodenough DA (1988) Localization of the tight junction protein, ZO-1, is modulated by extracellular calcium and cell-cell contact in Madin-Darby canine kidney epithelial cells. *J Cell Biol* 107:2389–2399.

Simon DB, Lu Y, Choate KA, Velazquez H, Al-Sabban E, Praga M, Casari G, Bettinelli A, Colussi G, Rodriguez-Soriano J, McCredie D, Milford D, Sanjad S, Lifton RP (1999) Paracellin-1, a renal tight junction protein required for paracellular Mg2+ resorption. *Science* 285:103–106.

Simon-Assmann P, Turck N, Sidhoum-Jenny M, Gradwohl G, Kedinger M (2007) In vitro models of intestinal epithelial cell differentiation. *Cell Biol Toxicol* 23:241–256.

Simonovic I, Rosenberg J, Koutsouris A, Hecht G (2000) Enteropathogenic Escherichia coli dephosphorylates and dissociates occludin from intestinal epithelial tight junctions. *Cell Microbiol* 2:305–315.

Singh U, Itallie CMV, Mitic LL, Anderson JM, McClane BA (2000) CaCo-2 cells treated with Clostridium perfringens enterotoxin form multiple large complex species, one of which contains the tight junction protein occludin. *J Biol Chem* 275:18407–18417.

Smales C, Ellis M, Baumber R, Hussain N, Desmond H, Staddon JM (2003) Occludin phosphorylation: identification of an occludin kinase in brain and cell extracts as CK2. *FEBS Lett* 545:161–166.

Sonoda N, Furuse M, Sasaki H, Yonemura S, Katahira J, Horiguchi Y, Tsukita S (1999) Clostridium perfringens enterotoxin fragment removes specific claudins from tight junction strands: Evidence for direct involvement of claudins in tight junction barrier. *J Cell Biol* 147:195–204.

Soête M, Camus D, Dubremetz JF (1994) Experimental induction of bradyzoite-specific antigen expression and cyst formation by the RH strain of Toxoplasma gondii in vitro. *Exp Parasitol* 78:361–370.

Soête M, Dubremetz JF (1996) Toxoplasma gondii: kinetics of stage-specific protein expression during tachyzoite-bradyzoite conversion in vitro. *Curr Top Microbiol Immunol* 219:76–80.

Speer CA, Dubey JP, Blixt JA, Prokop K (1997) Time lapse video microscopy and ultrastructure of penetrating sporozoites, types 1 and 2 parasitophorous vacuoles, and the transformation of sporozoites to tachyzoites of the VEG strain of Toxoplasma gondii. *J Parasitol* 83:565–574.

Staddon JM, Herrenknecht K, Smales C, Rubin LL (1995) Evidence that tyrosine phosphorylation may increase tight junction permeability. *J Cell Sci* 108 (Pt 2):609–619.

Staehelin LA (1973) Further observations on the fine structure of freeze-cleaved tight junctions. *J Cell Sci* 13:763–786.

Steed E, Rodrigues NTL, Balda MS, Matter K (2009) Identification of MarvelD3 as a tight junction-associated transmembrane protein of the occludin family. *BMC Cell Biol* 10:95.

Sterzenbach T, Lee SK, Brenneke B, von Goetz F, Schauer DB, Fox JG, Suerbaum S, Josenhans C (2007) Inhibitory effect of enterohepatic Helicobacter hepaticus on innate immune responses of mouse intestinal epithelial cells. *Infect Immun* 75:2717–2728.

Stevenson BR, Anderson JM, Goodenough DA, Mooseker MS (1988) Tight junction structure and ZO-1 content are identical in two strains of Madin-Darby canine kidney cells which differ in transepithelial resistance. *J Cell Biol* 107:2401–2408.

Stibbs HH (1985) Changes in brain concentrations of catecholamines and indoleamines in Toxoplasma gondii infected mice. *Ann Trop Med Parasitol* 79:153–157.

Straight SW, Shin K, Fogg VC, Fan S, Liu CJ, Roh M, Margolis B (2004) Loss of PALS1 expression leads to tight junction and polarity defects. *Mol Biol Cell* 15:1981–1990.

Straub KW, Cheng SJ, Sohn CS, Bradley PJ (2009) Novel components of the Apicomplexan moving junction reveal conserved and coccidia-restricted elements. *Cell Microbiol* 11:590–603.

Straub KW, Peng ED, Hajagos BE, Tyler JS, Bradley PJ (2011) The Moving Junction Protein RON8 Facilitates Firm Attachment and Host Cell Invasion in Toxoplasma gondii. *PLoS Pathog* 7:e1002007.

Stuart RO, Nigam SK (1995) Regulated assembly of tight junctions by protein kinase C. *Proc Natl Acad Sci U S A* 92:6072–6076.

Su C, Evans D, Cole RH, Kissinger JC, Ajioka JW, Sibley LD (2003) Recent expansion of Toxoplasma through enhanced oral transmission. *Science* 299:414–416.

Suar M, Jantsch J, Hapfelmeier S, Kremer M, Stallmach T, Barrow PA, Hardt WD (2006) Virulence of broad- and narrow-host-range Salmonella enterica serovars in the streptomycin-pretreated mouse model. *Infect Immun* 74:632–644.

Subramanian VS, Marchant JS, Ye D, Ma TY, Said HM (2007) Tight junction targeting and intracellular trafficking of occludin in polarized epithelial cells. *Am J Physiol Cell Physiol* 293:C1717–C1726.

Sudol M, Chen HI, Bougeret C, Einbond A, Bork P (1995) Characterization of a novel protein-binding module–the WW domain. *FEBS Lett* 369:67–71.

Sukthana Y (2006) Toxoplasmosis: beyond animals to humans. *Trends Parasitol* 22:137–142.

Sundstrom JM, Tash BR, Murakami T, Flanagan JM, Bewley MC, Stanley BA, Gonsar KB, Antonetti DA (2009) Identification and analysis of occludin phosphosites: a combined mass spectrometry and bioinformatics approach. *J Proteome Res* 8:808–817.

Susomboon P, Maneerat Y, Dekumyoy P, Kalambaheti T, Iwagami M, Komaki-Yasuda K, Kawazu SI, Tangpukdee N, Looareesuwan S, Kano S (2006) Down-regulation of tight junction mRNAs in human endothelial cells co-cultured with Plasmodium falciparum-infected erythrocytes. *Parasitol Int* 55:107–112.

Suss-Toby E, Zimmerberg J, Ward GE (1996) Toxoplasma invasion: the parasitophorous vacuole is formed from host cell plasma membrane and pinches off via a fission pore. *Proc Natl Acad Sci U S A* 93:8413–8418.

Suzuki T, Elias BC, Seth A, Shen L, Turner JR, Giorgianni F, Desiderio D, Guntaka R, Rao R (2009) PKC eta regulates occludin phosphorylation and epithelial tight junction integrity. *Proc Natl Acad Sci U S A* 106:61–66.

Swedlow JR, Hu K, Andrews PD, Roos DS, Murray JM (2002) Measuring tubulin content in Toxoplasma gondii: a comparison of laser-scanning confocal and wide-field fluorescence microscopy. *Proc Natl Acad Sci U S A* 99:2014–2019.

Sánchez-Pulido L, Martín-Belmonte F, Valencia A, Alonso MA (2002) MARVEL: a conserved domain involved in membrane apposition events. *Trends Biochem Sci* 27:599–601.

Takehara M, Nishimura T, Mima S, Hoshino T, Mizushima T (2009) Effect of claudin expression on paracellular permeability, migration and invasion of colonic cancer cells. *Biol Pharm Bull* 32:825–831.

Tamagawa H, Takahashi I, Furuse M, Yoshitake-Kitano Y, Tsukita S, Ito T, Matsuda H, Kiyono H (2003) Characteristics of claudin expression in follicle-associated epithelium of Peyer's patches: preferential localization of claudin-4 at the apex of the dome region. *Lab Invest* 83:1045–1053.

Tamura A, Kitano Y, Hata M, Katsuno T, Moriwaki K, Sasaki H, Hayashi H, Suzuki Y, Noda T, Furuse M, Tsukita S, Tsukita S (2008) Megaintestine in claudin-15-deficient mice. *Gastroenterology* 134:523–534.

Tang XX, Chen H, Yu S, Zhang L, Caplan MJ, Chan HC (2010a) Lymphocytes accelerate epithelial tight junction assembly: role of AMP-activated protein kinase (AMPK). *PLoS One* 5:e12343.

Tang Y, Clayburgh DR, Mittal N, Goretsky T, Dirisina R, Zhang Z, Kron M, Ivancic D, Katzman RB, Grimm G, Lee G, Fryer J, Nusrat A, Turner JR, Barrett TA (2010b) Epithelial NF-kappaB enhances transmucosal fluid movement by altering tight junction protein composition after T cell activation. *Am J Pathol* 176:158–167.

Taraszka KS, Higgins JM, Tan K, Mandelbrot DA, Wang JH, Brenner MB (2000) Molecular basis for leukocyte integrin alpha(E)beta(7) adhesion to epithelial (E)-cadherin. *J Exp Med* 191:1555–1567.

Tavelin S, Hashimoto K, Malkinson J, Lazorova L, Toth I, Artursson P (2003) A new principle for tight junction modulation based on occludin peptides. *Mol Pharmacol* 64:1530–1540.

Taylor S, Barragan A, Su C, Fux B, Fentress SJ, Tang K, Beatty WL, Hajj HE, Jerome M, Behnke MS, White M, Wootton JC, Sibley LD (2006) A secreted serine-threonine kinase determines virulence in the eukaryotic pathogen Toxoplasma gondii. *Science* 314:1776–1780.

Teller IC, Beaulieu JF (2001) Interactions between laminin and epithelial cells in intestinal health and disease. *Expert Rev Mol Med* 3:1–18.

Teo CF, Zhou XW, Bogyo M, Carruthers VB (2007) Cysteine protease inhibitors block Toxoplasma gondii microneme secretion and cell invasion. *Antimicrob Agents Chemother* 51:679–688.

Terai T, Nishimura N, Kanda I, Yasui N, Sasaki T (2006) JRAB/MICAL-L2 is a junctional Rab13-binding protein mediating the endocytic recycling of occludin. *Mol Biol Cell* 17:2465–2475.

Tomavo S, Fortier B, Soete M, Ansel C, Camus D, Dubremetz JF (1991) Characterization of bradyzoite-specific antigens of Toxoplasma gondii. *Infect Immun* 59:3750–3753.

Tramonti D, Andrew EM, Rhodes K, Newton DJ, Carding SR (2006) Evidence for the opposing roles of different gamma delta T cell subsets in macrophage homeostasis. *Eur J Immunol* 36:1729–1738.

Traweger A, Fang D, Liu YC, Stelzhammer W, Krizbai IA, Fresser F, Bauer HC, Bauer H (2002) The tight junction-specific protein occludin is a functional target of the E3 ubiquitin-protein ligase itch. *J Biol Chem* 277:10201–10208.

Turano C, Coppari S, Altieri F, Ferraro A (2002) Proteins of the PDI family: unpredicted non-ER locations and functions. *J Cell Physiol* 193:154–163.

Turksen K, Troy TC (2011) Junctions gone bad: Claudins and loss of the barrier in cancer. *Biochim Biophys Acta* .

Turner HL, Turner JR (2010) Good fences make good neighbors: Gastrointestinal mucosal structure. *Gut Microbes* 1:22–29.

Turner JR, Rill BK, Carlson SL, Carnes D, Kerner R, Mrsny RJ, Madara JL (1997) Physiological regulation of epithelial tight junctions is associated with myosin light-chain phosphorylation. *Am J Physiol* 273:C1378–C1385.

Umeda K, Matsui T, Nakayama M, Furuse K, Sasaki H, Furuse M, Tsukita S (2004) Establishment and characterization of cultured epithelial cells lacking expression of ZO-1. *J Biol Chem* 279:44785–44794.

Utech M, Ivanov AI, Samarin SN, Bruewer M, Turner JR, Mrsny RJ, Parkos CA, Nusrat A (2005) Mechanism of IFN-gamma-induced endocytosis of tight junction proteins: myosin II-dependent vacuolarization of the apical plasma membrane. *Mol Biol Cell* 16:5040–5052.

Utech M, Mennigen R, Bruewer M (2010) Endocytosis and recycling of tight junction proteins in inflammation. *J Biomed Biotechnol* 2010:484987.

Utepbergenov DI, Fanning AS, Anderson JM (2006) Dimerization of the scaffolding protein ZO-1 through the second PDZ domain. *J Biol Chem* 281:24671–24677.

Vaishnava S, Behrendt CL, Ismail AS, Eckmann L, Hooper LV (2008) Paneth cells directly sense gut commensals and maintain homeostasis at the intestinal host-microbial interface. *Proc Natl Acad Sci U S A* 105:20858–20863.

Vega S, Morales AV, Ocaña OH, Valdés F, Fabregat I, Nieto MA (2004) Snail blocks the cell cycle and confers resistance to cell death. *Genes Dev* 18:1131–1143.

Veiga E, Guttman JA, Bonazzi M, Boucrot E, Toledo-Arana A, Lin AE, Enninga J, Pizarro-Cerdá J, Finlay BB, Kirchhausen T, Cossart P (2007) Invasive and adherent bacterial pathogens co-Opt host clathrin for infection. *Cell Host Microbe* 2:340–351.

Velge-Roussel F, Dimier-Poisson I, Buzoni-Gatel D, Bout D (2001) Anti-SAG1 peptide antibodies inhibit the penetration of Toxoplasma gondii tachyzoites into enterocyte cell lines. *Parasitology* 123:225–233.

Velmurugan GV, Dubey JP, Su C (2008) Genotyping studies of Toxoplasma gondii isolates from Africa revealed that the archetypal clonal lineages predominate as in North America and Europe. *Vet Parasitol* 155:314–318.

Vetrano S, Rescigno M, Cera MR, Correale C, Rumio C, Doni A, Fantini M, Sturm A, Borroni E, Repici A, Locati M, Malesci A, Dejana E, Danese S (2008) Unique role of junctional adhesion molecule-a in maintaining mucosal homeostasis in inflammatory bowel disease. *Gastroenterology* 135:173–184.

Vietor I, Bader T, Paiha K, Huber LA (2001) Perturbation of the tight junction permeability barrier by occludin loop peptides activates beta-catenin/TCF/LEF-mediated transcription. *EMBO Rep* 2:306–312.

Vonlaufen N, Guetg N, Naguleswaran A, Müller N, Björkman C, Schares G, von Blumroeder D, Ellis J, Hemphill A (2004) In vitro induction of Neospora caninum bradyzoites in vero cells reveals differential antigen expression, localization, and host-cell recognition of tachyzoites and bradyzoites. *Infect Immun* 72:576–583.

Wachtel M, Frei K, Ehler E, Fontana A, Winterhalter K, Gloor SM (1999) Occludin proteolysis and increased permeability in endothelial cells through tyrosine phosphatase inhibition. *J Cell Sci* 112 (Pt 23):4347–4356.

Waghray M, Zavros Y, Saqui-Salces M, El-Zaatari M, Alamelumangapuram CB, Todisco A, Eaton KA, Merchant JL (2010) Interleukin-1beta promotes gastric atrophy through suppression of Sonic Hedgehog. *Gastroenterology* 138:562–72, 572.e1–2.

Wakabayashi Y, Chua J, Larkin JM, Lippincott-Schwartz J, Arias IM (2007) Four-dimensional imaging of filter-grown polarized epithelial cells. *Histochem Cell Biol* 127:463–472.

Walker ME, Hjort EE, Smith SS, Tripathi A, Hornick JE, Hinchcliffe EH, Archer W, Hager KM (2008) Toxoplasma gondii actively remodels the microtubule network in host cells. *Microbes Infect* 10:1440–1449.

Walter JK, Castro V, Voss M, Gast K, Rueckert C, Piontek J, Blasig IE (2009a) Redox-sensitivity of the dimerization of occludin. *Cell Mol Life Sci* 66:3655–3662.

Walter JK, Rueckert C, Voss M, Mueller SL, Piontek J, Gast K, Blasig IE (2009b) The oligomerization of the coiled coil-domain of occludin is redox sensitive. *Ann N Y Acad Sci* 1165:19–27.

Wan H, Winton HL, Soeller C, Gruenert DC, Thompson PJ, Cannell MB, Stewart GA, Garrod DR, Robinson C (2000) Quantitative structural and biochemical analyses of tight junction dynamics following exposure of epithelial cells to house dust mite allergen Der p 1. *Clin Exp Allergy* 30:685–698.

Wan KL, Carruthers VB, Sibley LD, Ajioka JW (1997) Molecular characterisation of an expressed sequence tag locus of Toxoplasma gondii encoding the micronemal protein MIC2. *Mol Biochem Parasitol* 84:203–214.

Wang Y, Zhen Y, Shi Y, Chen J, Zhang C, Wang X, Yang X, Zheng Y, Liu Y, Hui R (2005) Vitamin k epoxide reductase: a protein involved in angiogenesis. *Mol Cancer Res* 3:317–323.

Ward PD, Klein RR, Troutman MD, Desai S, Thakker DR (2002) Phospholipase C-gamma modulates epithelial tight junction permeability through hyperphosphorylation of tight junction proteins. *J Biol Chem* 277:35760–35765.

Ward PD, Ouyang H, Thakker DR (2003) Role of phospholipase C-beta in the modulation of epithelial tight junction permeability. *J Pharmacol Exp Ther* 304:689–698.

Watson AJM, Chu S, Sieck L, Gerasimenko O, Bullen T, Campbell F, McKenna M, Rose T, Montrose MH (2005) Epithelial barrier function in vivo is sustained despite gaps in epithelial layers. *Gastroenterology* 129:902–912.

Watson AJM, Duckworth CA, Guan Y, Montrose MH (2009) Mechanisms of epithelial cell shedding in the Mammalian intestine and maintenance of barrier function. *Ann N Y Acad Sci* 1165:135–142.

Watson CJ, Rowland M, Warhurst G (2001) Functional modeling of tight junctions in intestinal cell monolayers using polyethylene glycol oligomers. *Am J Physiol Cell Physiol* 281:C388–C397.

Webster JP (2001) Rats, cats, people and parasites: the impact of latent toxoplasmosis on behaviour. *Microbes Infect* 3:1037–1045.

Weiner HL, da Cunha AP, Quintana F, Wu H (2011) Oral tolerance. *Immunol Rev* 241:241–259.

Weiss LM, Ma YF, Takvorian PM, Tanowitz HB, Wittner M (1998) Bradyzoite development in Toxoplasma gondii and the hsp70 stress response. *Infect Immun* 66:3295–3302.

Weiss LM, Dubey JP (2009) Toxoplasmosis: A history of clinical observations. *Int J Parasitol* 39:895–901.

Wesch D, Peters C, Oberg HH, Pietschmann K, Kabelitz D (2011) Modulation of $\gamma\delta$ T cell responses by TLR ligands. *Cell Mol Life Sci* .

Westhofen P, Watzka M, Marinova M, Hass M, Kirfel G, Mueller J, Bevans CG, Mueller CR, Oldenburg J (2011) Human vitamin K 2,3-epoxide reductase complex subunit 1-like 1 (VKORC1L1) mediates vitamin K-dependent intracellular antioxidant function. *J Biol Chem* .

Westphal JK, Dörfel MJ, Krug SM, Cording JD, Piontek J, Blasig IE, Tauber R, Fromm M, Huber O (2010) Tricellulin forms homomeric and heteromeric tight junctional complexes. *Cell Mol Life Sci* 67:2057–2068.

Wetzel DM, Håkansson S, Hu K, Roos D, Sibley LD (2003) Actin filament polymerization regulates gliding motility by apicomplexan parasites. *Mol Biol Cell* 14:396–406.

Whitehead RH, VanEeden PE, Noble MD, Ataliotis P, Jat PS (1993) Establishment of conditionally immortalized epithelial cell lines from both colon and small intestine of adult H-2Kb-tsA58 transgenic mice. *Proc Natl Acad Sci U S A* 90:587–591.

Windeck T, Gross U (1996) Toxoplasma gondii strain-specific transcript levels of SAG1 and their association with virulence. *Parasitol Res* 82:715–719.

Wittchen ES, Haskins J, Stevenson BR (1999) Protein interactions at the tight junction. Actin has multiple binding partners, and ZO-1 forms independent complexes with ZO-2 and ZO-3. *J Biol Chem* 274:35179–35185.

Wong V (1997) Phosphorylation of occludin correlates with occludin localization and function at the tight junction. *Am J Physiol* 273:C1859–C1867.

Wong V, Gumbiner BM (1997) A synthetic peptide corresponding to the extracellular domain of occludin perturbs the tight junction permeability barrier. *J Cell Biol* 136:399–409.

Wood SR, Zhao Q, Smith LH, Daniels CK (2003) Altered morphology in cultured rat intestinal epithelial IEC-6 cells is associated with alkaline phosphatase expression. *Tissue Cell* 35:47–58.

Woodmansee DB (2003) Kinetics of the initial rounds of cell division of Toxoplasma gondii. *J Parasitol* 89:895–898.

Wu C, Keightley SY, Leung-Hagesteijn C, Radeva G, Coppolino M, Goicoechea S, McDonald JA, Dedhar S (1998) Integrin-linked protein kinase regulates fibronectin matrix assembly, E-cadherin expression, and tumorigenicity. *J Biol Chem* 273:528–536.

Wu Z, Milton D, Nybom P, Sjö A, Magnusson KE (1996) Vibrio cholerae hemagglutinin/protease (HA/protease) causes morphological changes in cultured epithelial cells and perturbs their paracellular barrier function. *Microb Pathog* 21:111–123.

Wu Z, Nybom P, Magnusson KE (2000) Distinct effects of Vibrio cholerae haemagglutinin/protease on the structure and localization of the tight junction-associated proteins occludin and ZO-1. *Cell Microbiol* 2:11–17.

Yamamoto M, Ramirez SH, Sato S, Kiyota T, Cerny RL, Kaibuchi K, Persidsky Y, Ikezu T (2008) Phosphorylation of claudin-5 and occludin by rho kinase in brain endothelial cells. *Am J Pathol* 172:521–533.

Yamamoto T, Kojima T, Murata M, Takano KI, Go M, Chiba H, Sawada N (2004) IL-1beta regulates expression of Cx32, occludin, and claudin-2 of rat hepatocytes via distinct signal transduction pathways. *Exp Cell Res* 299:427–441.

Yarovinsky F, Hieny S, Sher A (2008) Recognition of Toxoplasma gondii by TLR11 prevents parasite-induced immunopathology. *J Immunol* 181:8478–8484.

Yarovinsky F, Zhang D, Andersen JF, Bannenberg GL, Serhan CN, Hayden MS, Hieny S, Sutterwala FS, Flavell RA, Ghosh S, Sher A (2005) TLR11 activation of dendritic cells by a protozoan profilin-like protein. *Science* 308:1626–1629.

Ye D, Ma I, Ma TY (2006) Molecular mechanism of tumor necrosis factor-alpha modulation of intestinal epithelial tight junction barrier. *Am J Physiol Gastrointest Liver Physiol* 290:G496–G504.

Yin J, Yu FSX (2008) Rho kinases regulate corneal epithelial wound healing. *Am J Physiol Cell Physiol* 295:C378–C387.

Yolken RH, Dickerson FB, Torrey EF (2009) Toxoplasma and schizophrenia. *Parasite Immunol* 31:706–715.

Yu ASL, McCarthy KM, Francis SA, McCormack JM, Lai J, Rogers RA, Lynch RD, Schneeberger EE (2005) Knockdown of occludin expression

leads to diverse phenotypic alterations in epithelial cells. *Am J Physiol Cell Physiol* 288:C1231–C1241.

Yu QH, Yang Q (2009) Diversity of tight junctions (TJs) between gastrointestinal epithelial cells and their function in maintaining the mucosal barrier. *Cell Biol Int* 33:78–82.

Yuan ZG, Zhang XX, He XH, Petersen E, Zhou DH, He Y, Lin RQ, Li XZ, Chen XL, Shi XR, Zhong XL, Zhang B, Zhu XQ (2011) Protective immunity induced by Toxoplasma gondii rhoptry protein 16 against toxoplasmosis in mice. *Clin Vaccine Immunol* 18:119–124.

Zai A, Rudd MA, Scribner AW, Loscalzo J (1999) Cell-surface protein disulfide isomerase catalyzes transnitrosation and regulates intracellular transfer of nitric oxide. *J Clin Invest* 103:393–399.

Zeissig S, Bürgel N, Günzel D, Richter J, Mankertz J, Wahnschaffe U, Kroesen AJ, Zeitz M, Fromm M, Schulzke JD (2007) Changes in expression and distribution of claudin 2, 5 and 8 lead to discontinuous tight junctions and barrier dysfunction in active Crohn's disease. *Gut* 56:61–72.

Zhang L, Li J, Young LH, Caplan MJ (2006) AMP-activated protein kinase regulates the assembly of epithelial tight junctions. *Proc Natl Acad Sci U S A* 103:17272–17277.

Zhao YO, Khaminets A, Hunn JP, Howard JC (2009) Disruption of the Toxoplasma gondii parasitophorous vacuole by IFNgamma-inducible immunity-related GTPases (IRG proteins) triggers necrotic cell death. *PLoS Pathog* 5:e1000288.

Zheng A, Yuan F, Li Y, Zhu F, Hou P, Li J, Song X, Ding M, Deng H (2007) Claudin-6 and claudin-9 function as additional coreceptors for hepatitis C virus. *J Virol* 81:12465–12471.

Zheng B, He A, Gan M, Li Z, He H, Zhan X (2009) MIC6 associates with aldolase in host cell invasion by Toxoplasma gondii. *Parasitol Res* 105:441–445.

Zoumpopoulou G, Tsakalidou E, Dewulf J, Pot B, Grangette C (2009) Differential crosstalk between epithelial cells, dendritic cells and bacteria in a co-culture model. *Int J Food Microbiol* 131:40–51.